

INFORMATION TO USERS

This manuscript has been reproduced from the microfilm master. UMI films the text directly from the original or copy submitted. Thus, some thesis and dissertation copies are in typewriter face, while others may be from any type of computer printer.

The quality of this reproduction is dependent upon the quality of the copy submitted. Broken or indistinct print, colored or poor quality illustrations and photographs, print bleedthrough, substandard margins, and improper alignment can adversely affect reproduction.

In the unlikely event that the author did not send UMI a complete manuscript and there are missing pages, these will be noted. Also, if unauthorized copyright material had to be removed, a note will indicate the deletion.

Oversize materials (e.g., maps, drawings, charts) are reproduced by sectioning the original, beginning at the upper left-hand corner and continuing from left to right in equal sections with small overlaps. Each original is also photographed in one exposure and is included in reduced form at the back of the book.

Photographs included in the original manuscript have been reproduced xerographically in this copy. Higher quality 6" x 9" black and white photographic prints are available for any photographs or illustrations appearing in this copy for an additional charge. Contact UMI directly to order.

U·M·I

• University Microfilms International
A Bell & Howell Information Company
300 North Zeeb Road, Ann Arbor, MI 48106-1346 USA
313/761-4700 800/521-0600

Order Number 9123151

**Synthesis and evaluation of new nonlinear optical organic
compounds**

Mitchell, Michael Anthony, Ph.D.

The University of Arizona, 1991

U·M·I
300 N. Zeeb Rd.
Ann Arbor, MI 48106

NOTE TO USERS

**THE ORIGINAL DOCUMENT RECEIVED BY U.M.I. CONTAINED PAGES
WITH SLANTED AND POOR PRINT. PAGES WERE FILMED AS RECEIVED.**

THIS REPRODUCTION IS THE BEST AVAILABLE COPY.

SYNTHESIS AND EVALUATION OF NEW NONLINEAR
OPTICAL ORGANIC COMPOUNDS

by
Michael Anthony Mitchell

A Dissertation Submitted to the Faculty of the
DEPARTMENT OF CHEMISTRY
In Partial Fulfillment of the Requirements
For the Degree of
DOCTOR OF PHILOSOPHY
In the Graduate College
THE UNIVERSITY OF ARIZONA

1991

THE UNIVERSITY OF ARIZONA
GRADUATE COLLEGE

2

As members of the Final Examination Committee, we certify that we have read
the dissertation prepared by Michael Anthony Mitchell

entitled Synthesis and Evaluation of New Nonlinear Optical Organic
Compounds

and recommend that it be accepted as fulfilling the dissertation requirement
for the Degree of Doctor of Philosophy.

H. K. Hall, Jr. 1/10/91
Henry K. Hall, Jr. Date

James E. Mulvaney 1/10/91
James E. Mulvaney Date

Robert B. Bates 1/10/91
Robert B. Bates Date

David E. Wigley 1/10/91
David E. Wigley Date

John H. Enemark 1/10/91
John H. Enemark Date

Final approval and acceptance of this dissertation is contingent upon the
candidate's submission of the final copy of the dissertation to the Graduate
College.

I hereby certify that I have read this dissertation prepared under my
direction and recommend that it be accepted as fulfilling the dissertation
requirement.

H. K. Hall, Jr. 1/10/91
Dissertation Director Date

STATEMENT BY AUTHOR

This dissertation has been submitted in partial fulfillment of requirements for an advanced degree at The University of Arizona and is deposited in the University Library to be made available to borrowers under rules of the Library.

Brief quotations from this dissertation are allowable without special permission, provided that accurate acknowledgment of source is made. Requests for permission for extended quotation from or reproduction of this manuscript in whole or in part may be granted by the head of the major department of the Dean of the Graduate College when in his or her judgment the proposed use of the material is in the interests of scholarship. In all other instances, however, permission must be obtained from the author.

SIGNED: 

ACKNOWLEDGMENTS

Grateful acknowledgment is made to the Eastman Kodak Company for their financial support of this research, as well as their valuable collaboration. Special acknowledgment goes to Dr. Douglas Robello, Dr. Craig Willand, and Dr. Dave Williams for their consultation. Thanks also go to Dr. Hillary Hampsch for doing the EFISH measurements, and Dr. Werner Koehler for the ground state dipole moment measurements of the sulfone compounds.

The apparatus used to evaluate the ground state dipole moments could not have been built without the help of many friends. These friends are: Ron Clayton in the machine shop, Larry Cook and Ted White in the electronics shop, and Charlie Amling in the glass shop.

The journey to obtain any goal is filled not only with the learning of knowledge, but also the experiences needed to reach that goal. There are many people who helped me learn the science, and who have enriched my personal experiences. Special recognition belongs to Professor Henry Hall and Professor Jim Mulvaney, both of whom guided my research and growth. Also, the entire research group of Professor Hall, without whom day to day work would have been much more difficult. Of particular note in the group are Mr. M. Tomida for his initial studies, and Dr. Anne Padias who is an excellent scientist and friend. The completion of my degree would have been impossible without the love and support of my extraordinary wife Susan; for her I reserve the warmest gratitude possible.

TABLE OF CONTENTS

	Page
LIST OF SCHEMES.....	7
LIST OF TABLES.....	9
LIST OF FIGURES.....	11
ABSTRACT.....	12
CHAPTER 1. INTRODUCTION TO NONLINEAR OPTICAL MATERIALS.....	13
Introduction.....	14
Theoretical Background.....	18
Design of Nonlinear Optical Molecules.....	19
Design of Nonlinear Optical Materials.....	22
CHAPTER 2. NONLINEAR OPTICAL ENHANCEMENT STUDIES.....	33
<i>p</i> -Aminophenyl Sulfone Oligomers.....	34
Retrosynthesis.....	36
Synthesis.....	40
Measurements and Discussion.....	56
Future Studies.....	61
Experimental.....	63
CHAPTER 3. NEW NONLINEAR OPTICAL POLYMERIC MATERIALS.....	83
Poly {4'-carboalkoxy-4-methoxy- α' -cyano- α - aminostilbenes}.....	84
Retrosynthesis.....	89
Synthesis.....	90
Polymer Synthesis.....	96
Measurements and Discussion.....	97
Experimental.....	100
CHAPTER 4. MEASUREMENT OF SECOND ORDER HYPERPOLARIZABILITIES.....	109
Background.....	110
EFISH Measurements.....	111
Spectrophotometric Measurements.....	116
Ground State Dipole Moment.....	123
Transition Dipole Moment and Transition Frequency.....	128
Excited State Dipole Moment.....	132
Results and Discussion.....	137

TABLE OF CONTENTS --Continued

	Page
CHAPTER 5. CONCLUSION.....	154
APPENDIX A. ^1H NMR AND ^{13}C NMR SPECTRA.....	157
APPENDIX B. DSC AND SEC DATA.....	251
REFERENCES.....	265

LIST OF SCHEMES

Scheme	Page
1. Optical Properties of NLO Materials.....	15
2. NLO Photon Absorption and Emission of Molecules.....	17
3. Second Order Susceptibilities of Various Compounds.....	23
4. Poling Process to Produce NLO Polymer Matrix.....	26
5. NLO Comb Polymer and Poling Technique.....	27
6. Crosslinking Strategies to Form NLO Materials.....	28
7. Early Main Chain NLO Polymers.....	29
8. α -Cinnamate Homo- and Copolymers.....	30
9. Loss of Second Harmonic Generation (SHG) with Temperature.....	31
10. Retrosynthesis of <i>p</i> -Aminophenyl Sulfones <i>via</i> Bond a.....	37
11. Retrosynthesis of <i>p</i> -Aminophenyl Sulfones <i>via</i> Bond b.....	38
12. Polysulfone Synthesis.....	39
13. Retrosynthesis of <i>p</i> -Aminophenyl Sulfones <i>via</i> Bond c.....	39
14. Monomer Analogue Synthesis.....	41
15. Synthesis of the Hexamethylene Spaced <i>p</i> -Aminophenyl Sulfone Oligomers.....	43
16. Synthesis of the α,β -Unsaturated Sulfone 30	44
17. Synthesis of the Vinyl Sulfide 32	44
18. Synthesis of the 1,4-Disubstituted Cyclohexane 34	45
19. Synthesis of the Monomethylene Monomer.....	46
20. Reduction of Monomer 38	46
21. Possible Mechanisms for Monomethylene Monomer Reduction.....	47
22. Attempted Oligomer Synthesis via Nucleophilic Aromatic Substitution.....	48
23. Dimethylene Spaced Dimer Synthesis.....	49
24. Dimethylene Spaced Trimer Synthesis.....	51
25. Piperidine Spaced Dimer Synthesis.....	53
26. Piperidine Spaced Trimer Synthesis.....	54
27. Piperidine Monomer Analogue Synthesis.....	55

LIST OF SCHEMES--Continued

Scheme	Page
28. Desired Dimer Conformation.....	59
29. Undesired Dimer Conformation.....	59
30. Generic Target Stilbene Polymer.....	87
31. Retrosynthesis of the Stilbene Monomers.....	89
32. Synthesis of Acceptor Half of the Stilbene Monomer.....	90
33. Synthesis of Donor Half of the Stilbene Monomer.....	90
34. Synthesis of the Vinyl Chloride 83	92
35. Synthesis of Stilbene Monomers and Monomer Analogues.....	94
36. Homopolymer Synthesis.....	96
37. Copolymer Synthesis.....	97
38. EFISH Sample Cell.....	112
39. Experimental Setup for the EFISH Measurement.....	113
40. Second Harmonic Intensity Versus the Change in Cell Pathlength.....	115
41. Symmetry of <i>p</i> -Nitroaniline.....	120
42. One Transistor Oscillator Circuit for Ground State Dipole Moment Determinations.....	124
43. Capacitance Cell for Ground State Dipole Moment Determination.....	125

LIST OF TABLES

Table	Page
1. Effect of Donor/Acceptor Strength on the Hyperpolarizability of <i>p</i> -Substituted Benzene Compounds...	21
2. Effect of Increasing Size of π System on the Hyperpolarizability.....	21
3. Hyperpolarizabilities of the α -Cinnamate Copolymers.....	31
4. Ground State Dipole Moments of Hexamethylene Spaced Oligomers.....	56
5. Hyperpolarizabilities of the Dimethylene Spaced Oligomers.....	58
6. Hyperpolarizabilities of the Piperidine Spaced Oligomers...	60
7. Physical Characteristics of NLO Polymers.....	98
8. UV/Visible Data of Monomers and Polymers.....	99
9. Hyperpolarizability of <i>p</i> -Nitroaniline (1) by EFISH.....	116
10. Relation of β_{xxx} to β_x for Various Compounds.....	119
11. Compounds Used for the Evaluation of the Spectrophotometric Method of Hyperpolarizability Determination.....	122
12. Measured Dielectric Constants.....	127
13. Solvents Used for Excited State Dipole Moment Determinations.....	136
14. Measured Ground State Dipole Moments.....	137
15. Transition Frequencies and Transition Dipole Moments.....	142
16. EFISH Values of Some α -Cyanocinnamates.....	142
17. Results of Solvatochromic Determinations of the Excited State Dipole Moment of <i>p</i> -Nitroaniline (1, $\mu_e = 14\text{-}15\text{D}$) with Equations 24-30.....	144
18. Results of Solvatochromic Determinations of the Excited State Dipole Moment of 4-(Dimethylamino) Benzonitrile (95, $\mu_e = 11.1\text{D}$) with Equations 24-30.....	145
19. Results of Solvatochromic Determinations of the Excited State Dipole Moment of 2-Amino-7-Nitrofluorene (96, $\mu_e = 19\text{-}23\text{D}$) with Equations 24-30.....	146
20. Difference Between Excited and Ground State Dipole Moments Calculated From Equations 29 and 30 for Compounds 1, 95, and 96.....	150

LIST OF TABLES--Continued

Table		Page
21.	Hyperpolarizabilities (β_{xxx}) Determined by Spectrophotometric Method, Utilizing Equation 26.....	150
22.	Hyperpolarizabilities (β_{xxx}) Determined by Spectrophotometric Method, Utilizing Equation 29.....	151
23.	Hyperpolarizabilities of Monomers and Dimers Determined by Spectrophotometric Method (β_{xxx}), and by EFISH.....	152

LIST OF FIGURES

Figure		Page
1.	Dielectric Value in Dioxane Versus Concentration for Compound 1.....	138
2.	Dielectric Value in Dioxane Versus Concentration for Compound 97.....	139
3.	Dielectric Value in Dioxane Versus Concentration for Compound 87.....	140
4.	Integral Area Versus Concentration for Compound 48.....	141
5.	Frequency of Absorbance Calculated From Equation 26 Versus Experimental for Compound 1.....	147
6.	Frequency of Absorbance Calculated From Equation 26 Versus Experimental for Compound 95.....	148
7.	Frequency of Absorbance Calculated From Equation 26 Versus Experimental for Compound 96.....	149

ABSTRACT

Nonlinear optical (NLO) materials are of current interest because of their potential applications in the development of optical computers, switches, and information storage devices, as well as laser attenuation. Organic molecules with a donor group and an acceptor group connected through a pi system exhibit a large second order NLO response, the NLO characteristic of the most interest. Previous studies have suggested that by having the NLO molecular units connected in series there is a synergistic enhancement of the NLO effect. In an effort to study this enhancement various p-aminophenyl sulfone monomers, dimers, and trimers were synthesized and evaluated. The results from this study did not confirm such enhancement, and indicate that much more work needs to be done.

Also, another class of monomer which was expected to have a high NLO efficiency was synthesized. These monomers were polymerized via condensation polymerization to give the polyesters, which contained a stilbene moiety. These polymers were found to be tractable and possess a high glass transition temperature, which is very desirable.

Finally, a method based on simple spectrophotometric measurements, and ground state dipole moment measurements, was evaluated and refined. This method, while not as accurate as standard techniques, is low cost, and simpler to conduct.

CHAPTER 1**INTRODUCTION TO NONLINEAR OPTICAL MATERIALS**

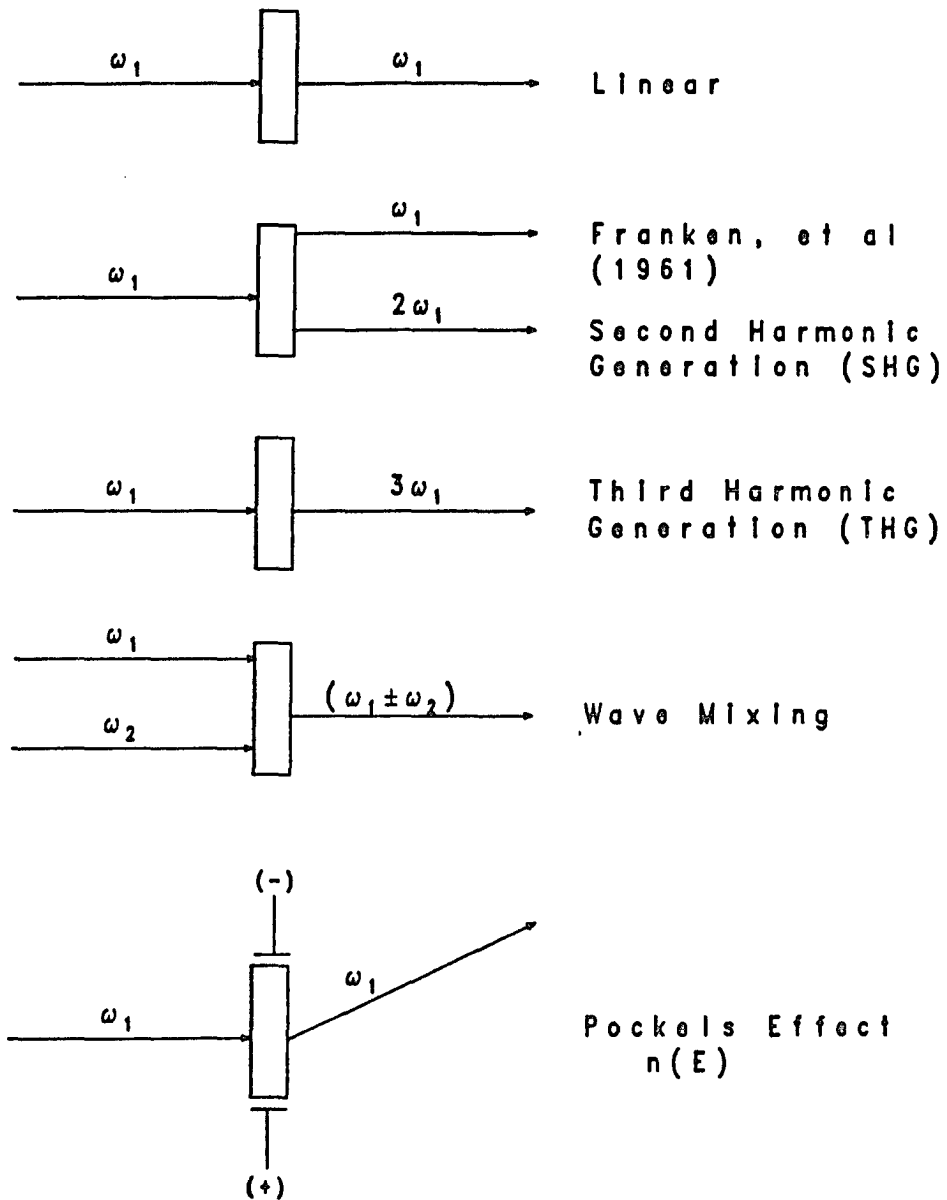
Introduction

When we wear glasses, use binoculars, telescopes, microscopes, mirrors or gratings, we manipulate light. All of these devices take advantage of the linear response of light with matter. In linear optics, light which enters matter, such as a lens, can be refracted, diffracted, or scattered, but the light which leaves the material is essentially the same type of light which entered the material. Linear optics has, of course, been thoroughly studied and, besides new polymers for contact lenses, there is little research in new materials.

Nonlinear optics (NLO) is also not an extremely new field of research. In 1875, Kerr^{1,2} showed that an electric field applied to glass could perturb its index of refraction. This effect, and the similar response observed by Pockels for crystals,³ are technically the first observed nonlinear optical responses. However, nonlinear optics is commonly viewed as those responses which arise from the interactions of very intense light, i.e. lasers, with matter.

In 1961, Franken and coworkers observed that red laser light from a ruby laser at 694 nm, when passed through a quartz crystal, gave not only the linear response, but also coherent light at 347 nm.⁴ This frequency doubling is one example of an NLO response (see Scheme 1). Other NLO responses include frequency tripling and wave mixing. In wave mixing, two different laser frequencies (ω_1 and ω_2) are incident onto an NLO material and a mixture of frequencies ($\omega_1 \pm \omega_2$) are obtained. Also of great interest are the electro-optic effects similar to those observed by Kerr and Pockel. In electro-optic devices, the index of refraction of the material is proportional to an applied electric field. Other interesting NLO effects such as the generation of a dc electric current and magnetic fields have been observed due to the incidence of laser light on crystals.^{4,5,6}

Essentially, nonlinear optics is the study of the dependence of the optical properties of a material on the intensity of the incident radiation. With the advent of lasers, field strengths of light could reach 3×10^{10} V/m; this is within the range of atomic fields, which are on the order of 10^9 to 10^{12} V/m.⁵ Qualitatively, photons are noninteracting, but NLO materials



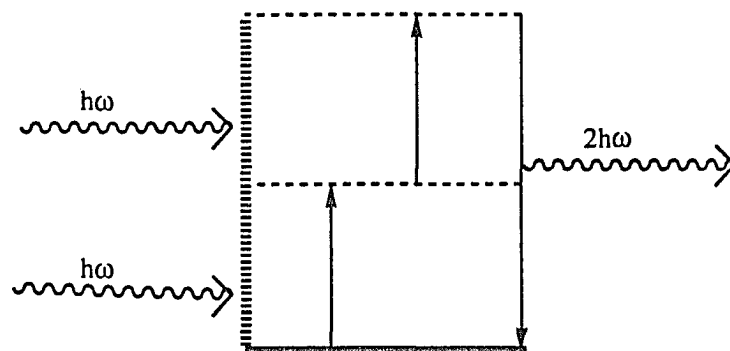
Scheme 1. Optical Properties of NLO Materials.

can overcome this tendency with a high density of photons. For example, frequency doubling is the result of two photons interacting. Electrons in the NLO material can simultaneously absorb two of the incident photons, and then a new photon of double the frequency is emitted (see Scheme 2). The difference in momentum between the incoming and outgoing photons is absorbed by the NLO material. As expected, the probability of a molecule or atom absorbing two photons simultaneously is small; however, conversion efficiencies as high as 50% have been observed.⁷ Similarly, third harmonic generation can be viewed as three photons incidenting simultaneously on a molecule which then emits one photon of triple the frequency. The probability of this event is even smaller than the frequency doubling, thus conversion efficiencies of only about 0.01% are common.⁵ The theoretical description of NLO effects was derived by Bloemberger in 1962, work for which he won the Nobel Prize in 1981.⁸

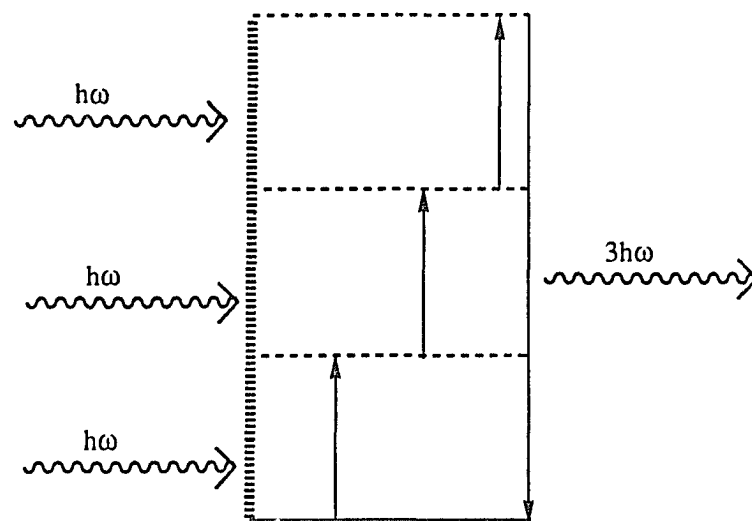
Obviously, there are many potential uses for NLO effects. Currently, frequency doubling properties find extensive use in laser attenuation.⁵ Primary laser sources are available from IR through the visible and UV down to about 116 nm. Frequency doubling is one of the major methods of effective conversion of infrared radiation into visible, and visible into ultraviolet radiation. It is interesting to note that wave mixing has allowed the formation of coherent radiation down to the XUV, near the soft x-ray range. Also, in wave mixing the term $\omega_1 - \omega_2$ may lie in the range of acoustic frequencies, basically generating ultrasonic waves from optical mixing.

The future applications of NLO materials are even more fascinating and exciting than the current uses. The next major technological advances will probably involve optical and opto-electronic devices. Optical switching is needed to make fiber optics communications more efficient; currently optical signals have to be converted into electronic signals to be switched. NLO materials could potentially be used in optical recording media.⁹ However, the current long term goal is optical based computers. Optical scientists believe neurocomputers (computers capable of parallel processing) could be built with optical devices. Because of the

Frequency Doubling:



Frequency Tripling:



Scheme 2. NLO Photon Absorption and Emission of Molecules.

characteristics of light (speed and noninteracting photons) faster, denser, and more powerful computers are possible.¹⁰⁻¹⁴ The next technological generation could be around the corner. The knowledge needed to make these new devices is either here or rapidly approaching, save one major obstacle - the materials needed. Improvements needed for materials for nonlinear optics include larger NLO responses, stabilities, and processibility. The purpose of this dissertation is to increase the body of information available concerning organic NLO materials, as well as improve upon a practical method for evaluating the NLO efficiencies of organic molecules.

Theoretical Background

The purpose of this section is primarily to define terms which will be used throughout this dissertation.

The mathematical expression used to describe the interaction of light with bulk materials is given in Equation 1.⁵

(1)

$$\Delta P = P_2 - P_1 = X^{(1)}E + X^{(2)}EE + X^{(3)}EEE + \dots$$

This equation states that the change in polarizability of the material is related to the electric field component (E) of the light. (E can also be due to an imposed electric field, such as the Kerr and Pockels effects). The chi values ($X^{(n)}$) are constants called the susceptibilities, so $X^{(1)}$ is the first order susceptibility, $X^{(2)}$ is the second order susceptibility, and so on. In linear optics, only the first term ($X^{(1)}E$) is important, but when laser light interacts with matter the higher order terms become significant. The susceptibilities are constant for a material at a particular wavelength. It is very important to note that the even ordered terms in this equation imply a symmetry requirement. An isotropic mixture (or centrosymmetric crystal) possesses even order susceptibilities which equal zero. This can be seen if

we isolate the second order term, and evaluate it in the positive and negative direction:

$$+P^{(2)} = X^{(2)}(+E)(+E) = X^{(2)}(-E)(-E) = -P^{(2)}$$

The only way $+P^{(2)}$ can equal $-P^{(2)}$ is if $P^{(2)}$ equals zero, thus $X^{(2)} = 0$. This symmetry requirement is the major obstacle for designing new second order NLO materials. As expected, the importance of the higher order terms becomes very small. Currently, there is active research into third order materials (those with high $X^{(3)}$'s), but as stated earlier, these responses are usually very weak. My work in this dissertation focuses on second order nonlinear optics. Hence, the goal of second order NLO materials research is to produce materials with high second order susceptibilities ($X^{(2)}$'s).

To obtain our goals we must first have an understanding of the molecular NLO effect. The interaction of light with matter at the molecular level is given in Equation (2).

(2)

$$\Delta\mu = \mu_2 - \mu_1 = \alpha E + \beta EE + \gamma EEE + \dots$$

Equation (2) is analogous to Equation (1) but, since we're dealing with molecules, there is a change in dipolarizability ($\Delta\mu$). Also, just as in Equation (1), the first term (αE) is the only one important for linear optics. Since we are interested in second order NLO materials, it follows that we want molecules with high second order molecular hyperpolarizabilities (β 's). The next section will deal with the design of organic molecules with high second order hyperpolarizabilities.

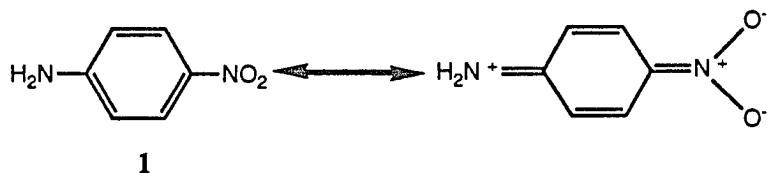
Design of Nonlinear Optical Molecules

Early NLO work showed anomalously high second order properties for various benzene derivatives (such as *m*-nitroaniline and 2-chloro-4-nitroaniline),¹⁵ and various dyes (such as 7-diethylamino-4-

methylcoumarin and auramine).^{16,17} However, it was Davydov and coworkers¹⁸ in 1970 who first made the connection between molecular charge transfer and second harmonic generation. This then became the major design component for organic molecules with large second order hyperpolarizabilities: molecules with strong charge transfer. These types of systems generally have a donor moiety connected to an acceptor substituent through a pi conjugated system:

D - Π - A


For example, *p*-nitroaniline:



Since this initial discovery, the factors effecting the intensity of the second order response have been thoroughly studied by Cheng *et al.*¹⁹ The main characteristics which determine the magnitude of β in these charge transfer systems are donor/acceptor strength and the extent of the pi system. Hyperpolarizabilities of some common donor and acceptor moieties for *p*-substituted benzenes are tabulated in Table 1. Table 1 is arranged such that the weakest donor/acceptor system is at the upper left, and the strongest system is at the lower right.


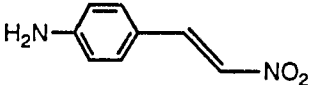
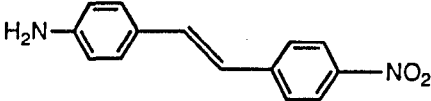
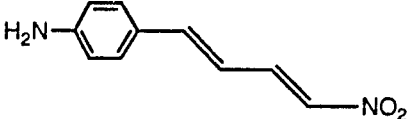
Increasing the size of the pi system also increases the magnitude of β , as shown in Table 2.²⁰

Table 1. Effect of Donor/Acceptor Strength on the Hyperpolarizability of p-Substituted Benzene Compounds (measured at 1907 nm).

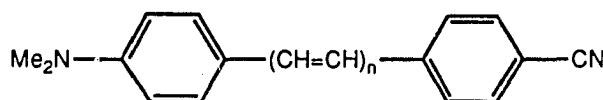


		β (x 10 ⁻³⁰ esu)			
A \ D		Me-	MeO-	MeS-	Me ₂ N-
-CN		0.7	1.9	2.8	5.0
-CHO		1.7	2.2	2.6	6.3
-NO ₂		2.1	5.1	6.1	12

Table 2. Effect of Increasing Size of Pi System on the Hyperpolarizability (measured at 1064 nm).

COMPOUND	β (x 10 ⁻³⁰ esu)
	34.5
	220
	450
	650

Attempts have even been made to derive predictive relations to estimate the effect of conjugation length. Duluc *et al.*^{21,22} showed that for the series of compounds **2**, an empirical relation could be derived ($\mu\beta = Cn^2$). However, care must be exercised when using such equations in more than a qualitative sense. In the relationship, μ is the ground state dipole moment, c is a constant, and n is the number of conjugated double bonds.



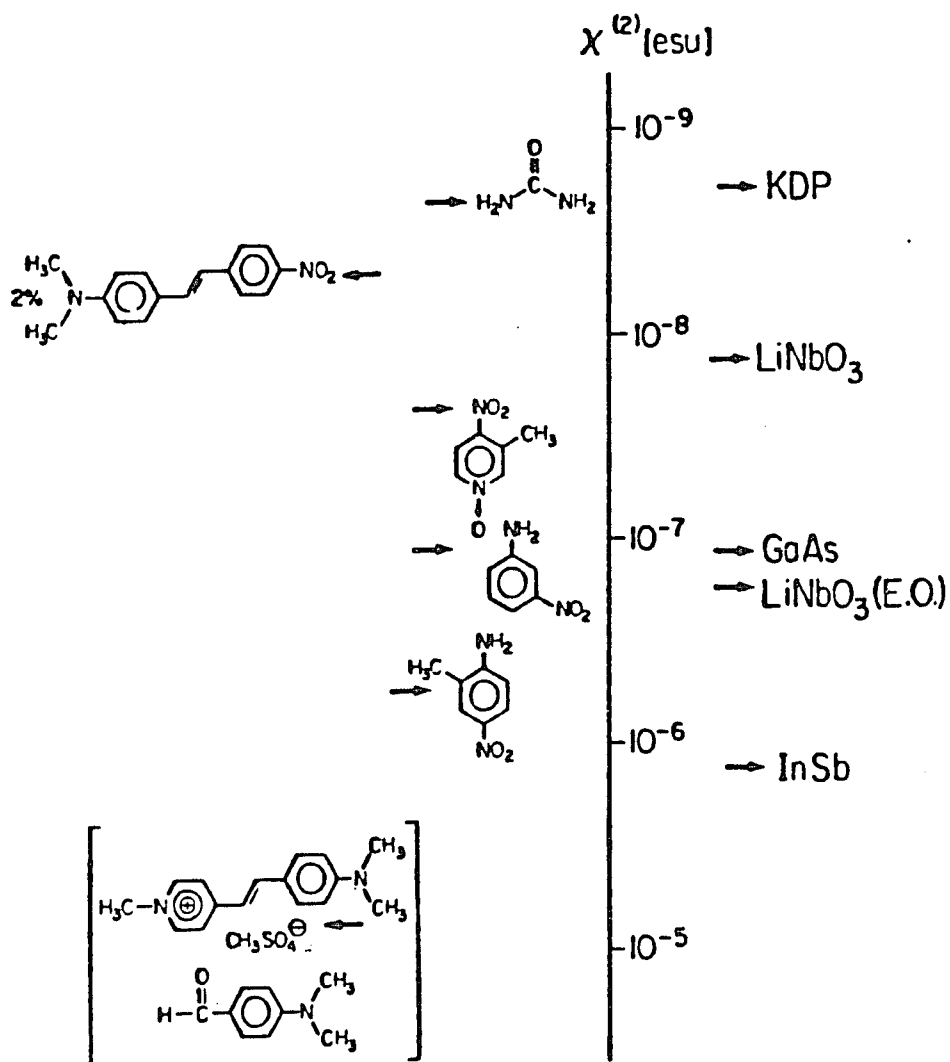
2 ($n=1, 2$, and 3)

Design of Nonlinear Optical Materials

The earliest and still the most commonly used materials for second order responses are crystals. Very large, single crystals are grown and cut to the proper dimensions for NLO experiments and devices.⁶ The most commonly used materials are the inorganic crystals, lithium niobate (LiNbO_3) and gallium arsenide (GaAs). Other inorganic crystals used include ammonium dihydrogen phosphate (ADP) and potassium dihydrogen phosphate (KDP).

The discovery that organic crystals could surpass the inorganic materials generated much research, since the organic disciplines were better understood and more well defined. Organic crystals such as 2-methyl-4-nitroaniline and 2-(N-prolinol)-5-nitropyridine have second order susceptibilities which are greater than GaAs or LiNbO_3 (see Scheme 3).²⁰ Organic materials also offer faster response times than inorganic materials,³ and provide greater design flexibility.⁴

While crystals are currently the best materials available, there are many problems associated with them. The major challenge is the fabrication of a large, defect-free crystal. There are organic crystals



Scheme 3. Second Order Susceptibilities of Various Compounds.

with high second order susceptibilities, but they are not as commonly used as LiNbO_3 , primarily because of fabrication difficulties. Another problem associated with all crystals is processing them into a useful form. A crystal can be cut, but production of thin films and irregular shapes is quite difficult. Thus, there are limitations to the optical devices which can be built and studied.

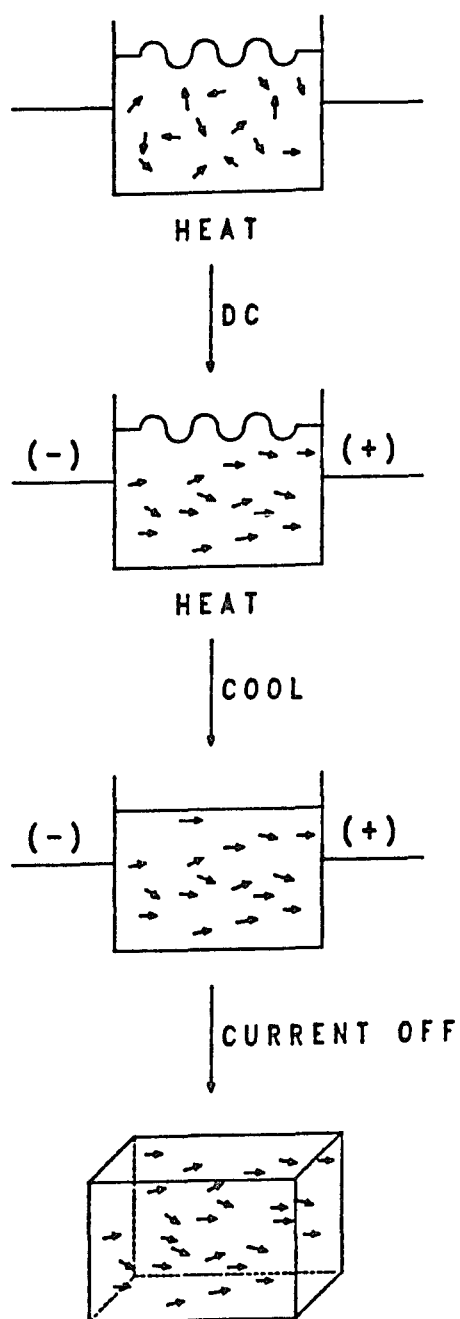
Another significant problem is the limited ability to predict if a molecule with a high β can be grown into a noncentrosymmetric crystal. For example, *p*-nitroaniline (**1**) has a high second order hyperpolarizability ($\beta^{1064\text{nm}} = 34.5 \times 10^{-30}$ esu), but a crystal of **1** has a second order susceptibility of zero. This results because **1** forms a centrosymmetric crystal, a trait common to most strongly dipolar organic molecules. Itoh *et al.*²³ have used CNDO/S3-CI calculations to obtain some predictive capability for the potential crystal structure of molecules. However, most methods for obtaining acentric crystals involve more conventional methods: use of chirality,²⁴ asymmetric hydrogen bonding,²⁵ molecules with smaller ground state dipoles,²⁶ and varying the anions in organic salts.²⁷ However, even if science reaches the point where crystals with the correct packing can be found easily, there still remain the inherent problems of crystal growth and device fabrication.

Due to the difficulties associated with crystalline materials, many researchers have turned to developing composite materials. Normally, these composite materials consist of an NLO chromophore dissolved in a polymer matrix, although inorganic hosts have also been utilized.²⁸ The lure of polymer composites (and polymers) is strong. These materials offer potentially large $\chi^{(2)}$'s, perhaps even larger than crystals,²⁰ and they offer high transparencies. Polymers offer great advantages in synthesizing the NLO material over crystal growth. Additionally, device fabrication should be much simpler with a processable polymer. And, of course, organic polymers possess the other desirable properties mentioned earlier for organic systems.

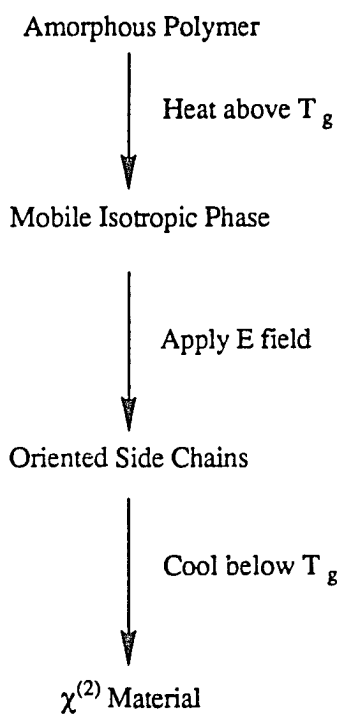
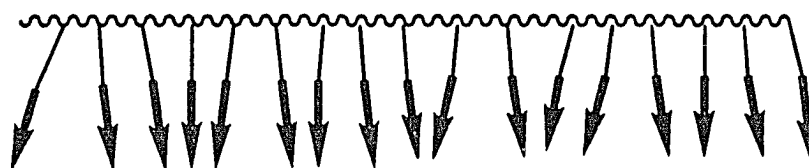
Early work in NLO polymeric materials centered on the host/chromophore systems.^{29,30} For example, as little as a 2% solution of 4-

dimethylamino-4'-nitrostilbene in a polymer host showed a $\chi^{(2)}$ higher than KDP (see Scheme 3).³¹ In this strategy, the materials are made by dissolving the chromophore in a polymer host (usually polymethyl methacrylate-PMMA) which is above its glass transition. Next, an electric potential is applied (10 KV/cm), which aligns the dipolar chromophores in one direction. The solution is then cooled down (with the potential still applied) to below the polymer's glass transition. The electrodes can then be removed and the $\chi^{(2)}$ material evaluated (see Scheme 4). While this concept seemed ideal, there are two major disadvantages. First, it is difficult to dissolve a high concentration of very polar chromophoric units into the relatively nonpolar polymer hosts. The second, and most devastating flaw, is that the chromophores are not truly locked into alignment. Typically, these materials show high $\chi^{(2)}$'s for only several months. There is enough molecular freedom to allow the chromophores to relax out of their imposed acentric alignment into an isotropic mixture. Isotropic mixtures, like centrosymmetric crystals, have $\chi^{(2)}$'s of zero. While this polymer matrix proved useless for providing materials for devices, the technique is still used to evaluate the NLO efficiencies of molecules.

The next generation of polymeric NLO materials were comb polymers, in which the NLO chromophore is a pendant attached to a polymer backbone (see Scheme 5). This concept increases the density of NLO units, because the chromophores are part of the polymer and they can not come out of solution. Also, tethering the chromophore to a polymer backbone should afford greater stability of the $\chi^{(2)}$ properties over time. The material production is similar to that of the polymer matrix: heat to amorphous melt, apply a potential, and cool. Unfortunately, these materials, like the polymer composites, lost second order susceptibilities over time.³² The latter observation seems to be due to two factors. First, it has been observed that increasing the spacer length between the polymer backbone and NLO unit speeds the rate of $\chi^{(2)}$ decay.³³ This is probably due to the unfavorable positioning of the dipoles parallel to each other. The second reason for the decay is theorized to be the possibility that the "teeth" of the comb polymer tend to mesh together to form the more favorable situation in which the

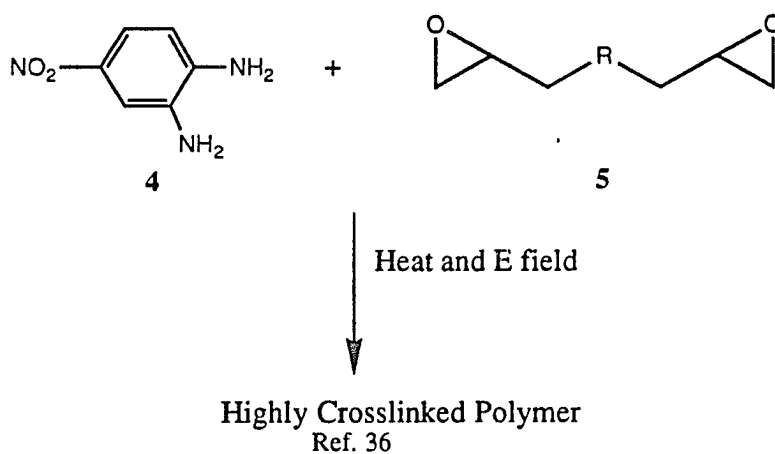
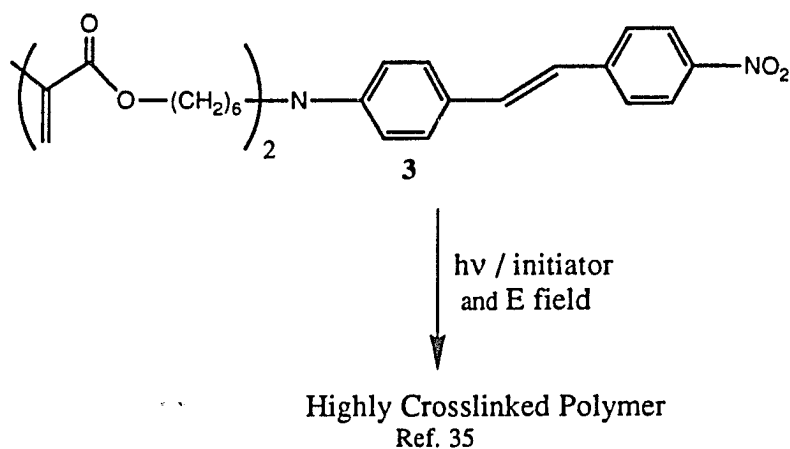


Scheme 4. Poling Process to Produce NLO Polymer Matrix.



Scheme 5. NLO Comb Polymer and Poling Technique.

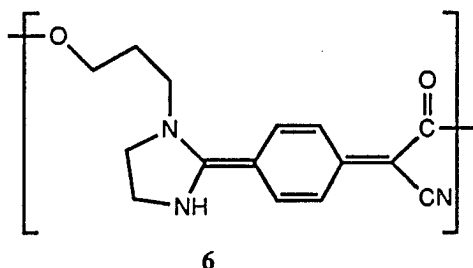
dipolar chromophores are parallel and opposing.³⁴ There have been interesting attempts to utilize crosslink curing while the electric field is applied to the comb polymers. While there is success in obtaining materials which retain adequate $\chi^{(2)}$'s over time, the degree of alignment is lower; thus, the magnitude of the susceptibilities obtained is low (see Scheme 6).^{35,36}



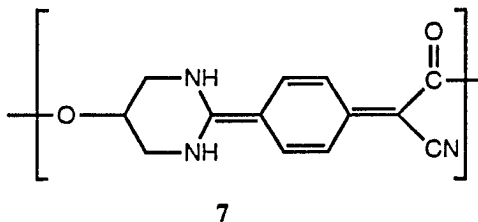
Scheme 6. Crosslinking Strategies to Form NLO Materials.

Hall, Green, Mulvaney, Noonan, and Williams were the first to attempt placing the NLO chromophores in the main chain of a polymer. Because an AB monomer can only polymerize in a head to tail fashion, it is possible to obtain a polymer chain with the dipoles all aligned in the same direction.

The first materials investigated by Hall et al. were the quinodimethane condensation polymers **6** and **7** shown in Scheme 7.³⁷ Unfortunately, the homopolymers showed no glass transitions. (A glass transition is essential, not only for processing, but also for optical clarity.) Also, the homopolymers were completely intractable. Copolymers with methyl 12-hydroxydodecanoate were tractable (soluble in hexafluoro-2-propanol and phenol/chlorobenzene), but again showed no glass transition temperatures.



and

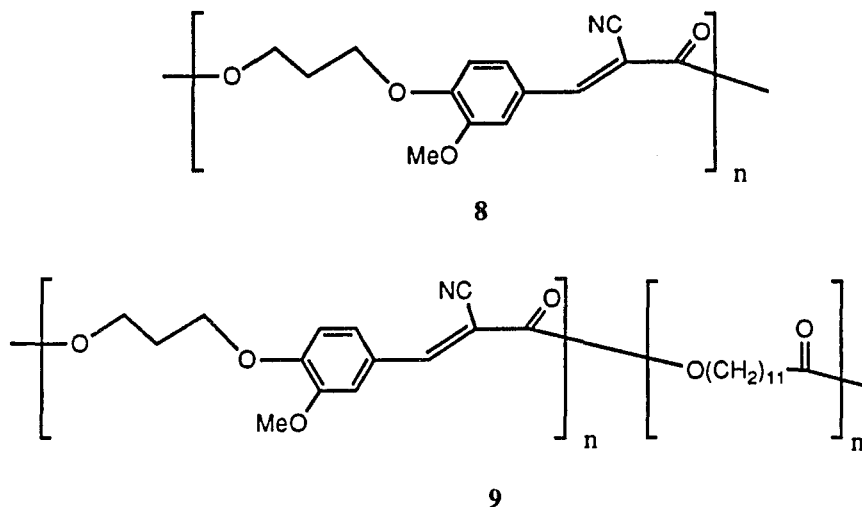


AB Polymer orients the dipoles head to tail.

Scheme 7. Early Main Chain NLO Polymers.

Attempting to obtain materials tractable in more reasonable solvents, and which possess glass transitions, Hall, Williams, and coworkers synthesized and evaluated the 4-oxy- α -cyanocinnamate homopolymers **8**

and copolymers **9** shown in Scheme 8.³⁸ The homopolymers were not tractable in reasonable solvents. However, the copolymers with methyl 12-dodecanoate were soluble in chloroform; thus, they could be



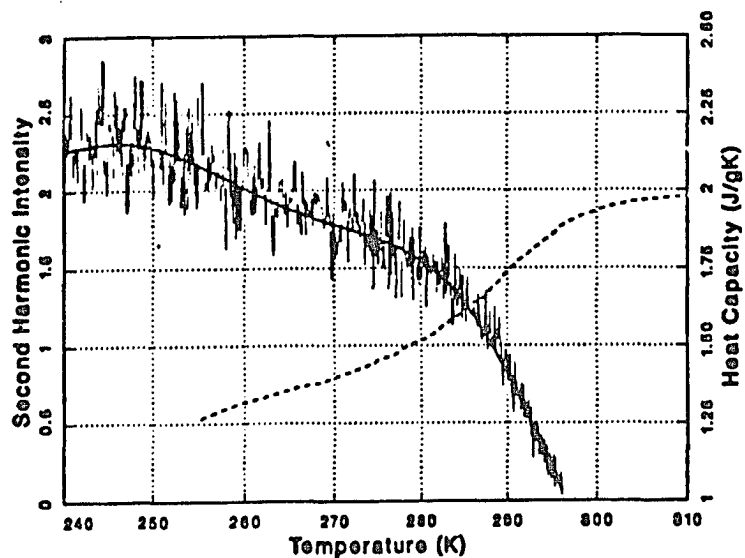
Scheme 8. α -Cinnamate Homo- and Copolymers.

evaluated for their molecular hyperpolarizability ($\mu_x\beta_x$) (see Table 3).^{39,40} The copolymer did possess a glass transition, but it was below room temperature. The low glass transition limits applications of this polymer, but low temperature poling experiments were done. There are two significant observations from this work. First, there appears to be a large enhancement in the hyperpolarizability due to the polymer structure. Table 3 shows that for polymer of MW = 17,000 there is a 15-fold enhancement, and polymer of MW = 70,000 shows a 20-fold enhancement in solution. These results are very exciting; they indicate that there is a large synergistic enhancement due to the AB copolymer structure! Unfortunately, the copolymer in the bulk poling experiments showed an absence of the enhancement. This loss is probably due to entanglement of the polymer chains, which inhibits the proper alignment. The second important result from this work is that below the copolymer's glass

transition, the second harmonic generation remained constant for several hours. This suggests that main chain NLO polymers may have the needed chronological stability. Because of the low glass transition, the second harmonic generation disappeared with heating (see Scheme 9).

Table 3. Hyperpolarizabilities of the α -Cinnamate Copolymers.

Molecular Weight, M	NLO Units (N)	$\mu_x\beta_x/N$ (10^{-48} esu)	Enhancement
Solution:			
Monomer	1	57
17,000	37	830	15
70,000	152	1140	20
Bulk:			
70,000	152	24	0.4



Scheme 9. Loss of Second Harmonic Generation (SHG) with Temperature.

The results of these latter experiments are very exciting and warrant further investigation. To this end, two projects were undertaken. The first was the synthesis and evaluation of a series of *p*-aminophenylsulfone monomers, dimers, and trimers. It was hoped that these systems would lead to a better understanding of the enhancement due to the AB polymer structure (Chapter 2). The second project focused on the synthesis of a new class of stilbene polymers, with the goal of obtaining soluble polymers with high glass transitions (T_g) (see Chapter 3).

Additional work was carried out on evaluating and improving upon a method of approximating the hyperpolarizability via spectrophotometric techniques (Chapter 4). This work was done out of the necessity of obtaining a less expensive and simpler method for evaluating molecular hyperpolarizabilities.

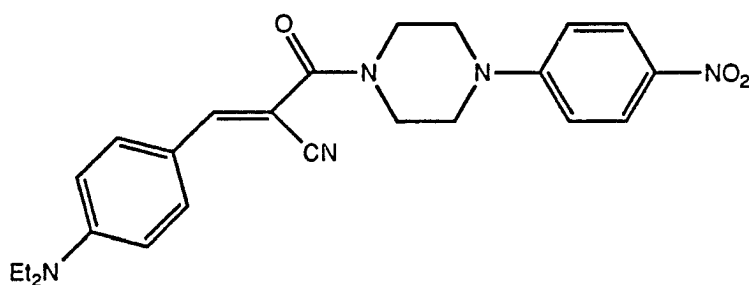
CHAPTER 2

NONLINEAR OPTICAL ENHANCEMENT STUDIES

p-Aminophenyl Sulfone Oligomers

The work by Hall *et al.* (see Chapter 1) indicated the possibility of synergistic enhancement of a molecule's hyperpolarizability (β_x), by having the organic dipole oriented in a head to tail fashion in an AB copolymer (see Introduction). While this observed enhancement remains somewhat anomalous, it suggests a potential to obtain very high second order susceptibilities (χ^2). This is a relatively new phenomenon, and consequently it has not been well studied.

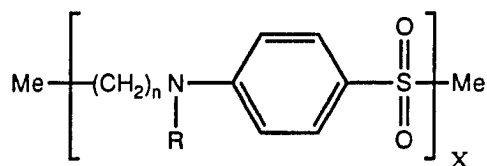
While this enhancement is anomalous, there are several other examples which add support to the validity of the results. First, there is the classic example of urea. In solution, urea has a second order hyperpolarizability of $(0.45 \pm 0.12) \times 10^{-30}$ esu. A simple additivity model would estimate the crystalline nonlinearity at 1.57×10^{-9} esu, which is somewhat lower than the experimental value of 3.4×10^{-9} esu.⁴¹ Zyss and Berthier theorize that hydrogen bonding in the crystal leads to a strong redistribution of the electron cloud, which gives rise to the enhancement in the crystal.⁴² The other example is the recent work by Katz and Schilling, involving more mainstream charge transfer organic molecules.⁴³ In their work, Katz and Schilling examined the ground state dipole moments of piperazine linked dichromophore **10**, and its individual chromophoric units.



In this work the authors claim to see an increase in dielectric orientational polarizability of between 0.5 and 2.0 Debye.

Obviously, there is a great need for more information concerning this NLO enhancement. The purpose of this work was to attempt to analyze the effect of having NLO-phores head to tail in an oligomeric system.

The main goal in designing the system for experimental study was to obtain homo-oligomer. *p*-Aminophenyl sulfone systems were chosen for several reasons. Copolymers always contain ambiguities concerning structure along the polymer chain. Thus, it is not known the degree to which the copolymer has alternating units. Also of prime importance was the need to form a tractable system. The homopolymers of the 4-oxy- α -cinnamates were all insoluble in reasonable solvents, such as chloroform, which are used to measure the hyperpolarizability (see Chapter 1). Finally, the target oligomers should be such that their synthesis would allow for construction with various spacer groups. The term oligomers refers to a wide range of degrees of polymerization. In this work it was desired to have very well defined small oligomers, i.e. monomers, dimers and trimers. It was believed that the *p*-aminophenyl sulfones **11** embodied all these characteristics.



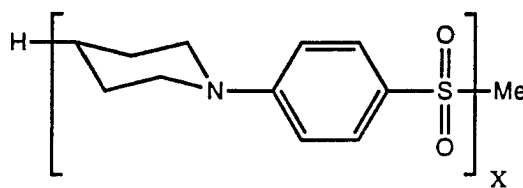
X=1, 2, or 3 ; n=2 or 6

11

Using retrosynthetic design it was possible to derive various monomers which would give homopolymer, as well as various spacer linkages. It was believed that the highly polarizable sulfone group would aid in the formation of soluble oligomers. Also, appendages on the amine group could be varied, if needed, to aid in the formation of tractable systems. Small oligomers could be prepared by either performing an oligomerization,

and separating out the desired small oligomers, or by constructing the small oligomers piece by piece.

The syntheses became the major task of this project. Once made, the oligomers would be evaluated for their NLO activity and, it was hoped, would show a chromophoric enhancement. Ideally, the second order hyperpolarizability of the trimer divided by three would be greater than that of the dimer divided by two. Additionally, the hyperpolarizability per unit of the dimer should be greater than that of the monomer. Also, it was expected that increasing spacer length would decrease any enhancement. A rigid spacer would be expected to increase enhancement because it would prevent rotations to unfavorable conformations. Thus, the 4-substituted piperidine linkage as in **12** was chosen.



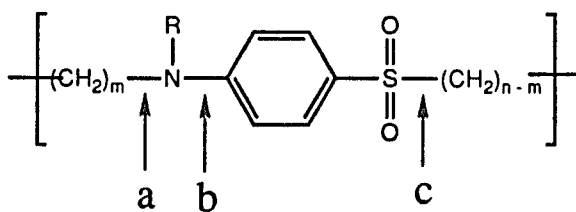
X=1, 2, or 3

12

These systems (dimethylene, hexamethylene, and piperidine spaced oligomers) became the targets to be synthesized and evaluated.

Retrosynthesis

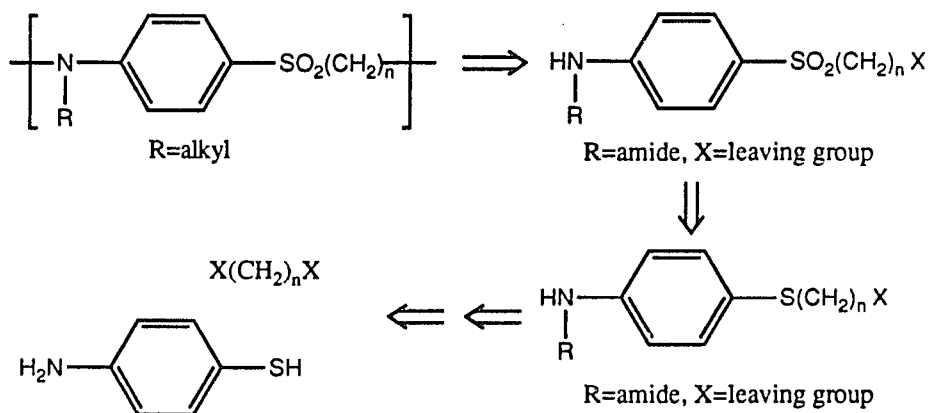
For the dimethylene and hexamethylene spaced oligomers, the three reasonable disconnections are shown on structure **13**.



13

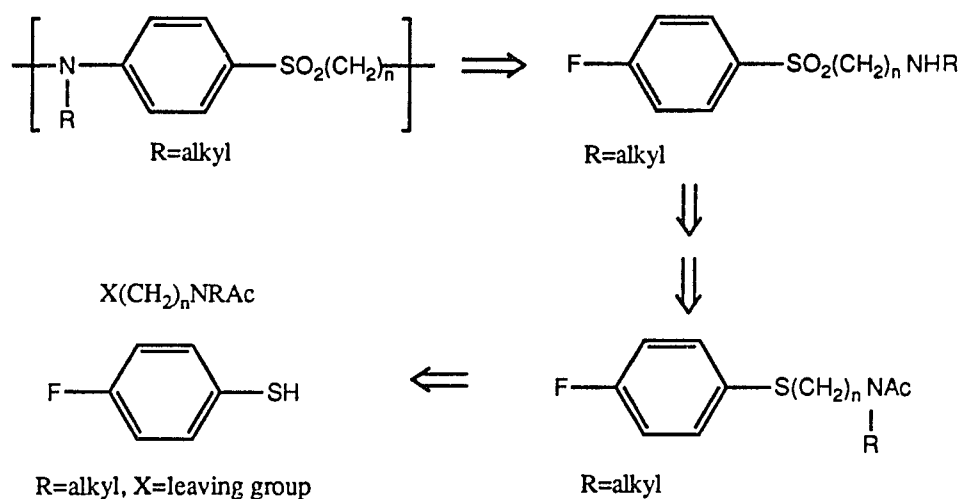
Bond a could be created by an N-alkylation reaction. Bond b could be formed by nucleophilic aromatic substitution, and bond c could be produced from an S-alkylation reaction, probably coming from the more nucleophilic sulfide rather than the sulfinate.

Disconnecting bond a affords the desired AB monomer (see Scheme 10). Because there was a risk of the amine oversubstituting to form a quaternary ammonium salt, it was decided to connect bond a from the amide. This had the additional advantage that because the amide would also serve to protect the amine, since the sulfone would be synthesized by an oxidation. Doing this retro-oxidation left an ω -(leaving group) sulfide. It was apparent that this sulfide could be readily obtained from the commercially available *p*-aminothiophenol.



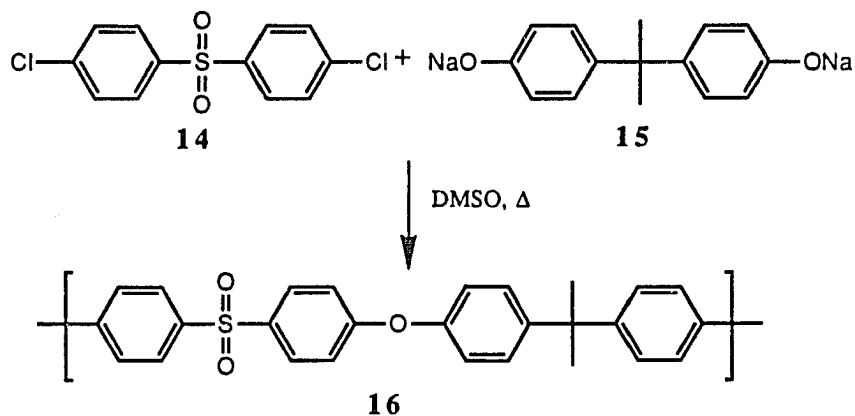
Scheme 10. Retrosynthesis of *p*-Aminophenyl Sulfones via Bond a.

Disconnection at bond **b** yielded a *p*-fluorophenyl sulfone; fluorine was chosen because it is an excellent leaving group in nucleophilic aromatic substitution reactions (see Scheme 11). It was believed that this method would work very well for the piperidine spaced systems because piperidine is an excellent nucleophile in these substitution reactions. The sulfone in this AB monomer would come from the sulfide, requiring protection of the amine as the amide. Disconnecting at the alkyl sulfide bond would leave the sulfide and ω -substituted amine, both of which could be derived from commercially available compounds.



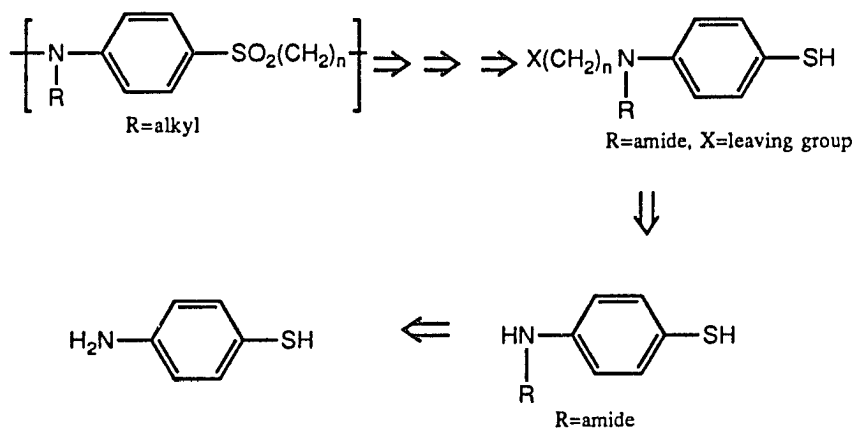
Scheme 11. Retrosynthesis of *p*-Aminophenyl Sulfones via Bond **b**.

This chemistry should be useful for polymerizations as well, since the synthesis of polymers by nucleophilic aromatic substitution is well known for the synthesis of polyarylether sulfones **16** (see Scheme 12).⁴⁴⁻⁴⁷



Scheme 12. Polysulfone Synthesis.

As mentioned previously, bond **c** could be derived from a sulfide substitution (see Scheme 13). Substitutions by sulfinates are known, but these reactions are usually difficult and low yielding. So, as with the other disconnections, the amine would be protected as the amide. The AB monomer then becomes a *N*-(ω -halo)-*p*-amide thiophenol. This monomer could in turn come from a commercially available *p*-amino thiophenol.

Scheme 13. Retrosynthesis of *p*-Aminophenyl Sulfones via Bond **c**.

In practice, all three of the synthetic routes derived were used, each having its own advantages and disadvantages. The hexamethylene spaced oligomer was easily prepared by the formation of bond a. It was attempted to conduct analogous chemistry to make the dimethylene spaced oligomers. However, the β -(leaving group) sulfones readily eliminated to form α,β -unsaturated sulfones. Attempts to synthesize the dimethylene spaced oligomers by the formation of bond b also failed; the amine was not nucleophilic enough. However, a variation of the formation of bond c synthesis worked very well to give the dimethylene spaced oligomers, while the piperidine spaced oligomers were best prepared by the connection at bond b.

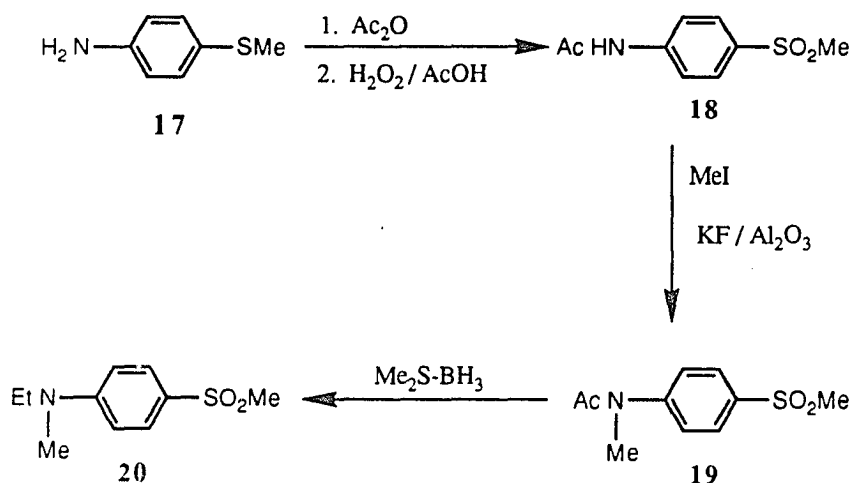
The trials and nuances of each of these syntheses will be discussed in the next section.

Synthesis

Monomer analogue synthesis

The synthesis of the monomeric analogue 20 was done more for modeling the synthesis than to obtain the monomeric analogue (see Scheme 14). A monomer analogue was made in one step from N,N-dimethyl trimethylsilyl amine (Aldrich) and *p*-fluorophenyl methyl sulfone. Dissolving these reactants in N,N-dimethylformamide (DMF) with a catalytic amount of cesium fluoride gave the monomeric unit in good yield. This procedure was performed by Mr. Tomida of these laboratories, and it is representative of formation via the nucleophilic aromatic substitution route. The reaction works well, but there is a mechanistic question as to whether the dimethylamino group comes exclusively from the silyl reagent or from the DMF. The other synthesis for the monomeric unit was designed to model the oligomer synthesis by the formation of the alkyl amine bond (route a). 4-(Methylmercapto)aniline 17 was protected as the acetamide, and then oxidized to the sulfone 18⁴⁸ in one flask in good yield. In the synthesis of an AB monomer, an ω -halo alkyl substituent attached to a sulfide would replace the methyl group. The amide was then N-methylated using 40% potassium fluoride supported on neutral alumina substrate, and

methyl iodide, in acetonitrile.^{49,50} These conditions are relatively mild compared to other methods of N-alkylation, and the potassium fluoride reagent generally affords higher yields. Compound **19** was obtained in 95% yield. The potassium fluoride reagent was prepared as described by Ando and Yamawaki;^{49,50} however, it is commercially available from Aldrich Chemical Company. The desired monomeric analogue **20** was prepared by a borane reduction in high yield.⁵¹ The overall yield for the four step monomer unit synthesis was 60%.



Scheme 14. Monomer Analogue Synthesis.

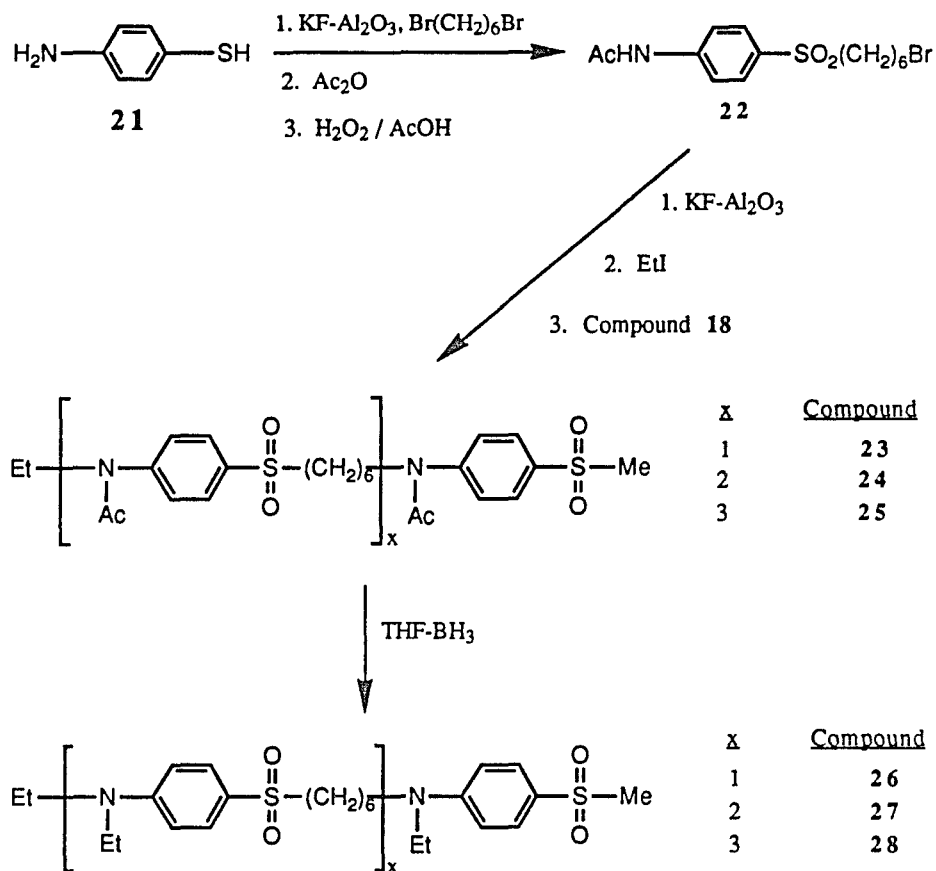
Oligomers with Hexamethylene Spacers Using Route a

The syntheses of the oligomers with hexamethylene spacers were accomplished using chemistry very similar to the monomeric modeling synthesis (see Scheme 15). *p*-Aminothiophenol (Aldrich) was reacted with a large excess of 1,6-dibromohexane, using the same potassium fluoride reagent that was used for the N-alkylation of amides.⁴⁹ After removal of the potassium fluoride reagent by filtration, acetic anhydride was added. Fortunately, the disubstituted hexane byproduct, 1,6-di(*p*-acetanilide mercapto) hexane, precipitated as the diamide, and the excess 1,6-dibromohexane could be removed by extraction with pentane. After the

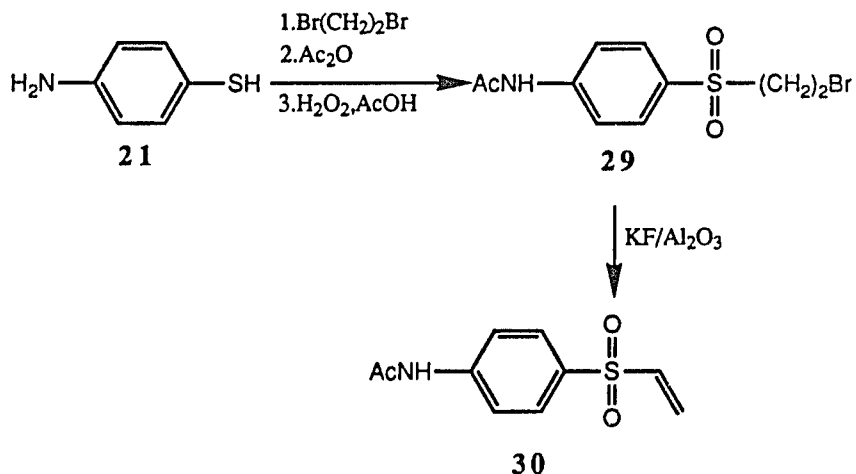
acetic acid/hydrogen peroxide oxidation to the sulfone, the desired AB monomer **22** was obtained in 37% yield over the three steps. The yield was not higher due to the formation of the disubstituted hexane byproduct, however, the 37% yield is still reasonable over three steps. Compound **22** is the AB monomer, which upon oligomerization condensed an equivalent of hydrogen bromide. The oligomerization was carried out by adding potassium fluoride reagent to a solution of the monomer. The formation of monomer, dimer, trimer, etc. was observed by TLC. After eleven hours, it appeared that the reaction had progressed enough, and a large excess of ethyl iodide was added to cap the amide ends of the molecules. After sufficient time had elapsed to complete the N-ethylations, the potassium fluoride reagent was filtered, and the solvent and excess ethyl iodide were evaporated. Without purification, more solvent, potassium fluoride reagent, and an excess of compound **18** were added to terminate the alkyl ends of the oligomers. When this final step was complete a mixture of the desired oligomers was obtained. Each of the oligomers (**23** - **25**) could then be isolated in pure form via column chromatography. The chromatographic separation was somewhat laborious, but very effective. Once the di, tri, and tetra-amides (**23** - **25**, respectively) were isolated, they were individually reduced with tetrahydrofuran/borane complex to give the desired oligomers (**26** - **28**). This method proved to be simpler than the dimethylsulfide/borane reduction used for the monomer analogues, and gave equally good yields. This synthesis worked well to give reasonable yields of the desired hexamethylene spaced oligomers.

Attempts to Make Oligomers with Short Spacers by Route a

In light of the success of this synthesis for the hexamethylene spaced oligomers, the same chemistry was utilized in an attempt to produce the dimethylene spaced oligomers. The (*p*-acetanilide) β -bromoethylsulfone **29** was synthesized in the same manner as compound **22**. However, this β -bromosulfone readily eliminated hydrogen bromide under the basic oligomerization conditions of the reaction to give the α,β -unsaturated sulfone **30** (see Scheme 16).

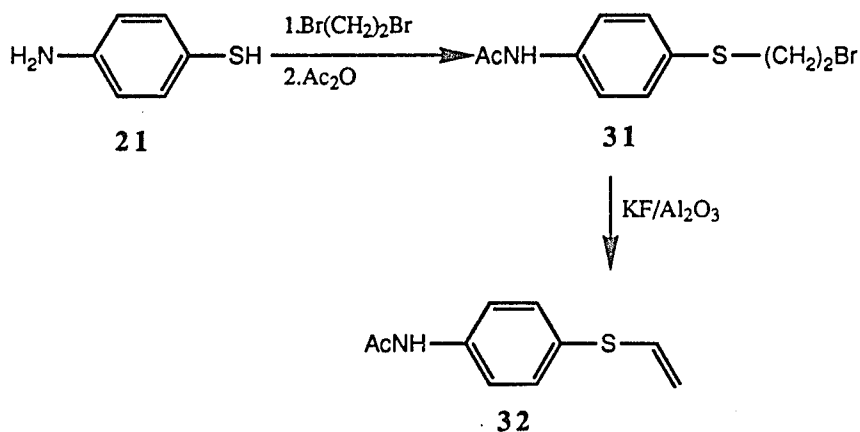


Scheme 15. Synthesis of the Hexamethylene Spaced *p*-Aminophenyl Sulfone Oligomers.



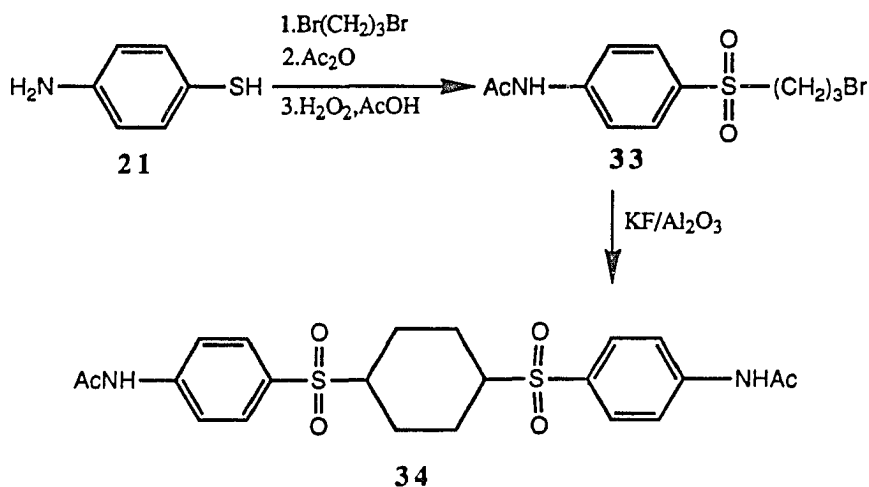
Scheme 16. Synthesis of the α,β -Unsaturated Sulfone **30**.

In retrospect, this was not surprising, and might have been predicted. Looking at the precursor of the sulfone, *p*-(2-bromo-1-ethylmercapto)-acetanilide **31**, offered an alternative route. A bromine two carbons away from a mercaptan should be an excellent leaving group. But once again, the major product resulted from an elimination to give the vinyl sulfide **32** (see Scheme 17).



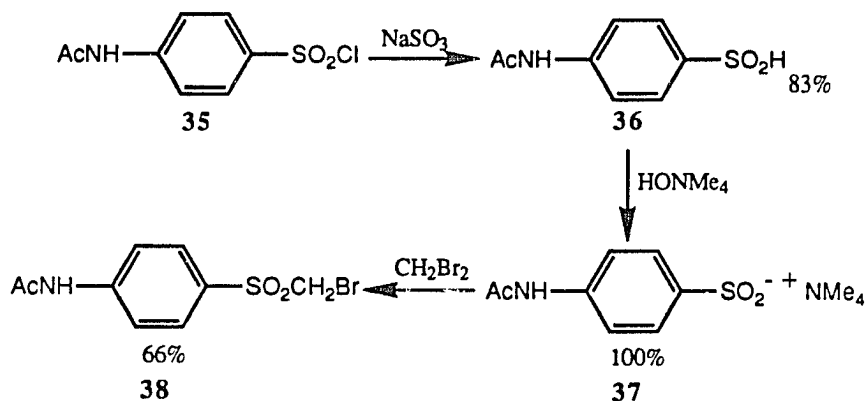
Scheme 17. Synthesis of the Vinyl Sulfide **32**.

Due to the difficulties encountered in the synthesis of the dimethylene spaced oligomers, we decided to turn instead to the trimethylene spaced series. Use of the same synthetic route gave the trimethylene monomer in good yield. Interestingly, when treated with the potassium fluoride reagent, the major product isolated was a 1,4-disubstituted cyclohexane **34** (see Scheme 18).



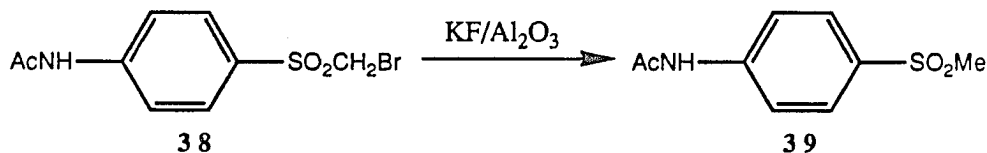
Scheme 18. Synthesis of the 1,4-Disubstituted Cyclohexane **34**.

We also attempted to synthesize the monomethylene spaced oligomers. In this case, the monomer **38** was produced by nucleophilic attack by the sulfinate (see Scheme 19).



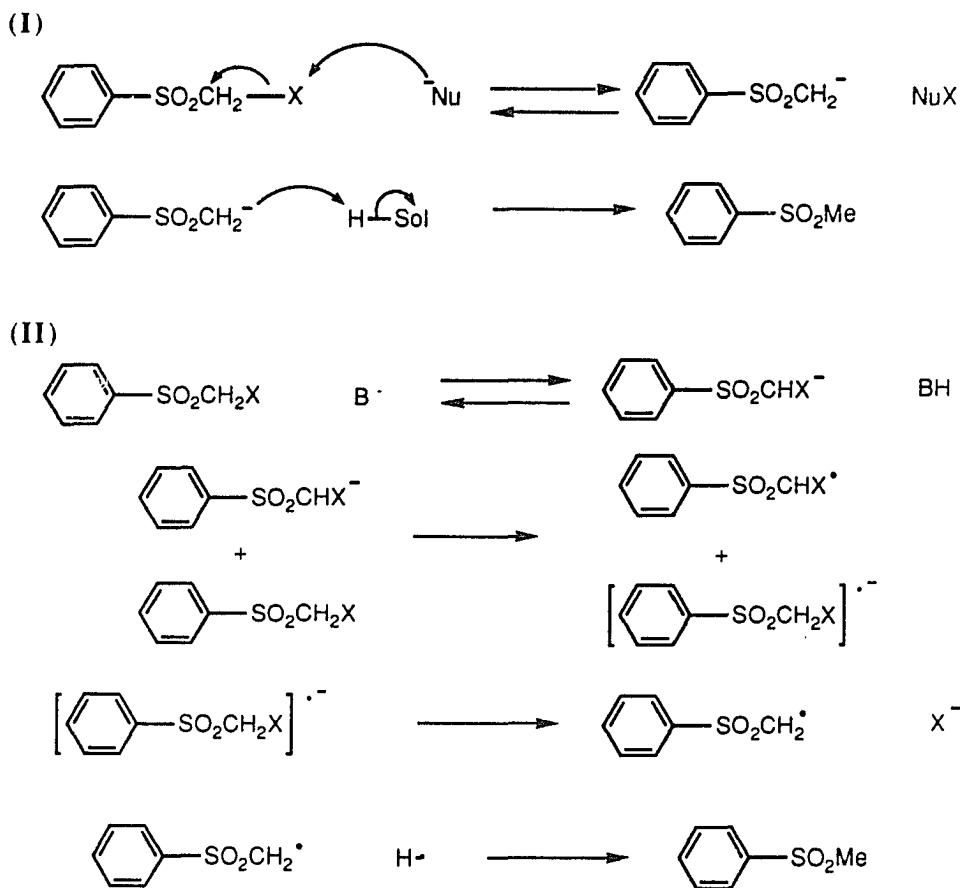
Scheme 19. Synthesis of the Monomethylene Monomer.

This monomer was then treated with the potassium fluoride/alumina reagent which interestingly reduced the bromomethyl sulfone to the methyl sulfone **39** (see Scheme 20).



Scheme 20. Reduction of Monomer **38**.

These reductive dehalogenations have recently been studied by Paradisi *et al.*⁵² Two possible mechanisms have been proposed, one involving nucleophilic attack at the halogen to give a carbanion which can pick up a proton (I), and the second involving a radical anion intermediate (II).



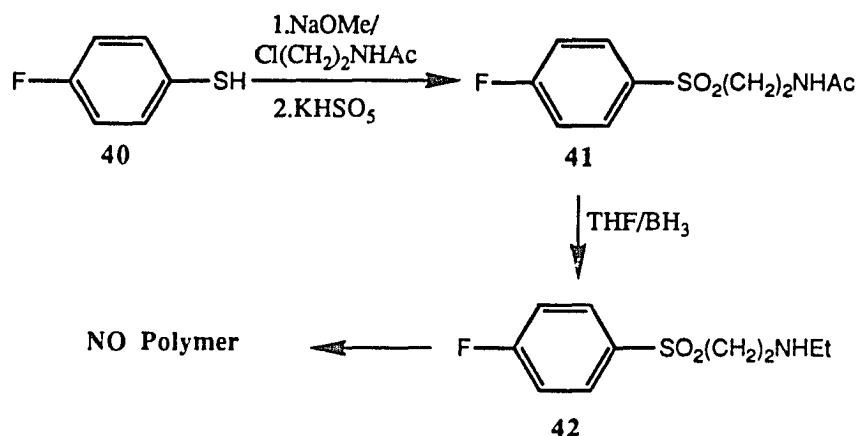
Scheme 21. Possible Mechanisms for Monomethylene Monomer Reduction.

While all of these unwanted reactions were educational, they failed to supply the desired oligomers.

Oligomers with Dimethylene Spacers by Route c

We then moved to the nucleophilic aromatic substitution reaction (see Scheme 22). The monomer was synthesized by reacting *p*-fluorothiophenol (**40**, Aldrich) with *N*-(2-chloroethyl)acetamide (Aldrich) in refluxing sodium methoxide, followed by oxidation with potassium hydrogen persulfate (OXONE).^{53,54} The amide **41** was then reduced using

THF/borane solution to the secondary amine **42**, the AB monomer which upon condensation would liberate a molecule of hydrogen fluoride.

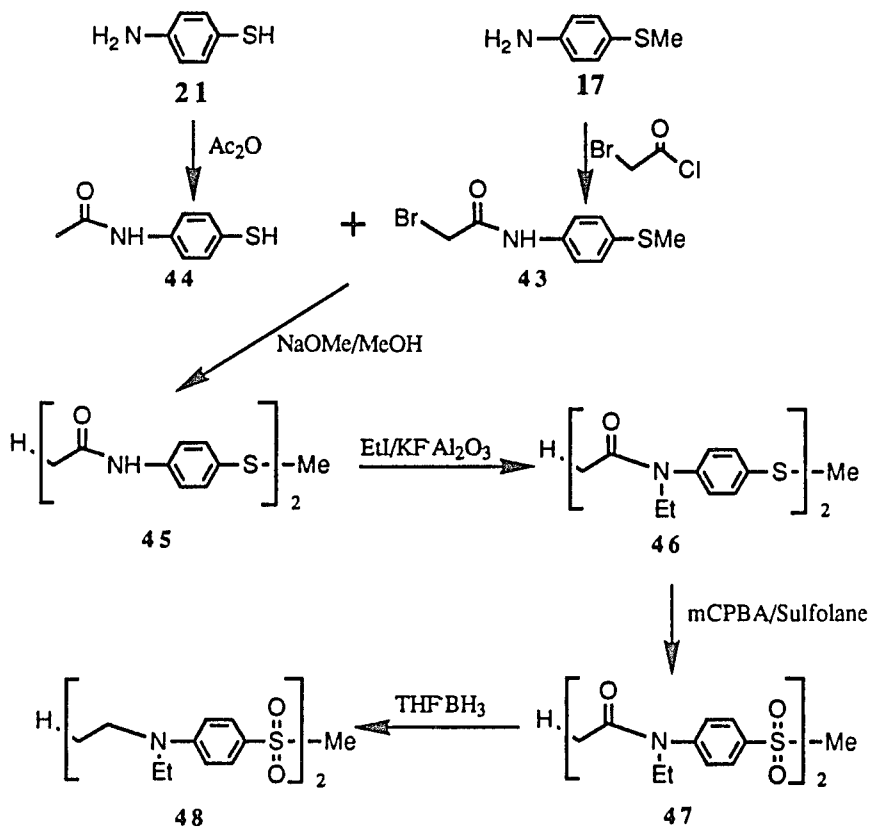


Scheme 22. Attempted Oligomer Synthesis via Nucleophilic Aromatic Substitution.

Unfortunately, all attempts at performing the polycondensations failed or gave ambiguous results. Increasing the temperature and reaction times led only to decomposition. The trimethylsilyl derivative of amine **42** was formed,^{55,56} in hopes that treatment with cesium fluoride would lead to oligomer, but this was also unsuccessful. It was apparent that this secondary "diethyl" amine **42** was not a strong enough nucleophile to successfully carry out this transformation. In an analogous situation, similar reactivities were observed: reactions of 4'-carbomethoxy-4-methoxy- α '-cyano- α -chlorostilbene with both dimethylamine and piperidine proceeded smoothly, while similar reaction with diethylamine gave none of the desired enamine (see Chapter 3).

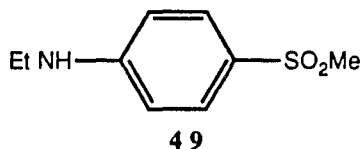
The desired dimethylene spaced dimer was ultimately prepared via an S-alkylation route (see Scheme 23). The key to the success of this synthetic scheme was the realization that the aniline moiety could be protected and set up for dimerization in one step. To do this, α -bromoacetyl chloride was used to protect *p*-(methylmercapto)aniline (**17**). The resulting α -bromoacetamide **43** was obtained in good yield. The other half of the dimer

came from the protection of *p*-aminothiophenol (**21**) as the acetamide **44**, in excellent yield. These two halves were coupled by using sodium methoxide to generate the sulfide anion of **44**. This then gave the basic dimer skeleton **45**, which could be converted to the desired dimethylene spaced dimer **48**. First, the dimer is di-*N*-ethylated using the now standard potassium fluoride/alumina conditions, in decent yield, to give **46**. The mercapto portions of the dimer were then oxidized to sulfone **47** in excellent yield using *m*-chloroperbenzoic acid (*m*-CPBA) in tetramethylene sulfone (Sulfolane).⁵⁷ Sulfolane was chosen because **46** was not readily soluble in more common solvents. Finally, the dimethylene spaced oligomer **48** was obtained under the standard THF/borane reduction conditions.



Scheme 23. Dimethylene Spaced Dimer Synthesis.

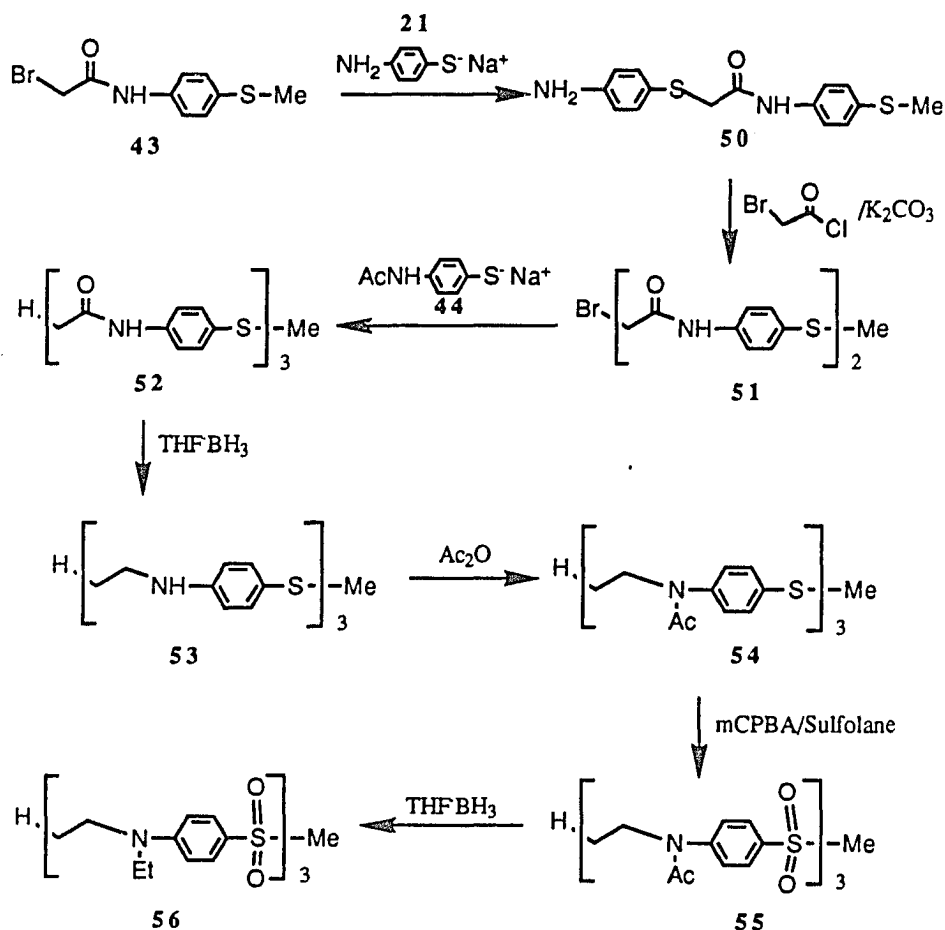
The yield of the final reduction was only 44%, with the major isolated byproduct being *p*-N-ethylaminophenyl methyl sulfone **49**.



Apparently the sulfone alpha to the carbonyl was facilitating degradation of the dimer. This would prove to be a problem in the trimer synthesis. However, the 22% yield of dimer **48** over all six steps was certainly adequate.

The dimethylene spaced trimer (see Scheme 24) was synthesized using a reaction sequence similar to that for the dimer. Generating sodium *p*-aminothiophenolate (**21**) from the thiophenol and sodium methoxide followed by addition of **43** afforded **50** in good yield. Compound **50** is an amine terminated dimer which could be converted to the trimer skeleton in two steps. First, protection of the amine with α -bromoacetyl chloride gave the α -bromoamide **51** in good yield. Compound **51** was then reacted with the sodium salt of **44** to give the basic trimer framework **52**. Originally, the dimethylene spaced trimer **56** was synthesized from **52** in three steps, just as the dimer **48** was synthesized from **45**. While it is true that the shortest distance between two points is a straight line, it is not always the easiest road to travel. Such was the case here; the N-alkylation of amide **52** gave only a 44% yield of the tri-N-ethylamide. Additionally, the final borane reduction gave only a 22% yield of **56** due to extensive cleavage of the trimer. Knowing that the cleavage was caused by the location of the sulfone alpha to the carbonyl, we were able to develop a better alternative. The low yielding N-ethylation was replaced by a borane reduction followed by formation of triamide **54**. The reduction of **52** to **53** went in good yield, and the reprotection of the triamine to triamide **54** proceeded in excellent yield. This sequence of reactions eliminated the need for the low yielding N-ethylation with the potassium fluoride reagent. Also, the amide protecting group was in the pendant, thus removing the problem of having the sulfone alpha to the amide. With the amine protected, compound **54** could be

oxidized to sulfone **55** using *m*-CPBA in Sulfolane, again in excellent yield. Finally, triamide sulfone **55** was reduced under standard borane conditions to dimethylene spaced trimer **56** in 75% yield. This final reduction gave a much better yield than the analogous reduction to form dimer **48** (44%). Excluding the final step, all the yields in this synthesis were greater than 85%, and the overall yield for trimer **56** was 38% over nine steps. The fact that this synthesis was very linear was compensated for by the high yields.



Scheme 24. Dimethylene Spaced Trimer Synthesis.

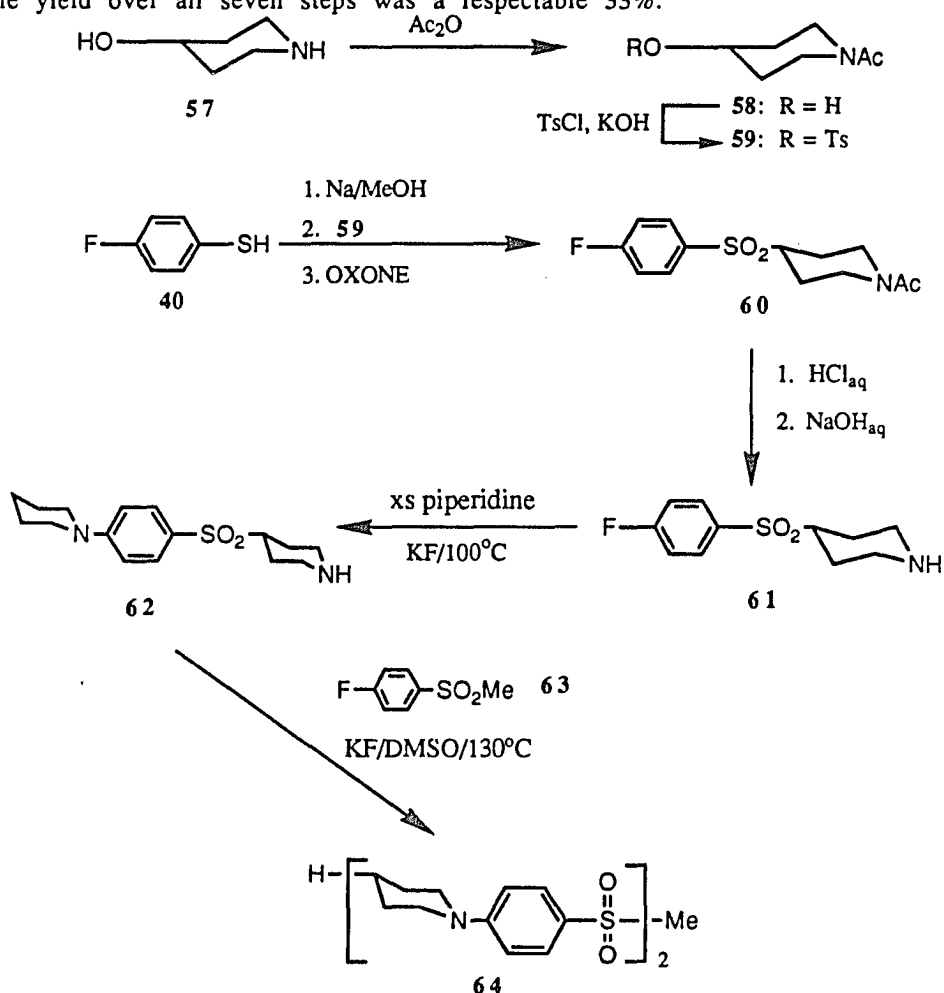
Oligomers with Piperidine Spacers by Route b

The piperidine spaced dimer (Scheme 25) and trimer (Scheme 26) were synthesized readily by nucleophilic aromatic substitution. The AB monomer **61** was made in three steps, but first the piperidine spacer had to be functionalized to protect the amine during oxidation and allow for substitution at the 4-position. These tasks were accomplished by reaction of 4-hydroxypiperidine **57** (Aldrich) with acetic anhydride. Then 4-hydroxypiperacetamide **58** was converted to tosylate **59** using *p*-toluenesulfonyl chloride in THF over potassium hydroxide. Compound **58** was produced in quantitative yield and tosylate **59** was made in 85% yield. Compound **59** was then reacted with sodium *p*-fluorothiophenolate (generated in sodium methoxide/methanol solution from **40**) to give 4-(*p*-fluorophenylmercapto)piperacetamide which was not isolated. The substitution solvent was the same as for the oxidation with OXONE (50% potassium hydrogen persulfate),⁵⁶ so a solution of the oxidizing agent was added directly when the substitution was complete. The desired sulfone **60** was synthesized in a 76% yield over two steps. The monomer **61** was then made by deprotection of the amide under standard conditions (refluxing aqueous hydrochloric acid, followed by basic workup) to give a fair yield.

Monomer **61** was oligomerized under various conditions. Typically, the monomer was dissolved in a high boiling polar solvent (DMSO or Sulfolane) and then heated at various temperatures. Anhydrous potassium fluoride (KF) was always added to absorb the hydrogen fluoride evolved, as well as act as a catalyst.⁴⁴ In all cases, cream to tan colored solids were obtained, which were only soluble in trifluoroacetic acid. Attempts to create shorter oligomers by adding piperidine and *p*-fluorophenylmethyl sulfone still did not yield soluble oligomer. Proton NMR in deuterated trifluoroacetic acid did indicate degrees of polymerization of about seven. However, these studies were abandoned because of the inability to form oligomers soluble in solvents other than trifluoroacetic acid.

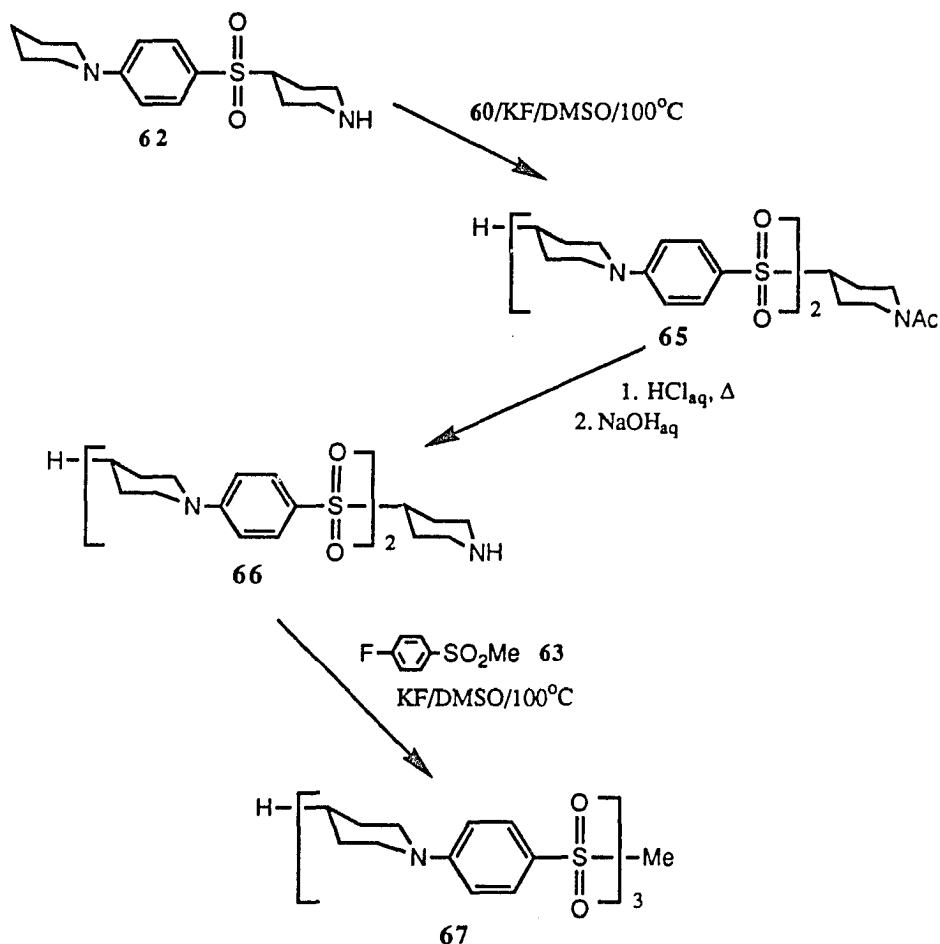
Monomer **61** was used to synthesize dimer in two steps. First, dissolving **61** in piperidine with anhydrous potassium fluoride at elevated temperatures gave a quantitative yield of the piperidine terminated

compound **62**. Compound **62** was then reacted with *p*-fluorophenylmethyl sulfone **63** in DMSO with potassium fluoride at 130°C. The piperidine spaced dimer **64** was obtained in fair yield. The compound was readily soluble in chloroform, but **64** would eventually turn pink when in contact with chloroform. This was a problem because chloroform was used in the purification. Reasoning that the color may be due to traces of HCl present in the chloroform, the pink dimer **64** was dissolved in acetonitrile and passed through basic alumina. This procedure removed the unwanted color. The yield over all seven steps was a respectable 33%.



Scheme 25. Piperidine Spaced Dimer Synthesis.

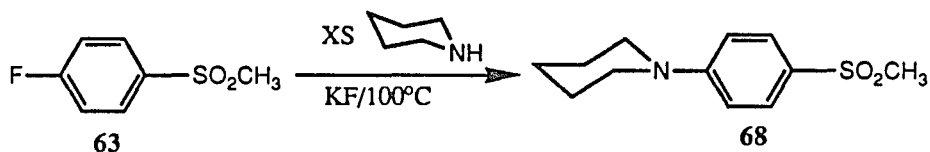
Piperidine trimer **67** was synthesized in similar fashion to dimer **64** (see Scheme 26). The piperidine terminated compound **62** was reacted with the precursor to the monomer (compound **60**) under the usual aromatic substitution conditions to give compound **65** in fair yield. This dimer with a piperamide end (**65**) could then be deprotected under standard acid catalyzed conditions to the free amine end (compound **66**) in excellent yield.



Scheme 26. Piperidine Spaced Trimer Synthesis.

Compound **66** was then reacted with *p*-fluorophenylmethyl sulfone **63** under the usual nucleophilic aromatic substitution conditions to give piperidine spaced trimer **67** in a poor yield (35%). It is not known why the final yield was so low, but it supplied enough material for the NLO studies and was therefore acceptable. The total yield from compound **62** was 25%.

Finally, the monomeric piperidine analogue **68** was easily synthesized in one step (Scheme 27). Dissolving *p*-fluorophenylmethyl sulfone **63** in piperidine and heating at 100°C with potassium fluoride gave **68** in 89% yield.



Scheme 27. Piperidine Monomer Analogue Synthesis.

All of the compounds synthesized were purified by either chromatography or recrystallization. The compounds were characterized by proton and carbon NMR and infrared spectroscopies.

Measurements and Discussion

Ground State Dipole Moments of Hexamethylene Spaced Oligomers

Seeking to establish possible cooperative effects, the ground state dipole moments of the hexamethylene spaced oligomers were measured by our collaborators at Eastman Kodak in Rochester, New York. The results are listed in Table 4.

Table 4. Ground State Dipole Moments of Hexamethylene Spaced Oligomers.

<u>Compound</u>	<u>$\Delta\mu$ (D \pm 0.7)</u>
Monomer (20)	7.7
Hexamethylene Dimer (26)	7.2
<u>Hexamethylene Trimer (27)</u>	<u>7.3</u>

The results in Table 4 are all within experimental error of each other. The hyperpolarizability (β_x) is not directly proportional to the ground state dipole moment, but from Equation 2 (Chapter 1), it is obvious that the hyperpolarizability is proportional to the difference between the ground state and excited state dipole moments. A perturbation which would cause a shift, or increase, in the hyperpolarizability would also effect a shift or increase in the molecular dipolarizability ($\Delta\mu$). Finally, an increase in the dipolarizability ($\Delta\mu$) would probably involve a disproportional increase in both the ground state and excited state dipole moments. That is, the ground state dipole would experience an increase that was not as large as the increase in the excited state dipole. Thus, ground state dipoles may indicate the possibility of an enhancement in the hyperpolarizability. Also, the ground state dipole moment provides a method for evaluating molecular orientation in solution. For example, if the dipole moments are viewed as vectors, then the dimer can be written as a vector sum. The dimer, if rigidly oriented head to tail, would have a vector sum of 15.4 ± 1.4 D.

$$\begin{array}{c} 7.7 \text{ D} \quad 7.7 \text{ D} \\ \longrightarrow \quad \longrightarrow \end{array} = \begin{array}{c} 15.4 \text{ D} \\ \longrightarrow \end{array}$$

And if the vectors of the dimer were perpendicular to each other then the vector sum would be $10.9 \pm 1 \text{ D}$.

$$\begin{array}{c} 7.7 \text{ D} \\ \longrightarrow \\ 7.7 \text{ D} \\ \uparrow \end{array} = \begin{array}{c} 10.9 \text{ D} \\ \nearrow \end{array}$$

That the dimer and the trimer have dipole moments within experimental error of the monomer indicates that the dipoles in these oligomers are completely decoupled from each other. The dipoles in the dimer and trimer act as if they were free monomers in solution. Additionally, if there is no enhancement in the ground state then no enhancement in the hyperpolarizability would be expected. Therefore, these oligomers were not studied further by EFISH.

It should be noted that the possibility exists that a system which shows no change in the ground state dipole moment may have an increase in the hyperpolarizability. If the excited states are perturbed, while there is little or no change in the ground state dipole, a change in the hyperpolarizability would occur. Interestingly, in principle, it is possible to increase the hyperpolarizability by lowering the ground state dipole without changing the excited state dipoles.

The result that there is no interaction between the chromophores in the dimer and trimer is not surprising. It has been well established that the synthesis of polymers with liquid crystal pendants usually requires a six to eight carbon spacer between the polymer backbone and the liquid crystal moiety. Without the long spacer the liquid crystal moiety is not sufficiently decoupled from the polymer chain to act as a mesogen.⁵⁸

Hyperpolarizabilities of Dimethylene Spaced Oligomers by EFISH

The second order hyperpolarizabilities of the dimethylene spaced oligomers were determined by the EFISH method by our collaborators at Eastman Kodak Company. The values obtained are reported in Table 5 as the quantity $\mu\beta$ (ground state dipole and hyperpolarizability product).

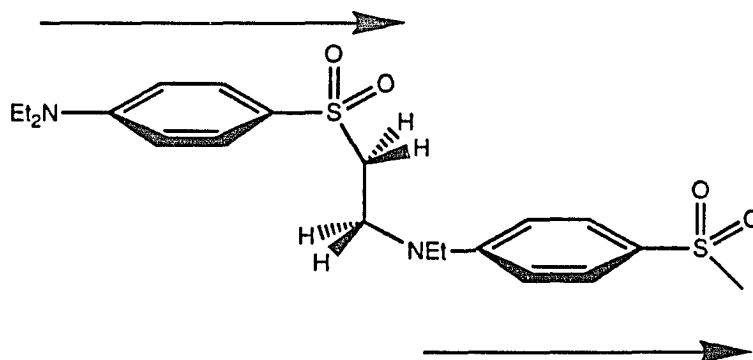
Table 5. Hyperpolarizabilities of the Dimethylene Spaced Oligomers.

<u>Compound</u>	<u>$\mu\beta$ ($\times 10^{-48}\text{esu}$)</u>	<u>$\mu\beta/\text{Unit}$ ($\times 10^{-48}\text{esu}$)</u>
Monomer (20)	26	26
Dimethylene Dimer (48)	66	33
Dimethylene Trimer (56)	69	23

The values of most interest are the unitized quantities ($\mu\beta/\text{chromophore}$). The results obtained show that the hyperpolarizabilities per NLO unit are all the same, within experimental error. These results are very unexpected, especially in light of the fact that the α -cyanocinnamate polymers showed an enhancement with a four atom spacer (- O (CH₂)₃ -). There are three possible explanations for these discrepancies between the sulfones and the α -cyanocinnamates.

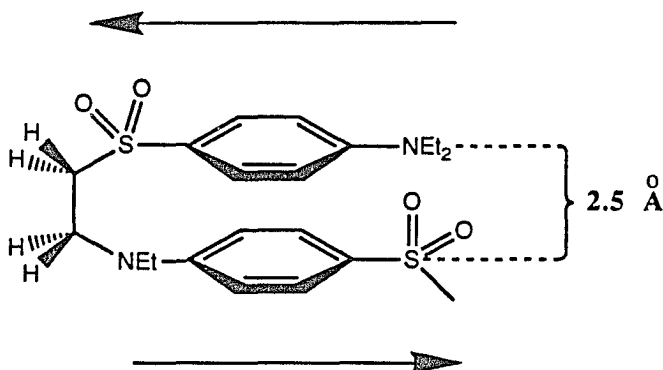
First, the ethylene spacer may impart sufficient freedom that the chromophores never sufficiently order themselves to produce an enhancement. This concept seems absurd knowing that the α -cyanocinnamates show an enhancement with a four atom spacer. However, we only evaluated dimer and trimer; it is possible that the much larger polymers lower the entropy of the system enough to allow the dipoles to orient into a favorable arrangement.

The second possible explanation is that the ethylene spacer compounds may possess a low energy conformer which orients the dipoles in opposing directions. Normally, the lowest energy conformation of two substituents in a 1,2-disubstituted ethane is anti, as shown in Scheme 28.



Scheme 28. Desired Dimer Conformation.

If the highly dipolar chromophores are eclipsed then a favorable pi-stacking can occur (see Scheme 29):



Scheme 29. Undesired Dimer Conformation.

This conformation may be competitive with the anti conformation for several reasons. The dipole moment of the eclipsed conformer would be very low, and thus probably more favorable in more nonpolar solvents. Also, there is the possibility of pi interactions between the aromatic rings, perhaps even charge transfer. Finally, it is theoretically possible that the lone pair of electrons on the amine can interact with the electron poor sulfone. Of course, the eclipsed conformation represents an extreme; there are gauche conformers which would also allow for similar pi stacking with

a distance of about 3.5 angstrom, which is a common pi stacking distance.^{59,60} However, UV/visible analysis does not show any shift in the absorption maximum which indicates that there is little or no such intramolecular interaction. This data also implies that there is no intermolecular aggregation.

The third option which may account for the discrepancy in results is the possibility that the earlier α -cyanocinnamate work was inaccurate. While the EFISH values for the α -cyanocinnamate polymers are probably reasonable, the molecular weights may be inappropriately small. The molecular weights were determined from gel permeation chromatography (GPC) by comparison to the retention times of polystyrene standards. If the α -cyanocinnamate polymer moves through the GPC at a faster rate than polystyrene of the same molecular weight, the results for the α -cyanocinnamate polymer will be erroneously small. A low molecular weight would in turn imply fewer NLO units; thus the hyperpolarizability per unit would seem larger than the actual value.

Whatever the cause, there is enough ambiguity in these model NLO systems to warrant further investigation.

Hyperpolarizabilities of Piperidine Spaced Oligomers by EFISH

The piperidine spaced oligomers were an attempt to create a more rigid and well defined system. It was believed that by placing the substituents on a ring they would be prevented from arranging themselves into unfavorable conformations. Unfortunately, the hyperpolarizabilities measured also showed no enhancement (Table 6).

Table 6. Hyperpolarizabilities of the Piperidine Spaced Oligomers.

<u>Compound</u>	<u>$\mu\beta$ ($\times 10^{-48}\text{esu}$)</u>	<u>$\mu\beta/\text{Unit}$ ($\times 10^{-48}\text{esu}$)</u>
Monomer (68)	45	45
Piperidine Dimer (64)	104	52
Piperidine Trimer (67)	136	45

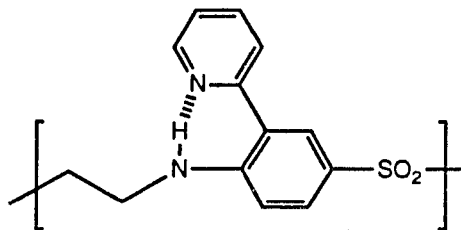
The value per chromophore, as for the dimethylene spacers, are all equal within experimental error. Computer analysis of the dimer indicated, as expected, that the sulfone substituent on the piperidine ring was equatorial. Unfortunately, the geometry about the sulfone forces the rest of the chromophore to be almost perpendicular to the other chromophore. The angle (Ar - S - piperidine) is 99° . (The computational analysis was done using MOPAC calculations with AM1 parameterization.) We would expect a maximum enhancement for the case where the two dipoles have an angle of 180° between them, and a complete loss of second order NLO activity when the angle was 0° . Since the angle between the chromophores is approximately 90° , it is not surprising that there is no enhancement of the hyperpolarizability.

Some work had suggested that the piperidine moiety is not as good a donor as other amines on an aromatic ring.⁶¹⁻⁶³ Theoretically, the hydrogens alpha to the amine could interact unfavorably with the ortho hydrogens on the aromatic ring. However, the fact that the $\mu\beta$ for piperidine monomer 68 is greater than that of monomer 20 indicates that the piperidine moiety is a much better donor.

To summarize, there was no enhancement in the hyperpolarizabilities in any of the systems synthesized for study. The hexamethylene spacer is simply too long to allow for favorable interactions between dipoles. In both the piperidine and dimethylene spaced systems, no enhancement was observed, probably because of the formation of conformers which could degrade any enhancement.

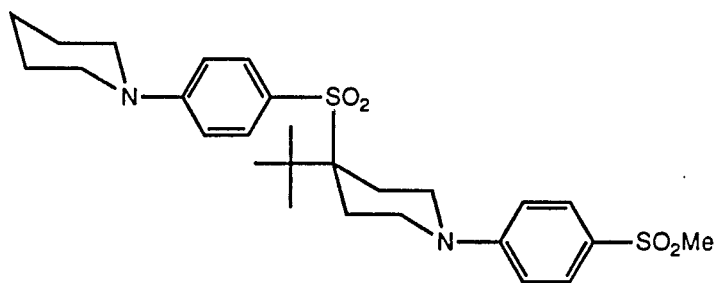
Future Studies

Future work for these molecular studies will have to prevent the formation of undesired conformations. One possibility is to install a hydrogen bonding group into the dimethylene spaced system which may prevent possible pi stacking (compound 69).



69

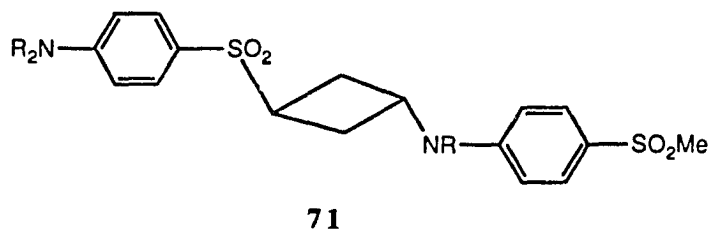
Another possibility is to place a bulkier group alpha to the sulfone in the piperidine spaced dimer. If this could be done, it may force the sulfone into an axial position (70).



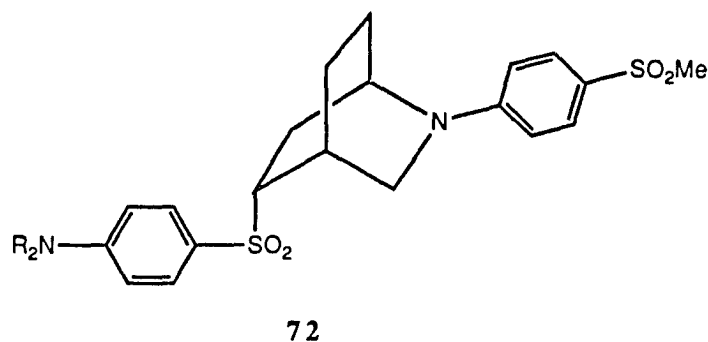
70

For experimental completeness, the *p*-aminophenyl sulfone analogues with a four atom spacer should be evaluated. This should be done because the α -cyanocinnamates showed an enhancement with a four atom spacer. Perhaps enough entropy to prevent pi stacking, but not enough distance to eliminate dipole interactions, would result.

Finally, new systems involving different and more rigid ring systems may be employed (compounds 71 and 72).



and,



These two ring systems rely on the 90° bend in the sulfone by placing the sulfone in an axial (or pseudo axial) position.

Experimental

General Methods

Melting points were uncorrected and determined on a Thomas Hoover melting point apparatus. Nuclear magnetic resonance spectra were recorded on a 250 MHz Bruker WM-250 spectrometer. Infrared spectra were recorded on a Perkin-Elmer 983 spectrometer. Elemental analyses were performed by Desert Analytics of Tucson, Arizona. The chromatographic grade silica gel used was 70-230 mesh, 60 Angstrom.

Synthesis of the Monomer

p-Methanesulfonylacetanilide (**18**):⁴⁸

4-(Methylmercapto)aniline **17** (1g, 7.2 mmol) and acetic anhydride (1.5g, 14.7 mmol) were dissolved in 4 ml of acetonitrile under argon. After stirring for 0.5 hours, a solution consisting of 30% hydrogen peroxide and 3.5 ml acetic acid was added dropwise. When the addition was complete, the reaction was warmed to 60°C and allowed to react for 12 hours. A trace of manganese dioxide was added and stirred for 2 hours. The solvent was then removed by high vacuum (5 mmHg) rotary evaporation. The product was recrystallized from ethyl acetate/acetone to give a 74% yield of **18**, mp = 186-187°C.

¹H-NMR (d₆DMSO) δ 10.39 (s, 1H), 7.81 (dd, 4H), 3.14 (s, 3H), 2.08 (s, 3H).

¹³C-NMR (d₆DMSO) δ 169.2, 143.8, 134.4, 128.3, 118.7, 43.9, 24.2.

IR (KBr) 3350, 1685, 1531, 1281, 1137 cm⁻¹.

Analysis Calculated: C 50.69%, H 5.20%, N 6.57%, S 15.03%, O 22.51%.

Found: C 50.68%, H 5.16%, N 6.62%, S 14.91%, O 22.63%.

p-Methanesulfonyl(N-methyl)acetanilide (**19**):^{49,50}

The sulfone **18** (3g, 14 mmol), 40% KF/alumina (8g, 55 mmol KF), and methyl iodide (5.3g, 37 mmol) were stirred in 100 ml of dry acetonitrile under argon. After 20 hours, the KF/alumina was filtered off, and the acetonitrile was then evaporated. The crude product was triturated with ethyl ether to give a 95% yield of **19** as a white solid, mp = 125-126°C.

¹H-NMR (CDCl₃) δ 7.93 (d, 2H), 7.37 (d, 2H), 3.26 (s, 3H), 3.03 (s, 3H), 1.93 (bs, 3H).

¹³C-NMR (CDCl₃) δ 169.8, 149.0, 128.8, 127.5, 44.3, 37.2, 22.5.

IR (KBr) 1653, 1300, 1150 cm⁻¹.

Analysis Calculated: C 52.85%, H 5.77%, N 6.16%, S 14.11%, O 21.12%.

Found: C 52.74%, H 5.73%, N 6.15%, S 14.17%, O 21.21%.

N-Ethyl,N-methylaminophenyl methyl sulfone (20):⁵¹

A 50 ml two neck round bottom flask was fitted with a six inch Vigreux distillation arrangement with a 25 ml receiver. The glassware was thoroughly dried, and under argon. The sulfone 19 was dissolved in 10 ml of anhydrous tetrahydrofuran and introduced into the reaction flask, followed by a 2 ml THF rinse. To the stirred solution, boron trifluoride etherate (1.3g, 8.9 mmol, 1.1 ml), was added, giving a precipitate. The contents were then heated to reflux. Next 10 ml of 1M borane-methyl sulfide complex in methylene chloride was added dropwise. After the addition was complete, the reaction was allowed to run for 6 hours at reflux. The methylene chloride, ethyl ether, and dimethyl sulfide were collected by fractional distillation, and the precipitate eventually went into solution. After the 6 hours, the THF was evaporated and 4 ml of 6M aqueous HCl was added. After refluxing for 1 hour, this solution was cooled in an ice bath and then neutralized with 6M aqueous NaOH. The aqueous layer was saturated with potassium carbonate and extracted with ethyl acetate. The ethyl acetate solution was dried over anhydrous magnesium sulfate, filtered, and then evaporated. The product was recrystallized from methanol/water to give an 85% yield of white crystalline 20, mp = 83-84°C.

¹H-NMR (CDCl₃) δ 7.59 (d, 2H), 6.57 (d, 2H), 3.34 (q, 2H), 2.88 (s, 3H),
2.87 (s, 3H), 1.04 (t, 3H).

¹³C-NMR (CDCl₃) δ 151.8, 128.7, 124.8, 110.4, 46.2, 44.7, 37.2, 11.0.

IR (KBr) 2972, 1291, 1134 cm⁻¹.

Analysis Calculated: C 56.31%, H 7.09%, N 6.57%, S 15.03%, O 15.00%.

Found: C 56.46%, H 7.10%, N 6.59%, S 15.11%, O 14.74%.

Synthesis of the Hexamethylene Spaced Oligomers

1-Bromo-6-(p-acetanilide sulfone) hexane (22):⁴⁸⁻⁵⁰

4-Aminothiophenol 21 was freshly Kugelrohr distilled (oven temp.= 100°C at 1 mmHg). 12g of crude 4-aminothiophenol gave 10.2g (82 mmol) of pure starting material which was dissolved in 50 ml of anhydrous

acetonitrile under argon. The latter solution was added dropwise to a slurry containing KF/alumina (70g, 6 eq. KF), 1,6-dibromohexane (50 ml, 0.325 mol, 4 eq.), and 100 ml anhydrous acetonitrile. After 3 hours, the KF/alumina was filtered away, and about 100 ml of acetonitrile evaporated off. Acetic anhydride (16g, 160 mmol) was then added. After 1 hour the solution was placed in an ice bath and then filtered to remove the byproduct 1,6-di(p-acetanilide sulfide)hexane (2.1g). The acetonitrile was removed by rotary evaporation to give an oil. This oil was extracted with 3 x 100 ml portions of pentane to remove the unreacted 1,6-dibromohexane. This left a crude solid which was dissolved in 80 ml acetonitrile. The oxidation was carried out by dripping a solution consisting of 100 ml of 30% hydrogen peroxide and 100 ml of glacial acetic acid into the acetonitrile solution. After stirring at 50°C for 15 hours, the reaction was quenched and allowed to stir for 3 hours, with a trace of manganese dioxide. After cooling, an oil formed which was removed by extraction with 2 x 100 ml portions of pentane. Neutralization with 6M aqueous sodium hydroxide solution precipitated the product **22**. This was filtered and then recrystallized twice from methanol to give a 37% yield of **4** as a waxy, white solid (mp = 95-98°C).

¹H-NMR (CDCl₃) δ 8.71 (s, 1H), 7.71 (s, 4H), 3.30 (t, 2H), 3.04 (bt, 2H), 2.13 (s, 3H), 1.70 (m, 4H), 1.33 (bt, 4H).

¹³C-NMR (CDCl₃) δ 169.5, 143.3, 132.7, 128.9, 119.4, 56.1, 33.5, 32.0, 27.3, 27.1, 24.4, 22.4.

IR (KBr) 3323, 1668, 1319, 1148 cm⁻¹.

Analysis Calculated: C 46.42%, H 5.56%, N 3.87%.

Found: C 46.46%, H 5.66%, N 3.79%.

Small Oligomers **23-25**:

The monomer **22** (5g, 14 mmol) was dissolved in 30 ml of anhydrous acetonitrile, and then 6g (41 mmol of KF) of 40% KF/alumina was added under argon. This slurry was stirred for 11 hours, after which ethyl iodide (2.6 ml, 33 mmol) and 2g additional KF/alumina were added. After stirring this mixture for another 9 hours, the used KF/alumina was filtered away and

the solvent evaporated to remove the excess ethyl iodide. Next, compound **18** (3g, 14 mmol) was added along with 30 ml of anhydrous acetonitrile. To this new solution a trace of potassium iodide and KF/alumina (6g, 41 mmol) were added and the slurry was stirred for 22 hours. The KF/alumina was then filtered away, and 20g of column chromatographic grade silica gel (70-230 mesh) was added. The solvent was then evaporated, and the silica/product was loaded on a 500 ml column of silica gel. The separation was started with 3% methanol in ethyl acetate. The first major fraction is unreacted **18** (0.92g recovered after recrystallization). The next major fraction was 1.004g of the dimer **23**. After **23** was off the column, the solvent was switched to 5% methanol in ethyl acetate. Next, the trimer **24** was recovered (1.026g). Finally, the solvent was switched to 10% methanol in ethyl acetate and 0.467g of the tetramer **25** was recovered.

Dimer 23: 14% Yield

$^1\text{H-NMR}$ (CDCl_3) δ 7.9(2d, 4H), 7.3 (2d, 4H), 3.7(q, 2H), 3.6 (t, 2H), 3.0 (bs, 5H), 1.8 (bs, 6H), 1.1-1.6 (m, 8H), 1.0 (t, 3H).
 $^{13}\text{C-NMR}$ (CDCl_3) δ 169.2, 169.0, 147.4, 147.3, 139.3, 137.9, 129.2, 128.7, 128.6, 55.6, 48.6, 44.0, 27.5, 27.1, 25.7, 22.6, 22.0, 13.0.
 IR (KBr) 2932, 1657, 1304, 1148 cm^{-1}

Trimer 24: 19% Yield

$^1\text{H-NMR}$ (CDCl_3) δ 7.9(2d, 6H), 7.3 (m, 6H), 3.7(q, 2H), 3.6 (t, 4H), 3.0 (bs, 7H), 1.8 (bs, 9H), 1.1-1.6 (m, 16H), 1.0 (t, 3H).
 $^{13}\text{C-NMR}$ (CDCl_3) δ 169.4, 147.5, 139.5, 138.2, 138.0, 129.5, 129.4, 128.9, 128.7, 55.8, 48.7, 44.2, 27.6, 27.2, 25.8, 22.8, 22.1, 22.0, 13.1.

Tetramer 25: 9% Yield

$^1\text{H-NMR}$ (CDCl_3) δ 7.9(2d, 8H), 7.3 (m, 8H), 3.7(q, 2H), 3.6 (t, 6H), 3.0 (bs, 9H), 1.8 (bs, 12H), 1.1-1.6 (m, 24H), 1.0 (t, 3H).
 $^{13}\text{C-NMR}$ (CDCl_3) δ 169.3, 147.5, 139.5, 138.2, 129.4, 128.9, 128.7, 128.6, 55.8, 48.8, 44.2, 27.6, 27.3, 25.9, 22.7, 22.2, 22.1, 13.1.

Hexamethylene Spaced Oligomers 26-28:

The resolved amides (23-25) were individually dissolved in 20 ml of anhydrous tetrahydrofuran under argon. To each of these solutions 1M THF/borane was added (4eq. per amide unit). The tetrahydrofuran solution was then refluxed for 42 hours. After cooling 5 ml of 6M aqueous hydrochloric acid was added slowly to each reaction. The mixtures were then made basic with 6M aqueous sodium hydroxide. The aqueous layer was then separated from the ether, and then each aqueous layer was extracted with ethyl acetate. The combined THF and ethyl acetate fractions were dried over anhydrous magnesium sulfate. After filtering the solvents were evaporated and the products were each purified by column chromatography to give the pure hexamethylene spaced oligomers 26-28.

Dimer 26: 62% yield of a viscous white oil.

$^1\text{H-NMR}$ (CDCl_3) δ 7.6(t, 4H), 6.6 (t, 4H), 3.3(bq, 6H), 3.2 (t, 2H), 2.9 (m, 5H),
1.2-1.7 (m, 8H), 1.1 (t, 9H).

$^{13}\text{C-NMR}$ (CDCl_3) δ 151.0, 150.9, 129.6, 124.6, 122.7, 110.3, 110.1, 56.4, 49.9, 44.9,
44.3, 27.9, 26.7, 26.2, 22.6, 12.0, 11.7.

IR (Neat) 2930, 1589, 1296, 1135 cm^{-1}

Analysis Calculated: C 60.70%, H 7.74%, N 5.66%.

Found: C 60.77%, H 7.98%, N 5.31%.

Trimer 27: 75% yield of a white glassy solid.

$^1\text{H-NMR}$ (CDCl_3) δ 7.6(m, 6H), 6.6 (t, 6H), 3.3(m, 8H), 3.2 (t, 4H), 2.9 (m, 7H),
1.2-1.7 (m, 16H), 1.1 (m, 12H).

$^{13}\text{C-NMR}$ (CDCl_3) δ 151.1, 151.9, 129.7, 129.1, 124.7, 123.0, 122.9, 110.3, 110.2,
56.5, 50.0, 44.9, 44.4, 28.0, 26.8, 26.3, 22.7, 12.1, 11.9.

IR (Melt) 2932, 1590, 1293, 1134 cm^{-1}

Analysis Calculated: C 61.47%, H 7.80%, N 5.51%.

Found: C 61.77%, H 7.97%, N 5.33%.

Tetramer **28**: 80% yield of a white glassy solid.

$^1\text{H-NMR}$ (CDCl_3) δ 7.6(m, 8H), 6.6 (m, 8H), 3.3(m, 10H), 3.2 (t, 6H), 2.9 (m, 9H),
1.2-1.7 (m, 24H), 1.1 (m, 15H).

$^{13}\text{C-NMR}$ (CDCl_3) δ 151.1, 151.0, 129.7, 129.0, 123.0, 122.8, 110.3, 110.2, 56.4,
50.0, 44.9, 44.4, 28.0, 26.7, 26.3, 22.7, 12.1, 11.8.

IR (Melt) 2931, 1590, 1295, 1133 cm^{-1}

Analysis Calculated: C 61.84%, H 7.83%, N 5.44%.

Found: C 62.07%, H 8.01%, N 5.26%.

Synthesis of the Dimethylene Spaced Dimer:

p-Acetamidothiophenol **44**:

2.3 g of p-aminothiophenol **21** was freshly Kugelrohr distilled (oven temperature of 100°C at 1mmHg) to give 1.87g (15 mmol) of pure starting material. The pure p-aminothiophenol was melted and 1.7g (1.1 eq.) of acetic anhydride was added slowly, and the solution was cooled in an ice bath as needed. After the addition of the acetic anhydride was complete, the reaction mixture was allowed to come to room temperature. Stirring for 0.5 hour was followed by Kugelrohr distillation, heating slowly to remove unreacted acetic anhydride and acetic acid. The product then distilled at an oven temperature of 160°C , and 0.2 mmHg to give white crystalline **44** in 99% yield, mp = $151\text{-}153^\circ\text{C}$.

$^1\text{H-NMR}$ ($d_6\text{Acetone}$) δ 9.18 (bs, 1H), 7.4 (dd, 4H), 4.16 (s, 1H), 2.07 (s, 3H).

$^{13}\text{C-NMR}$ ($d_6\text{Acetone}$) δ 168.6, 138.1, 130.4, 125.0, 120.5, 23.9.

IR (KBr) 3292, 1658, 1598, 1540 cm^{-1} .

Analysis Calculated: C 57.46%, H 5.42%, N 8.38%.

Found: C 57.60%, H 5.34%, N 8.18%.

4-(Methylmercapto)- α -bromoacetanilide **43**:

5g (36 mmol) of freshly distilled 4-(methylmercapto)aniline **17** was rinsed into a round bottom flask with 50 ml of anhydrous acetonitrile, under

argon. 20g (4 eq.) of powdered potassium carbonate was then added. Then a solution consisting of 6.21g (1.1 eq.) of α -bromoacetyl chloride in 30 ml of acetonitrile was added dropwise. After 1 hour the mixture was dumped into 400 ml of water. The product was filtered and then dried under vacuum over night. The product was recrystallized from ethyl acetate to give an 86% yield of tan colored needles (**43**), mp = 129-130°C.

$^1\text{H-NMR}$ ($d_6\text{DMSO}$) δ 10.4 (s, 1H), 7.4 (dd, 4H), 4.1 (s, 2H), 2.5 (s, 3H).

$^{13}\text{C-NMR}$ ($d_6\text{DMSO}$) δ 164.6, 136.0, 132.6, 127.0, 119.9, 30.4, 15.4.

IR (KBr) 3253, 3182, 3113, 2925, 1659, 1606, 1537, 817 cm^{-1} .

Analysis Calculated: C 41.55%, H 3.87%, N 5.38%.

Found: C 44.67%, H 4.18%, N 5.76%.

4-Methylmercapto- α -(p-acetamidophenylsulfide) acetanilide **45**:

2g (12 mmol) of **44** was dissolved in 30 ml of a freshly prepared 0.5M sodium methoxide/methanol solution. Then a slurry of 3.11g (12mmol) of **43**, finely powdered, in 20 ml of methanol was added. This mixture was stirred for 1.5 hours, and then 50 ml of water was added. The product was filtered then dried under vacuum overnight. Recrystallization from methanol (with a hot filtration) gave a 71% yield of pure **45** as white crystals, mp = 200-201°C.

$^1\text{H-NMR}$ ($d_6\text{DMSO}$) δ 10.1 (s, 1H), 10.0 (s, 1H), 7.2-7.6 (m, 8H), 3.8 (s, 2H), 2.4 (s, 3H), 2.0 (s, 3H).

$^{13}\text{C-NMR}$ ($d_6\text{DMSO}$) δ 168.4, 166.9, 138.2, 136.3, 132.1, 130.4, 128.6, 127.1, 119.9, 119.6, 24.0, 15.5.

IR (KBr) 3289, 1659, 1601, 1536, 1493, 825 cm^{-1} .

Analysis Calculated: C 58.93%, H 5.24%, N 8.09%.

Found: C 58.78%, H 5.33%, N 8.14%.

N,N'-Diethyl-4-methylmercapto- α -(p-acetamidophenylsulfide) acetanilide 46.^{49,50}

2.73g (8 mmol) of **45** was dissolved in 90 ml of anhydrous acetonitrile under argon. To this solution 1.5 ml of ethyl iodide and 4g of 40% KF/alumina were added, and this mixture was stirred. Every 2 hours 2g of 40% KF/alumina and 1 ml of ethyl iodide were added until the reaction appeared complete (8 hours total). This mixture was allowed to stir overnight. The KF/alumina was filtered and washed with 100 ml of ethyl ether. The solvents were then evaporated, and the product purified by column chromatography. An 83% yield of pure **46** was obtained as a white solid, mp = 91-92°C.

¹H-NMR (CDCl₃) δ 7.39 (d, 2H), 7.29 (d, 2H), 7.04-7.14 (m, 4H), 3.70-3.79 (m, 4H), 3.51 (s, 2H), 2.52 (s, 3H), 1.82 (s, 3H), 1.11 (q, 6H).

¹³C-NMR (CDCl₃) δ 169.7, 167.7, 140.9, 139.4, 138.1, 135.9, 130.1, 128.6, 128.4, 127.1, 44.5, 43.7, 36.8, 22.7, 15.3, 12.9, 12.8.

IR (KBr) 2971, 1642, 1487, 1409, 1302 cm⁻¹.

Analysis Calculated: C 62.66%, H 6.51%, N 6.96%.

Found: C 62.53%, H 6.65%, N 6.98%.

N,N'-Diethyl-4-methylsulfone- α -(p-acetamidophenyl sulfone) acetanilide 47.⁵⁷

Compound **46** was dissolved in 35 ml of Sulfolane, and 6.87g of 50% m-chloroperbenzoic acid (4 eq.) was added, all under argon. This solution was kept at 40°C for 4.5 hours. The solution was then dripped into 130 ml of 5% sodium bicarbonate solution. The white product was filtered and dried under vacuum to a constant weight to give a 98% yield of **47**, mp = 205-206°C.

¹H-NMR (d₆DMSO) δ 7.7 (2dd, 8H), 3.7 (m, 4H), 3.3 (s, 2H), 1.8 (s, 3H), 1.0 (m, 6H).

¹³C-NMR (d₆DMSO) δ 168.5, 147.4, 145.2, 137.9, 129.7, 129.0, 128.7, 128.4, 58.9, 43.4, 22.6, 13.1.

IR (KBr) 2990, 1656, 1306, 1139 cm⁻¹.

Analysis Calculated: C 54.06%, H 5.62%, N 6.00%.

Found: C 53.68%, H 5.52%, N 5.76%.

Dimethylene spaced p-aminophenyl sulfone dimer **48**:

2g of **47** (4.3 mmol) was mixed in 50 ml of dry tetrahydrofuran under argon. To the mixture 30 ml of 1M THF/borane solution was added. This solution was refluxed for 18 hours, then cooled, and 20 ml of 6M hydrochloric acid added dropwise. This solution was made basic with 6M sodium hydroxide solution, the THF was separated and the remaining aqueous layer was extracted with 3 x 50 ml portions of ethyl acetate. After the solvent was evaporated the product was purified by column chromatography, followed by recrystallization from methanol. A 44% yield of **48** was obtained as white crystals, mp = 155-156°C.

¹H-NMR (d₆DMSO) δ 7.6 (2d, 4H), 6.6 (2d, 4H), 3.7 (t, 2H), 3.35 (m, 6H), 3.22 (t, 2H), 2.9 (s, 3H), 1.12 (m, 9H).

¹³C-NMR (d₆DMSO) δ 151.3, 150.2, 129.7, 129.3, 126.4, 122.4, 110.8, 110.5, 52.9, 45.3, 44.9, 44.5, 44.0, 12.1.

IR (KBr) 2974, 1592, 1301, 1139 cm⁻¹.

Analysis Calculated: C 57.51%, H 6.89%, N 6.39%.

Found: C 57.53%, H 6.88%, N 6.34%.

Synthesis of the Dimethylene Spaced Trimer:

α-(p-Aminothiophenyl)-4-methylmercapto acetanilide **50**:

2.4g (19 mmol) of freshly distilled p-aminothiophenol **21** was dissolved in 30 ml of 0.6 M sodium methoxide/methanol solution. To this solution a slurry consisting of 4.9g (1 eq.) of **43** in 20 ml of methanol was added. As the reaction progressed **43** went into solution until there was no more solid. After 4 hours a precipitate formed. One half hour after the precipitate formed, the slurry was dumped into 100 ml of 0.25 M aqueous sodium hydroxide solution. The solid was isolated by filtration, and then recrystallized from methanol to give an 88% yield of white crystalline **50**, mp = 130-131°C.

$^1\text{H-NMR}$ (d_6DMSO) δ 9.97 (s, 1H), 7.5 (d, 2H), 7.2 (2d, 4H), 6.5 (d, 2H), 5.27 (s, 2H), 3.52 (s, 2H), 2.42 (s, 3H).

$^{13}\text{C-NMR}$ (d_6DMSO) δ 167.3, 148.9, 136.5, 134.0, 131.9, 127.1, 119.9, 118.2, 114.3, 41.2, 15.5.

IR (KBr) 3298, 1666, 1586, 1518, 817 cm^{-1} .

Analysis Calculated: C 59.18%, H 5.30%, N 9.20%.

Found: C 59.32%, H 5.23%, N 9.18%.

α -(α -Bromo-p-acetamidothiophenyl)-4-methylmercaptoacetanilide **51**:

4.5 g (15 mmol) of **50** was dissolved in 100 ml of anhydrous acetone under argon. To this solution 3g (2 eq.) of triethylamine was added, followed by the dropwise addition of a solution containing 2.6g (1.1 eq.) of α -bromoacetyl chloride in 20 ml of acetone. The reaction was cooled with an ice bath as needed to keep the temperature close to ambient. After the addition was complete, the resulting slurry was stirred for 0.5 hour. The slurry was then poured into 200 ml of 0.25M aqueous hydrochloric acid and filtered, rinsing liberally with water. After drying under vacuum a 90% yield of cream colored **51** was obtained, mp = 285°C (dec.), which was used without further purification.

$^1\text{H-NMR}$ (d_6DMSO) δ 10.45 (s, 1H), 10.16 (s, 1H), 7.53 (m, 4H), 7.4 (d, 2H), 7.2 (d, 2H), 4.02 (s, 2H), 3.78 (s, 2H), 2.42 (s, 3H).

$^{13}\text{C-NMR}$ (d_6DMSO) δ 166.8, 164.8, 137.3, 136.3, 132.1, 130.0, 129.9, 127.1, 119.9, 119.8, 30.3, 15.5.

IR (KBr) 3244, 3176, 1654, 1536, 827 cm^{-1}

p-Ethylmercaptoacetanilide trimer **52**:

0.31g (13 mmol) of 98% sodium hydride was dissolved in 25 ml of anhydrous dimethyl sulfoxide. To this solution 2.2g (13 mmol) of **44** was added, and this solution was stirred for 20 under argon atmosphere. Then a solution of 4.98g (12 mmol) of **51** in 30 ml of anhydrous DMSO was added. After 10 hours the product was precipitated by pouring the reaction mixture into 600 ml of 0.25M aqueous sodium hydroxide solution. The precipitate was filtered and rinsed with 50 ml of water followed by 300 ml of methanol.

After drying under vacuum a 96% yield of tan colored **52** was obtained, mp = 241-242°C, and used without further purification.

¹H-NMR (d₆DMSO) δ 10.18 (s, 1H), 10.14 (s, 1H), 9.98 (s, 1H), 7.5 (m, 6H), 7.4 (m, 4H), 7.2 (d, 2H), 3.75 (s, 4H), 2.42 (s, 3H), 2.02 (s, 3H).
¹³C-NMR (d₆DMSO) δ 168.3, 167.0, 166.8, 138.2, 137.6, 136.3, 132.1, 130.4, 130.2, 129.3, 128.5, 127.1, 119.9, 119.8, 119.6, 38.6, 24.0, 15.5.

IR (KBr) 3323, 1650, 1518, 819 cm⁻¹

p-Ethylmercaptoaniline trimer 53:

5g (9.8 mmol) of **52** was mixed in 250 ml of anhydrous tetrahydrofuran under argon. 100 ml of 1M THF/borane solution (10 eq.) was added, and the mixture heated to reflux. After refluxing for 22 hours (the starting material eventually went into solution), the reaction was carefully quenched with 50 ml of 6M aqueous hydrochloric acid. The resulting solution was then made basic (pH about 10) with 6M aqueous sodium hydroxide solution. After separating the THF and aqueous phases, the aqueous phase was extracted with ethyl ether. The combined organic extracts were extracted once with brine solution and dried over magnesium sulfate. After evaporation of the solvents the product was purified by column chromatography. An 87% yield of **53** was obtained as a viscous yellow oil.

¹H-NMR (CDCl₃) δ 7.2 (m, 6H), 6.45 (m, 6H), 3.91(bs, 3H), 3.19 (t, 4H), 3.08 (q, 2H), 2.89 (t, 4H), 2.37 (s, 3H), 1.20 (t, 3H).
¹³C-NMR (CDCl₃) δ 148.1, 147.5, 146.4, 134.8, 134.7, 131.1, 124.1, 119.8, 119.2, 113.4, 113.2, 113.0, 42.2, 42.0, 38.1, 35.8, 18.8, 14.5.

IR (Melt) 3395, 3015, 2964, 2915, 1594, 1502, 816 cm⁻¹

Analysis Calculated: C 63.93%, H 6.65%, N 8.95%.

Found: C 64.77%, H 6.79%, N 8.88%.

p-Ethylmercaptoacetanilide trimer 54:

3.5g (7.5 mmol) of **53** was dissolved in 20 ml of ethyl acetate and cooled with an ice bath. 3.4g (4.5 eq.) of acetic anhydride was added dropwise, and the mixture was allowed to warm while stirring (a precipitate

forms immediately). After 4 hours the slurry was poured into 100 ml of hexane, filtered and rinsed with 500 ml additional hexane to remove all of the acetic acid and unreacted acetic anhydride. After drying a 97% yield of white solid, mp = 196-197°C, was obtained. The product **54** was used without further purification.

$^1\text{H-NMR}$ (50% d_6DMSO , 50% CF_3COOH) δ 7.1 - 7.5 (m, 12H), 4.01 (bt, 4H), 3.85 (q, 2H), 3.22 (bs, 4H), 2.48 (s, 3H), 2.03 (s, 6H), 2.00 (s, 3H), 1.18 (t, 3H).

IR (KBr) 2982, 1649, 1490, 1392 cm^{-1}

Analysis Calculated: C 62.49%, H 6.26%, N 7.05%.

Found: C 63.12%, H 6.27%, N 7.05%.

p-Dimethylene sulfone acetanilide trimer **55**:⁵⁷

4g (6.7 mmol) of **54** was mixed in 50 ml of anhydrous Sulfolane at 44°C under argon. To this mixture 15.5g (6.7 eq.) of 50% *m*-chloroperbenzoic acid was added. After the addition of the *m*-CPBA, **54** eventually went into solution. The reaction proceeded for 22 hours and then it was quenched, and the product precipitated, by dripping the Sulfolane solution into 300 ml of 0.5M aqueous sodium hydroxide solution. The product was filtered and rinsed with water. After drying under vacuum a 92% yield of pure **55** was obtained as a white solid, mp = 203-205°C.

$^1\text{H-NMR}$ (d_6DMSO) δ 7.9 (m, 6H), 7.55 (d, 6H), 3.95 (bt, 4H), 3.72 (q, 2H), 3.65 (bt, 4H), 3.26 (s, 3H), 1.83 (s, 3H), 1.76 (s, 6H), 0.99 (t, 3H).

$^{13}\text{C-NMR}$ (d_6DMSO) δ 169.1, 147.5, 146.8, 146.4, 137.7, 137.2, 129.3, 129.1, 128.9, 128.5, 52.3, 43.5, 43.4, 42.5, 22.6, 22.5, 13.1.

IR (KBr) 2976, 2928, 1664, 1299, 1151 cm^{-1} .

Analysis Calculated: C 53.82%, H 5.39%, N 6.07%.

Found: C 53.64%, H 5.32%, N 5.94%.

p-Dimethylene phenyl sulfone (N-ethyl) amine trimer **56**:

Triamide **55** (2g, 3 mmol) was mixed in 50 ml of anhydrous tetrahydrofuran under argon. To this mixture 30 ml of 1M THF/borane (10 eq.) solution was added, and the mixture was heated to reflux. The triamide

eventually went into solution. After 17 hours at reflux, the reaction mixture was cooled to 0°C, and 20 ml of 6M hydrochloric acid was carefully added. The solution was then made basic (pH about 10) with 6M sodium hydroxide solution. The THF was separated and the aqueous phase was extracted with 3 x 50 ml portions of ethyl acetate. The combined organic phases were extracted once with 20 ml of brine solution, and then dried over magnesium sulfate. After filtering and evaporation of the solvent, the crude product was purified by column chromatography to give a 75% yield of white solid (56) which melts at 81°C.

$^1\text{H-NMR}$ (CDCl_3) δ 7.63 (m, 6H), 6.65 (d, 2H), 6.54 (m, 4H), 3.75 (m, 4H), 3.38 (m, 8H), 3.22 (bq, 4H), 2.95 (s, 3H), 1.16 (m, 12H).

$^{13}\text{C-NMR}$ (CDCl_3) δ 151.4, 150.6, 150.2, 129.9, 129.8, 129.4, 126.7, 124.5, 122.5, 111.0, 110.8, 110.6, 53.0, 45.4, 44.9, 44.6, 44.1, 43.9, 12.2.

IR (Melt) 2970, 1590, 1299, 1138 cm^{-1}

Analysis Calculated: C 57.29%, H 6.67%, N 6.47%.

Found: C 56.75%, H 6.77%, N 6.20%.

Synthesis of the Piperidine Spaced Dimer:

4-Hydroxypiperacetamide 58:

4-Hydroxypiperidine 54 was mixed with 5.6g (1.1 eq.) of acetic anhydride. The mixture was warmed gently to dissolve the amine. The resulting solution was then stirred at room temperature for 1 hour. The product is then Kugelrohr distilled to remove the acetic acid and unreacted acetic anhydride; the desired product distilled at an oven temperature of 130-135°C, at 0.05 mmHg. The product 58 is a white crystalline solid, mp = 68-69°C, and the yield was 99%.

$^1\text{H-NMR}$ (CDCl_3) δ 4.27 (bs, 1H), 3.7-3.8 (m, 1H), 3.70(septet, 1H), 3.5-3.6 (m, 1H), 2.9-3.1(m, 2H), 1.90 (s, 3H), 1.6-1.8 (m, 2H), 1.2-1.4(m, 2H).

$^{13}\text{C-NMR}$ (CDCl_3) δ 168.7, 65.9, 43.4, 38.6, 34.0, 33.3, 21.0.

IR (Melt) 3389, 2939, 1619, 1453 cm^{-1}

Analysis Calculated: C 58.72%, H 9.15%, N 9.78%.

Found: C 58.77%, H 9.44%, N 9.67%.

4-Tosyloxypiperacetamide **59**:

6g (42 mmol) of **58** was dissolved in 100 ml of anhydrous tetrahydrofuran, and 8g of p-toluenesulfonyl chloride was added, under argon. Then 4g (1.5 eq.) of powdered potassium hydroxide was added. Over the span of four days a total of 4g of additional powdered potassium hydroxide and 5g p-toluenesulfonyl chloride were added periodically. The disappearance of the alcohol was monitored by TLC. When the reaction was complete, the potassium hydroxide was filtered away (through a short plug of silica gel) and the THF evaporated. The resulting yellow oil was purified by column chromatography, using ethyl ether as the mobile phase. After evaporation of the ether a viscous oil was obtained which solidified by agitating under high vacuum. Compound **59** was obtained in an 85% yield as a white solid, mp = 77-82°C.

¹H-NMR (CDCl₃) δ 7.79 (d, 2H), 7.36 (d, 2H), 4.72 (septet, 1H), 3.3-3.7 (m, 4H), 2.45 (s, 3H), 2.07 (s, 3H), 1.6-1.9 (m, 4H).

¹³C-NMR (CDCl₃) δ 168.5, 144.7, 133.7, 129.7, 127.3, 77.1, 42.4, 37.5, 31.5, 30.5, 21.3, 21.0.

IR (Melt) 2954, 2868, 1644, 1352, 1174 cm⁻¹

Analysis Calculated: C 56.55%, H 6.44%, N 4.71%.

Found: C 56.60%, H 6.64%, N 4.65%.

Piperacetamide, 4-(p-fluorophenyl) sulfone **60**:^{5 6}

8.6g (67 mmol) of p-fluorothiophenol **40** was dissolved in 100 ml of a 0.7M sodium methoxide/methanol solution. After 20 minutes a solution of 20g (67 mmol) of **59** in 50 ml of methanol was added to the p-fluorothiophenol solution. The reaction mixture was refluxed for 18 hours. The reaction was then cooled to 0°C, and 100 ml of additional methanol added. A solution consisting of 62g OXONE (50% KHSO₅) in 250 ml of water was then slowly added to the chilled reaction mixture (total time for addition was about 15 minutes). This slurry was stirred at room temperature for 8 hours. Then 700 ml of water was added, and the resulting solution was extracted

with 6 x 200 ml of chloroform. The combined chloroform extracts were dried over anhydrous sodium sulfate. After filtering away the drying agent and evaporating the chloroform an oil was obtained. To this oil 50 ml of ethyl ether was added, and the product quickly crystallized. After filtering and drying the crystals a 76% yield of white **60** was obtained, mp = 125-126°C.

$^1\text{H-NMR}$ (CDCl_3) δ 7.89 (m, 2H), 7.30 (m, 2H), 4.73 (bd, 1H), 3.95 (bd, 1H), 3.0-3.2 (m, 2H), 2.51 (bt, 1H), 1.9-2.2 (m, 5H), 1.5-1.7 (m, 2H).

$^{13}\text{C-NMR}$ (CDCl_3) δ 168.6, 167.9, 163.8, 132.3, 131.8, 131.6, 116.7, 116.3, 61.2, 44.8, 39.9, 25.3, 24.8, 21.2.

IR (Melt) 3100, 2926, 1642, 1143 cm^{-1}

Analysis Calculated: C 54.72%, H 5.65%, N 4.91%.

Found: C 54.93%, H 5.68%, N 4.78%.

Piperidine, 4-(p-fluorophenyl) sulfone **61**:

11g (35 mmol) of the amide **60** was mixed into 100 ml of 1M aqueous hydrochloric acid solution, and the mixture was brought to reflux. After 6 hours at reflux the solution was cooled to 0°C and made basic (pH about 12) with 1M aqueous sodium hydroxide solution. The slurry was then extracted with 5 x 100 ml portions of chloroform, and the chloroform was then extracted once with 50 ml of brine solution. After drying the chloroform solution over anhydrous sodium sulfate, it was filtered and the chloroform then evaporated. The product was recrystallized (with hot filtration) from water to give a 68% yield of white crystalline **61**, mp = 99-100°C. A second crop was obtained, mp = 98-100°C, making a total yield of 79%.

$^1\text{H-NMR}$ (CDCl_3) δ 7.89 (m, 2H), 7.25 (m, 2H), 3.18 (bd, 2H), 3.02 (tt, 1H), 2.56 (td, 2H), 2.01 (bd, 2H), 1.4-1.7 (m, 3H).

$^{13}\text{C-NMR}$ (CDCl_3) δ 167.9, 163.8, 132.7, 132.0, 131.8, 116.6, 116.2, 62.3, 45.3, 26.2.

IR (Melt) 3270, 2957, 2817, 1267, 1145 cm^{-1}

Analysis Calculated: C 54.31%, H 5.80%, N 5.76%.

Found: C 52.62%, H 5.99%, N 5.44%.

Piperidine, 4-(p-piperidine-N-phenyl) sulfone **62**:⁴⁴

Compound **61** (2g, 8 mmol) was dissolved in 35 ml of piperidine. To this solution 2g (4 eq.) of anhydrous potassium fluoride was added, under argon. The reaction mixture was stirred and heated to 100°C. After 9 hours the solution was cooled and the salts were filtered off, rinsing with ethyl acetate. The piperidine and ethyl acetate were evaporated and the product was dried by heating to 80°C under vacuum (0.5 mmHg) for two days. The product **62** was a tan solid, mp = 126-128°C, 99% yield, which was used without further purification.

¹H-NMR (CDCl₃) δ 7.50 (d, 2H), 6.85 (d, 2H), 3.32 (bs, 4H), 3.14 (bd, 2H), 2.92 (tt, 1H), 2.52 (bt, 2H), 1.97 (bd, 2H), 1.4-1.7 (m, 9H).

¹³C-NMR (CDCl₃) δ 154.3, 130.6, 122.6, 113.2, 62.0, 48.2, 45.0, 26.0, 25.0, 24.0.

IR (KBr) 3302, 2916, 1588, 1264, 1122 cm⁻¹

Piperidine spaced dimer **64**:⁴⁴

1g (3 mmol) of **62** and 0.72g (1.4 eq.) of p-fluorophenyl methyl sulfone **63** were dissolved in 15 ml of anhydrous dimethyl sulfoxide, under argon. To the latter solution 1g (5 eq.) of anhydrous potassium fluoride was added. The mixture was stirred and heated to 130°C. The reaction mixture was maintained at this temperature for two days. Then the mixture was cooled and precipitated into 200 ml of water. The product was filtered and dried under vacuum. It was then dissolved in chloroform, loaded on a silica gel column, and the pure product eluted with 50/50 ethyl acetate/hexanes. The pink color was removed by dissolving **64** in acetonitrile and filtering through a plug of basic alumina. Evaporation of the acetonitrile afforded a 64% yield of **64** as a white solid, mp = 220°C (dec.).

¹H-NMR (CDCl₃) δ 7.68 (d, 2H), 7.58 (d, 2H), 6.84 (m, 4H), 3.91 (bd, 2H), 3.32 (bs, 4H), 2.9-3.1 (m, 4H), 2.81 (bt, 2H), 2.04 (bd, 2H), 1.5-1.8 (m, 8H).

¹³C-NMR (CDCl₃) δ 154.5, 153.5, 130.6, 129.0, 128.6, 122.3, 114.2, 113.3, 61.4, 48.2, 46.7, 44.8, 25.1, 24.6, 24.1.

IR (KBr) 2929, 1588, 1293, 1141 cm⁻¹

Analysis Calculated: C 59.71%, H 6.54%, N 6.06%.

Found: C 59.68%, H 6.58%, N 5.94%.

Synthesis of the Piperidine Spaced Trimer:

4-(Piperidine dimer) piperacetamide **65**:⁴⁴

Compound **62** (1.25g, 4 mmol) and 1.26g (1.1 eq.) of **60** were dissolved in 20 ml of anhydrous dimethyl sulfoxide, under argon. To the latter solution 1.18g (5 eq.) of anhydrous potassium fluoride was added, and the mixture was heated to 130°C. After 2 days at this temperature the reaction mixture was cooled and precipitated into 200 ml of water. After drying under vacuum, and purification by column chromatography, a 72% yield of white solid **65**, mp = 208°C (dec.), was obtained.

¹H-NMR (d₆DMSO) δ 7.61 (d, 4H), 7.10 (m, 4H), 4.46 (bd, 1H), 4.08 (bd, 2H), 3.92 (bd, 1H), 3.42 (bs, 6H), 2.8-3.1 (m, 3H), 2.5-2.6 (m, 1H), 2.02 (s, 3H), 1.8-2.0 (bm, 4H), 1.2-1.6 (m, 10H).

¹³C-NMR (d₆DMSO) δ 168.8, 154.2, 153.4, 130.6, 123.3, 122.3, 113.9, 113.4, 60.3, 60.2, 47.9, 45.7, 44.6, 25.7, 25.0, 24.4, 24.1, 21.4.

IR (KBr) 2930, 1649, 1587, 1296, 1136 cm⁻¹.

Analysis Calculated: C 60.71%, H 6.85%, N 7.32%.

Found: C 59.68%, H 6.75%, N 7.01%.

4-(Piperidine dimer) piperidine **66**:

Compound **65** (1.2g, 2 mmol) was mixed in 10 ml of 2M aqueous hydrochloric acid, and this mixture was heated to reflux. The starting material eventually went into solution. After 17 hours at reflux, the solution was cooled and made basic (pH about 12) with 6M sodium hydroxide solution. The product was filtered and then dried under vacuum. The product was then eluted through 50g of silica gel using 50/50 methanol/chloroform (forerun discarded) to give a 99% yield of compound **66**. Compound **66** is a tan solid, mp = 155°C (dec.).

$^1\text{H-NMR}$ ($d_6\text{DMSO}$) δ 7.54 (m, 4H), 7.03 (d, 4H), 4.00 (bd, 2H), 3.35 (bs, 4H), 2.8-3.1 (m, 7H), 2.35 (bt, 2H), 1.87 (bd, 2H), 1.70 (bd, 2H), 1.35-1.60 (m, 8H), 1.27 (bq, 2H).
 $^{13}\text{C-NMR}$ ($d_6\text{DMSO}$) δ 153.9, 153.0, 130.3, 123.5, 122.2, 113.6, 113.2, 61.1, 59.9, 47.6, 45.6, 44.6, 25.9, 24.8, 24.2, 23.8.
 IR (KBr) 3436, 2930, 1588, 1136 cm^{-1} .

Piperidine spaced trimer **67**:⁴⁴

0.95g (1.8 mmol) of **66** and 0.41g (1.3 eq.) of p-fluorophenyl methyl sulfone **63** were dissolved in 10 ml of anhydrous dimethyl sulfoxide, under argon. Anhydrous potassium fluoride (0.52g, 5 eq.) was then added to the DMSO solution. This mixture was heated to 130°C. After 24 hours the reaction mixture was cooled and the product precipitated into 150 ml of water. After filtering and then drying under vacuum, the product was purified by column chromatography. A 35% yield of the trimer **67** was obtained as a white solid, mp = 200°C (dec.).

$^1\text{H-NMR}$ (CDCl_3) δ 7.5-7.6 (m, 6H), 6.84 (d, 6H), 3.92 (bd, 4H), 3.32 (bs, 4H), 2.7-3.1 (m, 9H), 2.05 (bd, 4H), 1.6-1.8 (m, 10H).
 $^{13}\text{C-NMR}$ (CDCl_3) δ 154.4, 153.5, 153.4, 130.6, 130.5, 129.0, 128.6, 123.9, 122.2, 114.2, 113.9, 113.2, 61.3, 48.2, 46.7, 46.5, 44.8, 25.1, 24.5, 24.1.

IR (KBr) 2929, 1590, 1503, 1292, 1142, 1088 cm^{-1}

Analysis Calculated: C 59.54%, H 6.32%, N 6.13%.

Found: C 59.57%, H 6.20%, N 5.87%.

Synthesis of the Piperidine Monomer:

N-(4-Phenyl methyl sulfone) piperidine **68**:⁴⁴

1g (5.7 mmol) of p-fluorophenyl methyl sulfone **63** was dissolved in 25 ml of piperidine, under argon. To the piperidine solution 1.65g (5 eq.) of anhydrous potassium fluoride was added. The mixture was stirred at 100°C for 22 hours. The mixture was then cooled and rinsed through a short plug of silica gel using ethyl acetate. The solvent and piperidine were

evaporated and the product was recrystallized from ethyl acetate/hexanes. The first crop gave a 76% yield of white crystals, mp = 115-116°C. A second crop afforded an additional 13% of **68** (total yield = 89%), mp = 114-116°C.

$^1\text{H-NMR}$ (CDCl_3) δ 7.66 (d, 2H), 6.85 (d, 2H), 3.30 (bs, 4H), 2.95 (s, 3H), 1.60 (bs, 6H).

$^{13}\text{C-NMR}$ (CDCl_3) δ 154.3, 128.9, 127.1, 113.5, 48.4, 44.8, 25.1, 24.1.

IR (KBr) 3005, 2927, 2870, 1587, 1399, 1292, 1136, 1093, 783 cm^{-1}

Analysis Calculated: C 60.22%, H 7.16%, N 5.85%.

Found: C 60.55%, H 7.37%, N 5.69%.

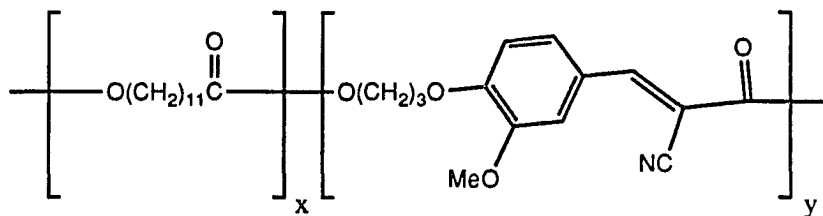
CHAPTER 3

NEW NONLINEAR OPTICAL POLYMERIC MATERIALS

Poly{4'-carboalkoxy-4-methoxy- α '-cyano- α -aminostilbenes}

The work of Hall and coworkers showed that a tractable AB copolymer could exhibit a large second order enhancement (see Chapter 1). In addition to this potentially great enhancement there are other benefits from having this main chain chromophore.^{39,40} First, a large density of chromophore (NLO) units can be obtained; this would lead to a material with high second order susceptibilities ($\chi^{(2)}$). Also, by arranging the NLO units in a head to tail fashion a more stable assembly should result, as compared to placing the chromophores in the pendant of a comb polymer.^{32,39} However, alignment of the entire main chain chromophore may be difficult to obtain.³² If tractable main chain chromophoric polymers with high glass transition temperatures can be obtained, processing methods may be able to form a bulk material in which there is a high degree of the appropriate orientation. For example, extrusion and electric poling methods may form films which would be useful in optical devices.

Hall and coworkers observed an enhancement for a copolymer 9 formed from the copolymerization of the NLO chromophore with methyl ω -hydroxydodecanoate.

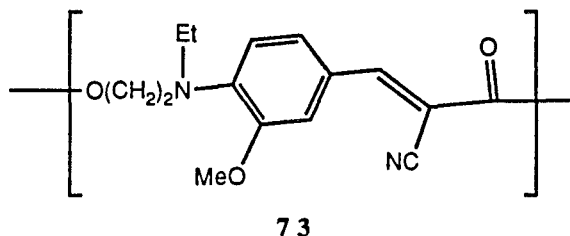


9

The enhancement most likely arises from the dipole-dipole interaction which occurs when two or more of the chromophores condense with each other. The dodecanoate comonomer probably does not contribute to the dipole-dipole stabilization, thus is not at all accountable for the enhancement. So if homopolymer can be formed a greater enhancement may be observed. And even if no enhancement is observed, the higher

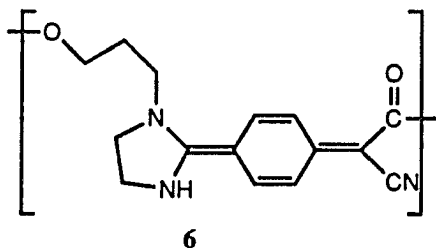
density of the NLO units should lead to materials with large second order susceptibilities. This then becomes the highest priority: To form an AB homopolymer with the chromophore in the main chain.

Intimately coupled with the desire for homopolymer is the necessity of forming tractable polymer. Researchers at AT&T Bell Laboratories,⁴³ as well as Hall and coworkers,^{37,38} have reported the synthesis of various main chain chromophore homopolymers. However, all the homopolymers synthesized by these groups have been insoluble in all but the most harsh solvents. Recently, Stenger-Smith and coworkers reported the synthesis of 4-amino- α -cyanocinnamic polyesters (73) which were soluble in common solvents.⁶⁴

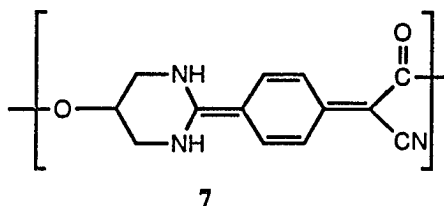


While forming homopolymers in the main chain tends to form intractable systems, the latter work indicates that careful design can yield the desired goals.

Another problem which is related to having the strong dipoles in the main chain of a homopolymer is the formation of crystalline regions. For example, the quinodimethane type homopolymers (6 and 7) synthesized by Hall *et al.* showed only crystalline melts at 86°C (by differential scanning calorimetry).³⁷

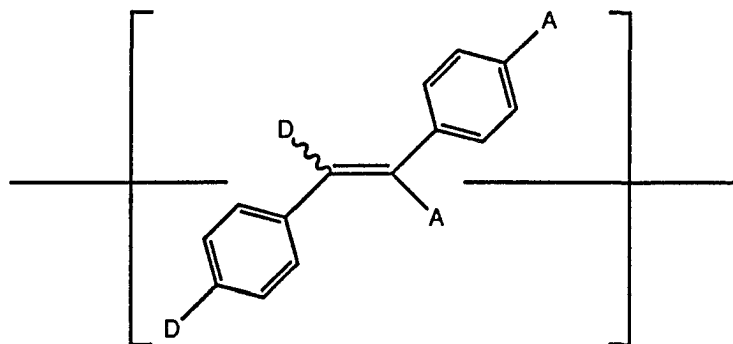


and,



Interestingly, the tractable cinnamate copolymer 9 synthesized by Hall and coworkers could be cast into glassy films. However upon heating and stretching the film it became opaque, indicating the formation of crystalline regions.³⁸ Polymers with high glass transitions would be more processable and form glassy, optically clear NLO materials. To date, the highest glass transition reported for a homopolymer is 90°C for the cinnamic polyesters 73 synthesized by Stenger-Smith *et al.*,⁶⁴ and the recent work with main chain *p*-aminophenyl sulfones ($T_g = 92^\circ\text{C}$) by Robello *et al.*³² So it is important to form polymers with high glass transition temperatures, which would contribute not only to processability, but also increase the temperature range at which these materials would be useful.

This then, is the desired outcome of this research: Tractable homopolymer, with a high glass transition temperature. To obtain the desired polymer it was decided to pursue the type of stilbene unit depicted in Scheme 30.

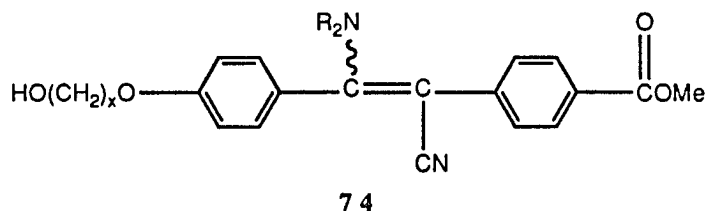


E and Z Isomers

Scheme 30. Generic Target Stilbene Polymer.

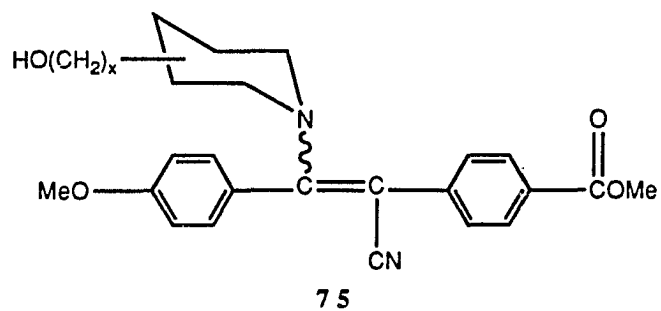
By polymerization of the E and Z mixture of isomers there should be enough irregularity along the polymer backbone to prevent the formation of crystalline regions. This lack of regular structure should also help to form a tractable polymer. Also, if the correct balance between alkyl substituents (R groups in **74**) and the NLO chromophores can be derived, it should be possible to maximize the glass transition.

The polymerizable units were originally placed at the 4 and 4' positions on the stilbene system. The other donor and acceptor moieties were chosen to be amino and cyano, respectively. These units were chosen because of their known strong donor and acceptor abilities. Thus the original target AB monomer became a 4'-carbomethoxy-4-hydroxyalkoxy- α' -cyano- α -aminostilbene **74**.



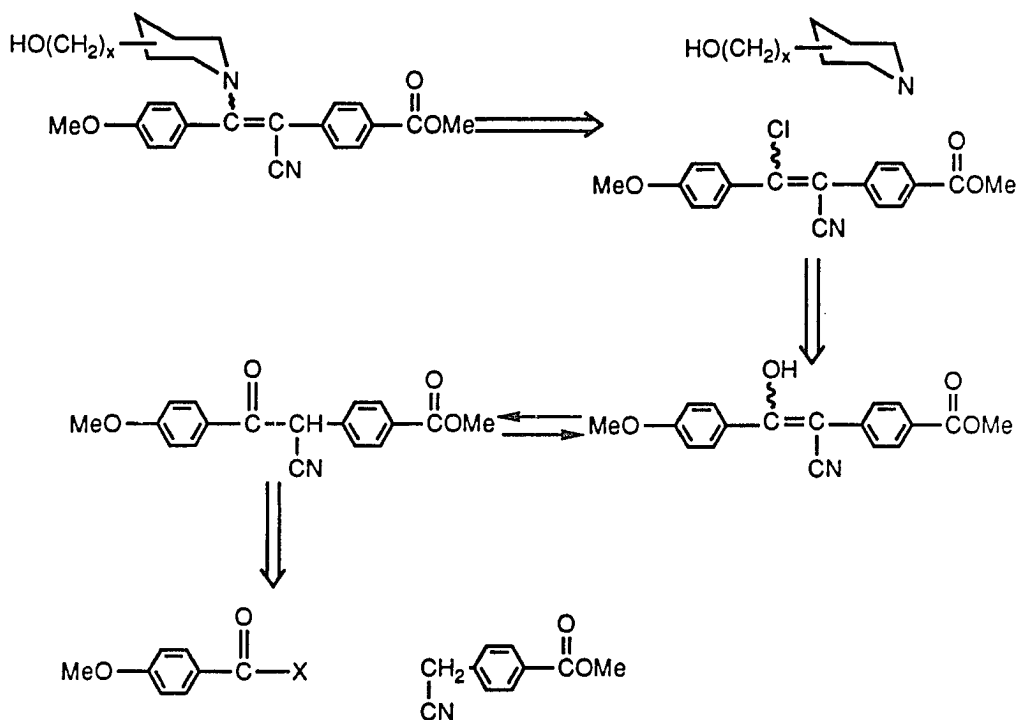
Later, the synthesis was shortened by placing the hydroxyl substituent at the end of an alkyl spacer attached to the amino moiety. Because various hydroxypiperidines are commercially available it was

decided to use these compounds as a hydroxy--spacer--amine. All these factors led to the choice of the target monomers **75**.



Retrosynthesis

Previous work by Moore and Robello,⁶⁵ as well as much work by Rappoport,^{66,67} indicated that the chloride in the activated vinylic system could be easily displaced by one of our hydroxypiperidines (see Scheme 31).

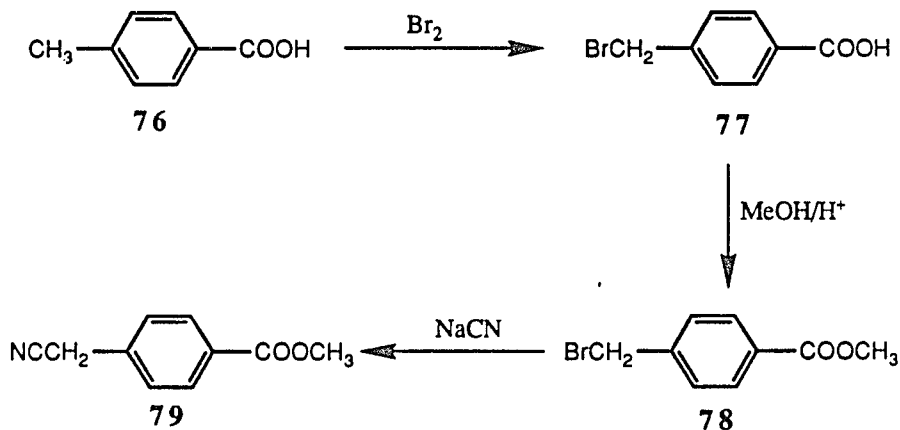


Scheme 31. Retrosynthesis of the Stilbene Monomers.

It was also known that the vinyl chloride could be made from the enol.^{68,69} The enol is, of course, a tautomer of the ketone, which should be accessible from a crossed Claisen condensation. The two starting materials could be easily synthesized, or perhaps even purchased.

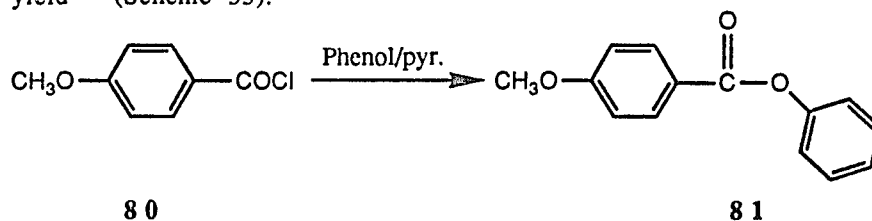
Synthesis

The synthesis of the amino cyanostilbene began with the construction of the two halves: a *p*-anisate and methyl α -cyano-*p*-toluate. Methyl α -cyano-*p*-toluate (**79**) was synthesized in three steps (see Scheme 32) starting from *p*-toluic acid⁷⁰ (**76**, Aldrich). First, *p*-toluic acid was brominated in the benzylic position via a free radical bromination to give α -bromo-*p*-toluic acid (**77**) in 50% yield. Then the acid was converted to the methyl ester **78** in 70% yield by a standard acid catalyzed esterification. The nitrile unit was added by nucleophilic substitution of the benzylic bromide with cyanide anion to give a 70% yield of compound **79**.



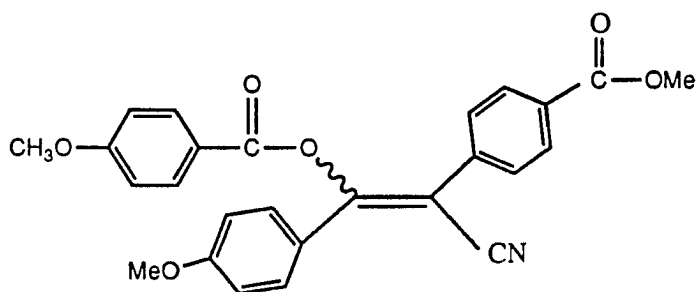
Scheme 32. Synthesis of Acceptor Half of the Stilbene Monomer.

p-Anisyl chloride **80** (Aldrich) was converted to the phenyl ester **81** using a phenol/pyridine solution. Phenyl *p*-anisate (**81**) was obtained in a 71% yield⁷¹ (Scheme 33).



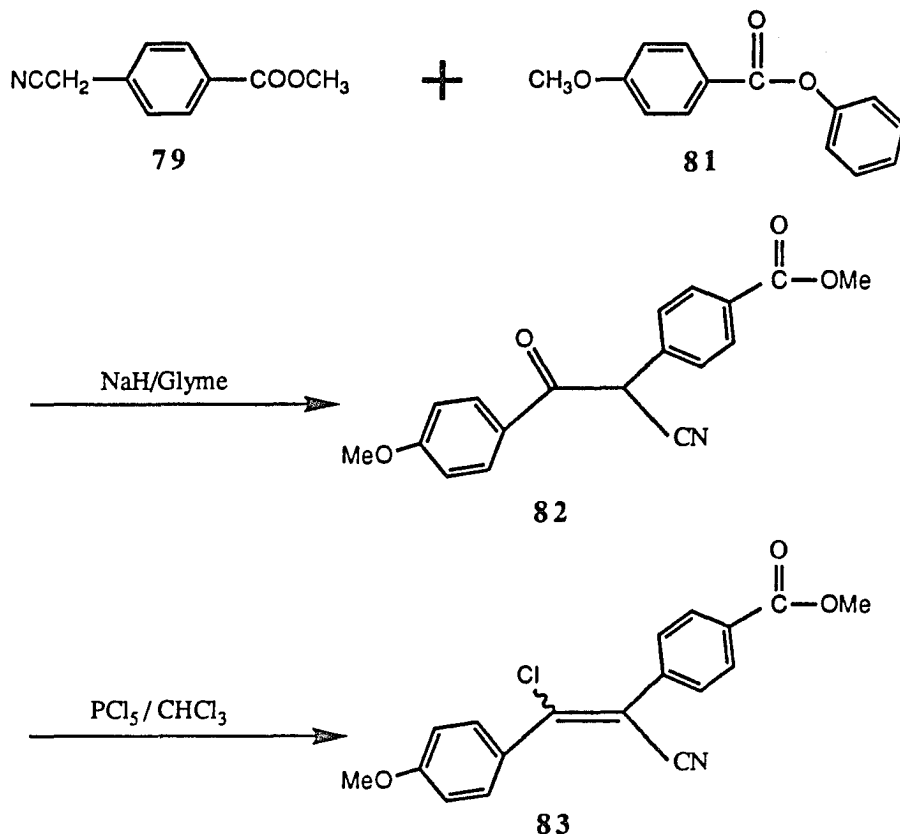
Scheme 33. Synthesis of Donor Half of the Stilbene Monomer.

The coupling of compounds **79** and **81** was accomplished via a crossed Claisen condensation (Scheme 34). One of the activated protons on **79** was removed with sodium hydride. The resulting anion then displaces the more stable phenolate anion from compound **81**. After acidic workup and purification a typical yield of 67% was obtained for the enol of **82**. Originally, the condensation of the chloride from *p*-anisyl chloride in a similar coupling to form **82** was attempted.⁶⁸ However, after the first condensation the resulting ketone **82** then readily lost another proton to form the enolate. This enolate quickly attacked another molecule of *p*-anisyl chloride to give vinyl ester **84**.



84

We then decided to use a less reactive acid derivative, methyl *p*-anisate, available from Aldrich. However, this compound did not react under any condensation conditions to give product **82**. Thus, the compound of intermediate reactivity, the phenyl ester **81**, was then chosen, which afforded the condensation product **82** in 67% yield.



Scheme 34. Synthesis of the Vinyl Chloride 83.

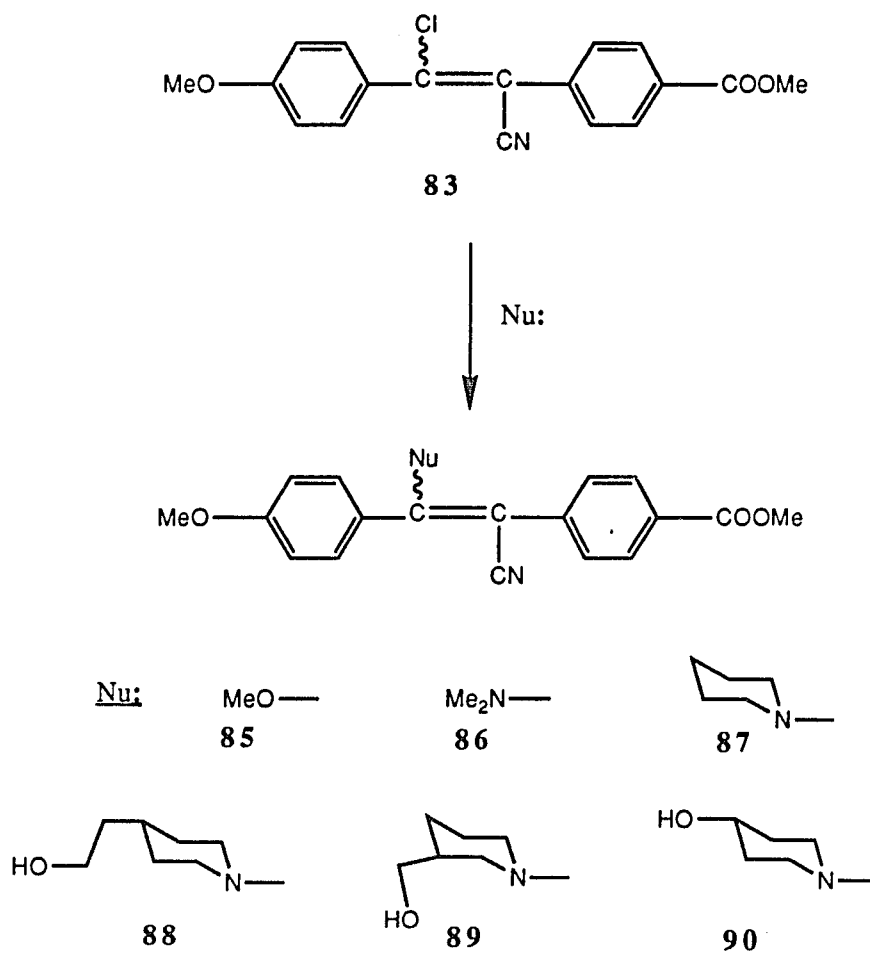
Compound 82 is very interesting. It appears to exist as the enol in the solid state, as indicated by the strong, broad -OH stretch at 3063 cm^{-1} in the infrared spectrum (KBr pellet). Also, in polar solvents, such as dimethylsulfoxide (DMSO); it appears to exist as the enol. This is apparent from the lack of the alkyl CH peak in the carbon NMR attached proton test (APT), as well as the absence of one hydrogen in the proton NMR (in d_6 -DMSO). The absence of the proton indicates that it is in an exchangeable form, in other words it is an hydroxyl proton. Also, both the proton and carbon NMR's show the presence of both E and Z isomers. However, in nonpolar solvents compound 82 exists as the ketone. This is clear from the NMR of 82 in chloroform: The carbon APT shows a CH peak at $\delta\ 45.7$, and the

proton shows as a sharp singlet at δ 5.61 corresponding to the one hydrogen. Also, the NMR spectrum in chloroform shows the presence of only one compound, not a mixture of isomers as was detected in d_6 -DMSO.

The enol **82** was converted to the vinyl chloride **83** with phosphorus pentachloride in methylene chloride^{68,69}. Many reagents and conditions were evaluated before these conditions were found to be optimal. A yield of 73% was obtained. The vinyl chloride then became the keystone compound from which all monomers and model compounds of this series were derived.

Initially a great deal of work was done on placing the polymerizable hydroxyl moiety at the end of a spacer attached to the 4-oxy substituent of the stilbene system. These compounds were derived from 4-hydroxybenzoic acid. In this synthesis it was necessary for the hydroxyl end to be protected because of the harsh conditions associated with both the coupling and the formation of the vinyl chloride. These aspects led to a complicated synthesis which quickly became very difficult. At this point it was decided to place the polymerizable hydroxyl at the end of a spacer attached to the amine nitrogen. This decision was made with the knowledge that the secondary amine is a better nucleophile than the hydroxyl under neutral conditions, and that various hydroxypiperidines are commercially available. The benefits of this route are a shorter, simpler synthesis to monomer (one step from **83**), and greater synthetic flexibility. This synthetic flexibility facilitated structural modifications which made it possible to fine tune the macroscopic polymer properties, simply by choosing different hydroxyamines.

The vinyl chloride **83** was then used in the preparation of various model compounds and monomers (see Scheme 35). The α -methoxystilbene (**85**) was easily prepared by dissolution of **83** in sodium methoxide/methanol solution and refluxing. Compound **85** was obtained in 76% yield as a mixture of E and Z isomers. The more prevalent isomer is assumed to be the more stable E isomer ("trans" stilbene). Analogous compounds prepared by Rappoport indicate that the protons on the vinylic methoxy of the Z isomer should be shifted further downfield as compared with the E isomer.^{66,72} This then indicates that the minor isomer ($C=C-OCH_3$, 3.69ppm)



Scheme 35. Synthesis of Stilbene Monomers and Monomer Analogues.

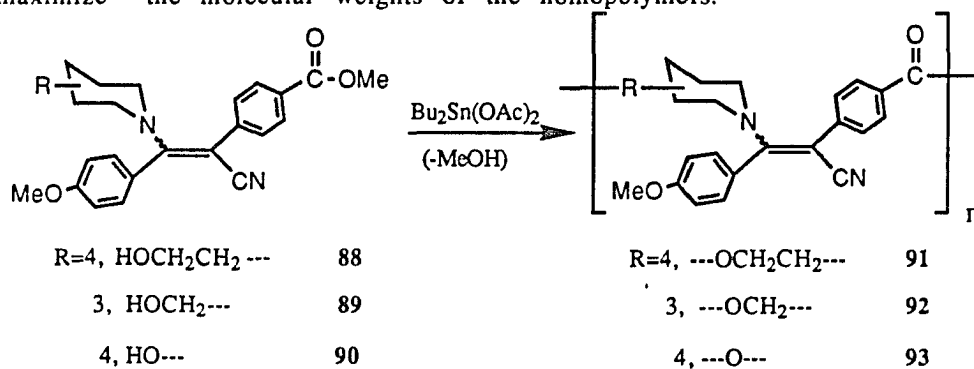
is the Z isomer, and the major product ($C=C-OCH_3$, 3.62 ppm) is the E isomer. Compound **83** was also reacted with an excess of dimethylamine in methylene chloride at room temperature to give the α -dimethylamino-stilbene **86** in very high yield. The product was obtained as an approximately 50/50 mixture of E and Z isomers.

Also, we attempted the substitution of the vinyl chloride **83** with diethylamine. However, even in a large excess in refluxing chloroform there was no reaction. This is due to the relatively bulky ethyl substituents decreasing the amines' nucleophilicity. Also, we attempted to synthesize the vinyl thioether from compound **83** and the sodium salt of butanethiol. However, these conditions deprotected the ester in the 4'-position, so this derivative was not made.

The piperidine analog **87** and all the monomers **88-90** were prepared by a similar method.⁶⁵ Compound **83** was refluxed in acetonitrile with 2-4 equivalents of the piperidine compounds to give all the desired enamines in typical yields of 95%. Compounds **87-90** were all isolated as roughly 50/50 mixtures of their E and Z isomers (determined by 1H NMR). The synthesis of all the enamines could be followed very easily by TLC because the products were all bright yellow.

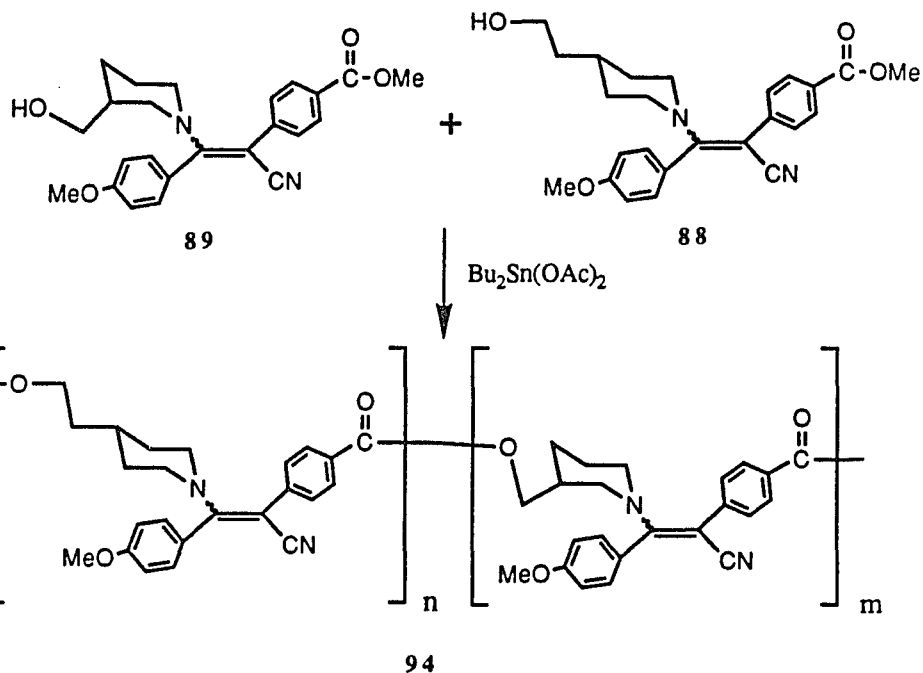
Polymer Synthesis

The monomers (88-90) were all polymerized by condensation polymerizations, with the loss of methanol (Scheme 36). The catalyst used was dibutyltin diacetate in a concentration of 2 mole percent. The polymerizations were carried out in a neat melt, two stage polycondensation.³⁸ First, heating at 100°C for one hour allows the formation of nonvolatile oligomers. The reaction mixture is then heated to 170-190°C and placed under high vacuum (about 0.4 mmHg). Fortunately, all the polymers (91-93) were soluble in chloroform which allowed for purification by precipitation in methanol. There was no attempt made to maximize the molecular weights of the homopolymers.



Scheme 36. Homopolymer Synthesis.

The copolymerization between monomers 88 and 89 was carried out under conditions designed to produce high molecular weight copolymer (see Scheme 37). To this end less catalyst was used, 0.3 mole percent dibutyltin diacetate. The heating sequence consisted of three steps. The first step and second step reaction times and temperatures were as in the homopolymerizations. To help increase molecular weight a third step was added, heating at 220°C under vacuum. Less catalyst and higher temperatures did afford copolymer of higher molecular weight than the homopolymers. The yield of copolymer 94 was 90%.



Scheme 37. Copolymer Synthesis.

All of the compounds synthesized were purified by either chromatography or recrystallization. The compounds were characterized by proton and carbon NMR and infrared spectroscopies. The polymers were all purified by precipitation and characterized by proton and carbon NMR, and infrared spectroscopies, as well as differential scanning calorimetry and size exclusion chromatography.

Measurements and Discussion

The synthesis of all the monomers worked quite well with overall yields of 33%. Compound 87 did have its hyperpolarizability evaluated by our collaborators at Eastman Kodak, and a value of $\mu\beta_x = 612 \times 10^{-48}$ esu was found. The ground state dipole moment was measured as described in Chapter 4, and found to be 7.07 Debye. Dividing the quantity $\mu\beta_x$ by the

dipole moment gives the value of the hyperpolarizability (β_x) as 87×10^{-30} esu. For reference, 4-N,N-dimethylamino-4'-nitrostilbene has a hyperpolarizability of $\beta_x = 450 \times 10^{-30}$ esu, which is very high. While the monomer analogue is not the best, it does have a respectable NLO activity. The polymer may have a huge hyperpolarizability due to the mere density of NLO-phoric units.

The polymerizations did supply material with the physical properties that were desired; the results are listed in Table 7.

Table 7. Physical Characteristics of NLO Polymers.

Polymer	M_w	M_n	PDI	$T_m(^{\circ}\text{C})$	$T_g(^{\circ}\text{C})$	Yield(%)
91	6270	4860	1.3	---	167	80
92	6750	5190	1.3	176	---	72
93	4720	3960	1.2	185	---	43
94	30200	12800	2.4	---	187	92

All of the homo- and copolymers were readily soluble in chloroform and acetone. The molecular weights of the homopolymers were not maximized. However, the copolymer was subjected to harsher conditions and less catalyst which gave polymer of molecular weight 30,200. Recent work by Robello *et al.*³² indicates that molecular weights of this magnitude are optimal. Lower molecular weights give more brittle polymers, and higher molecular weights make it too difficult to pole the bulk polymer.³² Only polymers 91 and 94 showed glass transitions (167 and 187°C, respectively), but these were very high. In fact, these are the highest glass transitions reported to date for a NLO polymer with the chromophore in the main chain. Both 92 and 93 only showed melt temperatures (176 and 185°C, respectively). This was not surprising for polymer 93 because of the rigid 4-oxypiperidine spacer. However, we expected the more unsymmetrical 3-methyleneoxypiperidine polymer 92 to possess a glass transition.

As expected, the polymer yields increased with time and temperature, except for polymer 93. This was not surprising because the secondary

alcohol of the monomer **90** can more easily eliminate, which would give lower yields of polymer with lower molecular weight. Also, the polymer **93** was not as thermally stable as the other polymers. The differential scanning calorimeter (DSC) characterization of polymer **93** showed decomposition exotherms above 220°C. Polymers **91**, **92**, and **94** were all stable to at least 300°C (the materials were not evaluated above 300°C).

These polymers, particularly **91** and **94**, are excellent candidates for further studies of their NLO efficiencies. The minor drawback of these materials would be that they possess two strong absorptions at 286 and 370 nm (see Table 8). This of course limits the optical range of usefulness for these materials, but there are still large areas of transparency.

Table 8. UV/Visible Data of Monomers and Polymers.

Compound	λ (nm) ^a	ϵ (cm ⁻¹ M ⁻¹)
88	286	5,340
	370	5,920
91 ^b	288	218,000
	372	257,000
89	288	3,420
	370	3,610
92 ^b	288	113,000
	370	133,000
90	286	14,700
	366	16,600
93 ^b	288	233,000
	370	276,000
94 ^b	288	2,080,000
	372	2,520,000

a. Spectral range 250-850 nm, in chloroform.

b. Values calculated from SEC molecular weights (see Table 7).

Experimental

General Methods

See **Experimental** section of Chapter 2. Differential scanning calorimetry (DSC) data were collected using a Perkin-Elmer DSC-4. Molecular weights were determined using size exclusion chromatography (SEC), which used a Beckman HPLC pump and UV detector with Showdex SEC columns, and evaluated as compared to polystyrene standards.

Synthesis

Methyl α -cyano-*p*-toluate (**79**):

Compound **79** was synthesized in three steps from *p*-toluic acid by the procedure of J.F. Codington and E. Mosettig.⁷⁰

Phenyl *p*-anisate (**81**):⁷¹

Phenol (1.04 g, 11 mmole) was dissolved in 8 ml of pyridine. A solution containing 1.70 g (10 mmole) of *p*-anisyl chloride **80** in 5 ml of chloroform was added dropwise to the phenol solution. The resulting mixture was stirred overnight. The next day 20 ml of chloroform was added, and the solution was extracted with 10% aqueous hydrochloric acid to until all the pyridine was removed. After many acid washes, the organic phase was washed once with water and then dried over anhydrous magnesium sulfate. The solvent was then evaporated and the product recrystallized from 95% ethanol to give a 71% yield of white crystalline **81**, mp=73-74°C (lit. mp=75-76°C).

¹H-NMR (CDCl₃) δ 8.13 (d, 2H), 7.3-7.4 (m, 2H), 7.15-7.25 (m, 3H), 6.94 (d, 2H), 3.81 (s, 3H).

¹³C-NMR (CDCl₃) δ 164.7, 163.8, 150.9, 132.1, 129.3, 125.6, 121.7, 113.7, 55.3.

IR (Melt) 3057, 2966, 2929, 2838, 1725 cm⁻¹

4'-Carbomethoxy-4-methoxy- α '-cyano- α -hydroxystilbene (**82**):⁷³

Compound **79** (7.5 g, 43 mmole) and compound **81** (10 g, 43 mmole) were dissolved in 50 ml of anhydrous glyme. This solution was dripped, by

cannulation, into a slurry containing 2 g (87 mmole) of sodium hydride in 20 ml of anhydrous glyme which had been chilled with an ice bath. The addition took 40 minutes, and everything was kept under argon. The glyme solution was stirred at room temperature for 20 hours. The glyme solution was then cooled in an ice bath and made acidic by the dropwise addition of 5% aqueous hydrochloric acid. At first a purple oil forms, but as the solution becomes more acidic the oil changes to a yellow precipitate. This precipitate was filtered and recrystallized twice from methanol to give a 67% yield of white crystalline product. Compound **82** is a mixture of E and Z enol isomers (mp=120-125°C).

¹H-NMR (d₆DMSO) Major isomer: δ 8.0 (d, 2H), 7.92 (d, 2H), 7.65 (d, 2H), 7.08 (d, 2H), 3.84 and 3.83 (2s, 6H).

Minor isomer: δ 7.75 (d, 2H), 7.25 (d, 2H), 7.11 (d, 2H), 6.90 (d, 2H), 3.79 (s, 3H), 3.75 (s, 3H).

¹³C-NMR (d₆DMSO) δ 170.0, 166.0, 161.3, 138.3, 131.0, 130.5, 130.3, 129.4, 127.5, 127.2, 120.7, 114.0, 113.8, 87.0, 55.5, 52.1.

¹H-NMR (CDCl₃) δ 7.96 (d, 2H), 7.87 (d, 2H), 7.46 (d, 2H), 6.85 (d, 2H), 5.70 (s, 1H), 3.83 (s, 3H), 3.77 (s, 3H).

¹³C-NMR (CDCl₃) δ 186.6, 165.9, 164.5, 135.4, 131.7, 131.6, 130.4, 128.2, 125.9, 116.3, 114.2, 55.4, 52.1, 45.7.

IR (KBr) 3063, 2217, 1712, 1589, 1512, 1280 cm⁻¹

Analysis Calculated: C 69.90%, H 4.85%, N 4.53%

Found: C 69.87%, H 4.81%, N 4.44%

4'-Carbomethoxy-4-methoxy-α'-cyano-α-chlorostilbene (**83**):^{68,69}

The enol **82** (8 g, 26 mmole) was dissolved in 70 ml of methylene chloride and this solution was cooled in an ice bath. Phosphorus pentachloride (5.5 g, 1 eq.) was added, and after 0.5 hour the solution was allowed to warm to room temperature. After stirring for another hour, 3 g (14 mmole) of additional phosphorus pentachloride was added. The reaction was then stirred at room temperature for 15 hours, and then was quenched with 50 g of ice. The organic layer was extracted with 1M aqueous sodium hydroxide solution, followed by a brine extraction. The methylene chloride

layer was then dried over anhydrous sodium sulfate. Filtration followed by evaporation of the solvent gave a crude product which was purified by chromatography (15% ethyl acetate, 85% hexanes). Compound **83** was isolated as a yellow solid which contained a mixture of E and Z isomers. The product, obtained in a 73% yield, had mp=89-105°C.

¹H-NMR (CDCl₃) Major isomer: δ 7.93 (d, 2H), 7.29 (d, 2H), 7.19 (d, 2H), 6.75 (d, 2H), 3.90 (s, 3H), 3.79 (s, 3H).

Minor isomer: δ 8.12 (d, 2H), 7.79 (d, 2H), 7.69 (d, 2H), 6.98 (d, 2H), 3.95 (s, 3H), 3.88 (s, 3H).

¹³C-NMR (CDCl₃) δ 166, 162 and 161.6, 148.9, 138 and 137.4, 131.4 and 130.6, 130.2, 129.9 and 129.8, 129.3, 128.5 and 126.7, 118 and 117.3, 113.9, 111.5, 55.4 and 55.3, 52.2.

IR (KBr) 2213, 1719, 1602, 1285, 1262, 1188 cm⁻¹

Analysis Calculated: C 65.96%, H 4.31%, N 4.27%, Cl 10.82%.

Found: C 65.68%, H 4.10%, N 4.15%, Cl 11.02%

4'-Carbomethoxy-4-methoxy-α'-cyano-α-methoxystilbene (**85**):⁶⁶

Compound **83** (0.2 g, 0.6 mmole) was mixed with 5 ml of freshly prepared 0.2 M sodium methoxide/methanol solution. This mixture was refluxed for one hour. After cooling, the reaction mixture was dripped into 20 ml of saturated sodium bicarbonate solution. The aqueous mixture was thoroughly extracted with ethyl ether, and the combined organic extracts were dried over anhydrous sodium sulfate. After filtering and evaporating the ether, very pure product was obtained as a mixture of E and Z isomers. Compound **85** was isolated as a yellow solid, mp=104-114°C, in 76% yield.

¹H-NMR (CDCl₃) δ 8.02 (d, 2H), 7.80 (d, 2H), 7.47 (d, 2H), 7.02 (d, 2H), 7.10 and 6.80 (2d from the minor isomer), 3.90 (s, 3H), 3.84 and 3.79 (s, 3H), 3.69 and 3.62 (s, 3H).

¹³C-NMR (CDCl₃) δ 171.8, 166.5, 161.7, 137.0, 130.8 and 131.5, 129.7 and 129.0, 128.8, 128.0, 123.8, 119.8, 114.6 and 114.4, 94.8, 59.1, 55.5, 52.2.

IR (KBr) 2958, 2204, 1712, 1279, 1251 cm⁻¹

Analysis Calculated: C 70.58%, H 5.30%, N 4.33%.

Found: C 70.66%, H 5.13%, N 4.24%.

Pure E isomer of **85** was obtained by recrystallization from ethanol to yield white crystals, mp=117-118°C, in a 55% recovery.

¹H-NMR (CDCl₃) δ 8.02 (d, 2H), 7.80 (d, 2H), 7.47 (d, 2H), 7.01 (d, 2H), 3.91 (s, 3H), 3.86 (s, 3H), 3.63 (s, 3H).

4'-Carbomethoxy-4-methoxy-α'-cyano-α-(N,N-dimethylamino)stilbene (**86**):

Compound **83** (0.2 g, 0.61 mmole) was dissolved in 1 ml of 3 M dimethylamine/methylene chloride solution at 0°C. After 2 hours 9 ml more of the 3 M dimethylamine solution was added, and the mixture was allowed to warm to room temperature. This solution was stirred overnight, and then filtered through a plug of silica gel, rinsing with acetonitrile. After evaporation of the solvent, the product was purified by chromatography (30% ethyl acetate in hexanes) to give a 90% yield of **86**. Compound **86** was isolated as a mixture of E and Z isomers. The yellow solid had mp=158-160°C.

¹H-NMR (CDCl₃) δ 7.93, 7.60, 7.41, 7.19, 7.06, 6.90, 6.70 (7d, 8H), 3.84, 3.78, 3.75, 3.71 (4s, 6H), 3.06 and 2.64 (2s, 6H).

¹³C-NMR (CDCl₃) δ 166.9, 166.7, 165.3, 163.5, 161.8, 161.3, 142.2, 141.7, 132.7, 132.1, 129.4, 129.0, 128.1, 127.6, 126.8, 126.1, 125.5, 123.4, 121.8, 114.1, 82.6, 80.9, 55.3, 55.2, 52.0, 51.7, 43.6, 43.1.

IR (KBr) 2933, 2183, 1713, 1272 cm⁻¹

Analysis Calculated: C 71.41%, H 5.99%, N 8.33%.

Found: C 71.23%, H 6.03%, N 8.02%.

4'-Carbomethoxy-4-methoxy-α'-cyano-α-piperidinostilbene (**87**):⁶⁵

Compound **83** (0.20 g, 0.61 mmole) was dissolved in 1 ml of acetonitrile (anhydrous) with 0.12 g of piperidine (2.1 eq.). This solution was refluxed for 3 hours under argon. After cooling, the reaction mixture was filtered through a plug of silica gel, rinsing with acetonitrile to insure complete recovery. The solvent was then evaporated, and the product was purified by chromatography. A 90% yield of compound **87** was obtained as a mixture of E and Z isomers. The product was a yellow solid, mp=161-162°C.

$^1\text{H-NMR}$ (CDCl_3) δ 8.02, 7.68, 7.55, 7.25, 7.18, 7.00, 6.78 (7d, 8H), 3.91, 3.86, 3.83, 3.78 (4s, 6H), 3.42 and 2.84 (2bs, 4H), 1.72 and 1.59 (2bs, 6H).

$^{13}\text{C-NMR}$ (CDCl_3) δ 167.2, 167.0, 165.8, 164.0, 162.2, 161.6, 142.4, 142.0, 132.5, 131.9, 129.6, 129.1, 128.4, 128.1, 127.5, 126.9, 126.7, 125.8, 123.5, 121.9, 114.2, 83.4, 81.6, 55.4, 55.3, 52.7, 52.2, 52.0, 51.9, 26.8, 26.6, 24.0, 23.8.

IR (KBr) 2932, 2181, 1709, 1276, 1251 cm^{-1}

Analysis Calculated: C 73.38%, H 6.43%, N 7.44%.

Found: C 72.89%, H 6.66%, N 7.12%.

4'-Carbomethoxy-4-methoxy- α' -cyano- α -(4-ethanolpiperidino)stilbene (88):⁶⁵

The procedure was the same as for the synthesis of compound 87. Here, 1 g (3 mmole) of 83 and 1.2 g (3 eq.) of 4-piperidinoethanol were dissolved in 20 ml anhydrous acetonitrile under argon. The solution was refluxed for 48 hours, and then worked up as in the previous procedure. After purification by chromatography a 95% yield of yellow solid, mp=77-78°C, was obtained. Compound 88 was isolated as an approximately 50/50 mixture of the E and Z isomers.

$^1\text{H-NMR}$ (CDCl_3) δ 7.94, 7.62, 7.47, 7.18, 7.10, 6.92, 6.72 (7d, 8H), 3.85, 3.80, 3.77, 3.67 (4s, 6H), 3.5-3.7 (m, 3H), 3.15 (bt, 1H), 2.99 (bd, 1H), 2.62 (bt, 1H), 2.02 (bs, 1H), 1.1-1.8 (m, 7H).

$^{13}\text{C-NMR}$ (CDCl_3) δ 166.8, 166.7, 165.1, 163.5, 161.9, 161.3, 142.2, 141.6, 132.4, 131.8, 129.4, 129.0, 128.1, 127.4, 126.8, 126.5, 125.5, 123.3, 121.8, 114.1, 83.4, 81.7, 60.2, 59.7, 55.2, 55.1, 51.9, 51.7, 51.3, 38.8, 38.7, 33.0, 32.9, 32.0, 31.7.

IR (KBr) 3441, 2925, 2183, 1712, 1601, 1503, 1278, 1254, 1017 cm^{-1}

Analysis Calculated: C 71.41%, H 6.71%, N 6.66%.

Found: C 69.68%, H 6.49%, N 6.40%.

4'-Carbomethoxy-4-methoxy- α '-cyano- α -(3-hydroxymethylpiperidino)-stilbene (**89**):⁶⁵

The procedure was the same as for the synthesis of compound **87**. Here, 1 g (3 mmole) of **83** and 1.13 g (3.2 eq.) of 3-piperidinomethanol were dissolved in 20 ml anhydrous acetonitrile, under argon. The solution was refluxed for 48 hours, and then worked up as for compound **87**. After purification by chromatography a 95% yield of yellow solid was obtained, mp=86-90°C. Compound **89** was isolated as an approximately 50/50 mixture of the E and Z isomers.

¹H-NMR (CDCl₃) δ 8.00, 7.67, 7.52, 7.24, 7.15, 6.97, 6.77 (7d, 8H), 3.91, 3.85, 3.82, 3.77 (4s, 6H), 2.9-3.6 (m, 4H), 2.4-2.7 (m, 1H), 2.14 (bs, 1H), 1.5-2.0 (m, 4H), 1.1-1.4 (m, 1H).

¹³C-NMR (CDCl₃) δ 166.9, 166.7, 165.4, 163.7, 161.9, 161.3, 142.1, 141.6, 132.4, 131.8, 129.5, 129.0, 128.1, 127.3, 126.9, 126.4, 125.5, 123.3, 122.2, 114.1, 83.7, 81.6, 64.9, 64.7, 55.2, 55.1, 54.9, 52.4, 51.9, 51.7, 39.8, 39.5, 26.8, 26.4, 25.7, 25.4.

IR (KBr) 3447, 2933, 2184, 1713, 1601, 1508, 1433, 1278, 1253 cm⁻¹

Analysis Calculated: C 70.92%, H 6.45%, N 6.89%.

Found: C 67.52%, H 6.19%, N 6.67%.

4'-Carbomethoxy-4-methoxy- α '-cyano- α -(4-hydroxypiperidino)stilbene (**90**):⁶⁵

The procedure was the same as for the synthesis of compound **87**. Here, 1 g (3 mmole) of **83** and 1.0 g (3.2 eq.) of 4-hydroxypiperidine were dissolved in 20 ml anhydrous acetonitrile, under argon. The solution was refluxed for 48 hours, and then worked up as for compound **87**. After purification by chromatography a 100% yield of yellow solid, mp=93-97°C, was obtained. Compound **90** was isolated as an approximately 50/50 mixture of the E and Z isomers.

¹H-NMR (CDCl₃) δ 8.01, 7.69, 7.53, 7.26, 7.16, 6.78 (6d, 6H), 6.96-7.01 (m, 2H), 3.6-4.0 (m, 7H), 3.3 (m, 1H), 3.1 (m, 1H), 2.7 (m, 1H), 2.5 (bd, 1H), 1.5-2.1 (m, 5H).

^{13}C -NMR (CDCl_3) δ 166.9, 166.7, 165.1, 163.4, 162.0, 161.4, 141.9, 141.5, 132.4, 131.7, 129.6, 129.0, 128.1, 128.0, 127.4, 127.1, 126.3, 125.7, 123.2, 121.7, 114.2, 83.9, 82.4, 66.4, 66.0, 55.3, 55.2, 52.0, 51.8, 48.7, 48.3, 34.8, 34.6.

IR (KBr) 3431, 2946, 2183, 1714, 1600, 1508, 1278, 1253 cm^{-1}

Analysis Calculated: C 70.39%, H 6.16%, N 7.14%.

Found: C 65.88%, H 5.83%, N 6.64%.

4'-Carbomethoxy-4-methoxy- α' -cyano- α -aminostilbene polyesters (**91**, **92**, and **93**):³⁸

A dry 10 ml conical flask was fitted with a distilling adapter. The top of the distilling adapter had a rubber collar in which a pipet with a capillary tip could fit tightly. The pipet tip was long enough to reach the bottom of the flask. The pipet top was connected to an argon inlet. The arm of the distilling adapter was connected to a three way stopcock which could be switched between a bubbler and vacuum. The monomer (**88**, **89**, or **90**; 1.2 mmole) and 6 μl (24 μmole) of dibutyltin diacetate were mixed in the flask, and the argon flowed through the mixture and apparatus. Polymerization was then allowed to occur at 100°C for 1 hour. The mixture was then heated to 170-190°C, and the pipet then removed and the top of the adapter stoppered. The reaction was placed under vacuum (about 0.4 mmHg). The polymerization was allowed to proceed for 1.5-6 hours. After this time, the polymer was cooled and dissolved in 5 ml of chloroform. The polymer was then precipitated into 50 ml of methanol. The product was filtered and then dried under vacuum.

Poly{4'-carbo-4-methoxy- α' -cyano- α -(4-piperidinoethoxy)stilbene} (**91**):

An 80% yield of yellow polymer was obtained (see Tables 7 and 8).

^1H -NMR (CDCl_3) δ 7.99 (t, 1H), 7.67 (t, 1H), 7.52 (bd, 1H), 7.1-7.3 (m, 2H), 7.00 (bd, 2H), 6.8 (m, 1H), 4.35 (bt, 2H), 3.7-4.0 (m, 4H), 3.0-3.3 (m, 2H), 2.7 (bs, 1H), 1.3-2.0 (m, 7H).

^{13}C -NMR (CDCl_3) δ 166.0, 165.8, 164.9, 163.2, 161.7, 161.1, 142.0, 141.5, 132.2, 131.6, 129.2, 128.7, 127.8, 127.5, 127.2, 126.7, 126.2, 125.3, 123.1, 121.5, 113.9, 83.3, 81.7, 62.0, 61.9, 55.1, 51.5, 51.0, 34.7, 32.6, 32.4, 32.1.

IR (KBr) 2925, 2184, 1711, 1601, 1503, 1271 cm^{-1}

Analysis Calculated: C 74.21%, H 6.23%, N 7.21%.

Found: C 72.67%, H 6.08%, N 6.91%.

Poly{4'-carbo-4-methoxy- α' -cyano- α -(3-piperidinomethoxy)stilbene} (92):

A 72% yield of yellow polymer was obtained (see Table 7 and 8).

^1H -NMR (CDCl_3) δ 6.7-8.0 (m, 8H), 1.2-4.3 (m, 14H).

^{13}C -NMR (CDCl_3) δ 165.8, 165.6, 165.1, 163.2, 161.8, 161.3, 142.1, 141.8, 141.5, 132.3, 131.7, 129.7, 129.3, 128.8, 127.9, 127.3, 126.5, 126.3, 126.2, 125.3, 125.0, 122.9, 121.3, 114.0, 83.5, 82.2, 65.9, 64.6, 55.2, 54.5, 54.1, 53.9, 52.2, 51.8, 36.6, 26.5, 26.3, 25.5, 25.3.

IR (KBr) 2936, 2185, 1712, 1602, 1508, 1268 cm^{-1}

Analysis Calculated: C 73.78%, H 5.92%, N 7.48%.

Found: C 72.13%, H 6.02%, N 7.33%.

Poly{4'-carbo-4-methoxy- α' -cyano- α -(4-piperidinoxy)stilbene} (93):

A 43% yield of yellow polymer was obtained (see Table 7 and 8).

^1H -NMR (CDCl_3) δ 8.0, 7.7, 7.5, 7.1-7.3, 7.0, 6.8 (7m, 8H), 5.0-5.3 (m, 1H), 2.7-3.9 (m, 7H), 1.6-2.2 (m, 4H).

^{13}C -NMR (CDCl_3) δ 165.3, 165.1, 165.0, 164.9, 163.3, 162.0, 161.4, 142.1, 141.5, 132.3, 131.7, 129.6, 129.0, 128.2, 127.9, 127.7, 127.5, 127.3, 126.1, 122.8, 121.5, 114.2, 69.1, 68.7, 55.2, 48.8, 48.7, 48.3, 48.0, 34.7, 31.4.

IR (KBr) 3477, 2948, 2186, 1712, 1602, 1505, 1256 cm^{-1}

Analysis Calculated: C 73.32%, H 5.59%, N 7.77%.

Found: C 65.47%, H 5.22%, N 6.90%.

Poly[4'-carbo-4-methoxy- α '-cyano- α '-(4-piperidinoethoxy) and (3-piperidinomethoxy)stilbene} copolymer (94):³⁸

The same experimental setup was used as in the homopolymerizations. Compounds 88 (0.26 g, 0.62 mmole) and 89 (0.25 g, 0.62 mmole) were mixed with 2 μ l (4 μ mole) of dibutyltin diacetate. A three stage polymerization was done by first heating to 100°C for 2 hours, with an argon flow. Vacuum was then applied and the sample heated at 190°C for 2.5 hours. Finally, while still under vacuum (0.4 mmHg) the sample was heated at 220°C for 2 hours. The polymer was then allowed to cool under vacuum overnight. The copolymer was purified by dissolution in chloroform and then precipitation into methanol. After filtration and drying the product under vacuum a 92% yield of yellow copolymer 94 was obtained (see Tables 7 and 8).

IR (KBr) 3441, 2931, 2186, 1711, 1602, 1537, 1503, 1267 cm^{-1}

CHAPTER 4
MEASUREMENT OF SECOND ORDER HYPERPOLARIZABILITIES

Background

The evaluation of optical nonlinearity is a difficult and meticulous task. This discussion will focus on methods for evaluating the second harmonic generation (SHG) of crystalline or poled polymer matrix materials. The technique utilized by our coworkers at Eastman Kodak to evaluate the molecular second order hyperpolarizability (β_x) will be described. Additionally, a technique that was adapted for use in our laboratory will be evaluated. This latter technique relies entirely on spectrophotometric measurement to approximate the hyperpolarizability (β_{xxx}).

The most direct method to evaluate SHG is to pump the crystal or matrix directly with laser light of frequency ω and measure the second harmonic (2ω).⁶ However, examining the literature reveals that very few materials are measured in this manner, because it requires that the power of the incident beam and the second harmonic be precisely known, as well as various other characteristics of the laser. All of these characteristics are very difficult to measure accurately. The materials whose absolute values have been determined by such a measurement are those needed as reference materials in other measurement techniques (for example gallium arsenide, ammonium dihydrogen phosphate (ADP), potassium dihydrogen phosphate (KDP), and quartz).

By using a reference in such experiment most of the problems associated with the laser beam characteristics can be negated. This is why most reported susceptibilities are comparative in nature. Also, the quality of the crystal being measured in a comparative measurement is less crucial than in an absolute measurement. While easier to perform than the absolute measurement, the sample in the comparative measurement must be a fairly large crystal (unless a polymer matrix is being measured).

In 1968 Kurtz^{74,75} devised a technique to evaluate powders and obtain a qualitative assessment of the material quickly. In the experiment the SHG is measured as a function of the particle size of the powder. From these measurements an assessment of whether an actual crystal of the sample will

show useful NLO properties can be made. This is a very useful technique because it eliminates the laborious task of growing optical quality crystals for all samples. A large number of samples can be evaluated quickly, and those which show promise grown into good quality crystals.

EFISH Measurements

The technique used to measure the hyperpolarizability of a molecule is the electric-field-induced second harmonic generation method (EFISH).⁷⁶⁻⁷⁹ The method is for evaluating small molecules and polymers in nonviscous solvents. This solution is placed in a cell consisting of an optical flat with a wedge cut out. Electrodes are placed on both sides covering the wedge cut out (see Scheme 38). The solution contained in the wedge is pulsed by an electric field E (10 KV/cm) for about 100 microseconds. This pulsing causes the dipoles in solution to orient in the direction of the electric field. A laser beam of frequency ω is incident perpendicular to the electric field (with the electric field component of the light in the same direction as the field E). The light exiting the sample cell is passed through a monochromator, and the second harmonic (SHG) light at 2ω is separated and its intensity is measured with a photomultiplier tube (see Scheme 39).

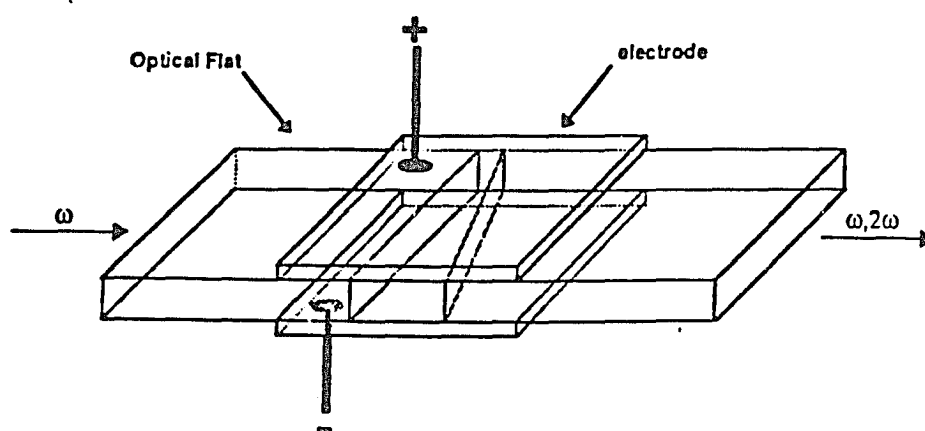
In this arrangement the intensity of the second harmonic generated $I_{2\omega}$ is given by Equation 3:

(3)

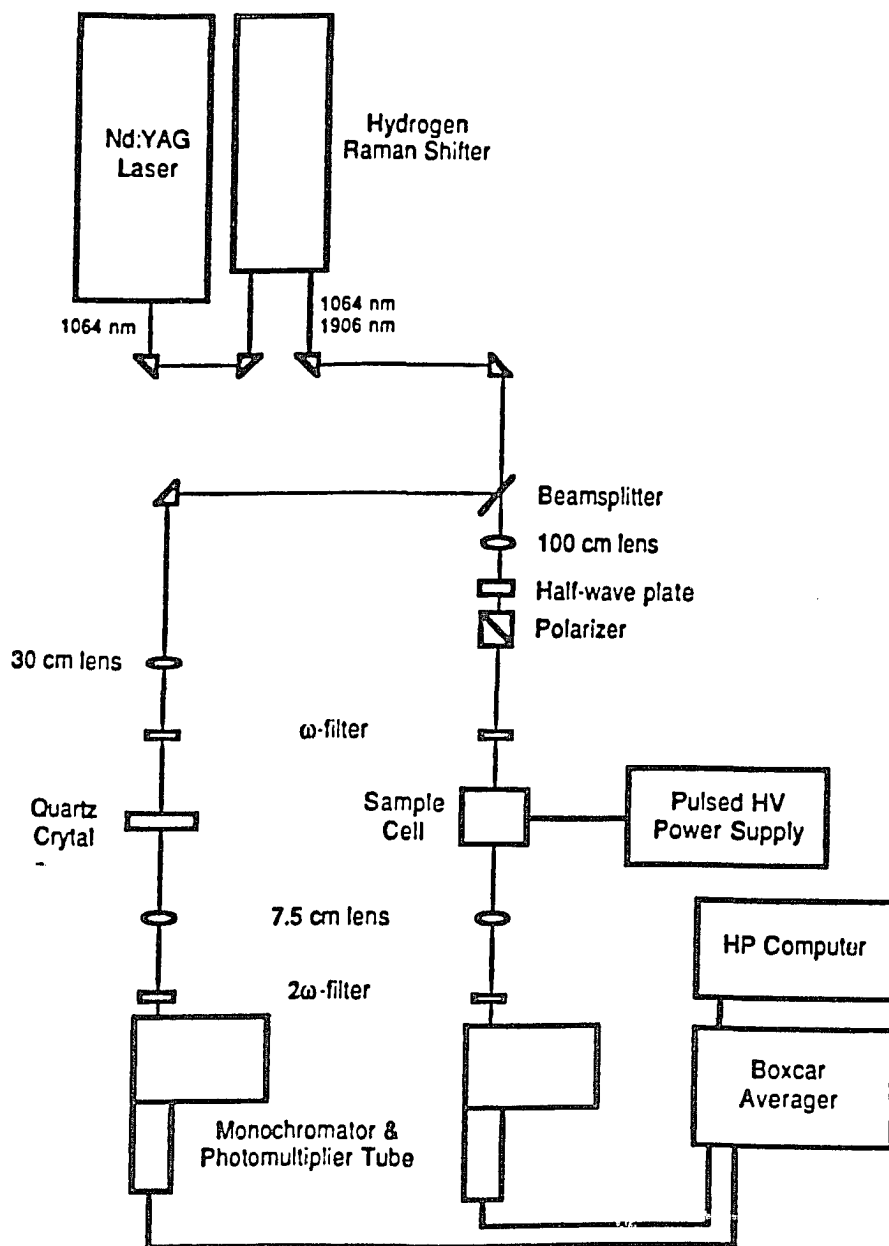
$$I_{2\omega} = G(\omega)l_c^2\Gamma^2I_\omega^2E^2\sin^2((L/l_c)(\pi/2))$$

where:

- I_ω = intensity of the laser beam
- E = electric field
- L = path length
- l_c = coherence length = $1/(4(n_{2\omega}^2 - n_\omega^2))$
- $G(\omega)$ = a function of the indices of refraction (n_ω and $n_{2\omega}$) for the solution and the windows



Scheme 38. EFISH Sample Cell.⁷⁷



Scheme 39. Experimental Setup for the EFISH Measurement.

The Γ is the third order nonlinear response of the solution to the DC field and the field at frequency ω (Equation 4):

(4)

$$\Gamma = f \sum N(m) ((\mu(m)\beta(m)/(5KT)) + \gamma(m))$$

where:

$$f = [(n_\omega^2 + 2)/3]^2 [(n_{2\omega}^2 + 2)/3] [\epsilon_0(\epsilon + 2)/(\epsilon + 2\epsilon_0)]$$

N = molecular number density

ϵ_0 = static dielectric constant

ϵ = dielectric constant for frequencies faster than dipole relaxation

$$\gamma = 1/5 (\gamma_{xxxx} + \gamma_{yyyy} + \gamma_{zzzz} + 2\gamma_{xxyy} + 2\gamma_{xxzz} + 2\gamma_{yyzz})$$

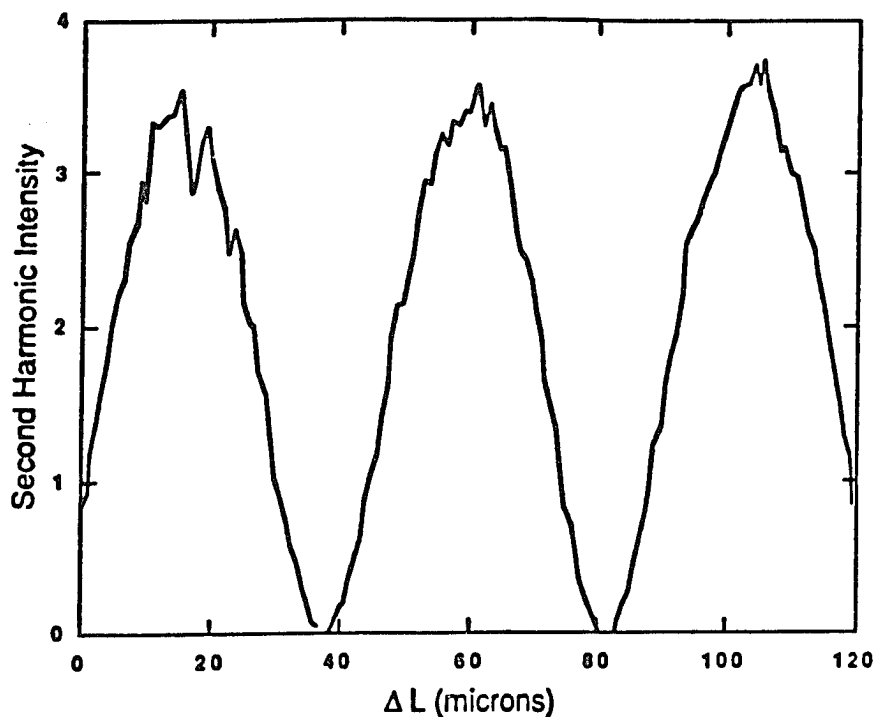
The quantity f is the local field correction factor which relates the fields present at the molecule to those of the applied fields. The γ represents the third order contribution. Normally the γ term is neglected because it is usually less than one tenth of the β term. It is important to note that, if the x-axis is defined as the axis which lies along the dipole, the value being measured is β_x . The β_x is the vector part of the hyperpolarizability tensor:

(5)

$$\beta_x = \beta_{xxx} + 1/3 (\beta_{xyy} + 2\beta_{yxy} + \beta_{xzz} + 2\beta_{zxz})$$

Equation 3 implies that the SHG intensity oscillates as a sine function as the path length changes. This periodic behavior is due to the difference in the phase velocities of the incident and SHG radiation ($n_{2\omega} = n_\omega$). Thus by varying the path length and measuring the SH intensity an experimental plot can be obtained (see Scheme 40). The path length is varied by moving the incident beam along the width of the special EFISH cell shown in

Scheme 38. The values of Γ and I_c can then be determined by using a nonlinear least-squares algorithm to fit the experimental data to Equation 3.



Scheme 40. Second Harmonic Intensity Versus the Change in Cell Pathlength.

The above procedure is done at various concentrations and the values for Γ obtained are plotted versus the number density N . A linear least-squares analysis gives the slope which is proportional to the quantity $\mu\beta_x$, which is a commonly reported value. In practice the value of the bulk susceptibility component X_{xxx} is approximated as:

(6)

$$X_{xxx} = ((I_{SH})^{1/2})/\text{period}.$$

This is done at several concentrations and the resulting X_{xxx} 's are plotted versus the number density (in molecules/mL) to give a line which obeys the relation:

(7)

$$X_{xxx} = X_{\text{solvent}} + (N\mu\beta_x E_0)/(5KT)$$

Although EFISH is the method of choice, it is not without problems. First, the experimental setup is very expensive, being far out of the price range for the typical academic laboratory. Second, it is a very difficult experiment to run properly. Third, the values determined are very dependent on conditions such as solvent, choice of incident radiation, and the EFISH technique. For example, *p*-nitroaniline (**1**) has been reported to have the following values for β_x at 1.06 μm incident laser (Table 9):

Table 9. Hyperpolarizability of *p*-Nitroaniline (**1**) by EFISH.

Solvent	β_x ($\times 10^{-30}$ esu)*	Reference
Dioxane	29	80
	16.9	81
Methanol	20.0-24.5	82
	34.5	83
Melt	34.5	84

* Measured at $\lambda = 1.06 \mu\text{m}$.

These problems are inherent due to the complexity of an EFISH measurement, and there is a great need for a relatively simple method of determining the hyperpolarizability.

Spectrophotometric Measurements

Recently two groups have reported methods for determining β_{xxx} (Equation 5) that involve only UV/visible and ground state dipole moment

measurements.^{80,85} Both procedures are based on work done by Oudar and Zyss^{20,86} where they derive an expression for β_{xxx} for a highly symmetrical chromophore.

Zyss and Oudar start with the relation for the peak amplitude $P_i^{2\omega}$ of the second harmonic dipole:

(8)

$$P_i^{2\omega} = \beta_{ijk}^{2\omega} E_j^\omega E_k^\omega$$

where E_j^ω is the peak amplitude of the fundamental electric field and the hyperpolarizability tensor $\beta_{ijk}^{2\omega}$ is given by:

(9)

$$\beta_{ijk}^{2\omega} = \frac{1}{2\hbar^2} \sum_{pq} \left\{ \mu_{op}^i (\mu_{pq}^j \mu_{qo}^k + \mu_{pq}^k \mu_{qo}^j) \frac{\omega_p \omega_q + 2\omega^2}{(\omega_p^2 - 4\omega^2)(\omega_q^2 - \omega^2)} + \mu_{op}^k \mu_{oq}^i \mu_{qo}^j \frac{\omega_p \omega_q + 2\omega^2}{(\omega_p^2 - \omega^2)(\omega_q^2 - \omega^2)} \right\}$$

where the sum is over all energy states. Equations 8 and 9 are obtained from time-dependent quantum-mechanical perturbation theory. The two-level model approximation is used on Equation 9 to reduce the cumbersome equation to a simpler form. The two-level model makes the approximation that there are only two energy levels: the ground state $|g\rangle$, and the excited state $|e\rangle$. The four terms which result from this approximation (p and q can be g or e) allow Equation 9 to be simplified to:

(10)

$$\beta_{ijk}^{2\omega} = \frac{1}{2\hbar^2} \left\{ \frac{\mu_{ge}^j \mu_{ge}^k (\mu_{ee}^i - \mu_{gg}^i)}{\omega_e^2 - \omega^2} + \mu_{ge}^i (\mu_{ge}^j (\mu_{ee}^k - \mu_{gg}^k) + \mu_{ge}^k (\mu_{ee}^j - \mu_{gg}^j)) \frac{\omega_e^2 + 2\omega^2}{(\omega_e^2 - 4\omega^2)(\omega_e^2 - \omega^2)} \right\}$$

For the special case where $i = j = k = x$ (x being the axis running through the dipole) the simple form of Equation 10 results:

(11)

$$\beta_{xxx} = \frac{3(\mu_e - \mu_g)\mu_{eg}^2}{2\hbar^2} \times \frac{\omega_{eg}^2}{(\omega_{eg}^2 - 4\omega^2)(\omega_{eg}^2 - \omega^2)}$$

where: μ_e = excited state dipole moment
 μ_g = ground state dipole moment
 μ_{eg} = transition dipole moment
 ω_{eg} = frequency of transition
 ω = incident laser frequency

The $\beta_{xxx}^{2\omega}$ in Equation 11 is the same β_{xxx} term in Equation 5, and β_{xxx} is often referred to as β_{cl} (the portion of β_x due to charge transfer). Theoretical calculations have shown that for *p*-nitroaniline (1) β_{xxx} can account for 75% of β_x . In addition, the developers of the method to measure β_{xxx} observe values which are between 38 and 80% of the measured EFISH value (see Table 10).⁸⁰

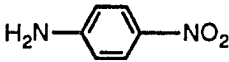
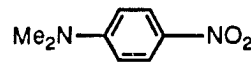
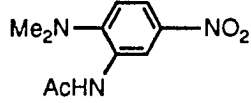
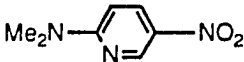
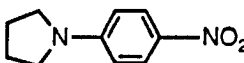
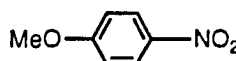

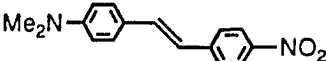
Because the second term in Equation 5 is unknown and Equation 11 is the result of the two-level approximation, determining β_{xxx} can give only a feel for the quantity of the hyperpolarizability. This "feel" for the hyperpolarizability is adequate because as pointed out earlier, there are sizeable inconsistencies in EFISH measurements. However, the real value of determining β_{xxx} lies in its usefulness in observing trends in small molecules with related structure. For example, researchers at Celanese Research Company used a more empirical but similar method to observe the effects of increasing pi conjugation and altering donor and acceptor substituents.⁸⁵

Other benefits of determining β_{xxx} include the ease of measurement, and the low cost of the method. To determine the transition dipole, μ_{eg} , and the transition frequency, ω_{eg} , a UV/visible spectrometer is needed, and to find the excited state dipole, μ_e , a UV/visible spectrometer or a fluorescence spectrophotometer can be utilized. These are both instruments that most research institutions possess. The ground state dipole can be determined by

various experimental setups, but can be done relatively inexpensively. The details of these measurements will be given in the following sections.

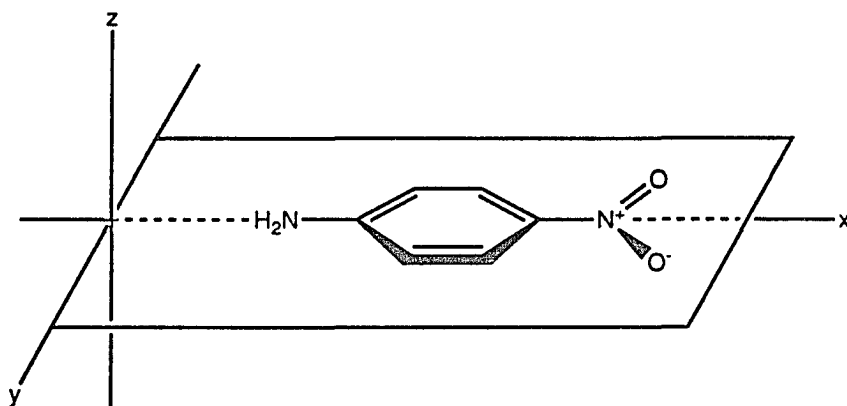
Returning to Equation 11 there are several assumptions which need to be qualified. The first of these assumptions is the applicability of the two-

Table 10. Relation of β_{xxx} to β_x for Various Compounds.

Compound	Hyperpolarizability (10^{-30} esu) at 1.06 μm		
	β_x	β_{xxx}	β_{xxx}/β_x (%)
	26	17	59
	57	22	39
	36	16	44
	38	23	61
	45	34	76
	13	5.7	44
	23	10.6	46
	450	323	72

level model approximation. This approximation is commonly used in quantum theory. In this approximation, all terms except for the ground and first excited state are ignored. Because the first excited state is a low energy charge transfer state the higher excited states are relatively inaccessible for organic SHG molecules. That is to say, the frequencies of incident and second harmonic are well below the frequencies of transition to higher excited states. Thus the two-level model is applicable to the kind of donor/acceptor molecules that are of interest in SHG. It must be noted that the two state model may be inadequate for more complex systems.¹⁹

The other assumptions involve the direction of the ground state dipole μ_g , excited state dipole μ_e , and transition dipole μ_{eg} vectors. The quantities in Equation 11 (μ_e , μ_g , and μ_{eg}) are written and experimentally determined as scalar quantities. Thus, Equation 11 is rigorously applicable only to molecules which have the ground state, excited state, and transition dipoles pointing in the same direction. In fact, this is applicable to many SHG molecules, for example *p*-nitroaniline (**1**). The pi system of **1** has a C_2 axis running through the dipole and two planes of symmetry (see Scheme 41).



Scheme 41. Symmetry of *p*-Nitroaniline.

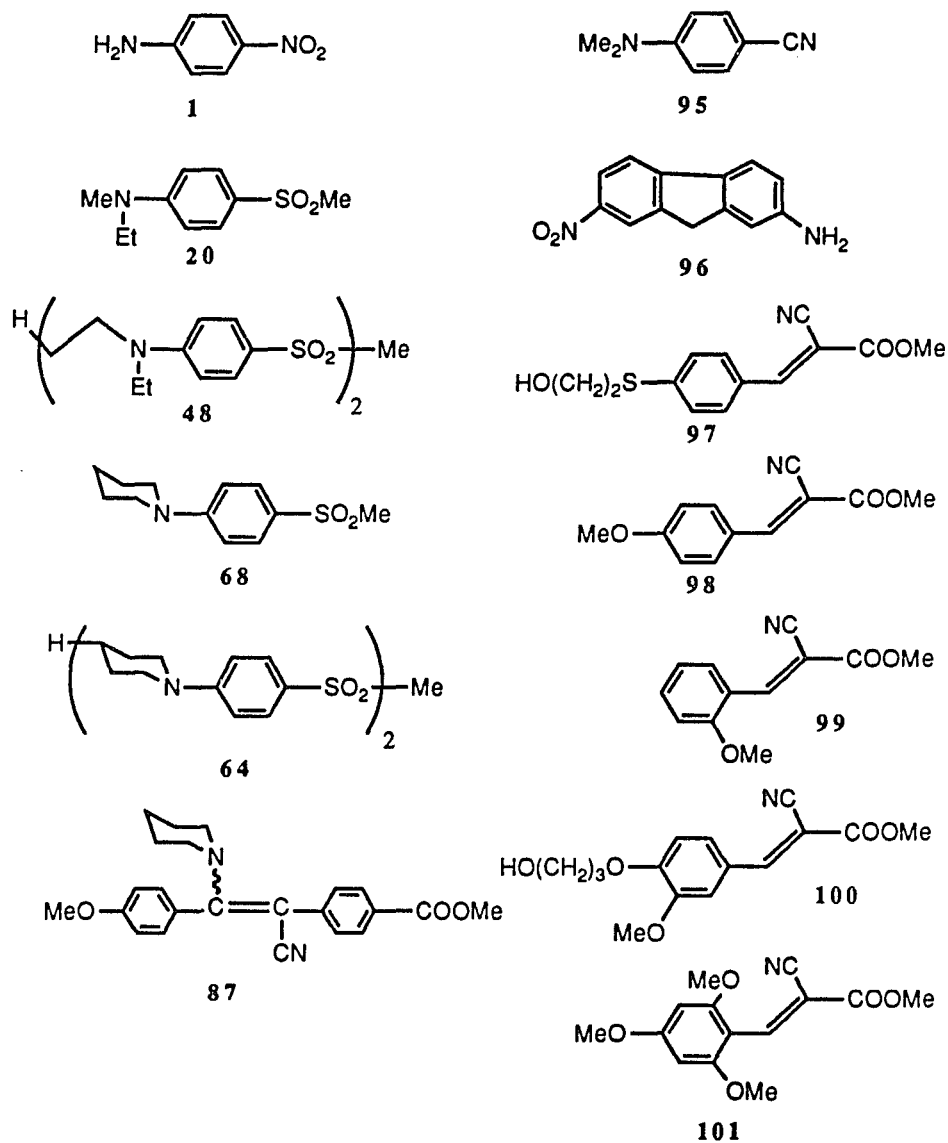
The symmetry in **1** dictates that the ground state and excited state dipole moments lie in the same direction on the x axis. According to Oudar and Zyss⁸⁶ the transition dipole of molecules with symmetry like **1** can either be parallel to the x axis or perpendicular to one of the mirror planes. However, when a molecule, like **1**, has an intramolecular charge transfer, the transition dipole is usually directed along the axis of the transition. So it is a fair assumption that, for NLO molecules like **1**, all the dipole moments (ground and excited states, and transition) are parallel to each other and the x axis. Equation 11 would therefore be completely applicable to molecules with symmetry similar to **1**. Molecules with NLO polarizabilities like **1** are said to have one-dimensional properties.

Turning to a two-dimensional case makes the problem much more complicated. For example, the molecule DMNP (2-dimethylamino-5-nitropyridine) has only one plane of symmetry for its pi symmetry. Thus the two vectors μ_{eg} and $(\mu_e - \mu_g)$ must lie in this plane at some unknown angle to each other. So Equation 11 becomes even more approximate for a molecule with two-dimensional properties. Since Equation 11 is only being used to give a "feel" for β_x , or to determine β_{xxx} to compare molecules of related composition, it will be approximated that μ_{eg} and $(\mu_e - \mu_g)$ are parallel.

The three-dimensional case is not considered because the hyperpolarizabilities of organic molecules are due primarily to the pi conjugated systems. The portion of the hyperpolarizabilities perpendicular to the molecular plane of compounds like **1** and DMNP is very near zero. Also, simple rotation of the molecule about the x-axis would imply that the perpendicular components cancel, and do not contribute to the SHG.

The compounds which had one or more of their properties (mg, meg, weg, me, bxxx, and bx) measured by the solution based method or by EFISH are listed in Table 11.

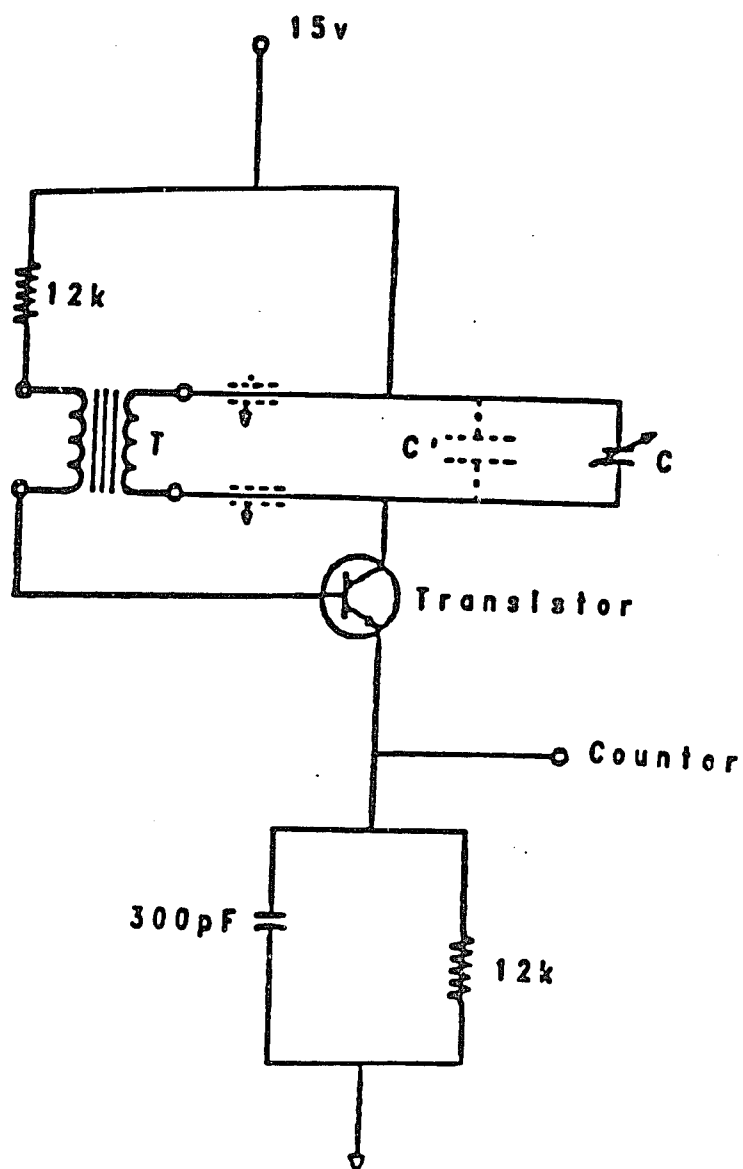
Table 11. Compounds Used for the Evaluation of the Spectrophotometric Method of Hyperpolarizability Determination.



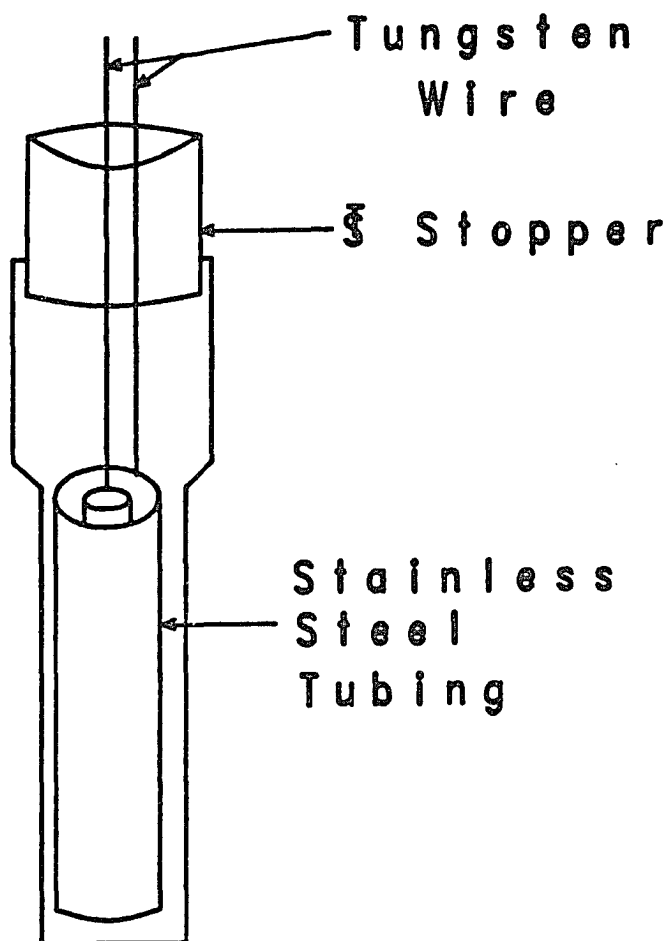
Ground State Dipole Moment

Most systems used for measuring the ground state dipole moment of a molecule involve a capacitance cell in conjunction with a capacitance bridge. Since time and money were two major constraints, the necessary equipment was borrowed from the undergraduate physical chemistry laboratory at the University of Arizona. The existing system was based on the heterodyne beat-frequency method described in the Garland and Shoemaker text,⁸⁷ which utilizes a one-transistor oscillator in the basic circuitry. A modification of this system was used and is described herein.

A schematic of the system's electronics is shown in Scheme 42. This circuit had been built by Prof. Kukulich according to the method described by Bonilla and Vassos.⁸⁸ An approximate cost of the necessary materials is about five hundred dollars. While the measurement setup was adequate, the cell design was too impractical for our needs. The heterodyne cell requires 100 milliliters of 0.01 M to 0.1 M solution, which is quite a large amount of sample. Instead, a cell based on the design described by Harris, Twieg, and coworkers⁸⁰ was constructed. The actual cell design, as shown in Scheme 43, consists of a female standard taper 14/22 test tube, with the cell suspended from the male standard taper 14/22 top. The capacitance cell is two coaxial stainless steel tubes, the inner having a diameter of 0.6 cm and the outer having a diameter of 1.0 cm. The tubes are rigidly held apart by tiny glass spacers, three at the top and three at the bottom. Both tubes are 7.0 cm in length. The tubes are suspended from the stopper with two 7.0 cm tungsten wires, one wire attached to each tube. The tungsten wires have crimped on pin connectors on the outside of the stopper, which are used to connect the cell to the measurement apparatus. To decrease the sample volume needed, a glass rod is mounted down the center of the inner stainless steel tube, and the test tube is tapered from a diameter of 5.0 cm at its top to 1.2 cm at the bottom. A fill line is located 5.5 cm from the bottom of the tube. Thus, the total volume needed is only 4.5 mL, which attests to the excellence of the glass shop employed.



Scheme 42. One Transistor Oscillator Circuit for Ground State Dipole Moment Determinations.



Scheme 43. Capacitance Cell for Ground State Dipole Moment Determination.

The principle behind using the cell to find the dielectric constant of a solution involves the capacitance:⁸⁸

(12)

$$\epsilon_s = C_s/C_v = C_s/C_A$$

where ϵ_s is the dielectric constant of the solution, C_s is the capacitance of the solution, C_v is the capacitance of vacuum, and C_A is the capacitance of air. C_A is taken to be approximately equal to C_v . There is a frequency of oscillation (f) across a capacitor which can be related to the capacitance:

(13)

$$f = 1/(2\pi \sqrt{LC_T}) = k/\sqrt{C_T}$$

where L is the inductance, k is a constant for a given circuit, and C_T is the total capacitance given by:

(14)

$$C_T = C_s + C'$$

where C' is the parasitic capacitance. Solving for C_T in Equation 14 and taking the difference between the cell circuit when closed and when open eliminates the parasitic capacitance C' :

(15)

$$C_s = k^2 (1/f_{\text{closed}}^2 - 1/f_{\text{open}}^2)$$

The f_{closed} is the frequency of oscillation for the completed circuit, and the f_{open} is the frequency of oscillation when the negative lead from the measuring unit is not attached to the capacitance cell. The dielectric constant ϵ_s for a solution is then found by taking the ratio:

(16)

$$\epsilon_s = C_s/C_A = (1/f^2_{\text{closed}} - 1/f^2_{\text{open}})_s / (1/f^2_{\text{closed}} - 1/f^2_{\text{open}})_A.$$

The setup was tested by measuring the dielectric constants for various solvents (see Table 12).

Table 12. Measured Dielectric Constants.

Solvent	ϵ_{exp}	ϵ_{lit}	Deviation (%)
Dioxane	2.1456	2.2090	2.9
Chloroform	4.867	4.726	3.0
Dichloromethane	9.209	8.930	3.1
Tetrahydrofuran	7.79	7.58	2.8

This is good agreement ($\pm 3\%$) considering the solvents were purified only by drying over 3 angstrom molecular sieves.

The ground state dipole moments μ_g of compounds were determined using the Guggenheim-Debye equation:⁸⁰

(17)

$$\mu_g = \left(\frac{9kT}{4\pi N_0} \right) \left(\frac{3}{(\epsilon+2)(n^2+2)} \right) \left(\frac{(\epsilon_s - n_s^2) - (\epsilon - n^2)}{C} \right)$$

where K is Boltzmann's constant, T is the temperature, N_0 is Avogadro's number, ϵ and n are the dielectric constant and index of refraction of the solvent respectively, ϵ_s and n_s are the dielectric constant and index of refraction of the solution, and C is the concentration of the solution.

Rearranging Equation 17 gives a linear relation:

(18)

$$\epsilon_s - n_s^2 = MC + (\epsilon - n^2)$$

where

$$M = \{ (4\pi N_0(\epsilon + 2)(n^2 + 2)) / 27KT \} \times \mu_g^2$$

The index of refraction of the dilute solutions, n_s , is about equal to that of the solvent, n , ($n_s = n$). Thus, a plot of $\epsilon_s - n^2$ versus concentration gives a line whose slope (determined by a least squares linear analysis) is proportional to the ground state dipole moment μ_g .

All determinations of μ_g were done in Aldrich Gold Label 1,4-Dioxane. The temperature was held constant at $30.0 \pm 0.2^\circ\text{C}$.

Transition Dipole Moment and Transition Frequency

The determinations of the transition dipole moment μ_{eg} and the transition frequency ω_{eg} were done in the solvent that was or would be used for the EFISH. The solvents were all Aldrich spectrometric grade and were dried over 3 angstrom sieves prior to use. The chloroform chosen was stabilized with amylene, not ethanol. The instrument used was a Hewlett Packard model 8452A diode array UV/visible spectrometer. The method used was that outlined by Harris, Twieg, and coworkers,⁸⁰ which was derived from work done by Liptay.⁸⁹

The transition frequency ω_{eg} is simply the frequency at the band maximum of the UV/vis absorption spectrum of the molecule. The transition dipole moment μ_{eg} can be calculated from the area of the absorption band:

(19)

$$\mathcal{A} = \int \epsilon M d\omega = \frac{2\pi\omega_{eg}N_0nM\mu_{eg}^2}{3(2303)\epsilon_0ch}$$

The integral absorption can be estimated as the area under an isosceles triangle:

(20)

$$\mathcal{A} = \epsilon M W_{1/2}$$

where: \mathcal{A} = area (integral absorption)
 ϵ = extinction coefficient ($\text{m}^{-1}\text{mole}^{-1}$)
 M = concentration (moles m^{-3})
 $W_{1/2}$ = width at half the peak height (m^{-1})
 ω_{eg} = transition frequency (m^{-1})
 N_0 = Avogadro's number
 n = index of refraction
 ϵ_0 = vacuum permittivity (MKS units)
 c = speed of light (MKS units)
 h = Planck's constant (MKS units)

By substituting the estimated area and solving for the transition moment, Equation 21 is derived:

(21)

$$\mu_{eg} = ((3(2303)\epsilon_0 c h W_{1/2} \epsilon) / (2\pi \omega_{eg} N_0 n))^{1/2}$$

The index of refraction is taken as that of the solvent. To convert the value of μ_{eg} into Debyes, the result from Equation 21 must be multiplied by 0.1x (speed of light in cm/s) and divided by 10^{-18} , a conversion factor. If there are problems in using Equation 21, they most likely stem from a units error.

The absorbance spectrum of the compound is taken at several concentrations. From these spectra the transition frequency ω_{eg} and the width at the half height $W_{1/2}$ are measured. The extinction coefficient is determined by the standard technique of calculating the slope of a least squares plot of the absorbance versus concentration (a Beer's Law plot).

With more unsymmetrical absorption bands (for example the ethylene spaced dimer 48) a more precise method was used to determine the

integral absorption for the transition dipole. Using a computer upgraded Olis Cary-14 UV/visible spectrophotometer, the area was determined using the drop line method in the computer software. Unfortunately, the software was only capable of giving the area in units of $\text{abs} \times \text{nm}$, thus a conversion factor had to be derived, since the area must be in $\text{abs} \times \text{cm}^{-1}$. Starting with the definition of the integral absorption:

$$\mathcal{A}_\lambda = \int_{\lambda_a}^{\lambda_b} A d\lambda$$

where \mathcal{A}_λ is the integral absorption in nm , A is the absorbance, and λ is the wavelength. Converting the change in wavelength into wavenumbers we have:

$$d\lambda = (d\lambda/d\omega)d\omega = (d\omega^{-1}/d\omega)d\omega = \omega^{-2}d\omega$$

Substituting for $d\lambda$ in the integral absorption we obtain the following relation for the integral absorption in nm and the result in wavenumbers.

$$\mathcal{A}_\lambda = A \int_{\omega_a}^{\omega_b} \omega^{-2} d\omega = A(\omega_b^{-1} - \omega_a^{-1})$$

Some simple algebra then gives the integral absorption in a more convenient form:

$$\mathcal{A}_\lambda = A(\omega_b^{-1} - \omega_a^{-1}) = A[(\omega_a - \omega_b)/\omega_a \omega_b]$$

This relation can then be reduced to:

$$\omega_a \omega_b \mathcal{A}_\lambda = -A(\omega_b - \omega_a)$$

We then recognize that the term on the right of the equation is simply the integral absorption in wavenumbers:

$$\mathcal{A}_\omega = \int_{\omega_a}^{\omega_b} A d\omega = A(\omega_b - \omega_a)$$

Making the substitution then gives the equation for the conversion of the integral absorbance in nanometers into wavenumbers:

$$\omega_a \omega_b \mathcal{A}_\lambda = -\mathcal{A}_\omega$$

Finally, the area in wavenumbers should be in inverse centimeters (cm^{-1}), so we need to multiply the left side of the equation by the conversion factor of 10^{-7} cm/nm. Also, area cannot be a negative quantity so we have to take the absolute value to obtain the relation in the proper final form:

(22)

$$\mathcal{A}_\omega = (\omega_a \omega_b \mathcal{A}_\lambda \times 10^{-7}) \text{cm}^{-1}$$

where ω_a and ω_b are the limits of the integral.

Having the integral absorption in wavenumbers allowed for the direct use of Equation 19. Plotting the integral absorbance \mathcal{A}_ω versus the concentration a linear relation is observed, where the slope m is equal to a collection of constants:

$$m = \frac{2\pi\omega_{eg}N_0nM\mu_{eg}^2}{3(2303)\epsilon_0ch}$$

Solving this relation for the transition dipole moment μ_{eq} gives Equation 23.

Solving this relation for the transition dipole moment μ_{eq} gives Equation 23.

(23)

$$\mu_{eg} = \left\{ \frac{3(2303)\epsilon_0 chm}{2\pi\omega_{eg}N_0nM} \right\}^{1/2}$$

Finding the slope m then allows for simple calculation of the transition dipole moment μ_{eq} .

Excited State Dipole Moment

The excited state dipole moments μ_e were evaluated by solvatochromic measurements of both the UV/visible absorbance spectra and the fluorescence spectra. Solvatochromic measurements find the most use in solvent polarity determinations,^{90,91} but the same relations can yield approximations of the excited state dipole moments. Solvatochromic theory results from work by McRea,⁹² Liptay,^{89,93} and others⁹⁴⁻⁹⁸ who attempted to explain and predict shifts in UV/visible and fluorescence spectroscopies due to solvent characteristics. The characteristics used are the dielectric constant and the index of refraction. For typical chromophores bathochromic (or red) shifts are observed with increasing solvent polarity, but hypsochromic (blue) shifts are not uncommon.

Previous work by Harris and Twieg *et al.*,⁸⁰ in addition to much work by Koutek^{99,100} suggest that the following relationships have the most promise for giving approximate excited state dipole moments:

Absorption Shifts:Equation 24 (McRea)^{80,92}

$$\nu_{\text{sol}}^{\text{a}} = A \left(\frac{n^2-1}{2n^2+1} \right) + B \left(\frac{\epsilon-1}{\epsilon+2} - \frac{n^2-1}{n^2+2} \right) + \nu_{\text{vac}}^{\text{a}}$$

$$\text{Where } B = \frac{2(\mu_{\text{g}}-\mu_{\text{e}})\mu_{\text{g}}}{a^3hc}$$

Equation 25 (Block and Walker)^{97,99}

$$\nu_{\text{sol}}^{\text{a}} = A \left(\frac{n^2-1}{2n^2+1} \right) + B \left(\frac{0.5\epsilon \ln \epsilon + 3(\epsilon-1)(1/\ln \epsilon) - 2\epsilon-1}{0.5\epsilon \ln \epsilon - 3(\epsilon-1)(1/\ln \epsilon) + \epsilon+2} - \frac{n^2-1}{n^2+2} \right) + \nu_{\text{vac}}^{\text{a}}$$

$$\text{Where } B = \frac{2(\mu_{\text{g}}-\mu_{\text{e}})\mu_{\text{g}}}{4\pi a^3 hc \epsilon_0}$$

Equation 26 (Bakhshiev)^{94,100,101}

$$\nu_{\text{sol}}^{\text{a}} = A \left(\frac{n^2-1}{n^2+2} \right) + B \left(\frac{\epsilon-1}{\epsilon+2} - \frac{n^2-1}{n^2+2} \right) \left(\frac{2n^2+1}{n^2+2} \right) + \nu_{\text{vac}}^{\text{a}}$$

$$\text{Where } B = \frac{2(\mu_{\text{g}}-\mu_{\text{e}})\mu_{\text{g}}}{a^3hc}$$

Fluorescence Shifts:Equation 27 (McRea)⁹²

$$\nu_{\text{sol}}^{\text{f}} = A \left(\frac{n^2-1}{2n^2+1} \right) + B \left(\frac{\epsilon-1}{\epsilon+2} - \frac{n^2-1}{n^2+2} \right) + \nu_{\text{vac}}^{\text{f}}$$

$$\text{Where } B = \frac{2(\mu_{\text{g}}-\mu_{\text{e}})\mu_{\text{e}}}{a^3hc}$$

Fluorescence Shifts, continued:Equation 28 (Block and Walker)^{97,99}

$$\nu_{\text{sol}}^f = A \left(\frac{n^2-1}{2n^2+1} \right) + B \left(\frac{0.5\epsilon \ln \epsilon + 3(\epsilon-1)(1/\ln \epsilon) - 2\epsilon-1}{0.5\epsilon \ln \epsilon - 3(\epsilon-1)(1/\ln \epsilon) + \epsilon+2} - \frac{n^2-1}{n^2+2} \right) + \nu_{\text{vac}}^f$$

$$\text{Where } B = \frac{2(\mu_g - \mu_e)\mu_e}{4\pi a^3 h c \epsilon_0}$$

Difference between absorption and fluorescence shifts:Equation 29 (Bakhshiev)^{94,100,101}

$$\nu_{\text{sol}}^a - \nu_{\text{sol}}^f = A \left(\frac{n^2-1}{n^2+2} \right) + B \left(\frac{\epsilon-1}{\epsilon+2} - \frac{n^2-1}{n^2+2} \right) \left(\frac{2n^2+1}{n^2+2} \right) + C$$

$$\text{Where } B = \frac{2(\mu_e - \mu_g)^2}{a^3 h c}$$

Equation 30 (Koutek)¹⁰⁰

$$\nu_{\text{sol}}^a - \nu_{\text{sol}}^f = A \left(\frac{\epsilon-1}{\epsilon+2} - \frac{n^2-1}{n^2+2} \right) \left(\frac{2n^2+1}{n^2+2} \right) + B$$

$$\text{Where } A = \frac{2(\mu_e - \mu_g)^2}{a^3 h c}$$

Where: ν_{sol}^a = Absorption maximum in the solvent
 ν_{sol}^f = Fluorescence maximum in the solvent
 ν_{vac}^a = Absorption maximum in a vacuum
 ν_{vac}^f = Fluorescence maximum in a vacuum
 n = Index of refraction of the solvent
 ϵ = Dielectric constant of the solvent

μ_g = Ground state dipole moment c = Speed of light
 ϵ_0 = Permittivity of a vacuum a = Onsager field radius
 μ_e = Excited state dipole moment h = Planck's constant

In solvatochromic determinations of the excited state dipole moment the change in spectrophotometric absorption or emission is measured as a function of solvent. The procedure consists of dissolving the chromophore of interest in various solvents which encompass a broad range of dielectric constants and refractive indices. The absorbance or fluorescence is related to the solvent properties by means of a multiple linear regression. The multiple linear regression yields the coefficients **A** and **B**, and the constant ν^a_{vac} , ν^f_{vac} , or **C**. The appropriate constant is then used to calculate the excited state dipole moment. The ground state dipole moment can be obtained as described previously. The terms *h* and *c* are constants, and the constant ϵ_0 is taken as one when working in electrostatic units. The Onsager field radius *a* is defined as the radius of the solvent sphere about the molecule. The choice of the magnitude of the field radius is arbitrary; in this work values from 0.5 to 0.7 times the length of the molecule were evaluated for *a* (these factors will be called the "Onsager Factor's" in this work).

The values for *n* and ϵ were taken from the CRC Handbook of Chemistry and Physics. The criterion for solvent choice is essentially any solvent which lacks anomalous interactions with the chromophore may be used.^{99,100} Thus hydrogen bonding solvents such as water and alcohols, were not used. Also, solvents capable of pi stacking or other pi interactions, such as benzene and dimethylsulfoxide, were not used. Initial studies included the use of polychlorinated solvents, but erroneous results were obtained. There are several factors which may lead to the anomalous results observed with chlorinated solvents. First, the C-Cl bond has a high partial moment giving the relatively nonpolar solvent a more polar character. Second, the chloro substituent can hydrogen bond to acidic hydrogens. Third, chlorinated solvents usually contain traces of hydrochloric acid, which can cause the anomalous results. So the use of chloroform and methylene chloride in spectral shift measurements was eliminated. Also, dioxane was not used because of its unusual polar character.

The solvents used are listed in Table 13. All solvents were spectroscopy grade, dried over 3 angstrom sieves for at least 48 hours before

use. The UV/visible spectra were recorded on a computer upgraded Olis Cary-14 spectrophotometer, and fluorescence spectra were recorded on a Spex 1681 Fluorolog spectrophotometer. Both spectrometers were used with a resolution of 0.5 nm. The UV/visible spectral data were collected with five readings per datum, and the fluorescence spectral data were collected with an integration time of one second.

Table 13. Solvents Used for Excited State Dipole Moment Determinations.

Solvent	n_D^{25}	ϵ^{25}
Hexane	1.327	1.88
Cyclohexane	1.424	2.015
Ethyl Ether	1.352	4.235
Tetrahydrofuran	1.404	7.58
Ethyl Acetate	1.370	6.02
Acetonitrile	1.342	38.8
2-Butanone	1.377	18.51
Acetone	1.357	20.7

The absorbance and fluorescence maxima were processed using both Lotus and Symphony spread sheet programs on an IBM PC. The Lotus program was used to calculate the coefficients A, B, and C using the multiple linear regression function. These results were then transferred to the Symphony program to make use of its superior graphics abilities. The results were graphed as $(U_{sol})_{exp}$ versus $(U_{sol})_{calc}$, where the calculated results were obtained by using the multiple linear regression results and solvent parameters in the appropriate equation (24-30). The linear correlations were calculated from the Lotus spread sheet to evaluate the quality of the equations used. Also, the difference ($\mu_e - \mu_g$) was calculated directly from Equations 29 and 30, without the need for the values of the ground state dipole moment.

Results and Discussion

Ground State Dipole Moment

As reported in Table 12 our capacitance cell and meter work reasonably well. Better results could be obtained with more expensive setups, but for our purposes this arrangement was more than accurate enough. All samples tested obeyed a linear relationship except at the concentration extremes. At low concentrations there is not enough solute to support a significant change in capacitance and the reading drops to the dielectric value of the pure solvent. At high concentrations voltage leakage becomes a problem and the values become erroneously high. Usually the best concentrations to evaluate are between 0.01 and 0.1 M (this is typical for ground state dipole moment measurements). Results of several measurements are shown in Table 14, and in Figures 1-3.

Table 14. Measured Ground State Dipole Moments.

<u>Compound</u>	<u>μ_g (Debye):</u>	
	<u>Experimental</u>	<u>Literature</u>
1	7.14	7.13
97	3.84	
87	7.07	

Transition Dipole Moment and Transition Frequency

The transition dipole μ_{eg} and the transition frequency ω_{eg} were easily determined from the UV/visible spectra at various concentrations. The first method outlined for the determination of μ_{eg} seems adequate in most cases, but future experiments should take advantage of the Olis software in determining the integral absorptions. Evaluating the area by the dropline method, as the software does, is simply more accurate than the triangle approximation. The results of many determinations of transition dipole μ_{eg} and transition frequency ω_{eg} are listed in Table 15, and the plot of area versus concentration for the dimethylene spaced dimer is shown in Figure 4.

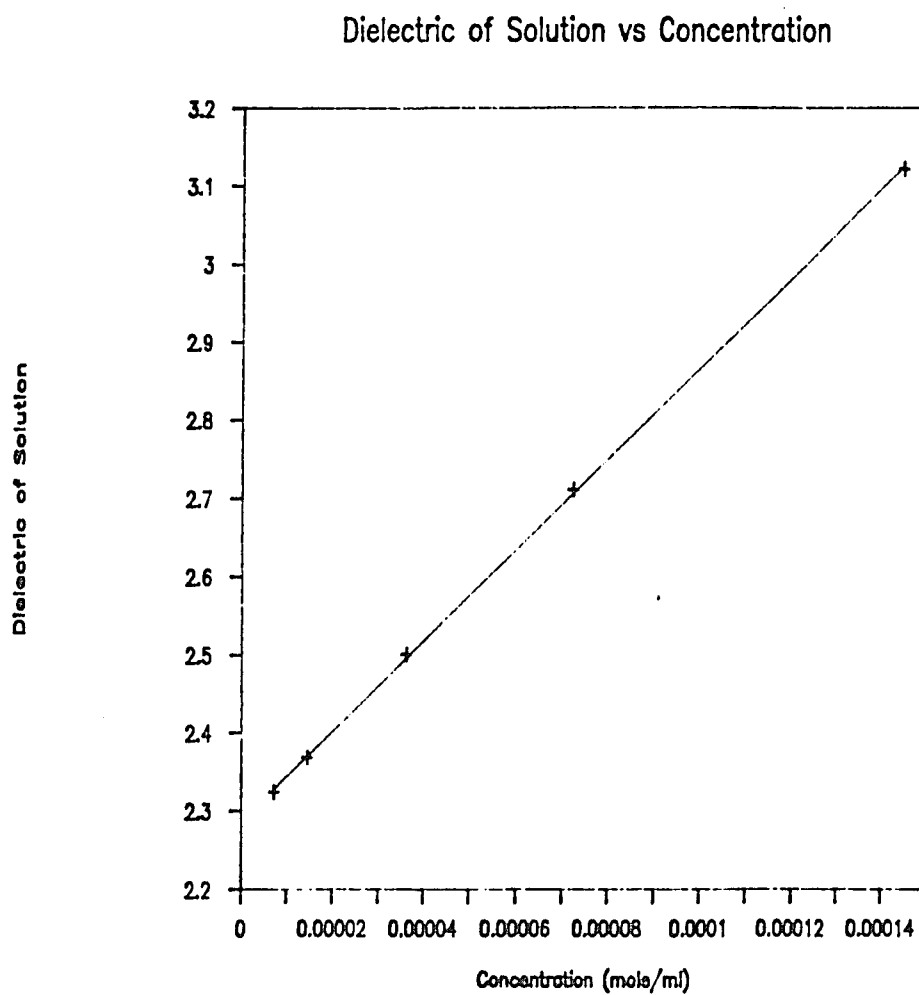


Figure 1. Dielectric Value in Dioxane Versus Concentration for Compound 1.

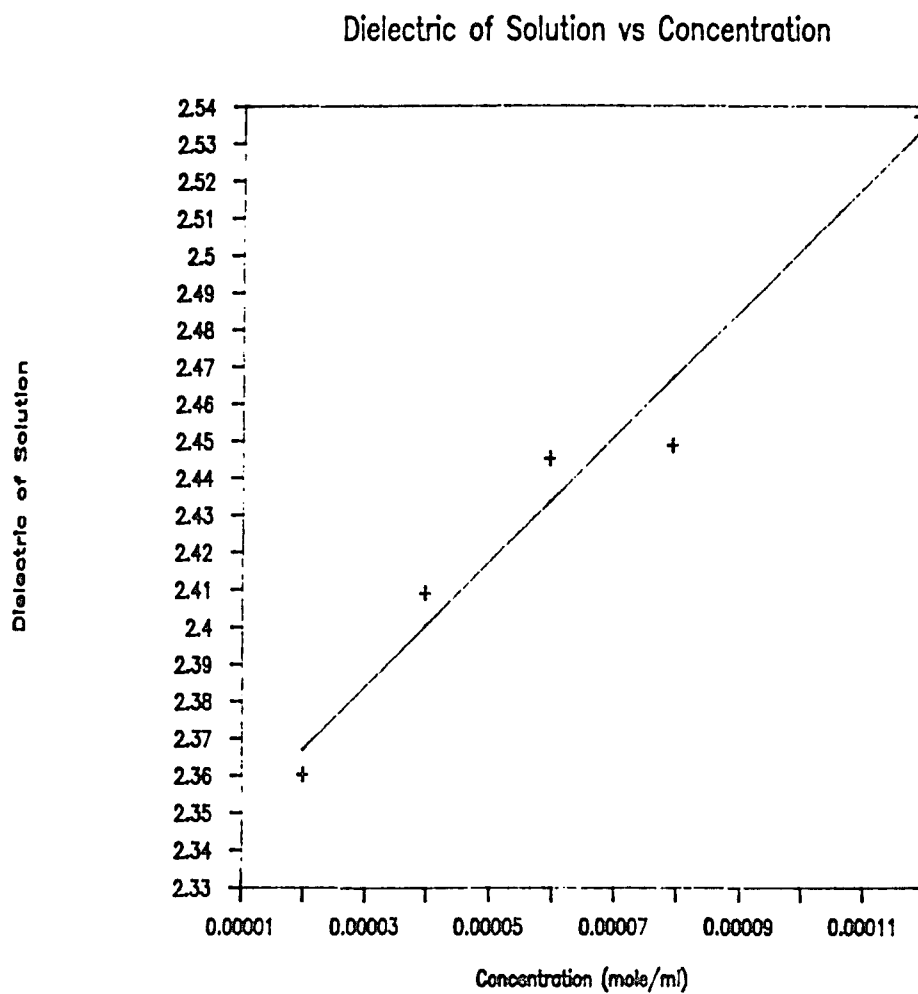


Figure 2. Dielectric Value in Dioxane Versus Concentration for Compound 97.

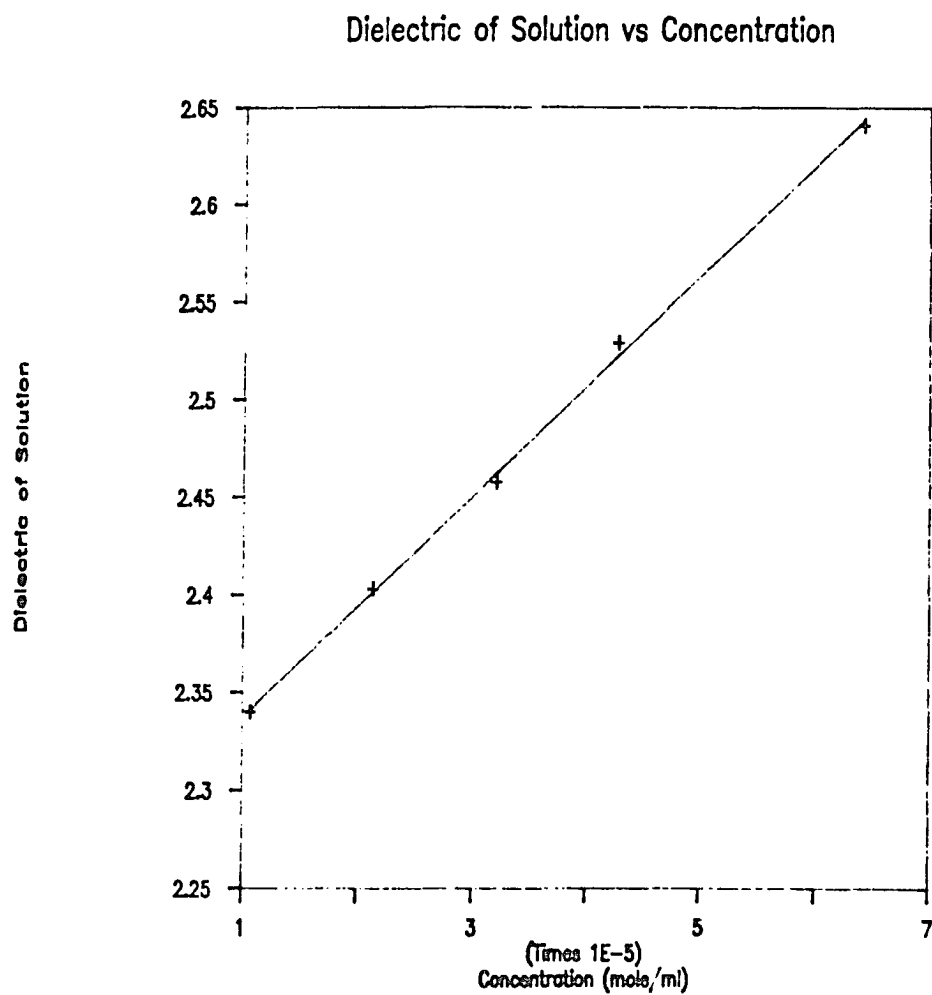


Figure 3. Dielectric Value in Dioxane Versus Concentration for Compound 87.

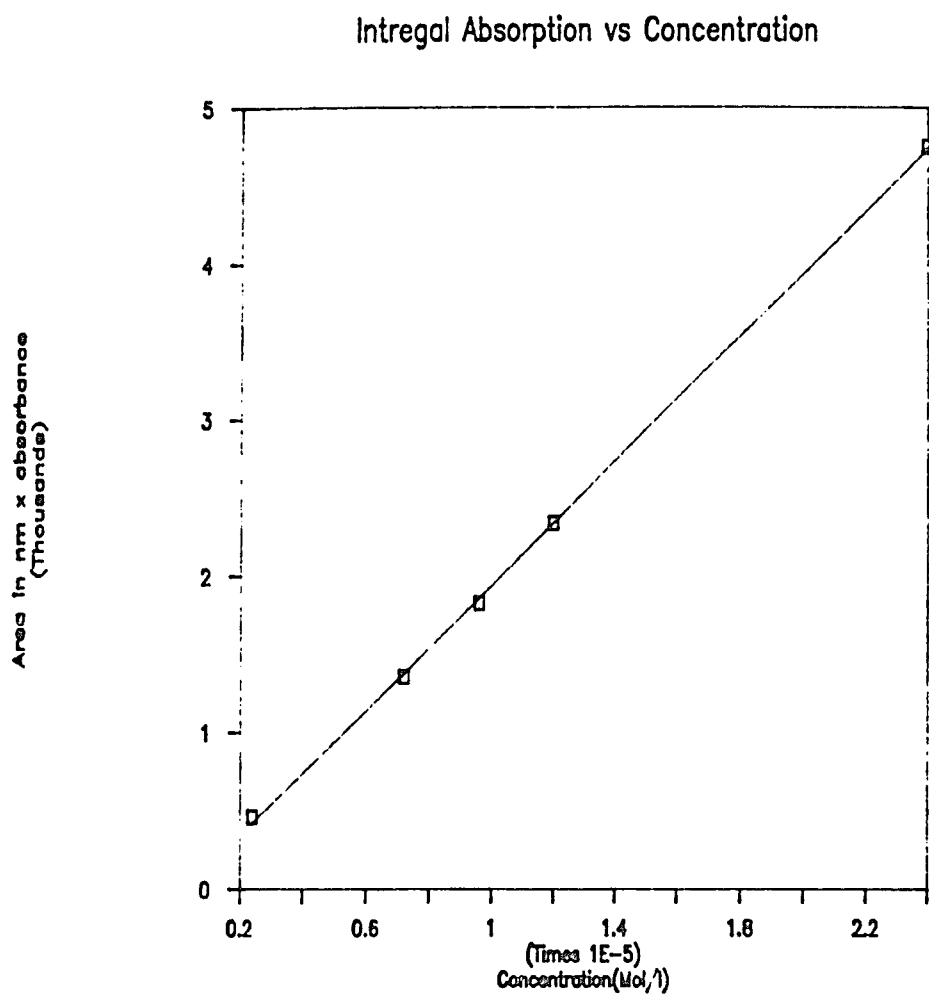


Figure 4. Integral Area Versus Concentration for Compound 48.

Table 15. Transition Frequencies and Transition Dipole Moments.

Compound	$\epsilon(\text{l mole}^{-1} \text{ cm}^{-1})$	$\mu_{eg}(\text{D})$	$\omega_{eg}(\text{cm}^{-1})$
1	14,136	4.77	28,249
97	22,449	5.10	27,285
87	18,333	5.54	26,955
68	20,600	8.92	34,436
64	40,700	10.6	34,483
20	23,314	7.39	34,965
48	-----	10.7	34,916
98	28,000	2.89	28,944
99	14,143	4.77	28,249

Excited State Dipole Moment

The excited state dipole moment (μ_e) determinations are the most approximate part of the determination of β_{xxx} . Early on in the method development anomalous results were obtained for the excited state dipole moment of *p*-sulfide- α -cyanocinnamate (97). The measured value by a method described in the literature was $\mu_e = 40$ D, which gave a $\mu_e\beta_{xxx} = 576 \times 10^{-48}$ esu. This result is a factor of 10 greater than that of similar *p*-oxy- α -cinnamates previously reported (see Table 16).^{39,40}

Table 16. EFISH Values of Some α -Cyanocinnamates.

Compound	$\mu\beta_x$
100	$57 \times 10^{-48} \text{ esu}$
101	$113 \times 10^{-48} \text{ esu}$

While it is true that the sulfur analogue should have a higher hyperpolarizability than the oxy systems because sulfur is a better and more polarizable donor,^{19,80} it probably should not be ten times as great. These questionable results prompted a more intensive investigation of the method for evaluating μ_e . Three compounds whose excited state dipole

moments were determined by electrochromic techniques (methods considered more accurate than solvatochromic measurements) were chosen to evaluate many methods and equations. The compounds chosen were: *p*-nitroaniline (**1**, literature $\mu_e=14-15D$),⁸⁰ 4-(dimethylamino)benzonitrile (**95**, literature $\mu_e=11.1D$),¹⁰² and 2-amino-7-nitrofluorene (**96**, literature $\mu_e=19-23D$).¹⁰² The UV/visible and fluorescence spectra of each of these compounds were measured in the solvents listed in Table 13, and their μ_e 's were calculated from the equations 24-30 with varying Onsager factors. The results are tabulated in Tables 17-19.

Examination of the data immediately shows that no method is consistently superior to any other method. Some methods work better for some compounds, with most methods failing for 4-(dimethylamino)-benzonitrile (**95**). The best overall results were obtained by the two UV/visible absorption equations: Equation 24 calculated with an Onsager factor of 0.6 ($\pm 16\%$ error), and Equation 26 calculated with an Onsager factor of 0.7 ($\pm 12\%$ error). The experimental absorbance values are plotted against the theoretical values calculated from Equation 26, and the plots for Compounds **1**, **95**, and **96** are shown in Figures 5-7, respectively. It must be stressed that these results are only for the three compounds tested here, and these equations may fail with other compounds. There seems to be no relation between the quality of the linear regression (Linear Correlation) and the accuracy of the results. This latter fact is indicative of the randomness of the solvatochromic measurement of the excited state dipole.

We had hoped that the difference in absorption and fluorescence measurements would yield better and more consistent results. Equations 29 and 30 offer a unique opportunity to calculate the difference $\mu_e - \mu_g$ without the need to measure the ground state dipole moment. This difference value could then be plugged directly into Equation 11. However, as shown in Table 20, the results are again erratic.

Table 17. Results of Solvatochromic Determinations of the Excited State Dipole Moment of *p*-Nitroaniline (**1**, $\mu_e = 14\text{-}15\text{D}$) with Equations 24-30.

Onsager Factor	Equation	μ_e	% Error	Linear Correlation
0.5	24	9.8	-30	0.9207
	25	14.8	0	0.7965
	26	9.3	-34	0.9248
	27	10.5	-25	0.9470
	28	11.7	-16	0.8525
	29	10.9	-22	0.8873
	30	10.2	-27	0.5793
0.6	24	11.7	-16	0.9207
	25	20.3	35	0.7965
	26	10.8	-23	0.9248
	27	12.2	-13	0.9470
	28	13.9	-1	0.8525
	29	12.0	-14	0.8873
	30	11.2	-20	0.5793
0.7	24	14.3	0	0.9207
	25	28.0	87	0.7965
	26	13.0	-7	0.9248
	27	14.1	0	0.9470
	28	16.2	8	0.8525
	29	13.3	-5	0.8873
	30	12.2	-13	0.5793

Table 18. Results of Solvatochromic Determinations of the Excited State Dipole Moment of 4-(Dimethylamino)benzonitrile (95, $\mu_e = 11.1\text{D}$) with Equations 24-30.

Onsager Factor	Equation	μ_e	% Error	Linear Correlation
0.5	24	9.2	-17	0.9958
	25	14.8	33	0.9556
	26	8.7	-21	0.9953
	27	14.3	28	0.9143
	28	16.8	51	0.8937
	29	15.2	37	0.8889
	30	14.7	33	0.8604
0.6	24	11.2	0	0.9958
	25	20.8	87	0.9556
	26	10.3	-6	0.9953
	27	17.4	57	0.9143
	28	20.8	87	0.8937
	29	17.9	61	0.8889
	30	17.3	56	0.8604
0.7	24	13.9	25	0.9958
	25	29.2	163	0.9556
	26	12.5	12	0.9953
	27	20.9	88	0.9143
	28	25.3	128	0.8937
	29	20.9	88	0.8889
	30	20.1	81	0.8604

Table 19. Results of Solvatochromic Determinations of the Excited State
Dipole Moment of 2-Amino-7-nitrofluorene (96,
 $\mu_e = 19\text{-}23\text{D}$) with Equations 24-30.

Onsager Factor	Equation	μ_e	% Error	Linear Correlation
0.5	24	12.3	-35	0.4952
	25	27.3	19	0.5252
	26	11.2	-41	0.5008
	27	16.3	-14	0.9600
	28	19.3	0	0.9305
	29	16.6	-13	0.9012
	30	18.0	-5	0.7984
0.6	24	16.3	-14	0.4952
	25	42.3	84	0.5252
	26	14.5	-24	0.5008
	27	20.1	0	0.9600
	28	24.1	5	0.9305
	29	19.6	0	0.9012
	30	21.5	0	0.7984
0.7	24	22.0	0	0.4952
	25	63.1	174	0.5252
	26	19.0	0	0.5008
	27	24.3	6	0.9600
	28	29.4	28	0.9305
	29	23.0	0	0.9012
	30	25.3	10	0.7984

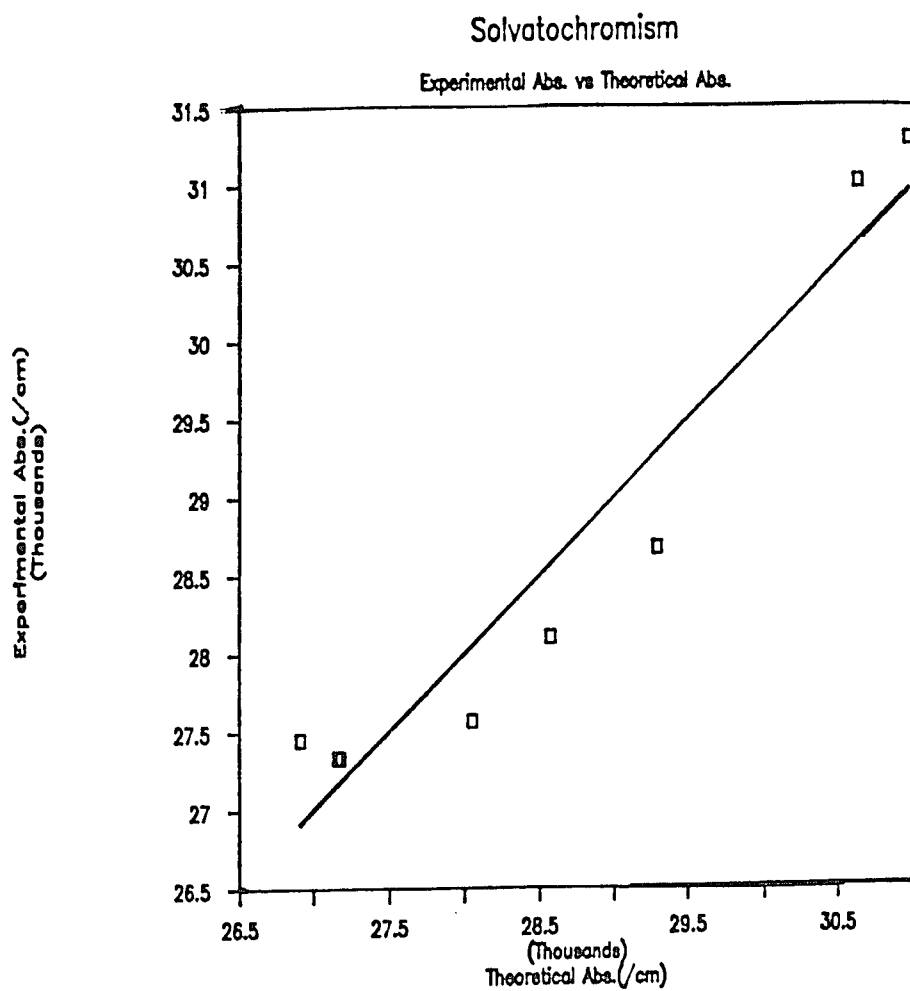


Figure 5. Frequency of Absorbance Calculated From Equation 26 Versus Experimental for Compound 1.

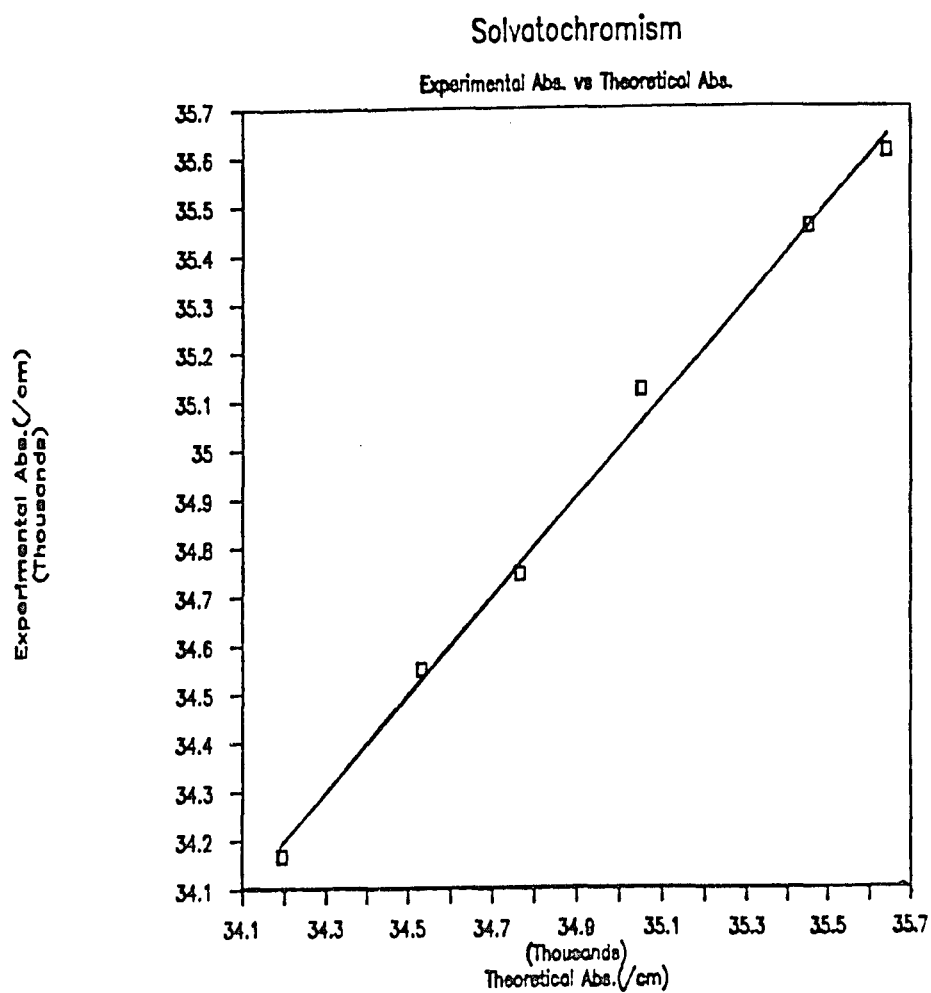


Figure 6. Frequency of Absorbance Calculated From Equation 26 Versus Experimental for Compound 95.

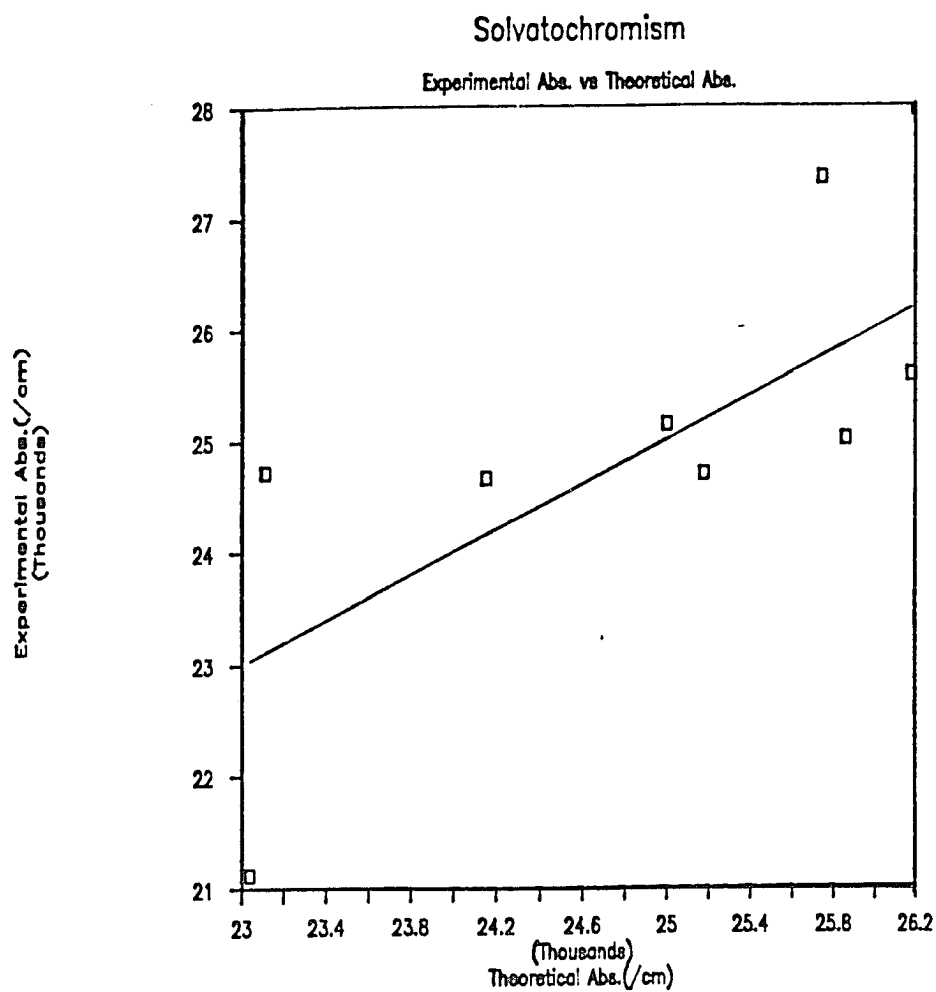


Figure 7. Frequency of Absorbance Calculated From Equation 26 Versus Experimental for Compound 96.

Table 20. Difference Between Excited and Ground State Dipole Moments
Calculated From Equations 29 and 30 for Compounds 1,
95, and 96.

Equation	Factor	$\mu_e - \mu_g$ in Debye (lit.)		
		1(6.6-6.9D)	96(12.4-16.2D)	95(4.6D)
29	0.5	3.7	9.8	8.7
	0.6	4.9	12.8	11.4
	0.7	6.2	16.2	14.4
30	0.5	3.1	11.2	8.2
	0.6	4.0	14.7	10.8
	0.7	5.1	18.5	13.6

With the exception of 4-(dimethylamino)benzonitrile (95), Equation 29 seems to work well to give the difference in dipoles (at a Onsager factor of 0.7). However, like all the equations, they are subject to unpredictable anomalies, as demonstrated by the high values for 95.

Second Order Hyperpolarizability

Because of the potentially gross errors from solvatochromic measurements of μ_e , hyperpolarizabilities calculated from these values should be viewed critically. With these facts in mind, the β_{xxx} values of various compounds were calculated using Equation 26 (with an Onsager factor of 0.7). The results from these calculations are listed in Table 21.

Table 21. Hyperpolarizabilities (β_{xxx}) Determined by Spectrophotometric Method, Utilizing Equation 26.

Compound	μ_e (D)	$\beta_{xxx}(x 10^{-30}\text{esu})$	$\beta_x(x 10^{-30}\text{esu})$
1	13	13	29
97	37	134	--
98	5	0.44	--
87	18	40	86

The values for both cinnamates are unreasonable, the thioether cinnamate **97** being high, and the ether cinnamate **98** being low. Expected values for β_x of these compounds should be around 10×10^{-30} to 50×10^{-30} esu. In both cases it appears that the fluorescence relationship gives more reasonable results, in particular Equation 29:

Table 22. Hyperpolarizabilities (β_{xxx}) Determined by Spectrophotometric Method, Utilizing Equation 29.

Compound	$\mu_c(D)$	$\beta_{xxx}(x 10^{-30} \text{esu})$
97	18	58
98	11	5

There seems to be some characteristic of the cinnamates which tends to give erroneous results. Realizing that 4-(dimethylamino)benzonitrile (**95**) also gave large errors by the solvatochromic measurements, it may be assumed that nitriles in general behave outside the predictive capabilities of these solvatochromic equations. However, Equation 29 did give the expected values of β_{xxx} for the cyanoenamine E/Z mixture of **87**; this may be because the nitrile moiety is a minor component of compound **87**. These facts illustrate the limitations of the solvatochromic determinations of μ_e , and thus limitations in the β_{xxx} calculations.

The *p*-aminophenyl sulfone monomers (compounds **20** and **68**) and dimers (compounds **48** and **64**) were evaluated by the spectrophotometric method to determine if the method could be extended to dimeric systems. The results indicate that the method does work for dimers, despite violating the assumptions made in the derivation of Equation 11 (see Table 23).

Table 23. Hyperpolarizabilities of Monomers and Dimers Determined by Spectrophotometric Method (β_{xxx}), and by EFISH.

Compound	$\beta_{xxx}(\times 10^{-30}\text{esu})^*$	$\beta_x(\times 10^{-30}\text{esu})$
20	302	26
48	655	66
68	332	45
64	817	104

* Utilizing Equation 29, with Onsager factor = 0.7.

The spectrophotometric method correctly predicted that the hyperpolarizabilities of the dimers were about twice those of the monomers. Also, the values of the piperidine phenyl sulfones (68 and 64) are greater than those of dimethylene aminophenyl sulfones (20 and 48), as was found by the EFISH results. However, the β_{xxx} values are all approximately a factor of ten greater than the EFISH values.

To conclude, these experiments lead to some generalizations concerning the spectrophotometric method. First, the data imply that results from these measurements should not be compared directly with EFISH values. This is because, as seen for the α -cinnamates and *p*-aminophenyl sulfones, the method can give erroneously high results. Anomalous results appear to arise from functional groups which do not behave as the excited state dipole equations predict that they should in solution. Due to this latter statement, as well as the assumptions concerning the vector orientations of the various dipole moments in the derivation of Equation 11, the second characteristic of this method is that compounds of unlike structures should not be compared by this method. This result has been corroborated by other recent work.^{19,103}

On a positive note, the third property of the method is that compounds of similar structure can be compared. This is seen nicely in the *p*-aminophenyl sulfone results, as well as in work done by others.^{80,85}

The *p*-aminophenyl sulfone results also show that this method works for dimeric compounds. However, due to the solvatochromic measurement

of the excited state dipole moment, the method is inherently limited for the evaluation of oligomers and polymers. There are two reasons for this limitation: Solubility in many solvents will be difficult, and the Onsager field radius will vary unpredictably with the solvent for a given polymer.

CHAPTER 5

CONCLUSION

The three projects performed for this dissertation will aid in the development of new nonlinear optical (NLO) polymeric materials. The molecular studies illustrated the pitfalls in designing systems with well defined orientations. The polymers synthesized in the second project showed that main chain NLO polymers with the desired physical properties can be made. The evaluation and improvements of the spectrophotometric method of approximating the hyperpolarizabilities may prove helpful in allowing more researchers enter the organic NLO field.

While the main goal of the p-aminophenyl sulfone project (an observable well defined enhancement) was not obtained, the studies did supply some valuable lessons. First, we confirmed that a long six carbon spacer would not show an enhancement. Second, we demonstrated that a short spacer does not necessarily allow the correct orientation to produce an enhancement. Third, we learned that more rigid systems need to be carefully designed to ensure the appropriate geometry needed. Fourth, we showed that piperidine donors lead to significantly higher hyperpolarizabilities than acyclic amines.

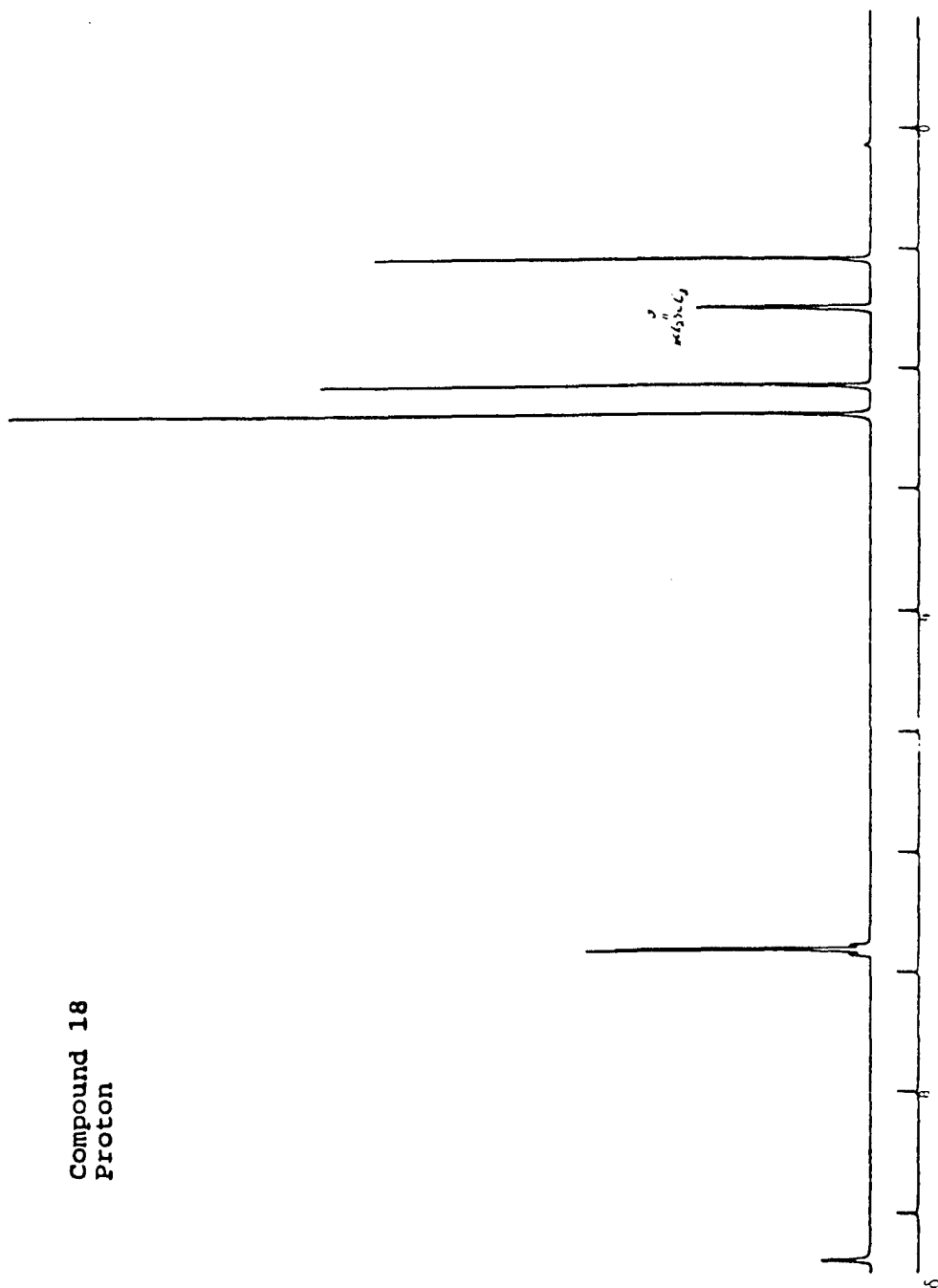
In the synthesis of the stilbene polymers we produced tractable homopolymer and copolymer which contained only NLO chromophores in the main chain. These polymers have very high glass transitions. This may prove to be the most significant result from this dissertation. The use of E and Z olefinic copolymer to impart enough irregularity in the polymer chain without decreasing the concentration of NLO units gave soluble materials with high glass transitions. These results may lead to commercially useful NLO organic polymers. The next avenue of research in this area should be to incorporate stronger NLO-phores (such as E/Z 4'-amino-4-nitrostilbene) into the main chain polymers. The double donor/double acceptor system does not seem to increase the hyperpolarizability, this result is supported by theoretical work done by Marks *et al.*¹⁰⁴

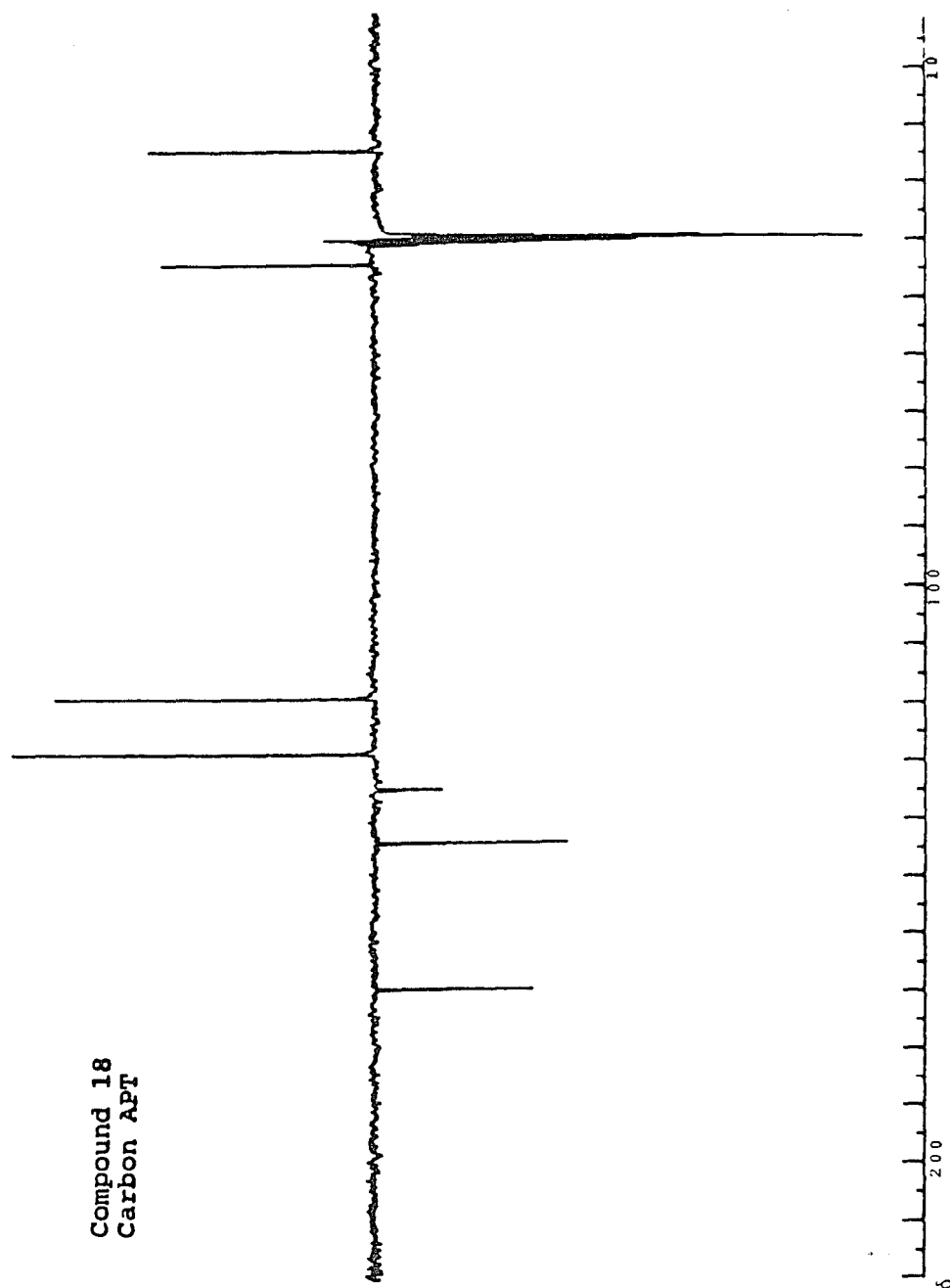
The low cost method of approximating the hyperpolarizability seems to be marginally useful. The main drawback to the method is the crude excited state dipole moment measurement. This obstacle could be overcome

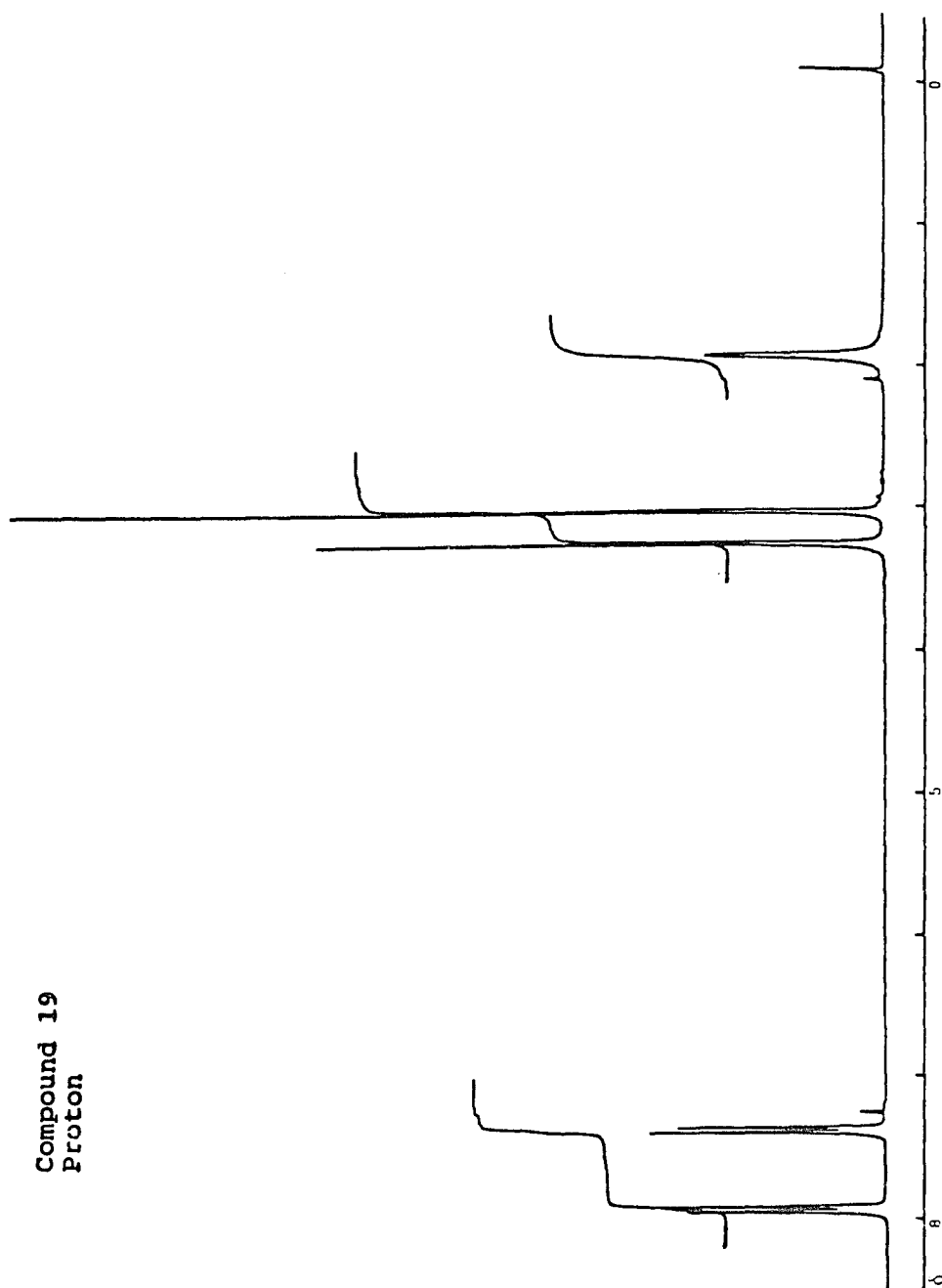
by using electrochromic techniques as opposed to the solvatochromic technique used here. However, electrochromic methods require more expensive and complicated instrumentation. Summarizing, the method evaluated here fails for the comparison of unlike compounds, and can give erroneous results. However, relative qualitative assessments can be performed with this method for compounds of similar structure. Our studies indicate that the method also works for dimeric systems. The solvatochromic determination of the excited state dipole moment probably bars the use of this method for polymers due to solubility problems, as well as the difficulty of estimating the Onsager field radius for a polymer in various solvents.

APPENDIX A
 ^1H NMR AND ^{13}C NMR SPECTRA

Compound 18
Proton

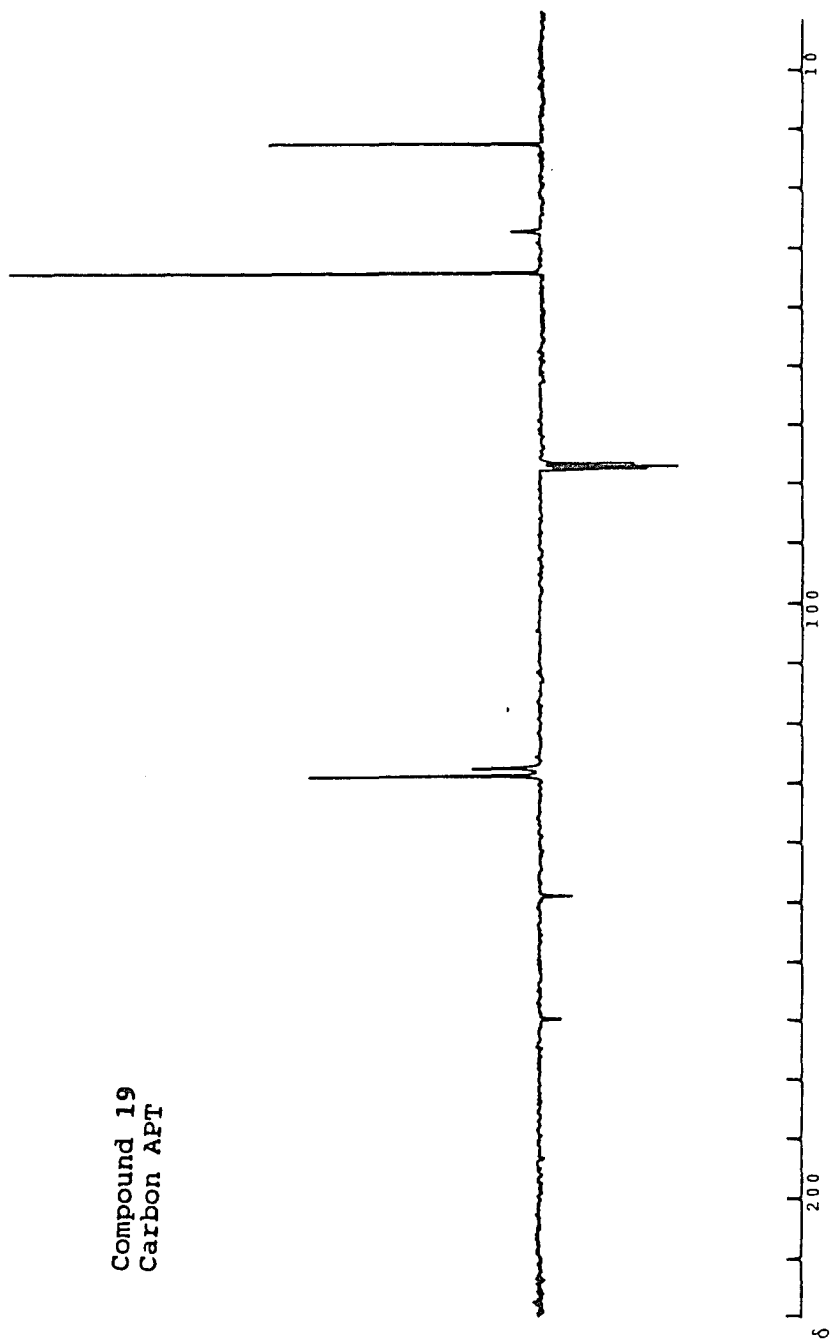


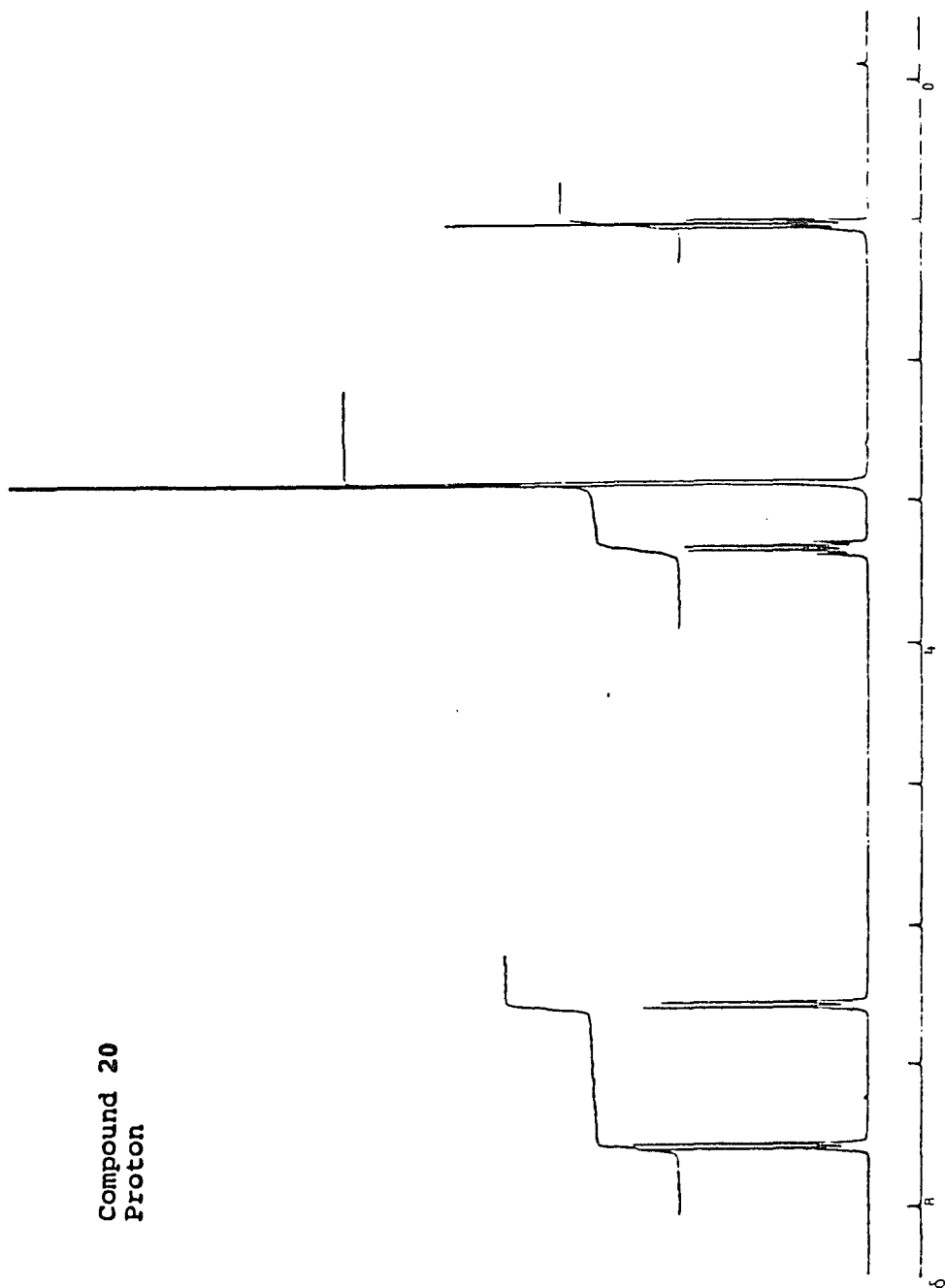




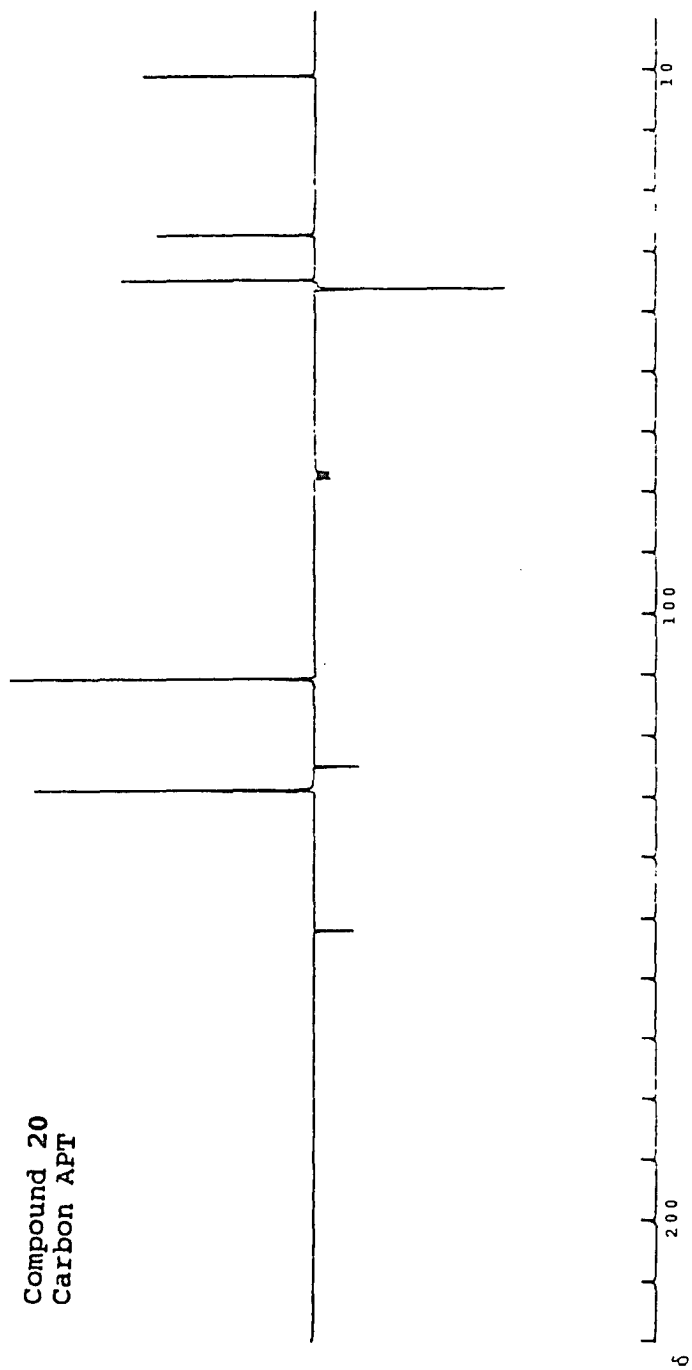
Compound 19
Proton

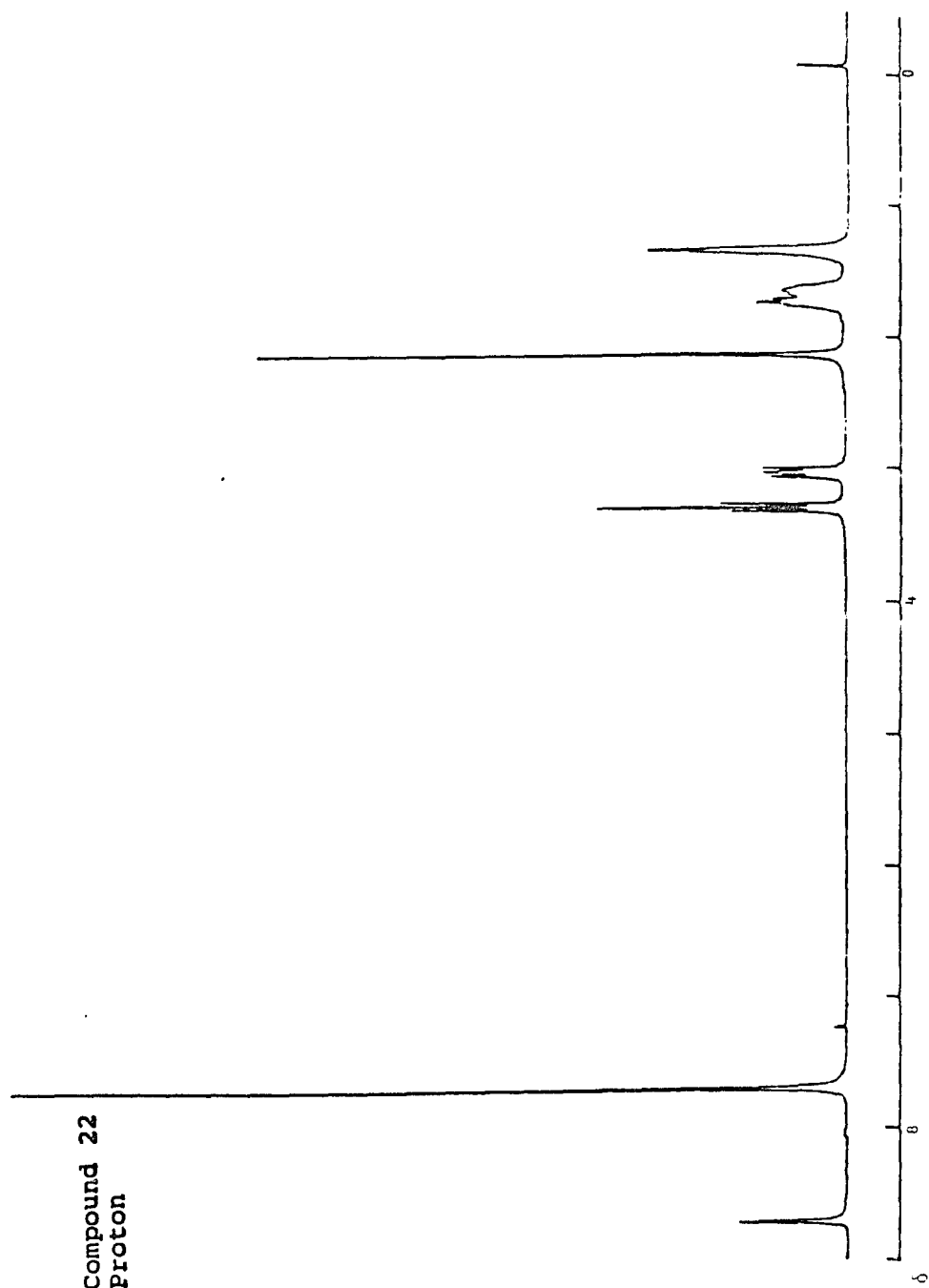
Compound 19
Carbon APT

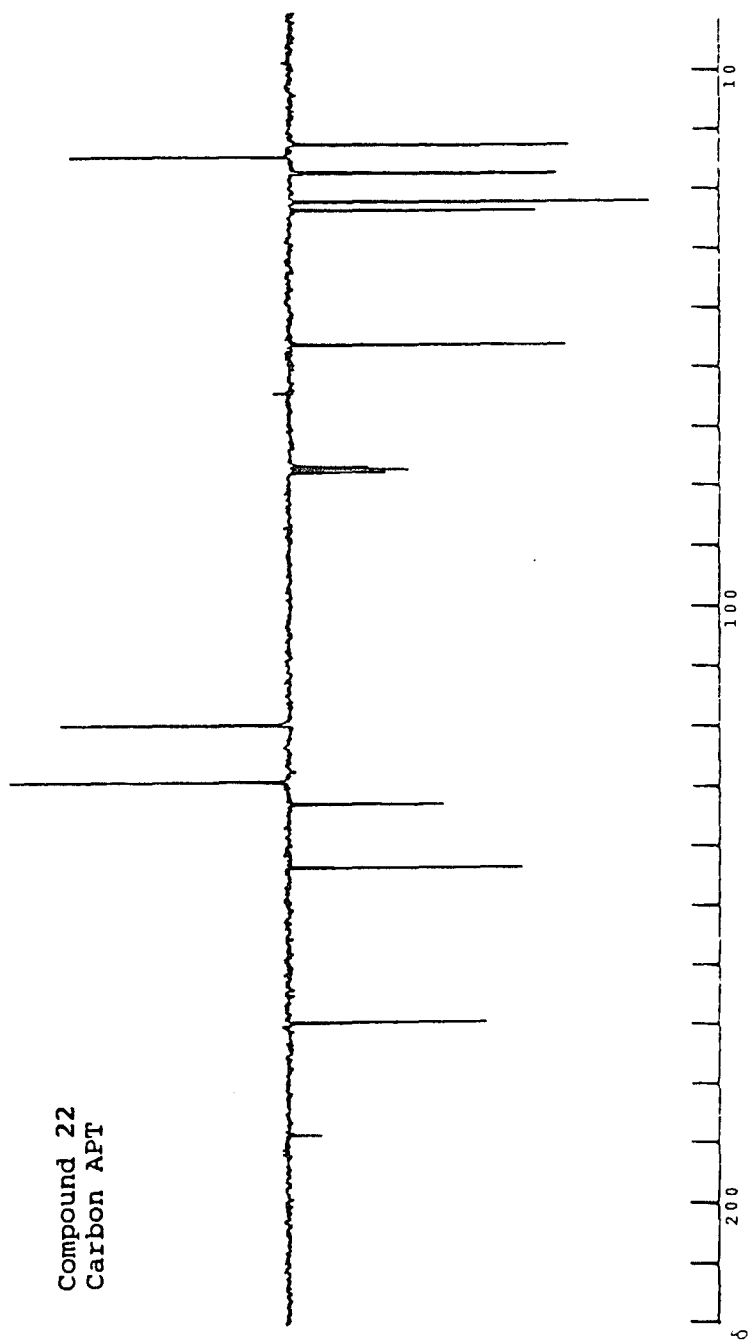




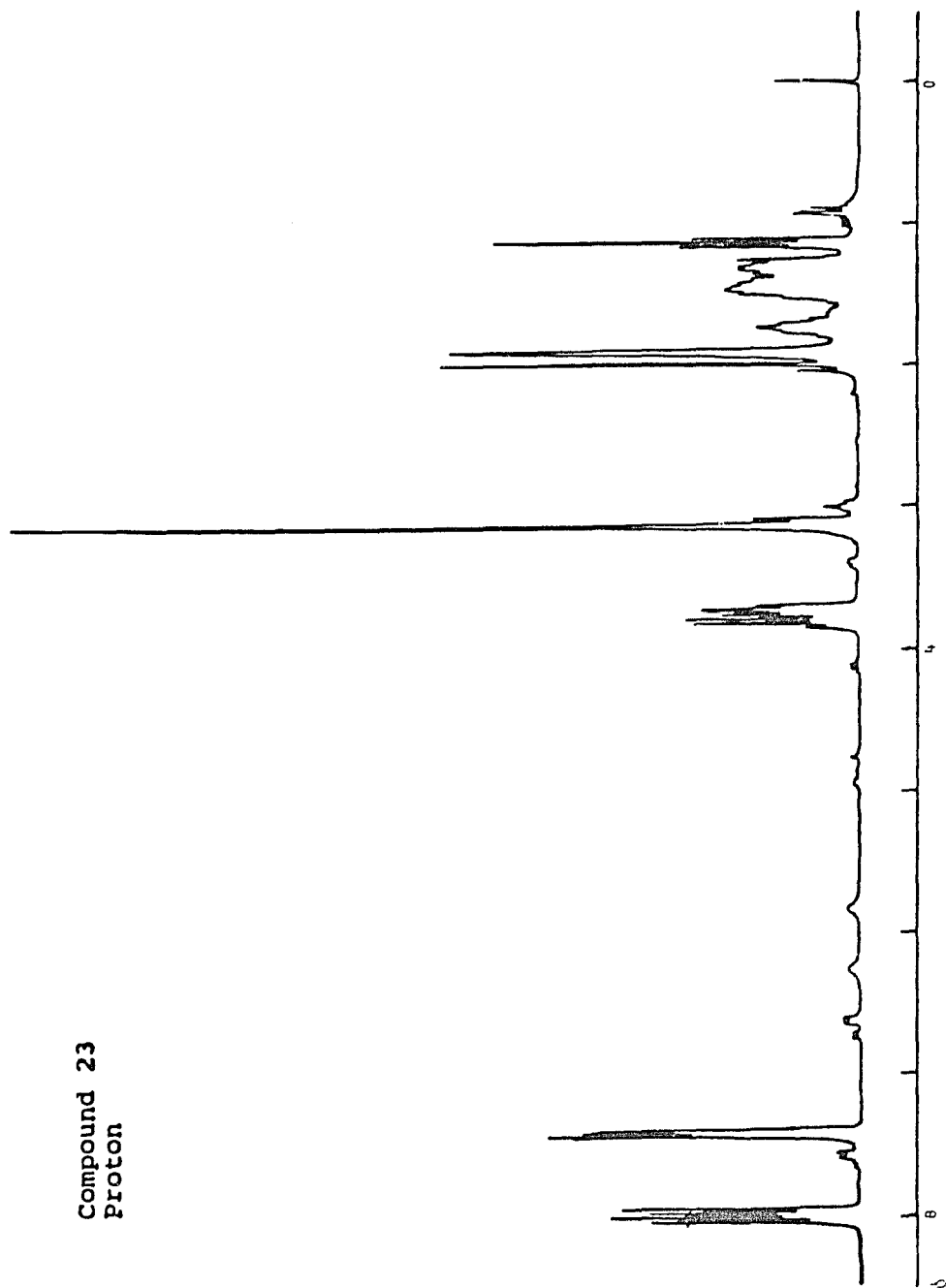
Compound 20
Carbon APT

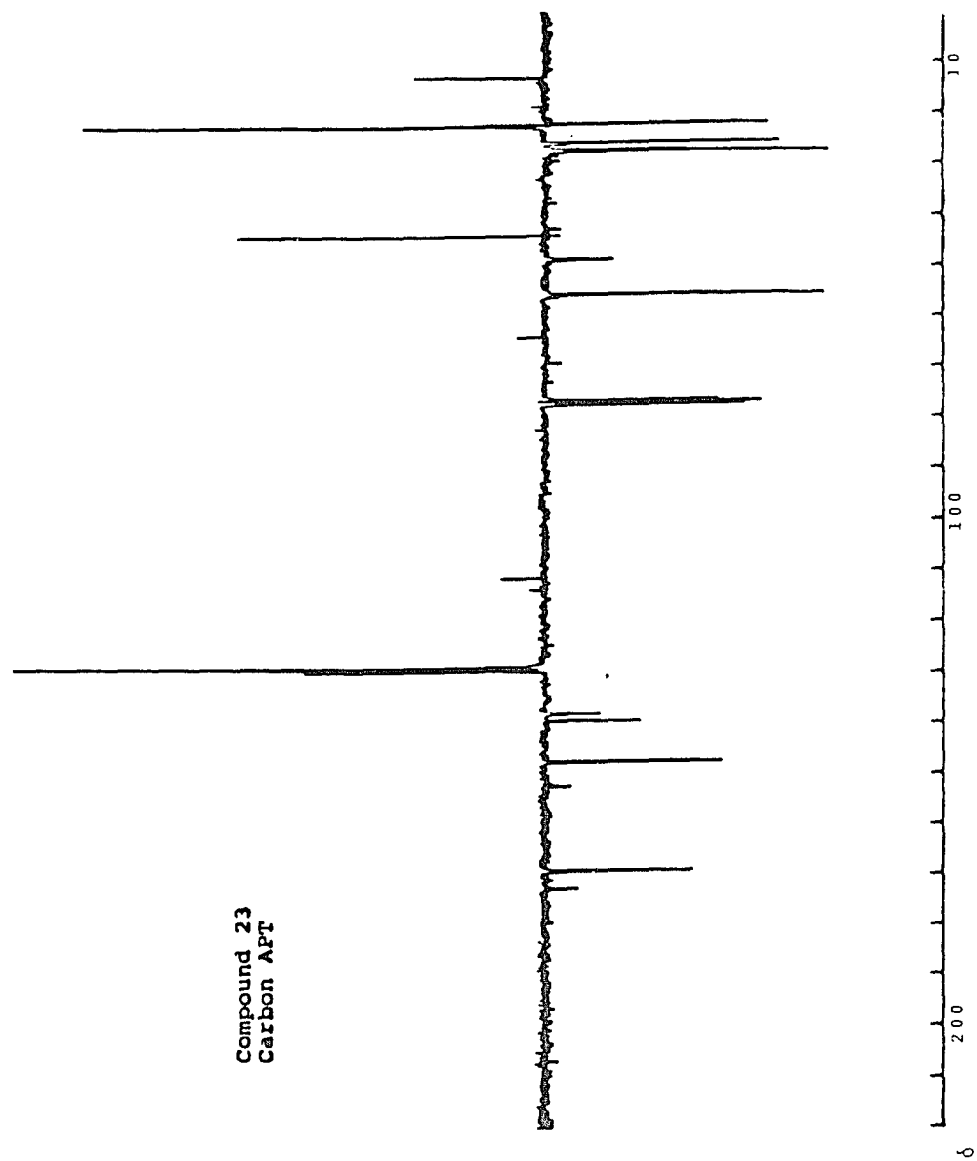


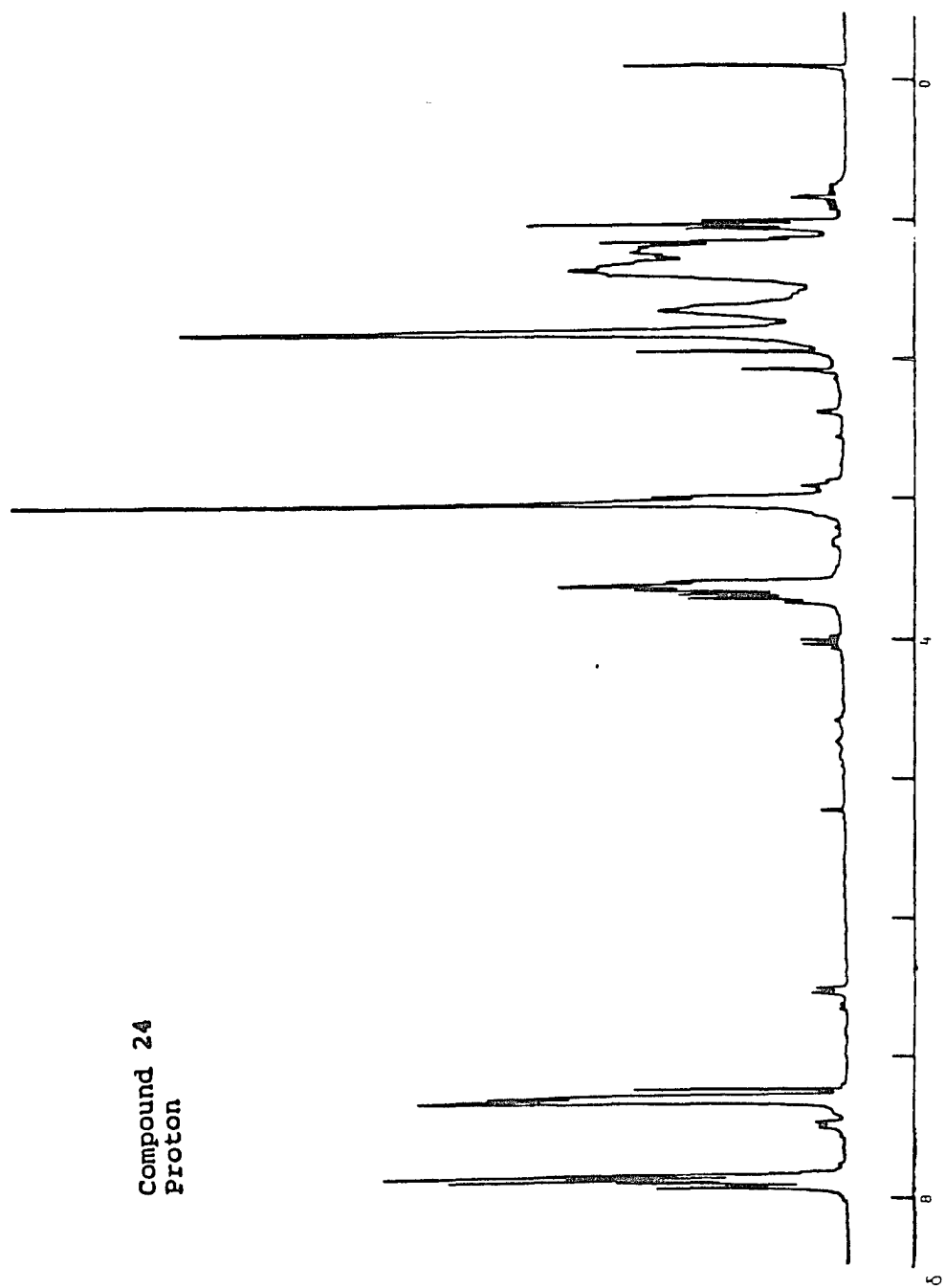


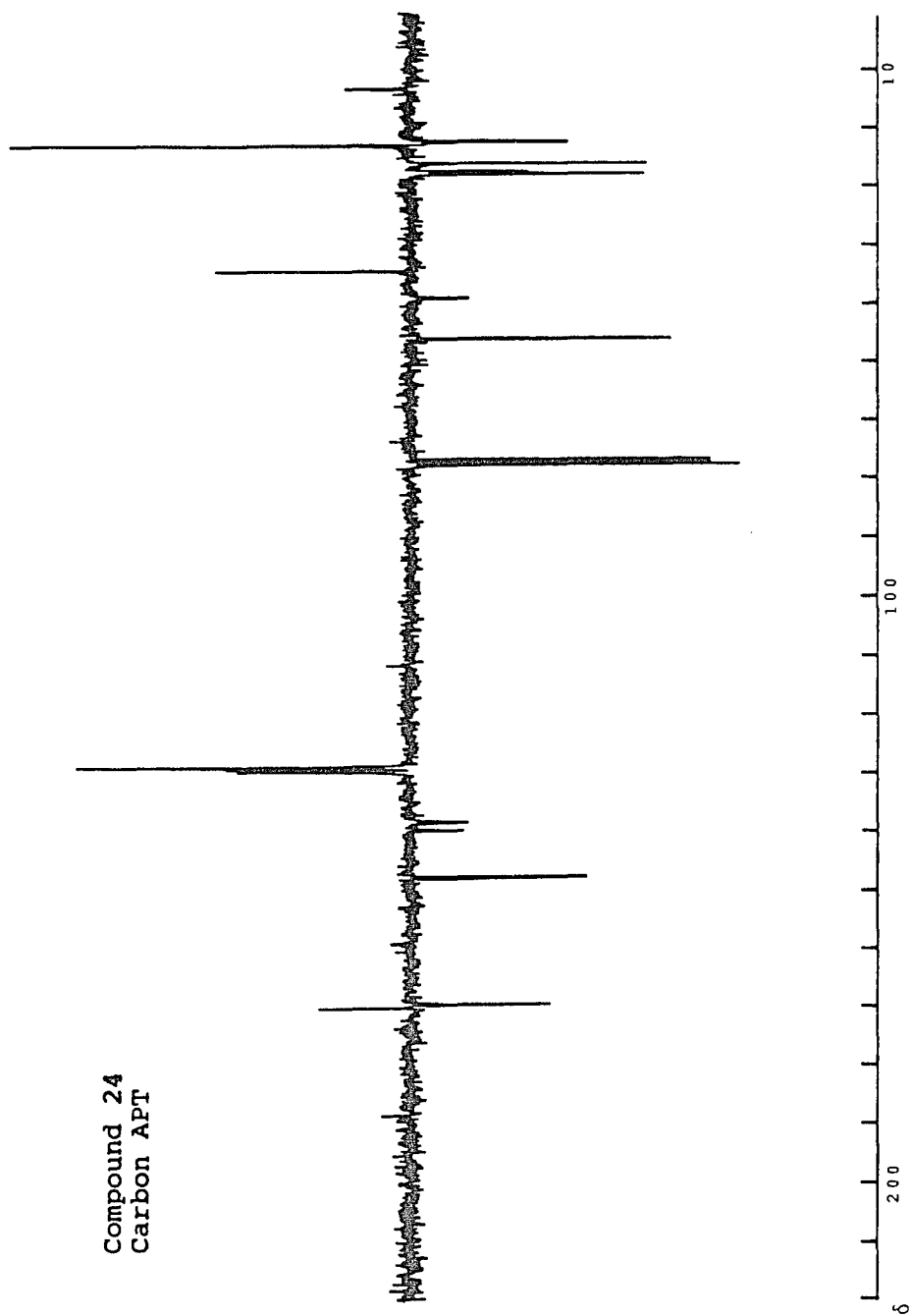


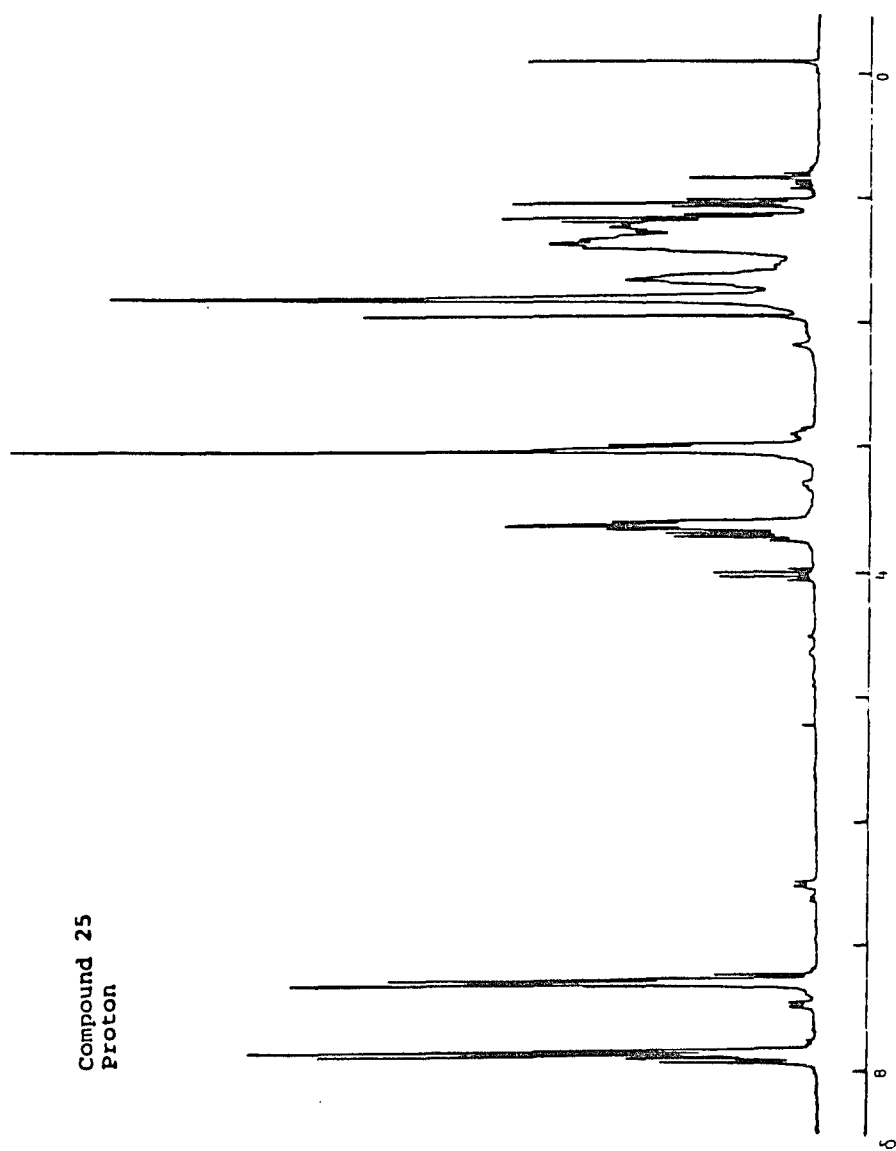
Compound 23
proton



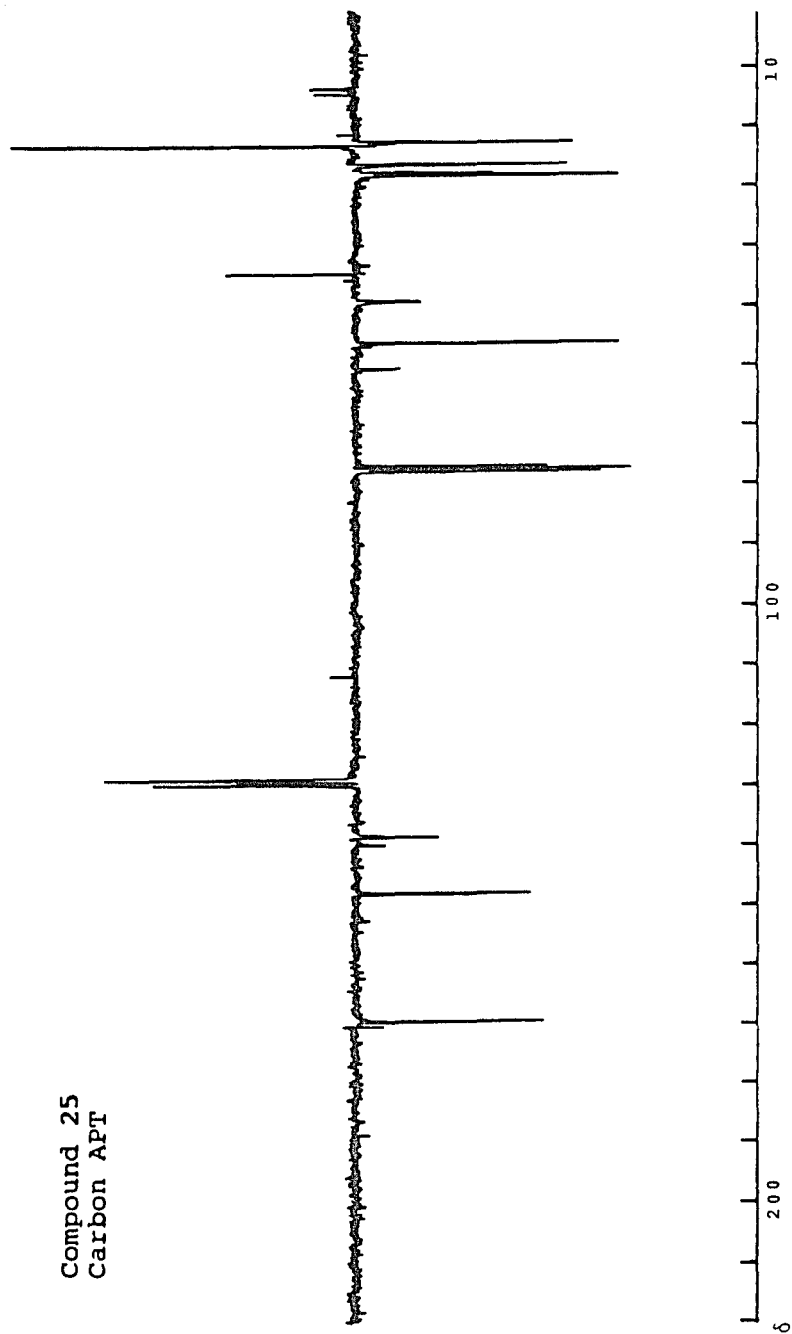




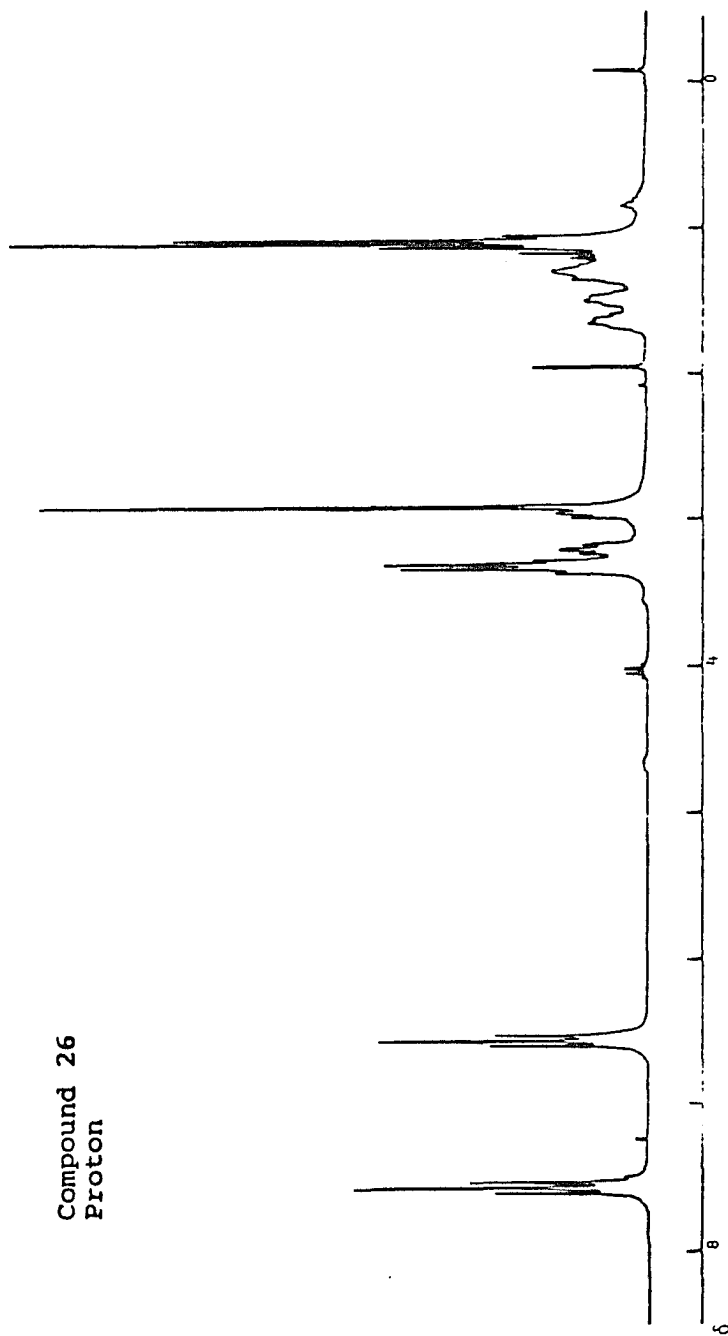


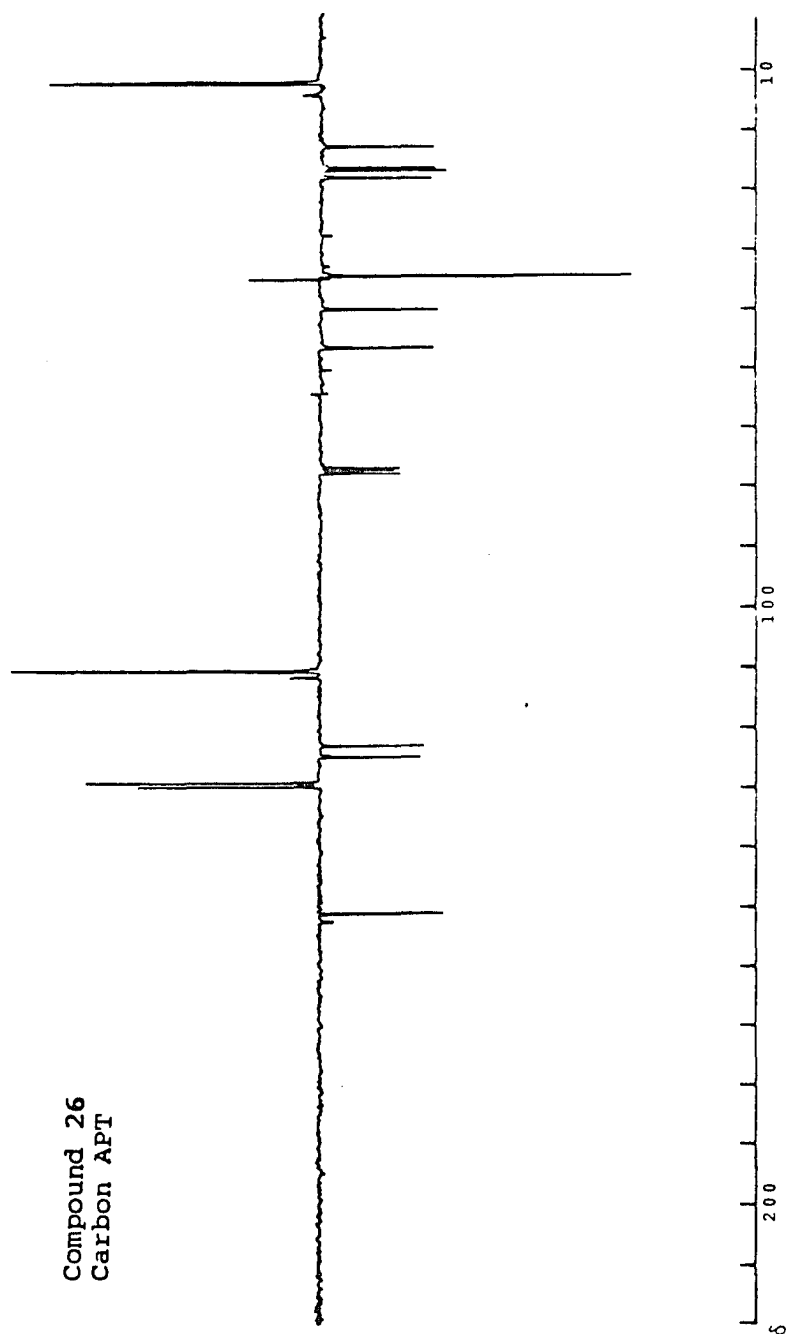


Compound 25
Carbon APT

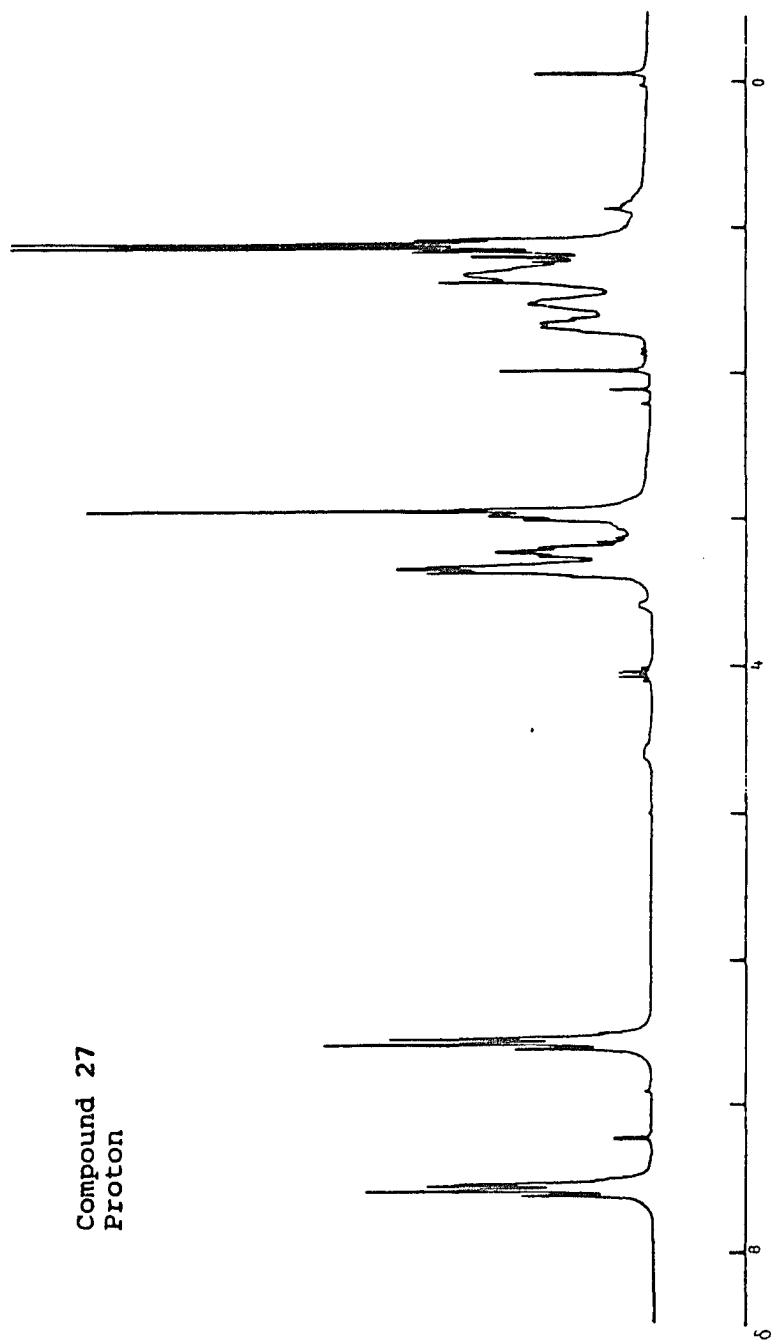


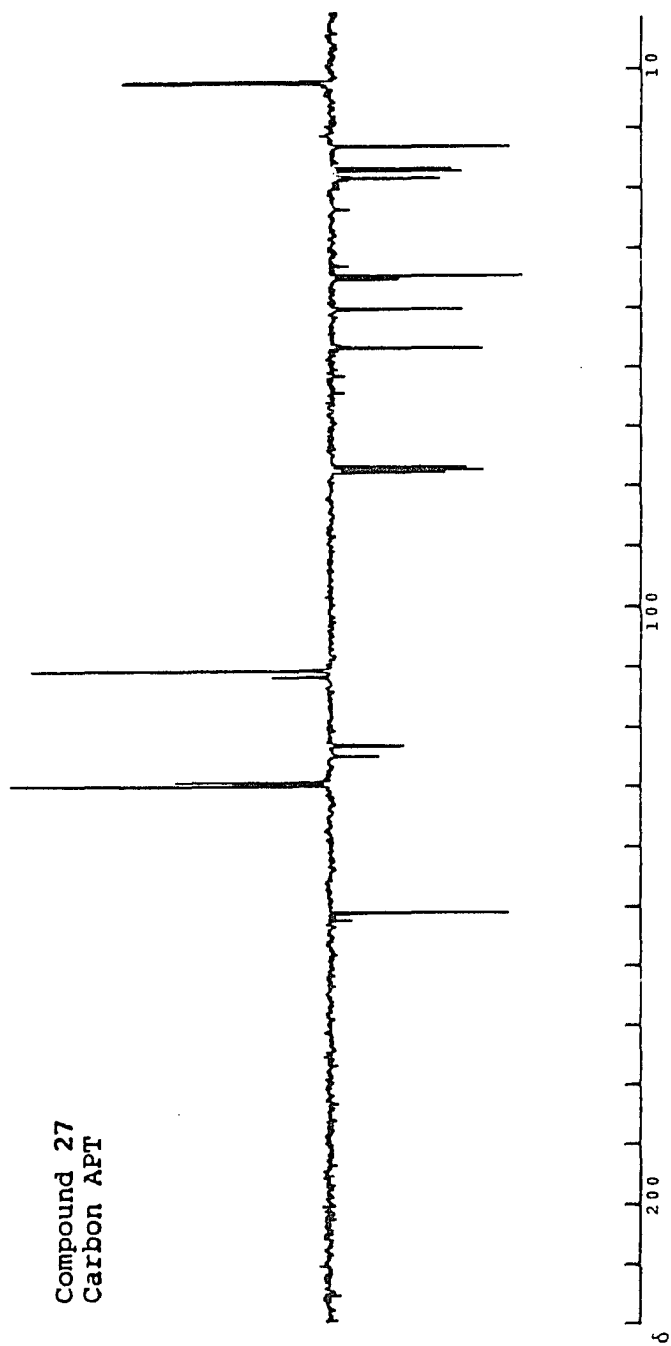
Compound 26
Proton



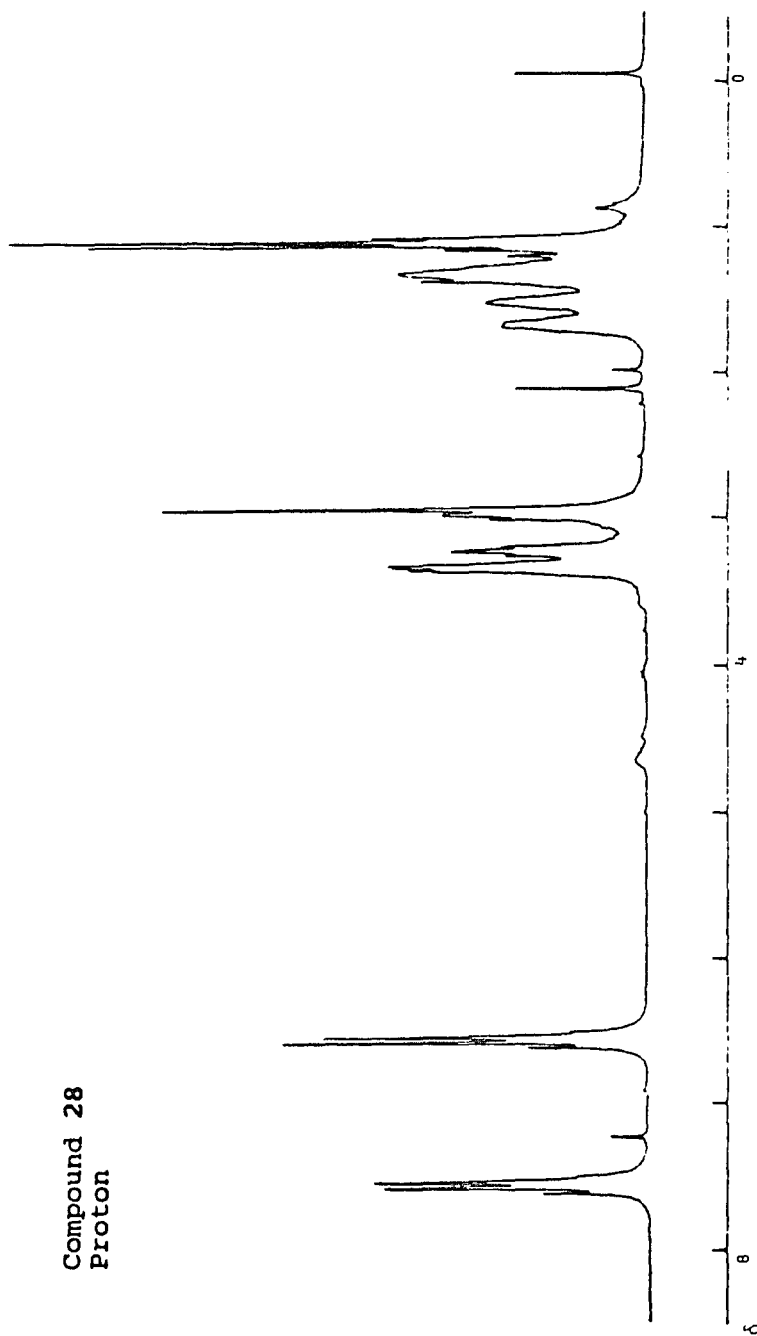


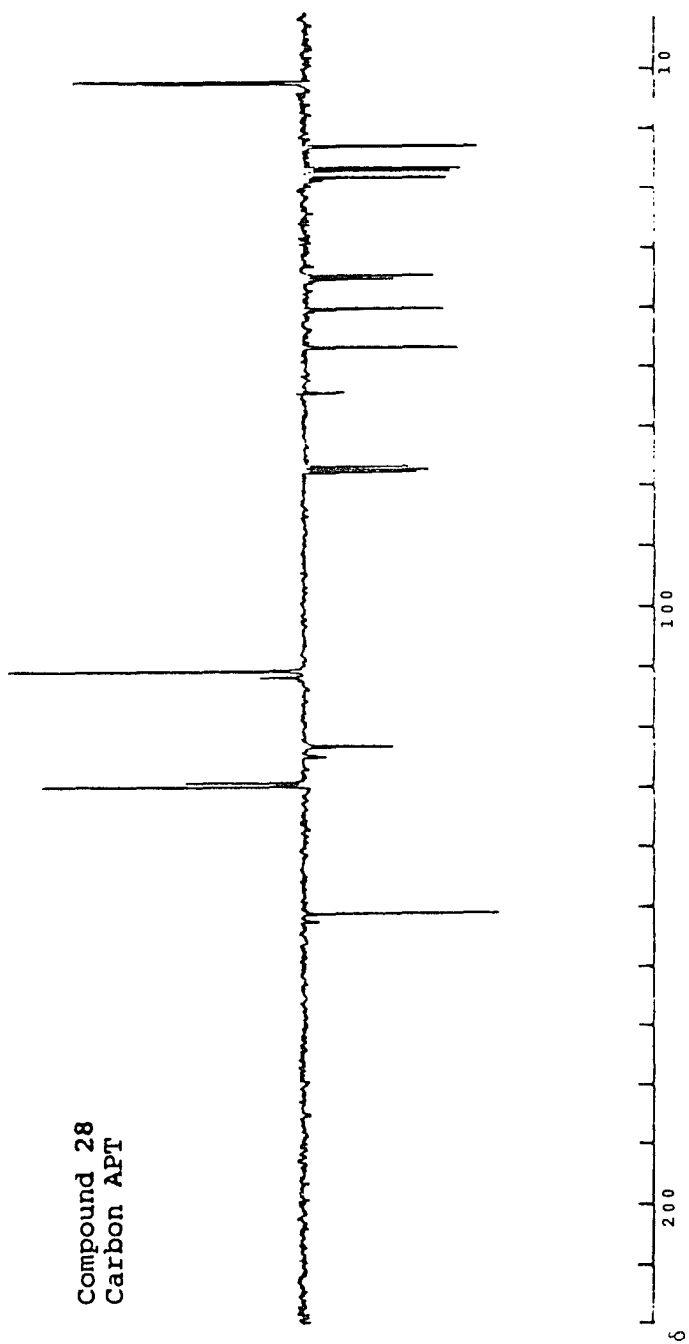
Compound 27
Proton



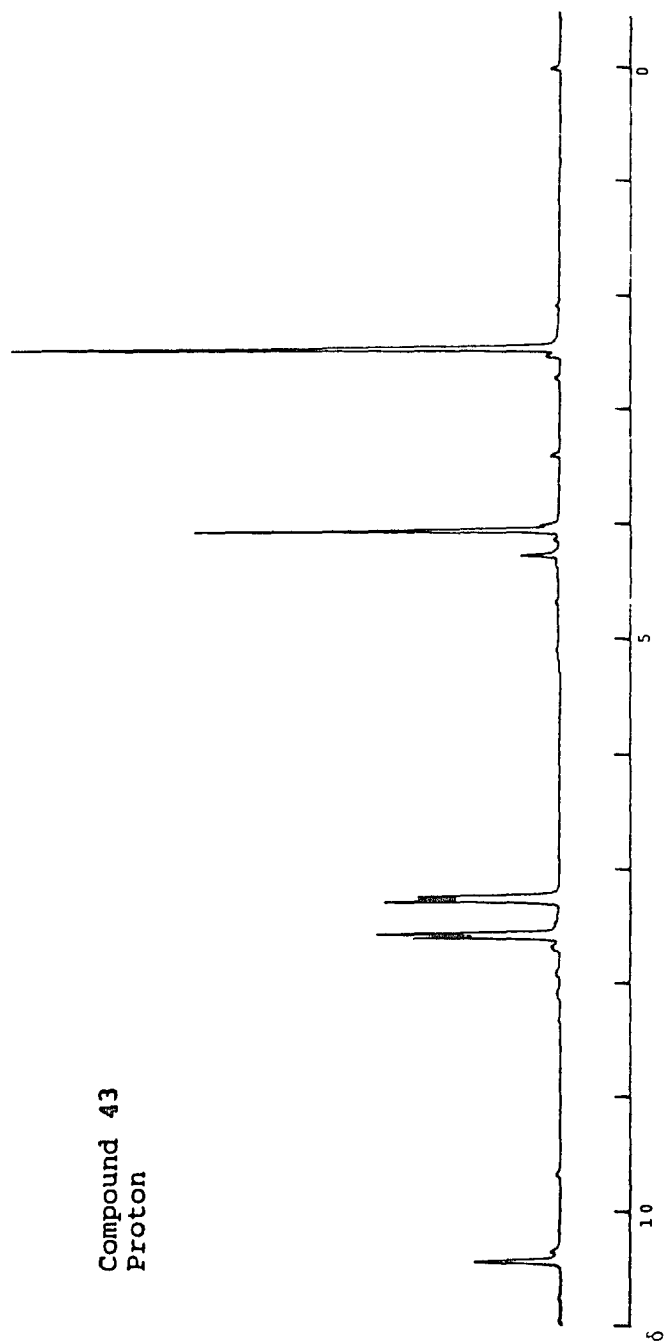


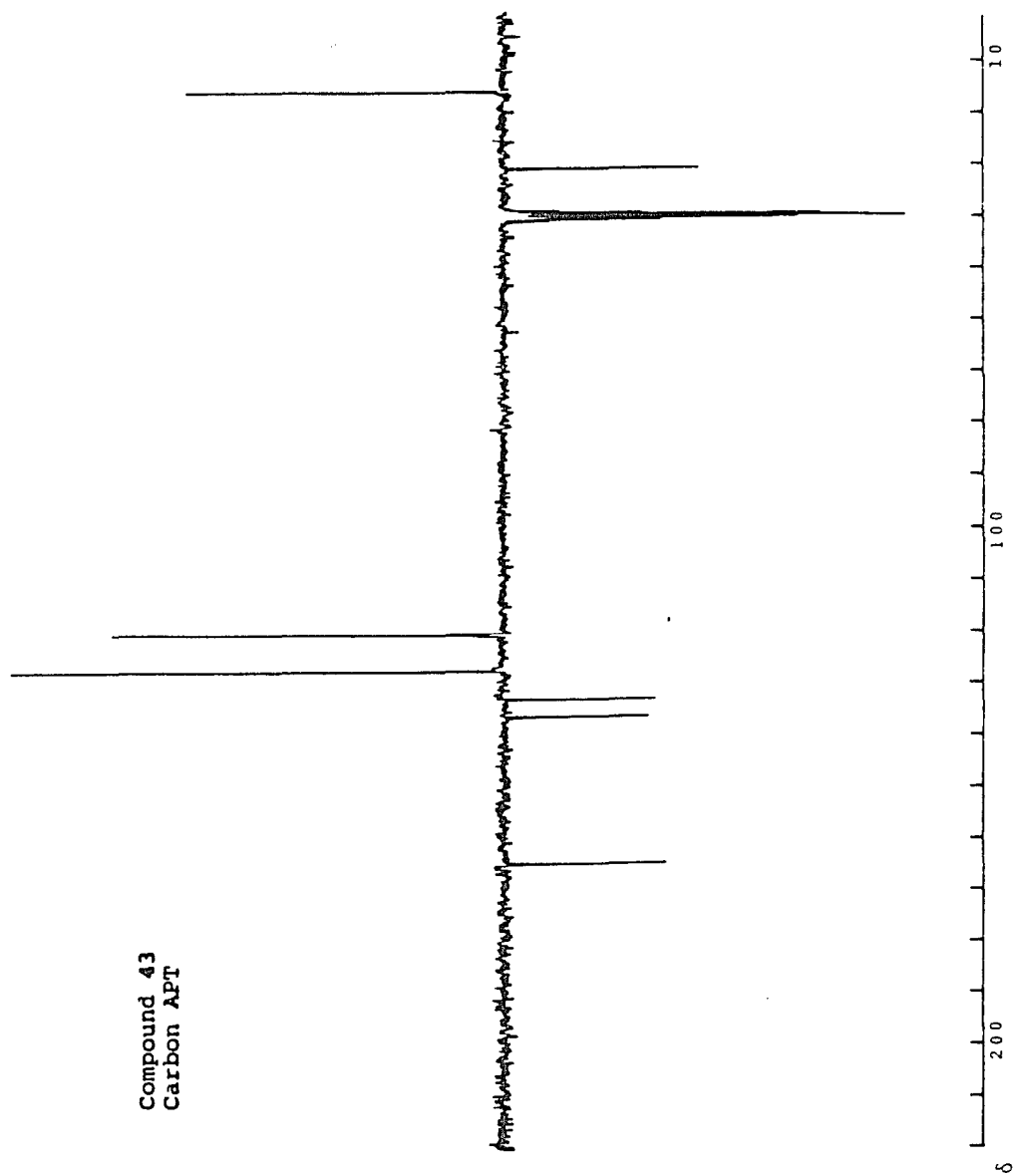
Compound 28
Proton



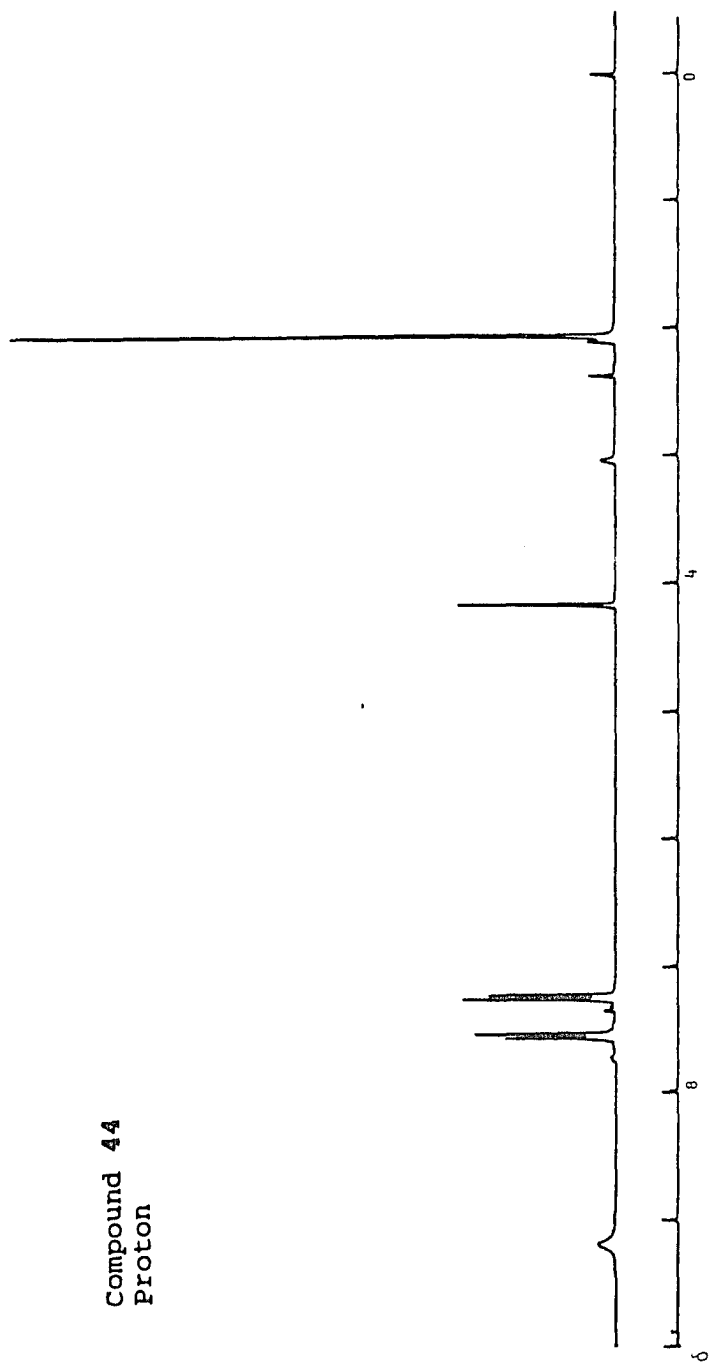


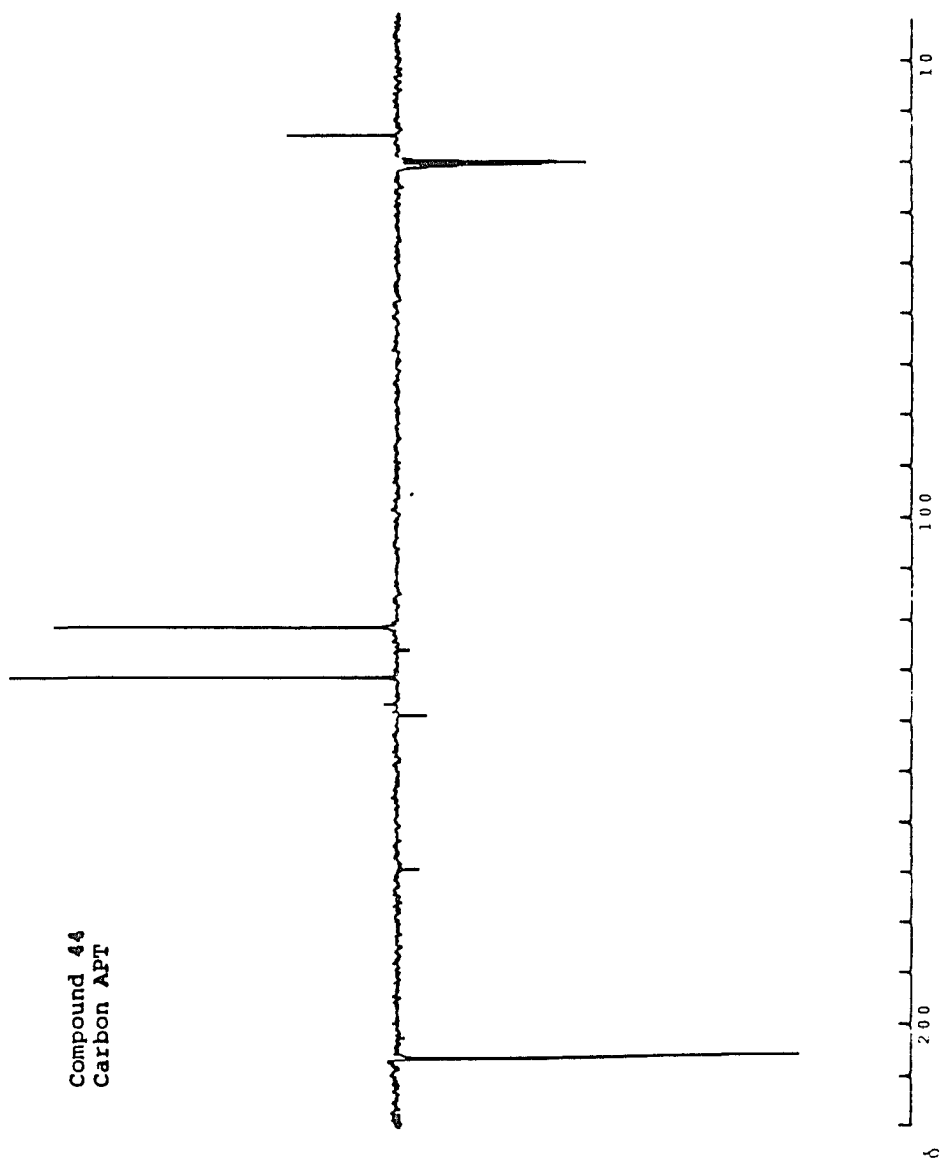
Compound 43
Proton

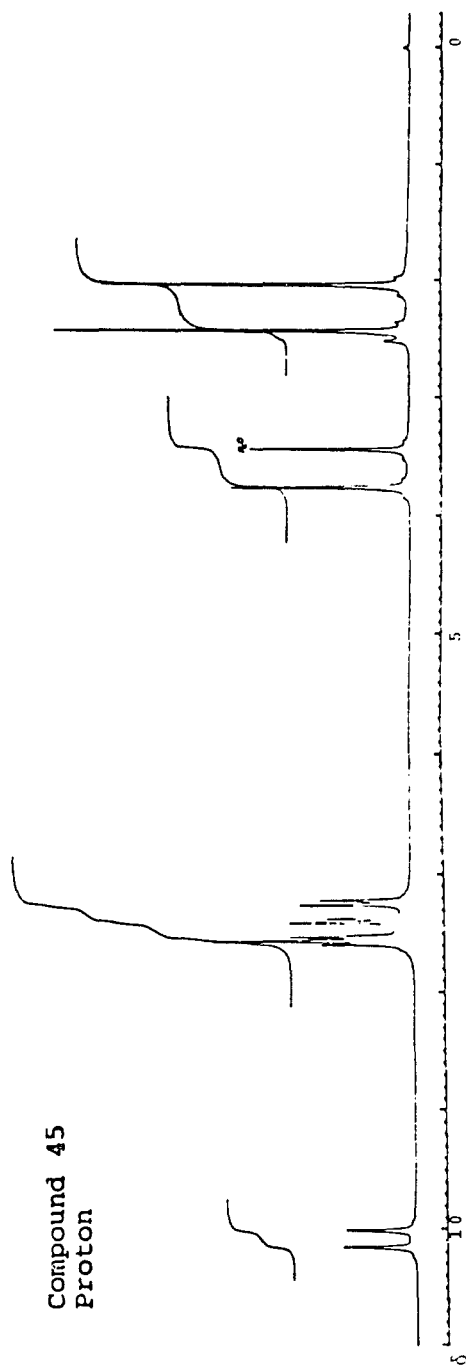




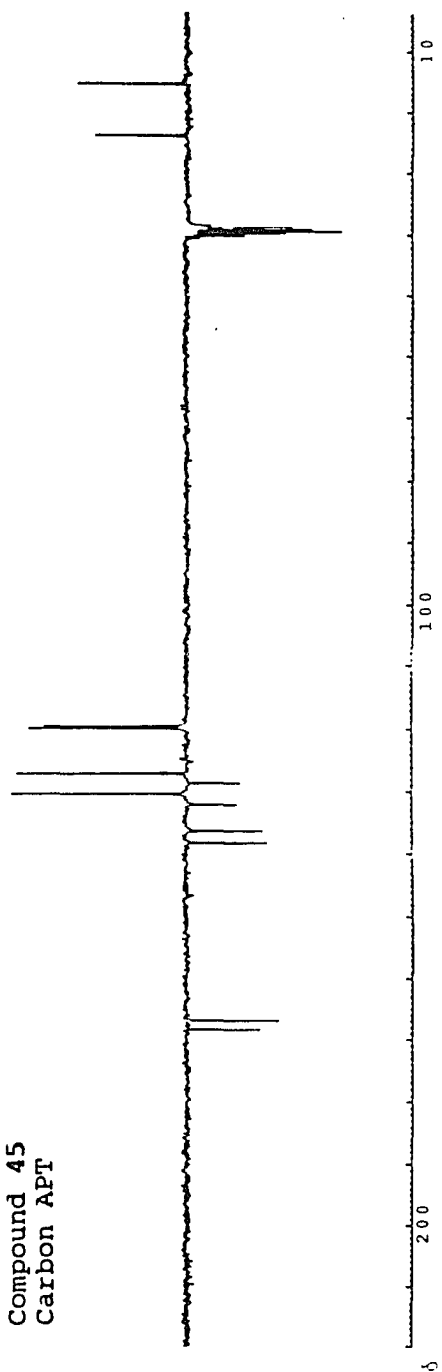
Compound 44
Proton

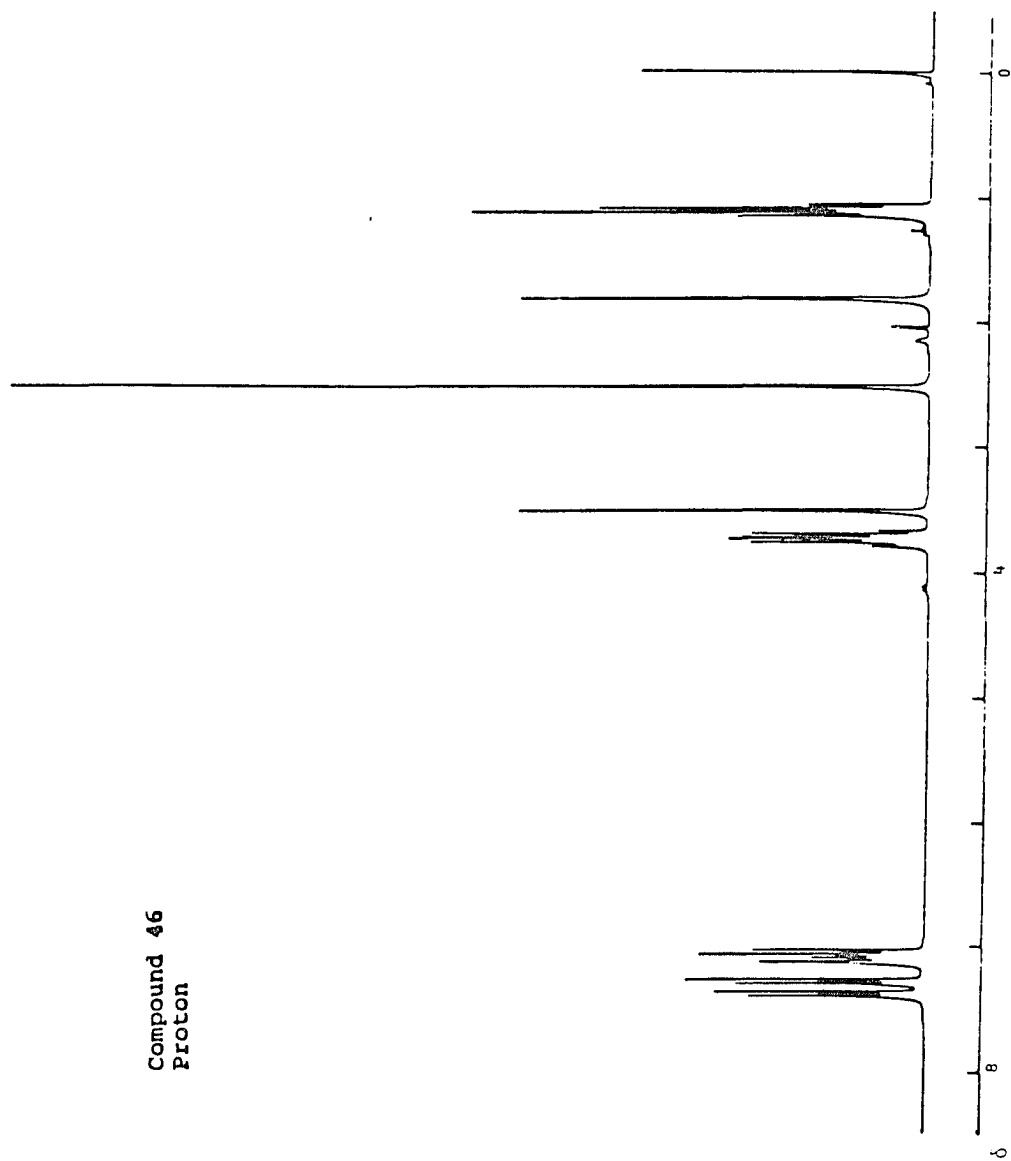


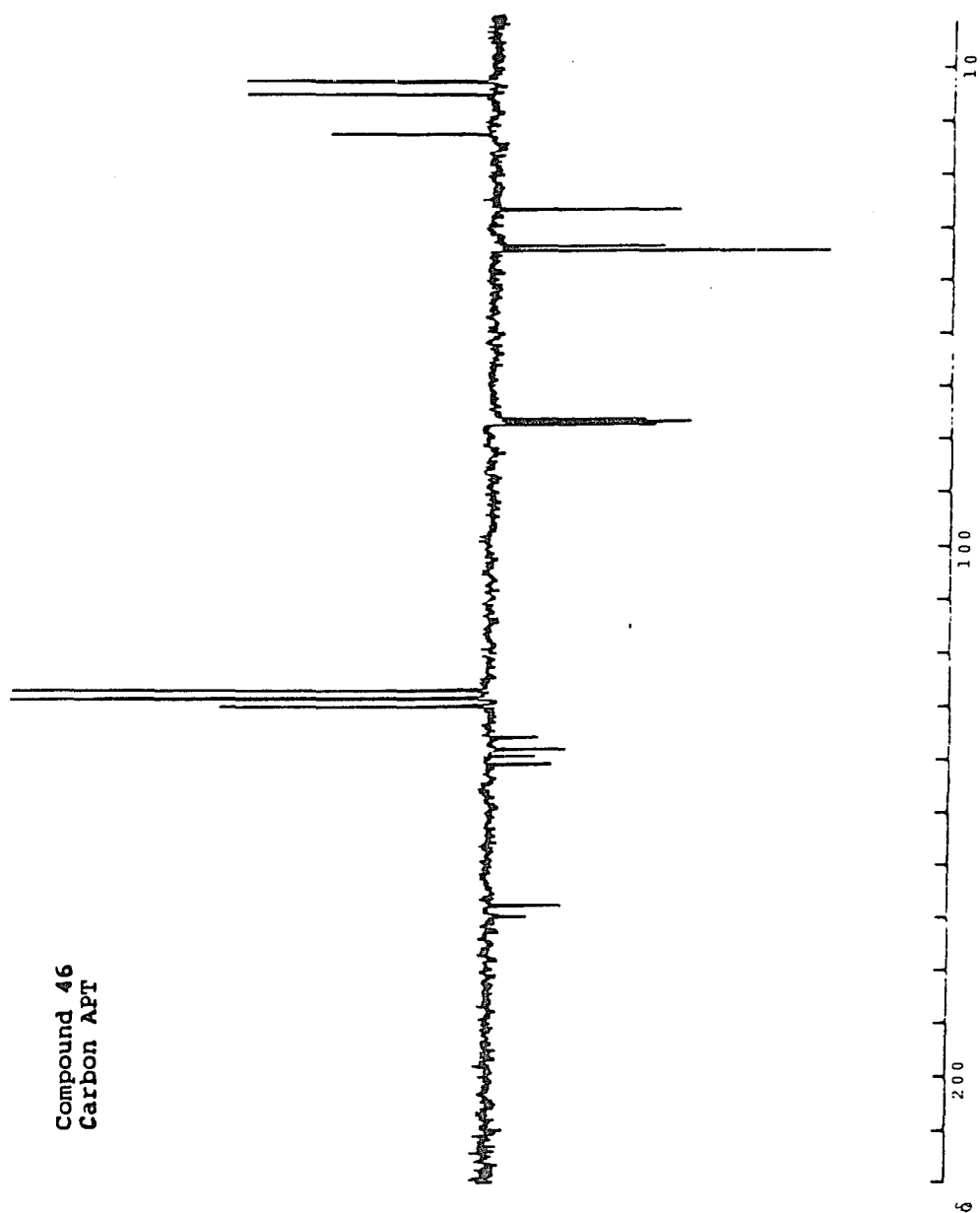




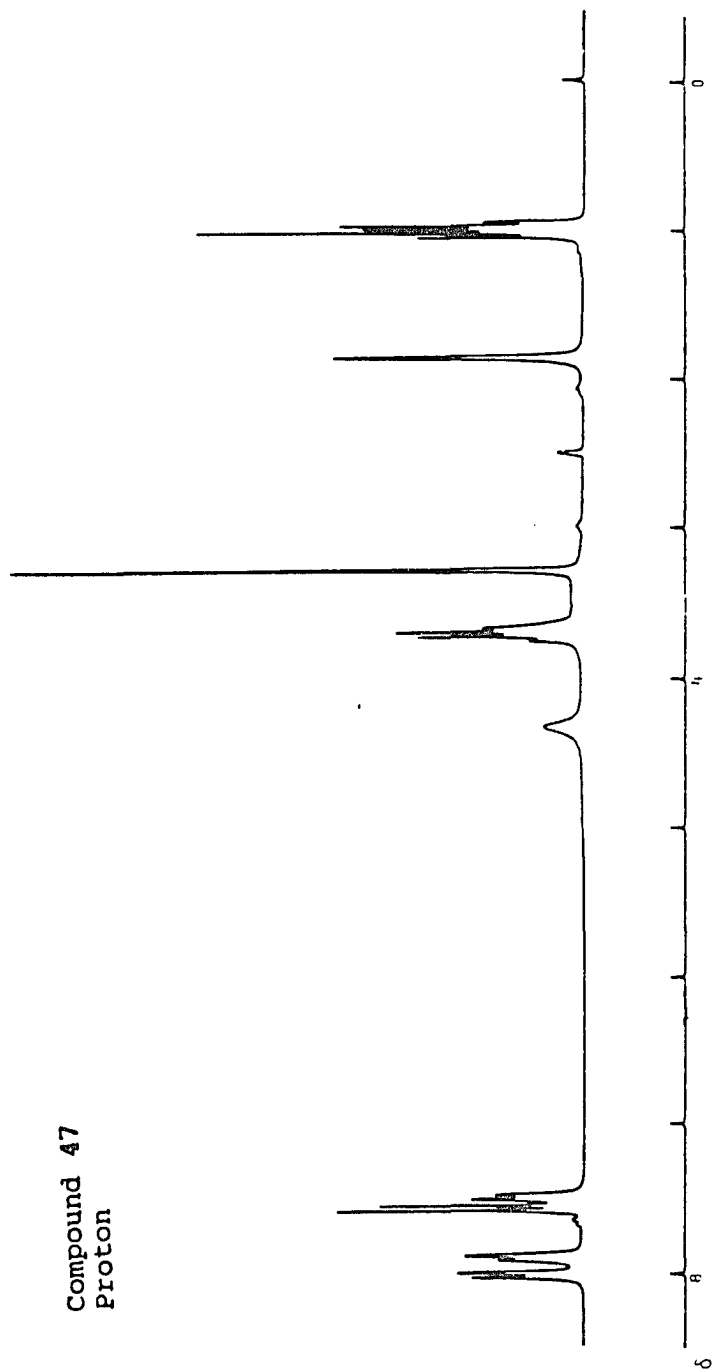
Compound 45
Carbon APT

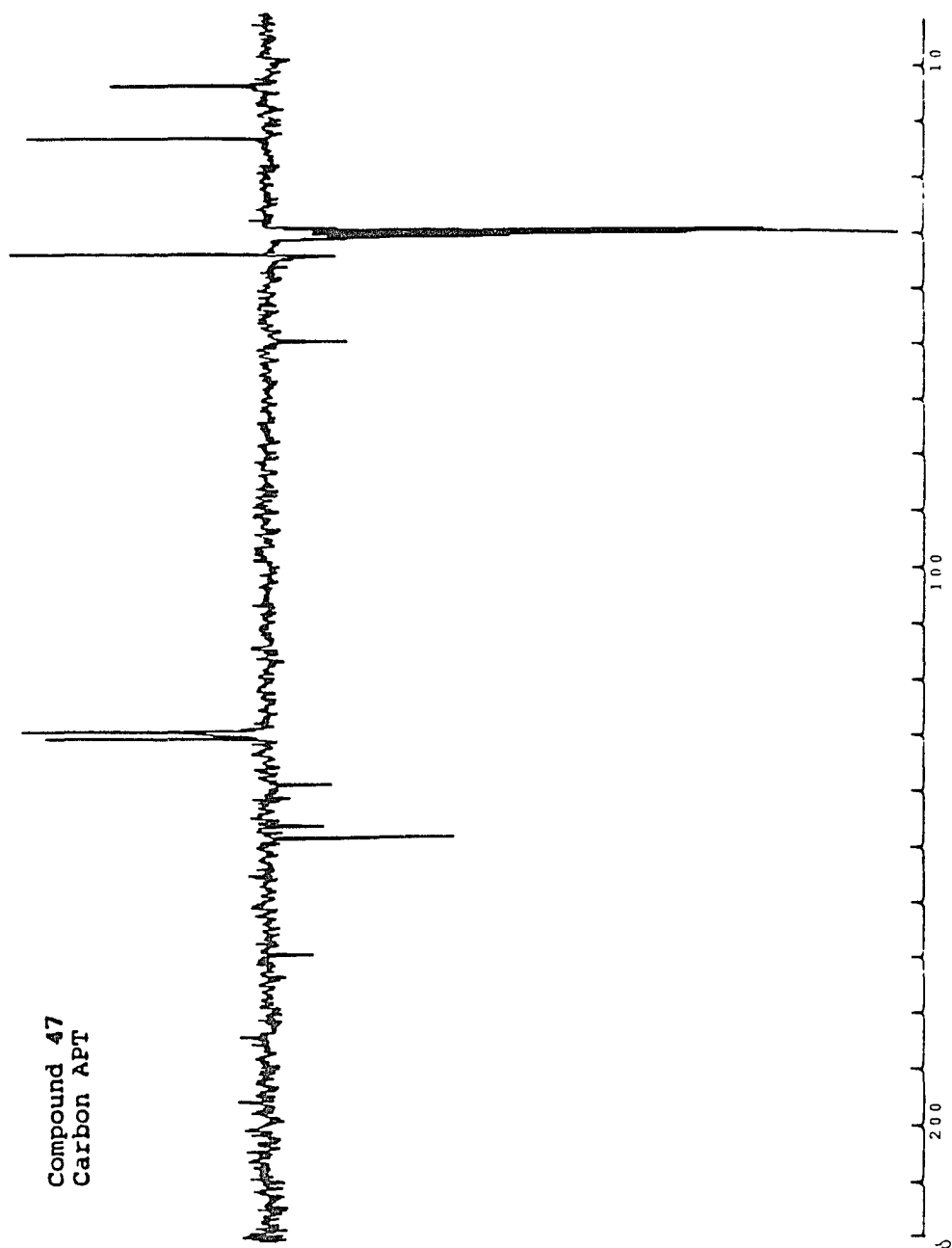


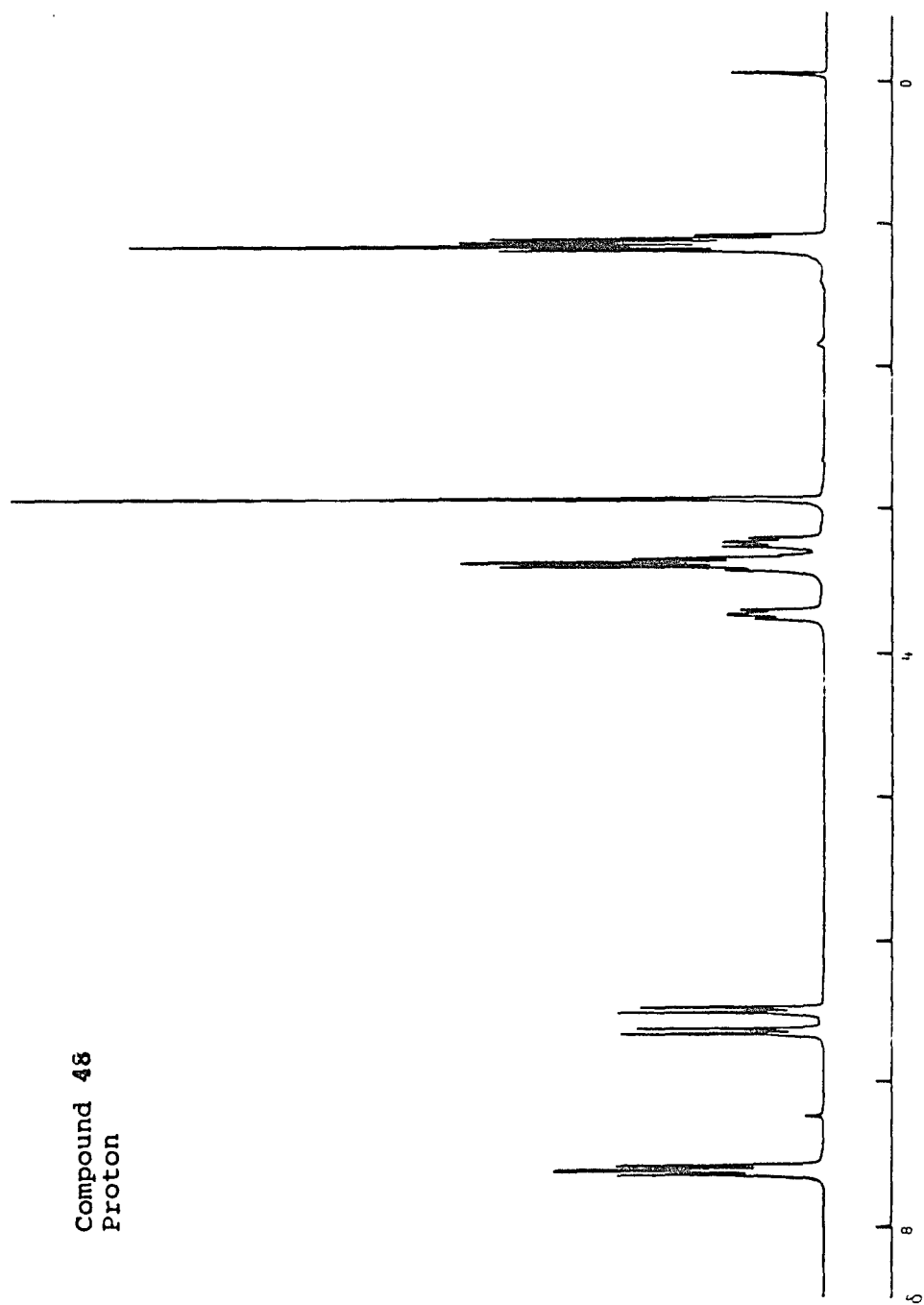




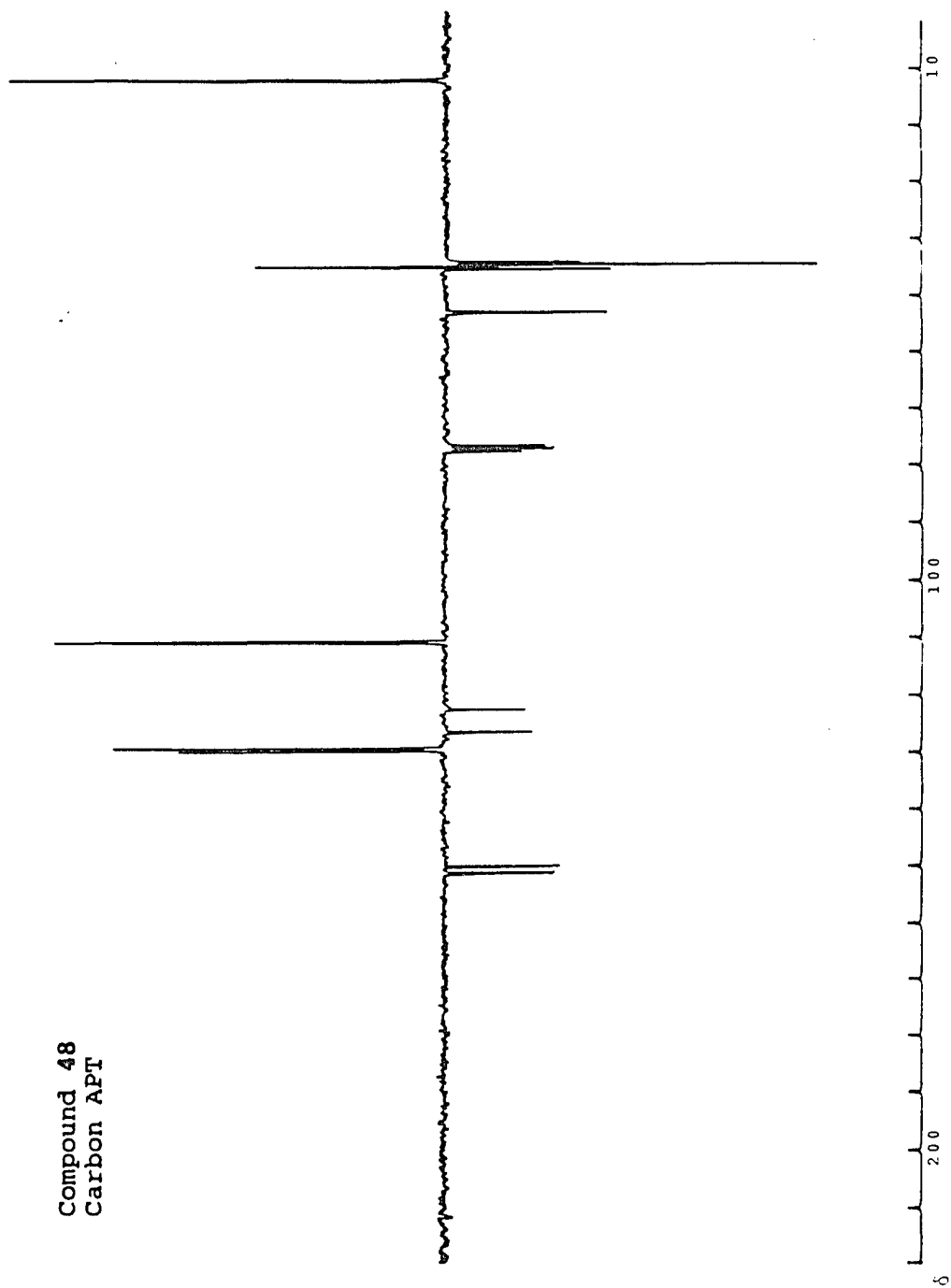
Compound 47
Proton

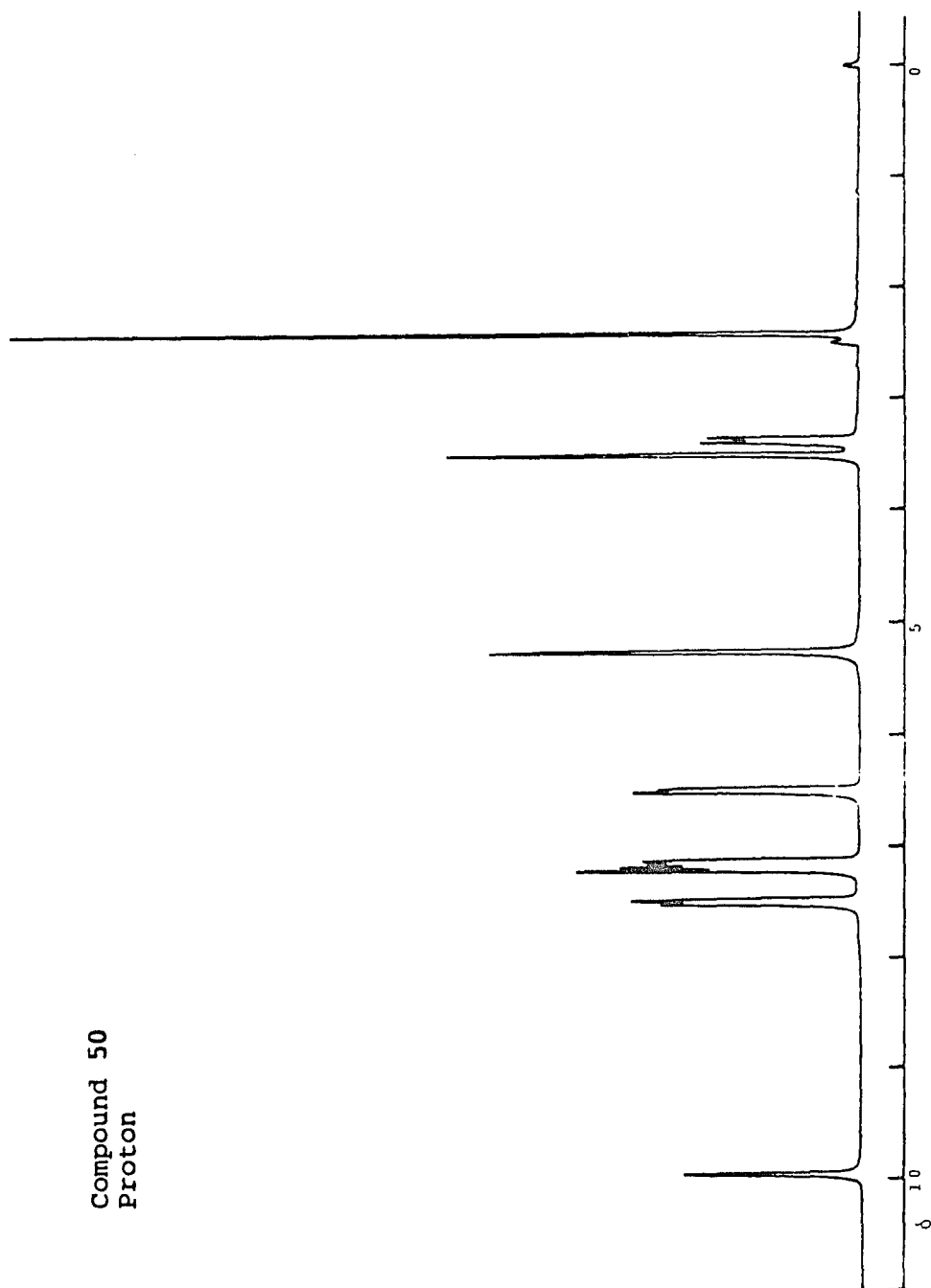


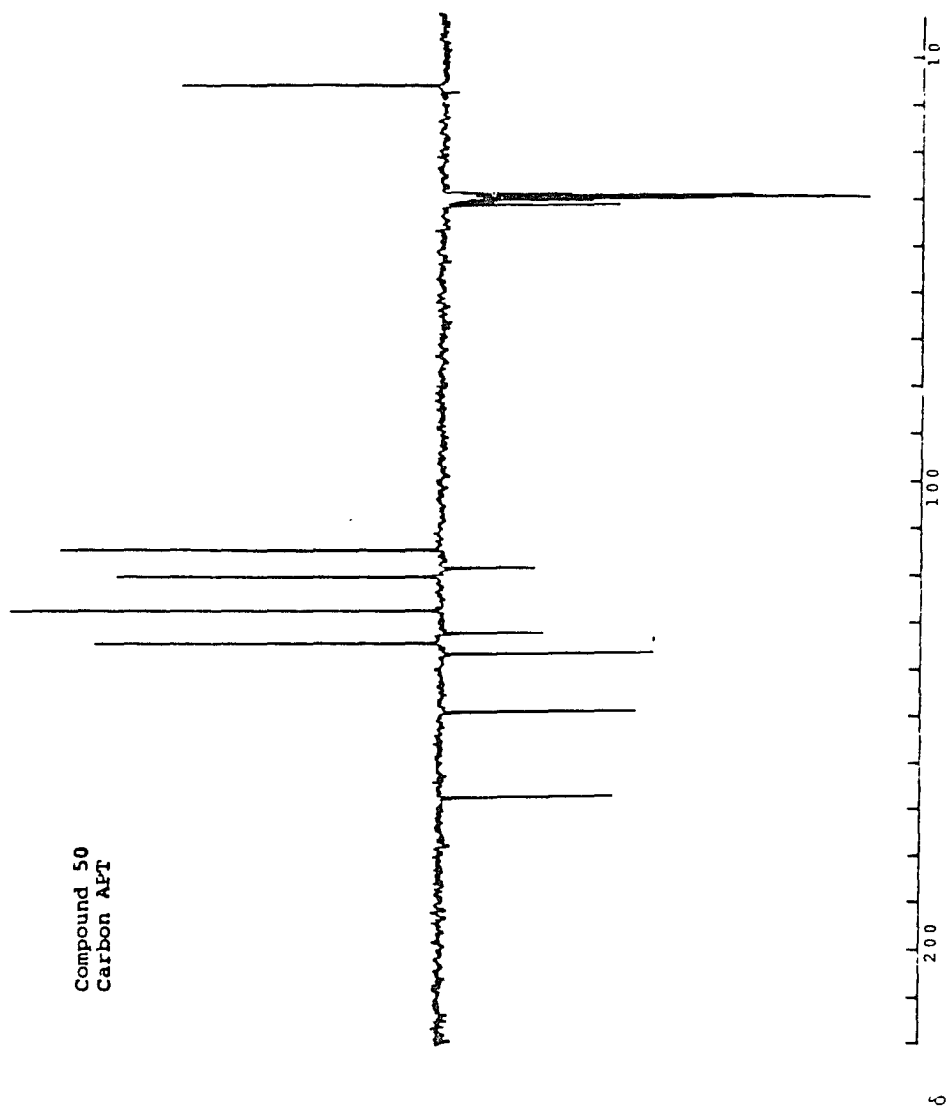




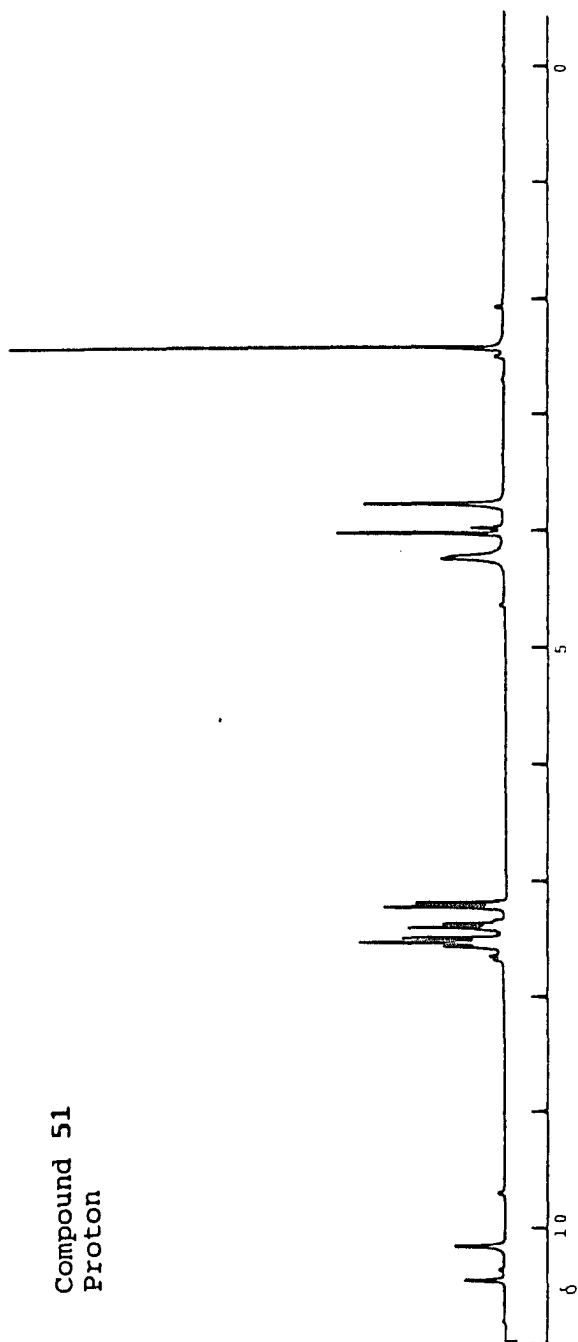
Compound 48
Carbon APT



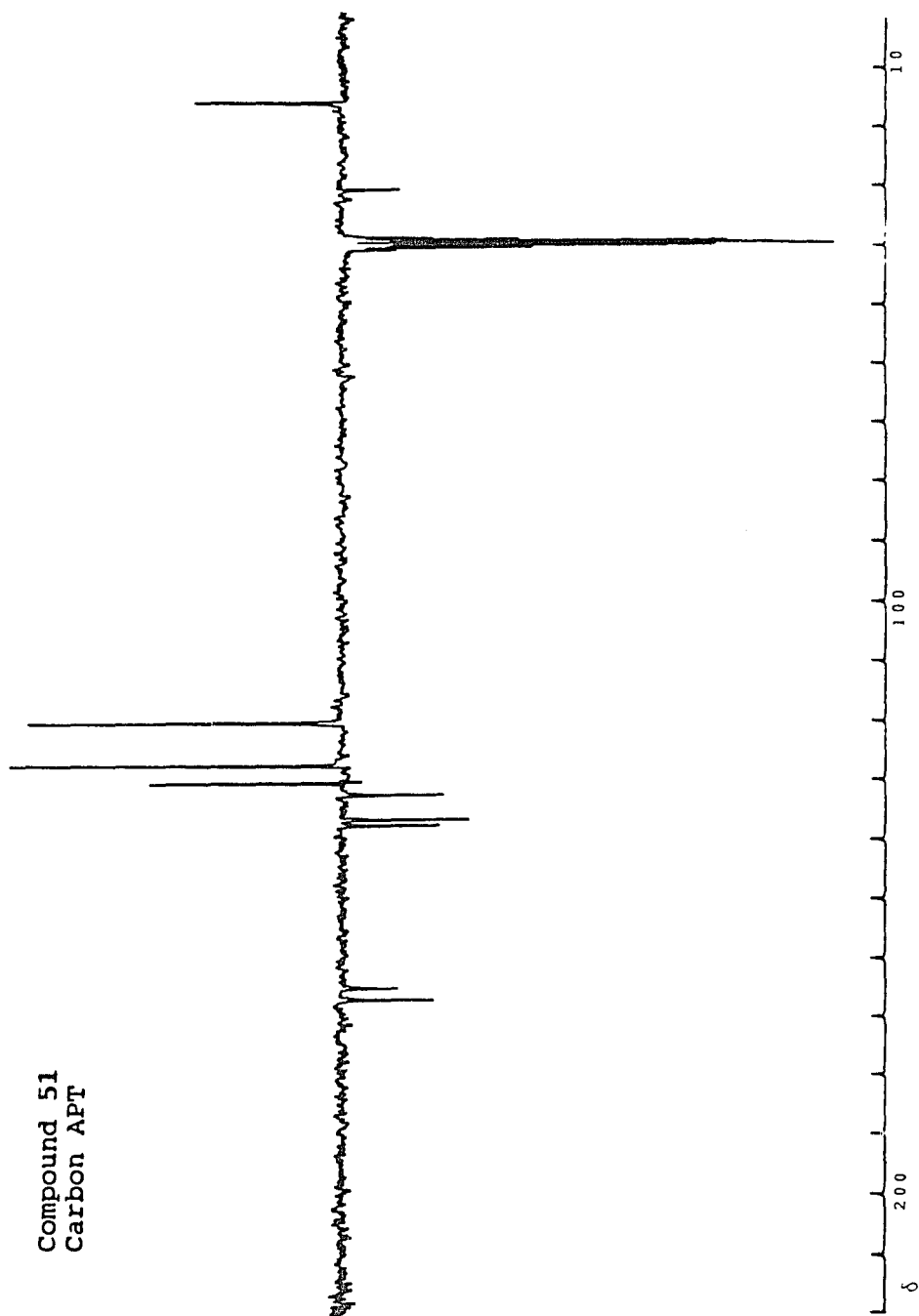




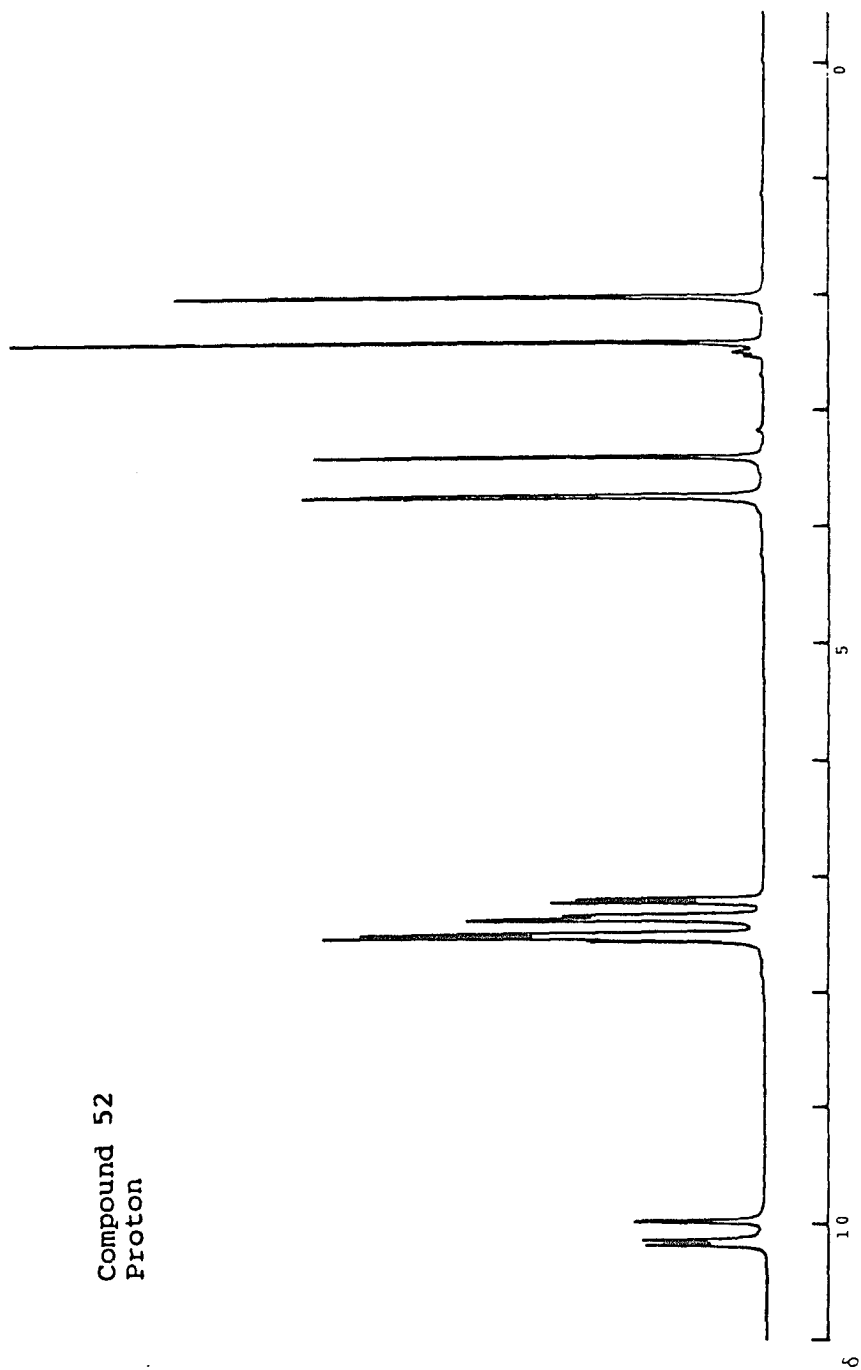
Compound 51
Proton

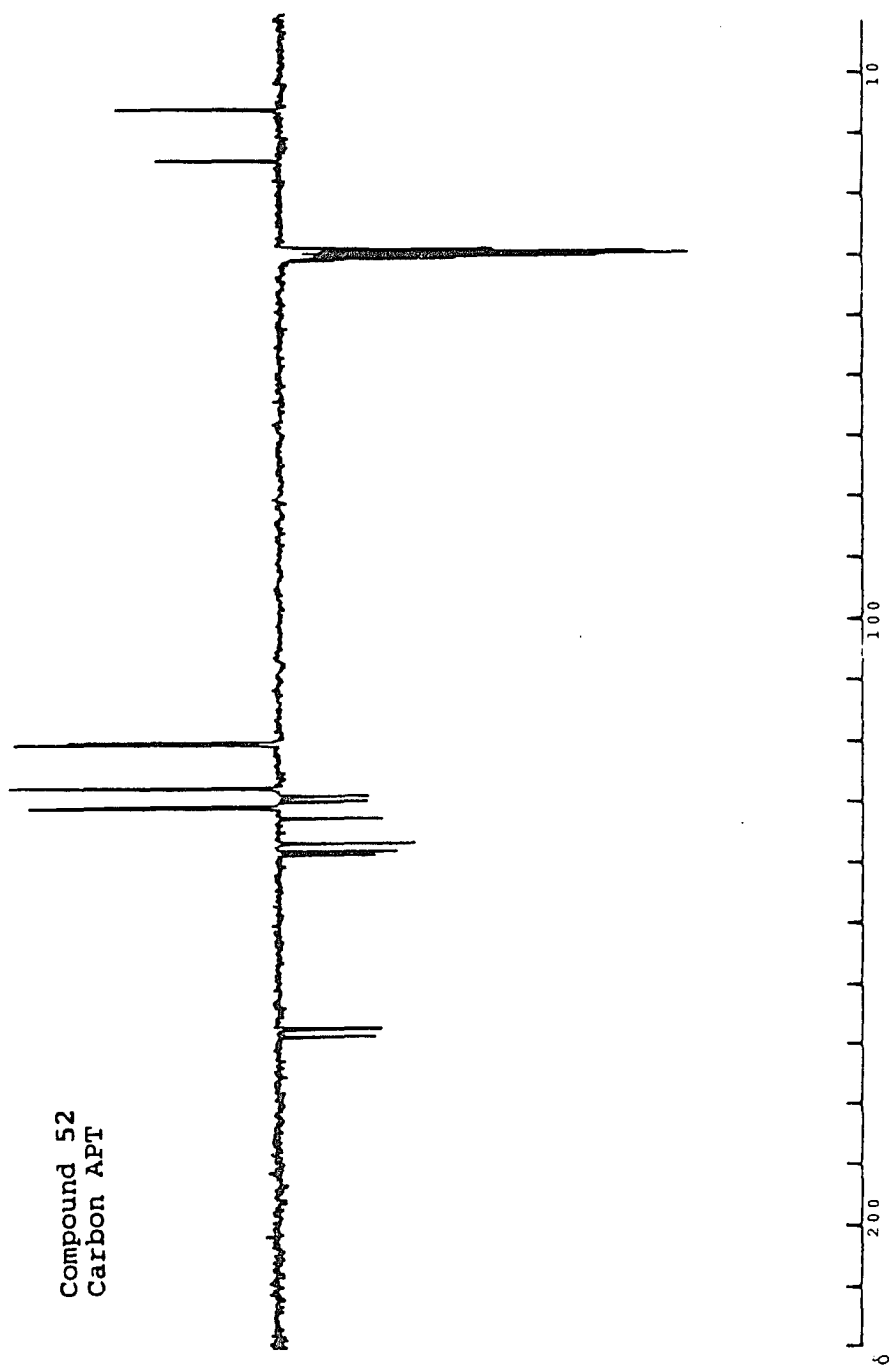


Compound 51
Carbon APT

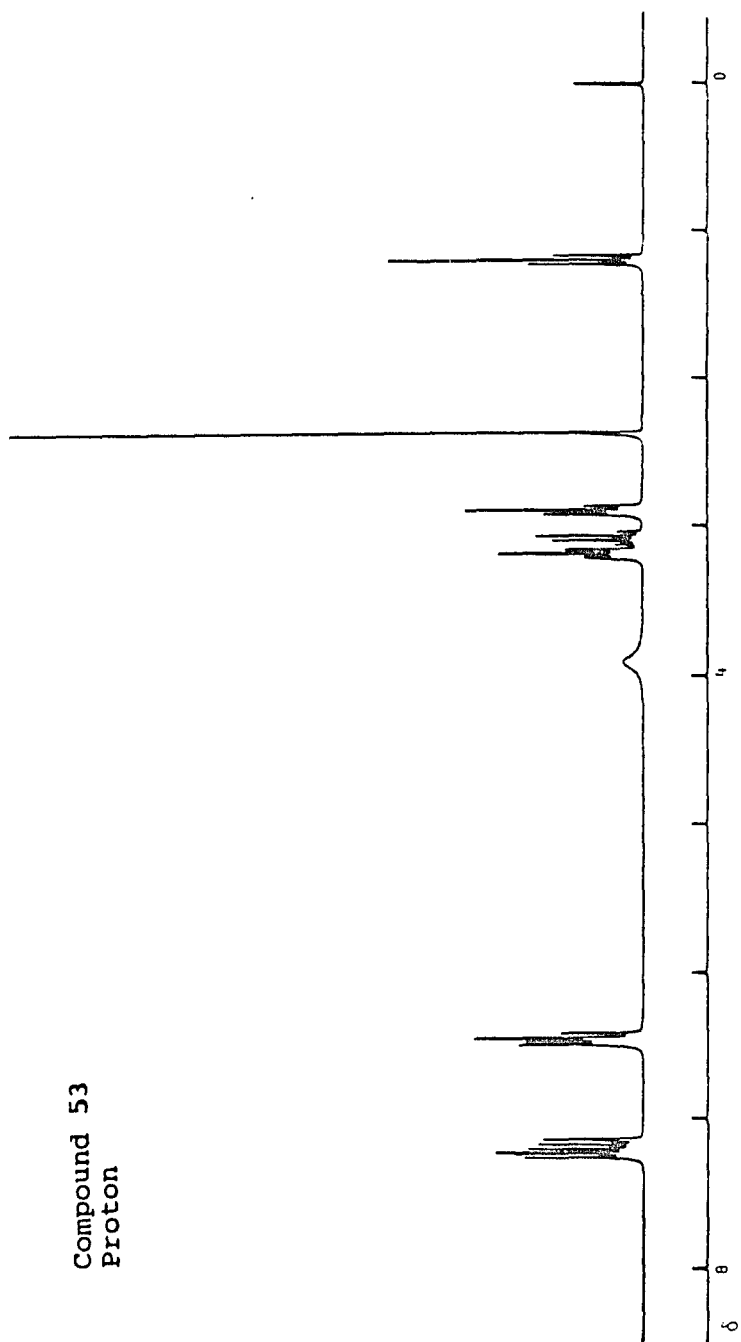


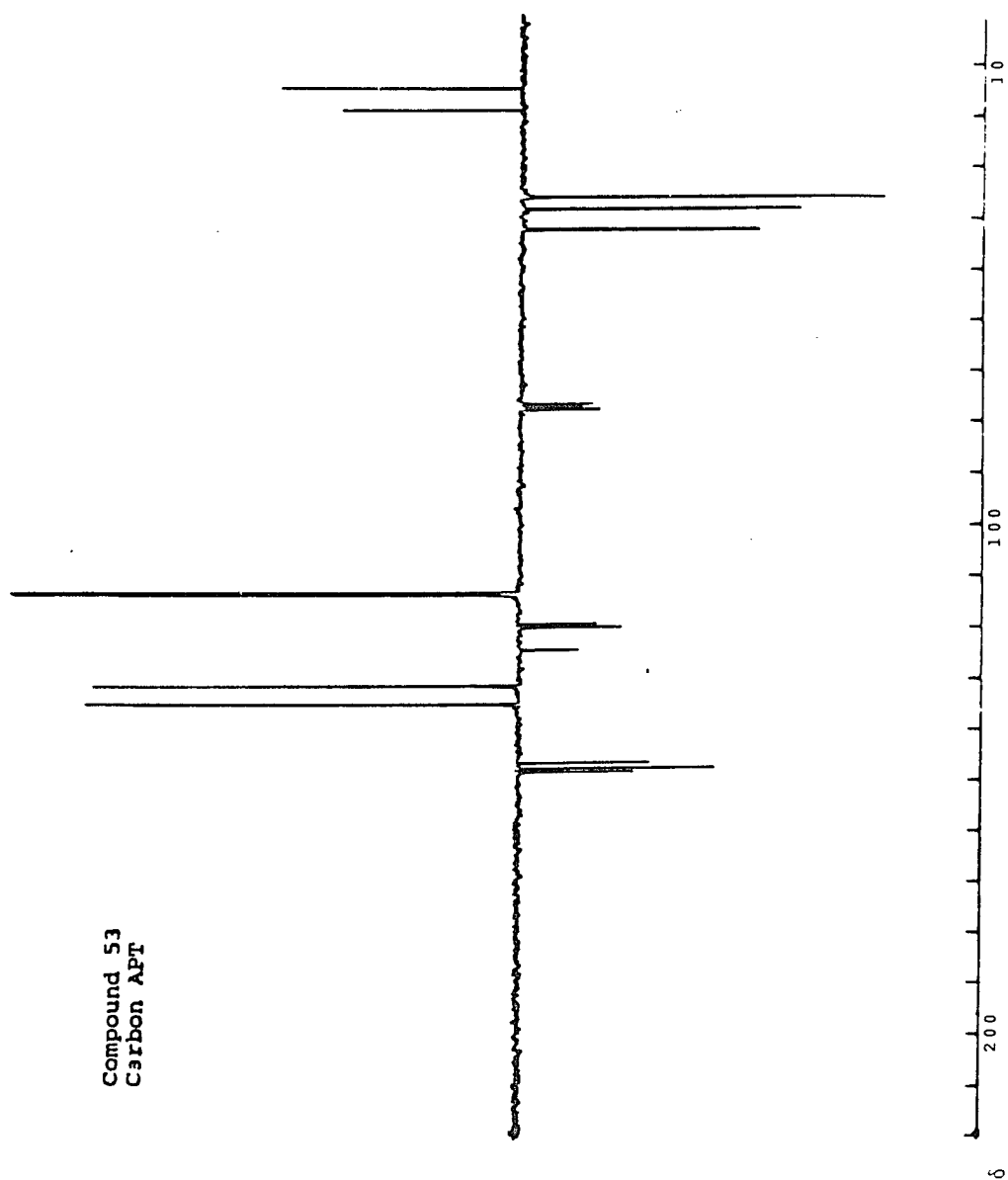
Compound 52
Proton

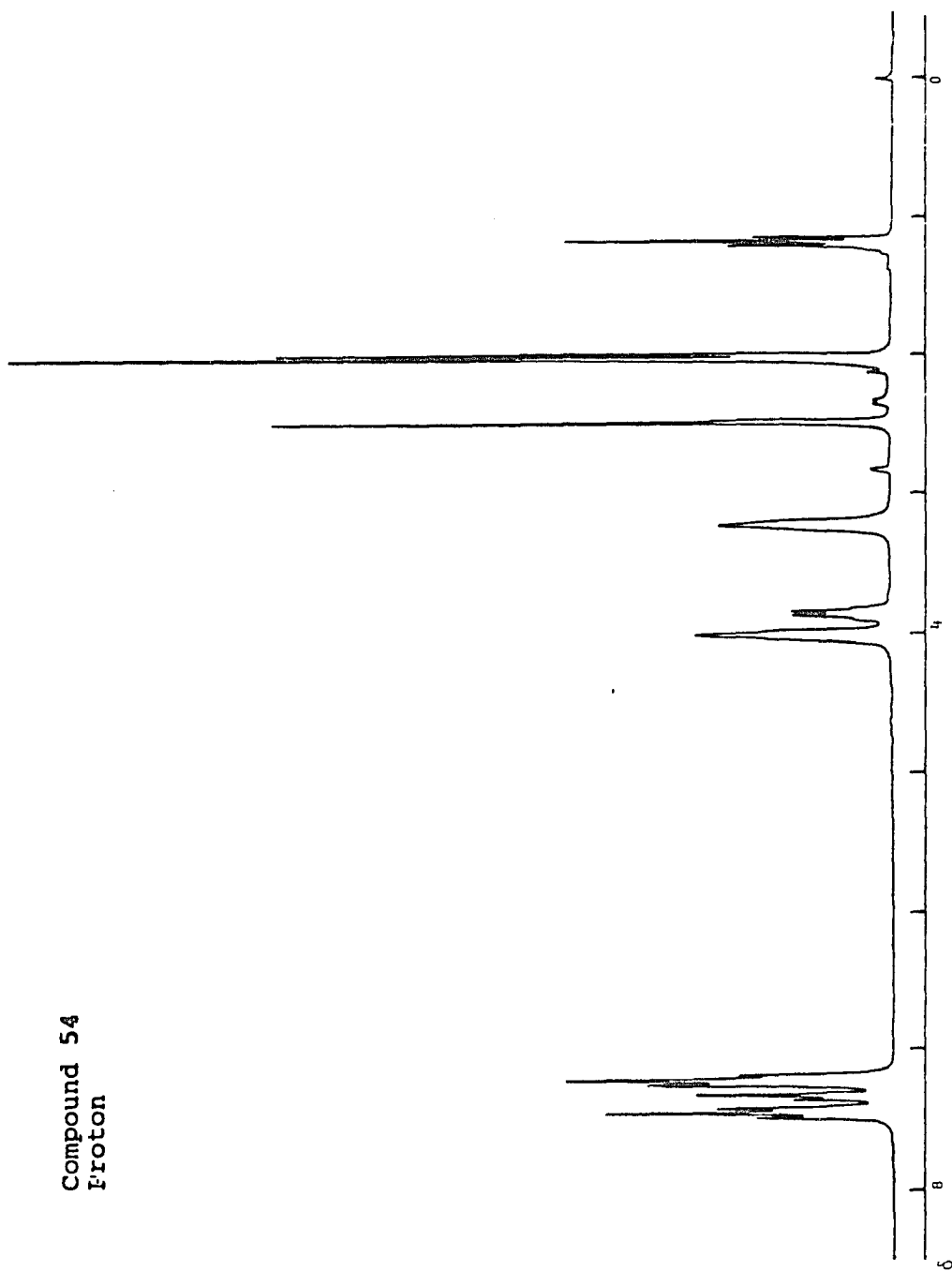


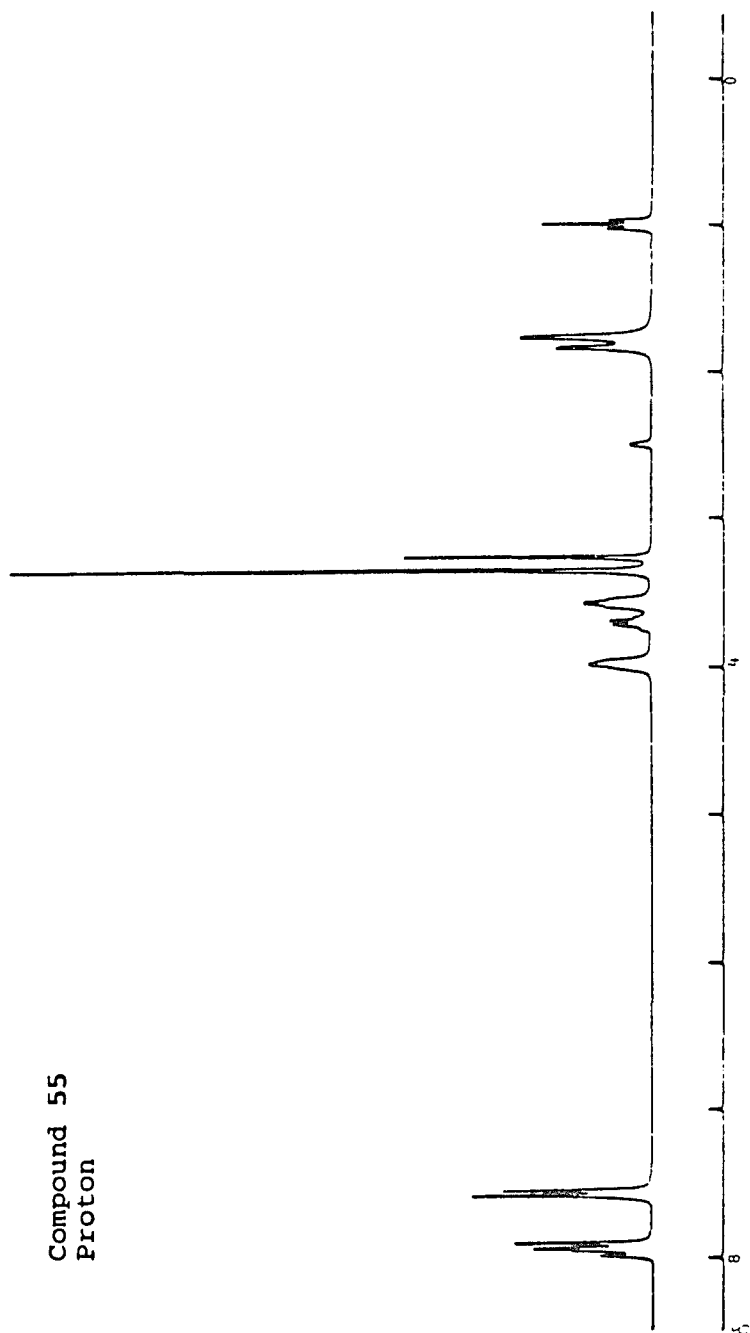


Compound 53
Proton

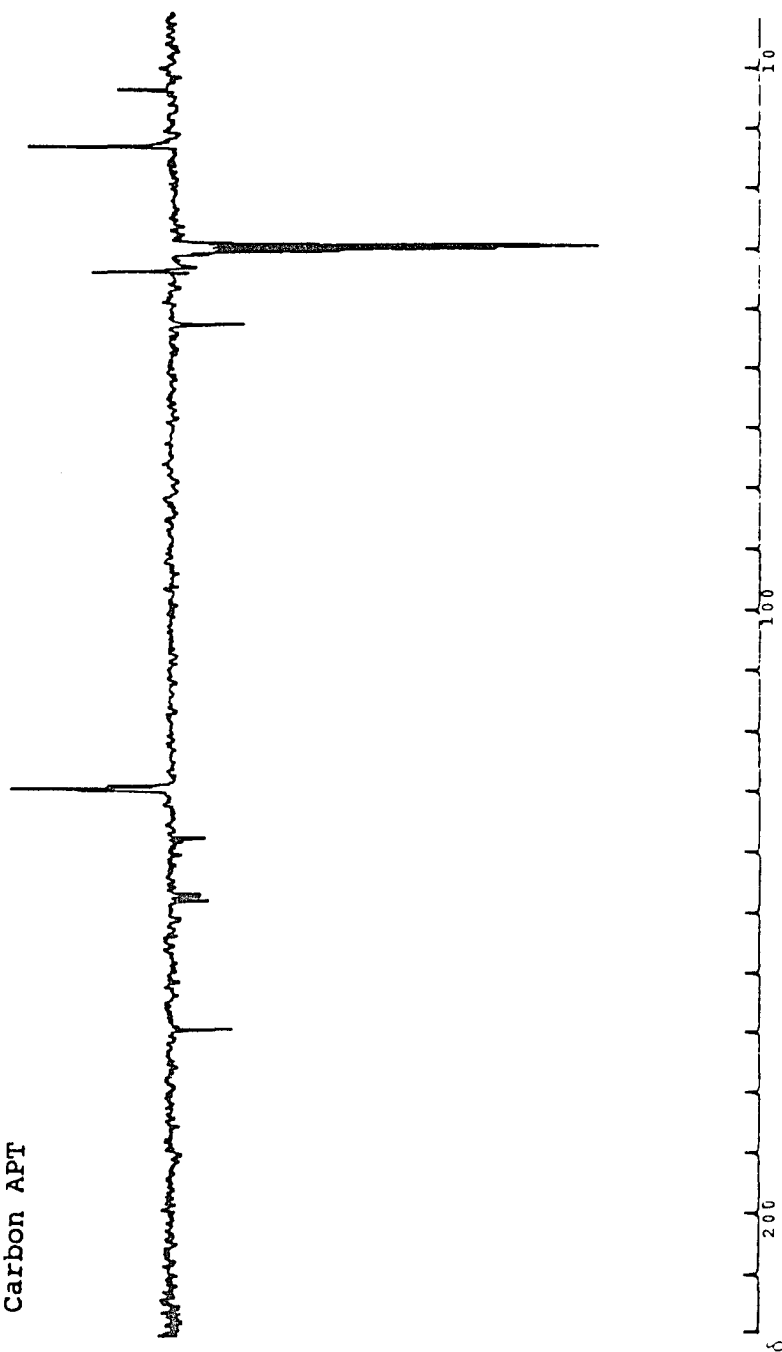


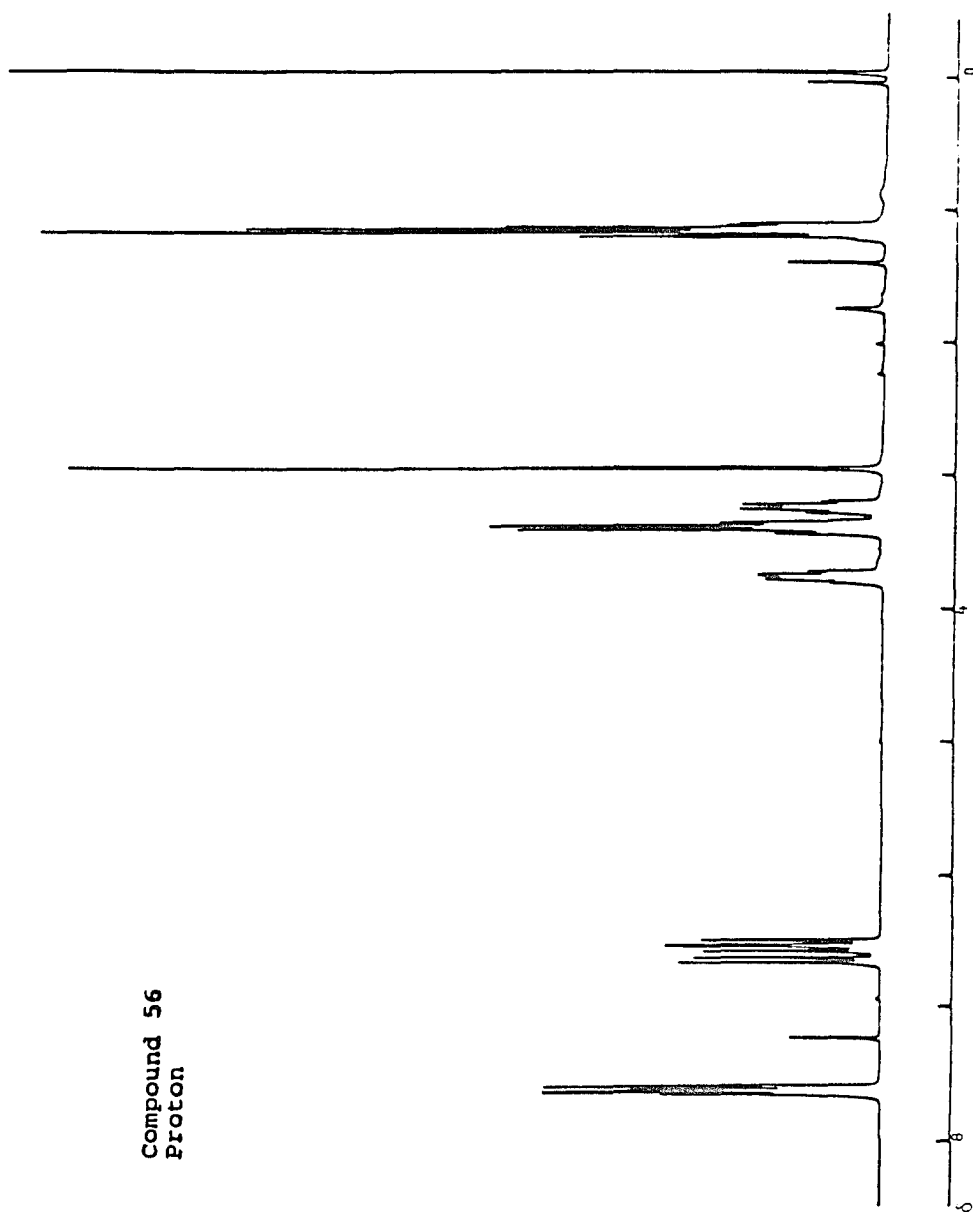






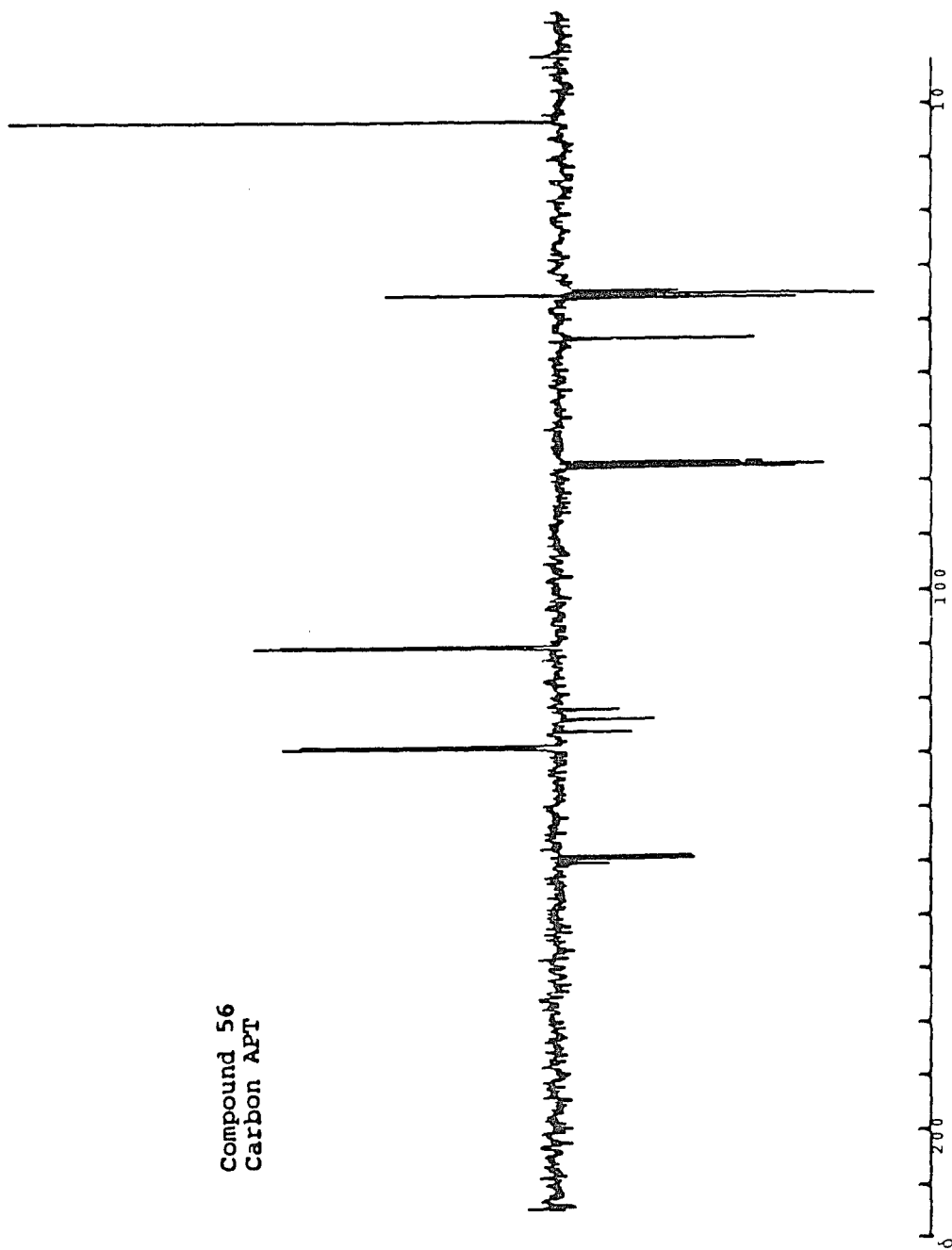
Compound 55
Carbon APT



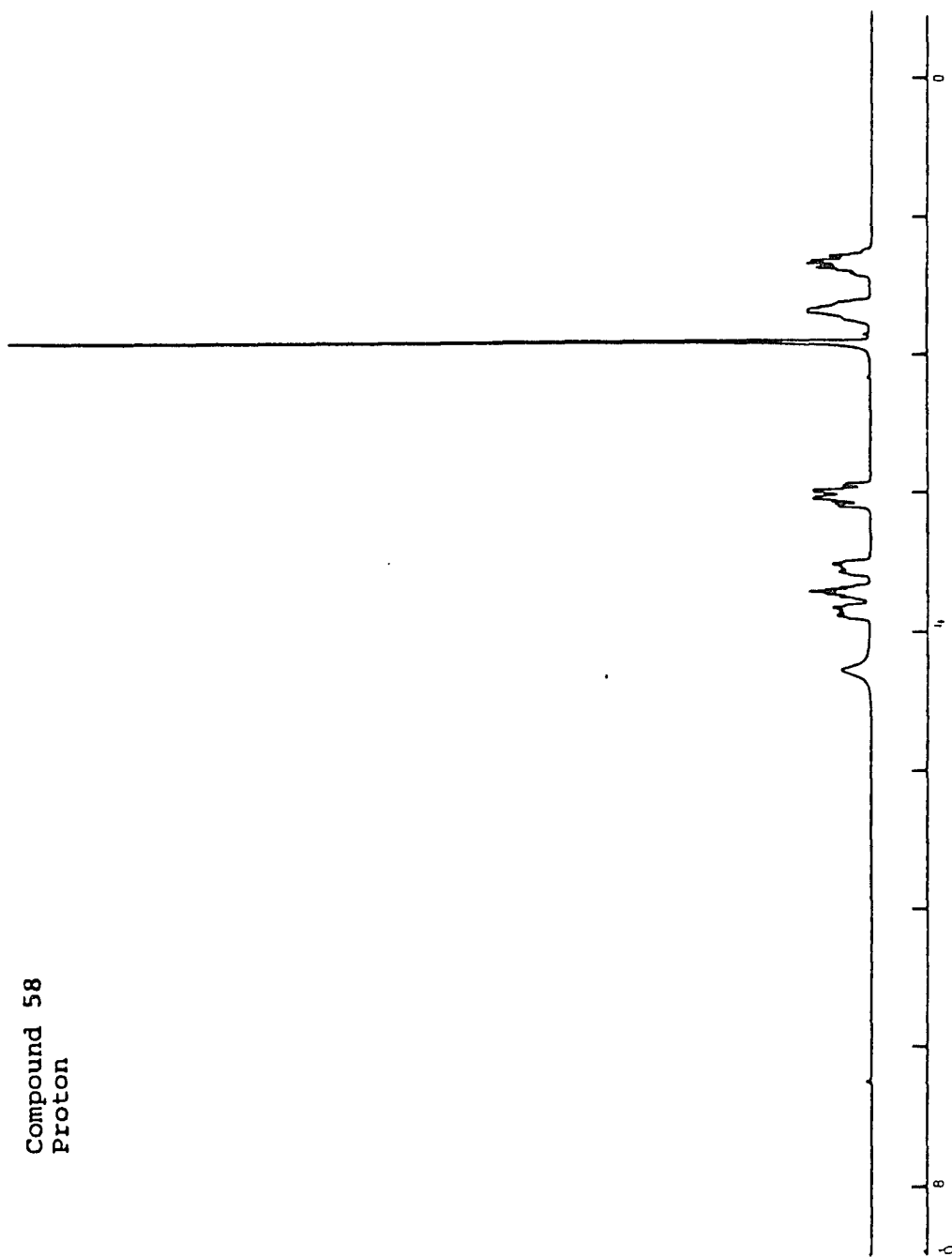


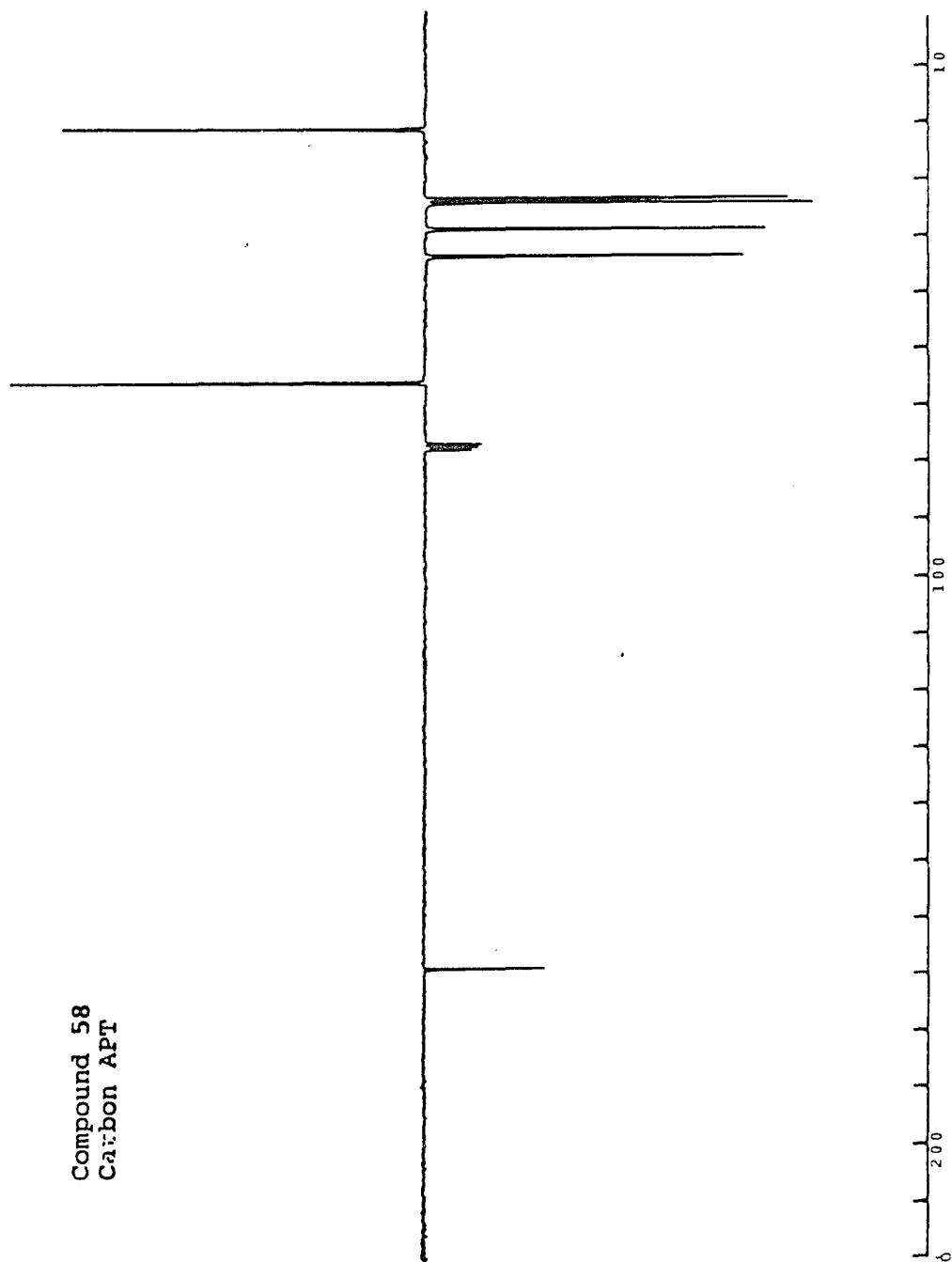
Compound 56
Proton

Compound 56
Carbon APT

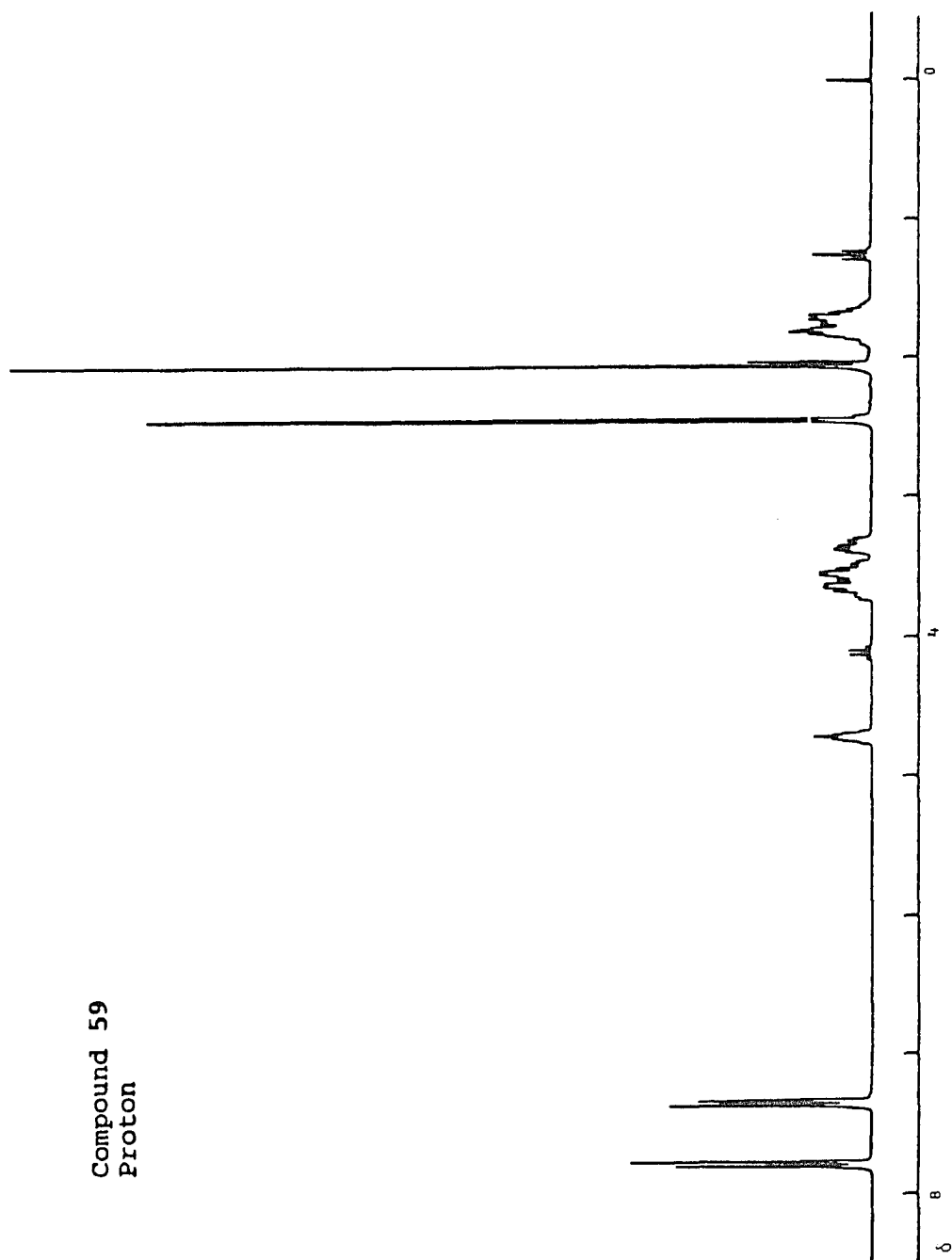


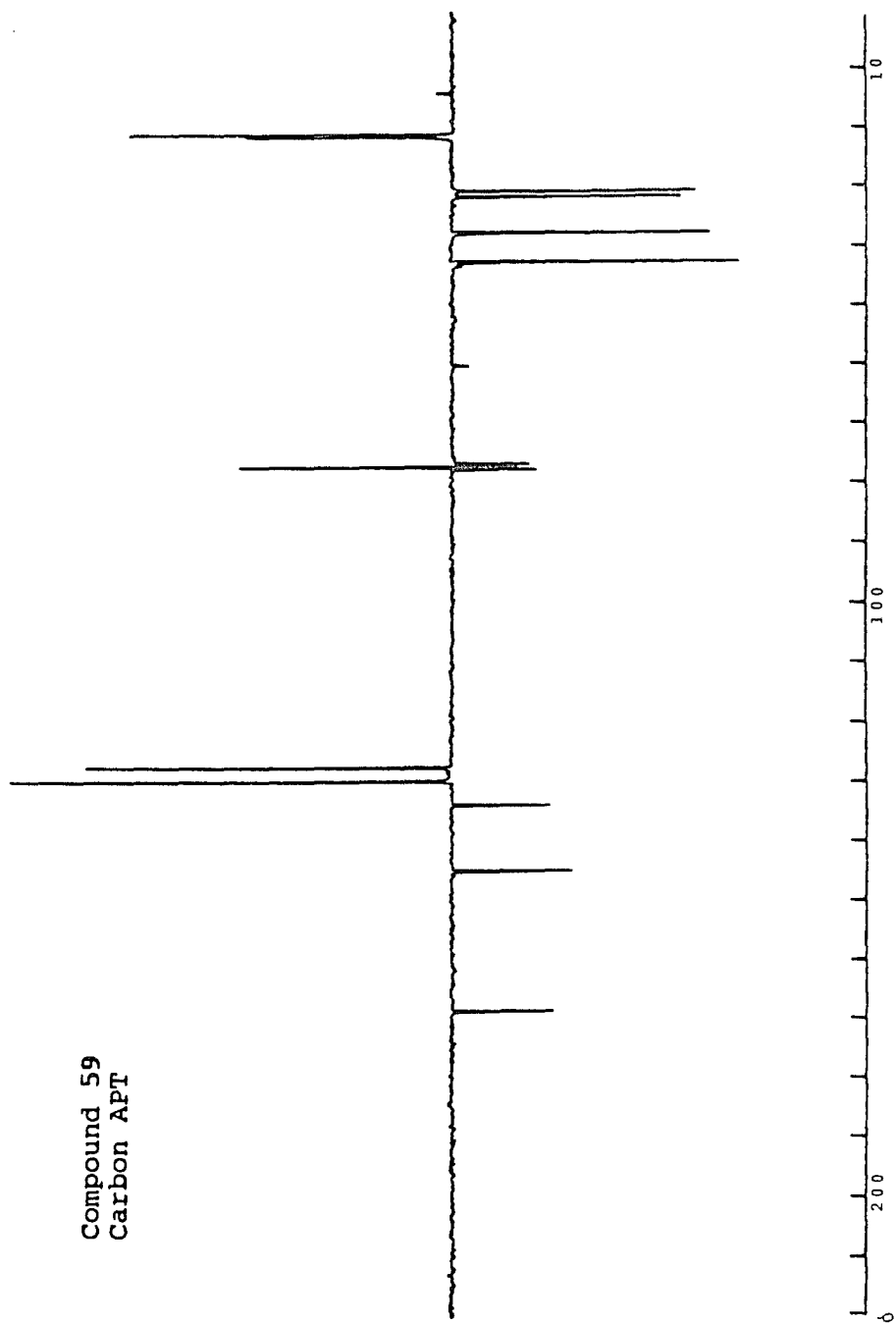
Compound 58
Proton



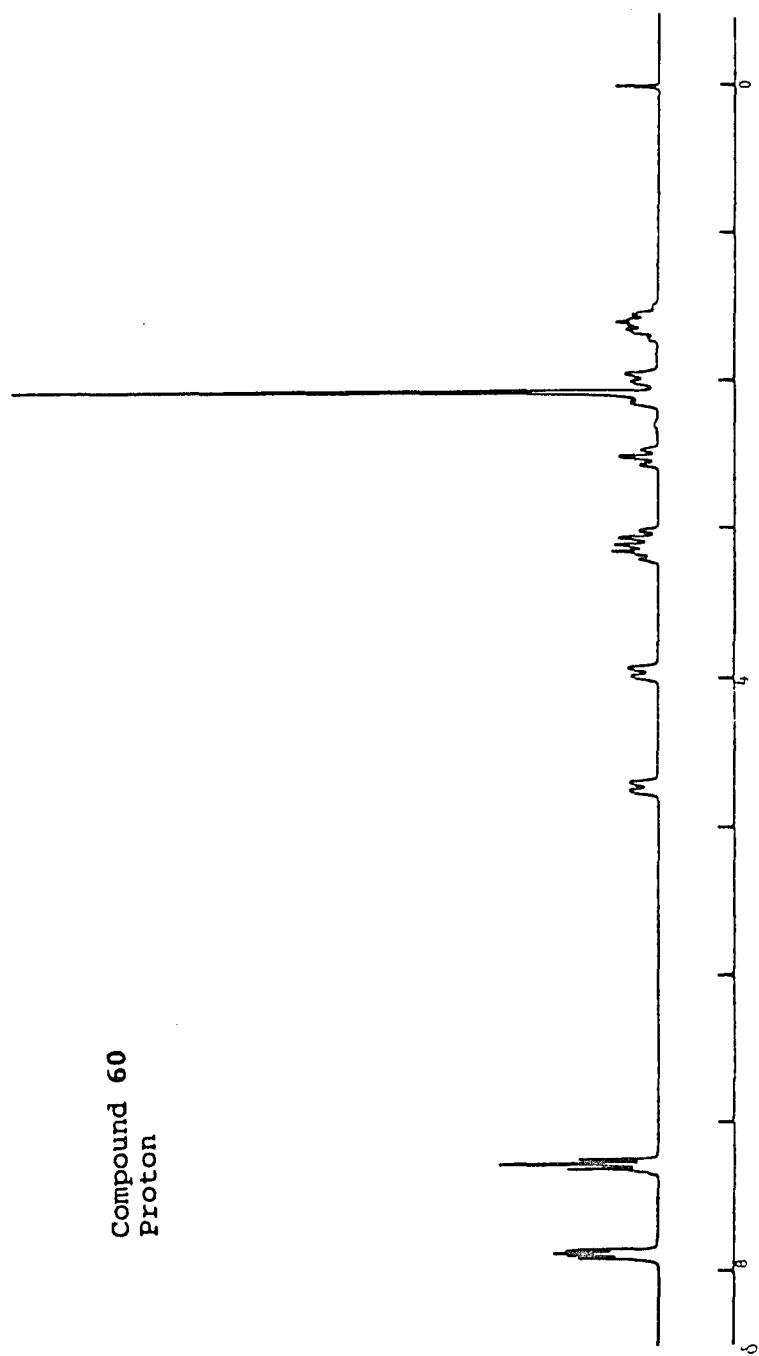


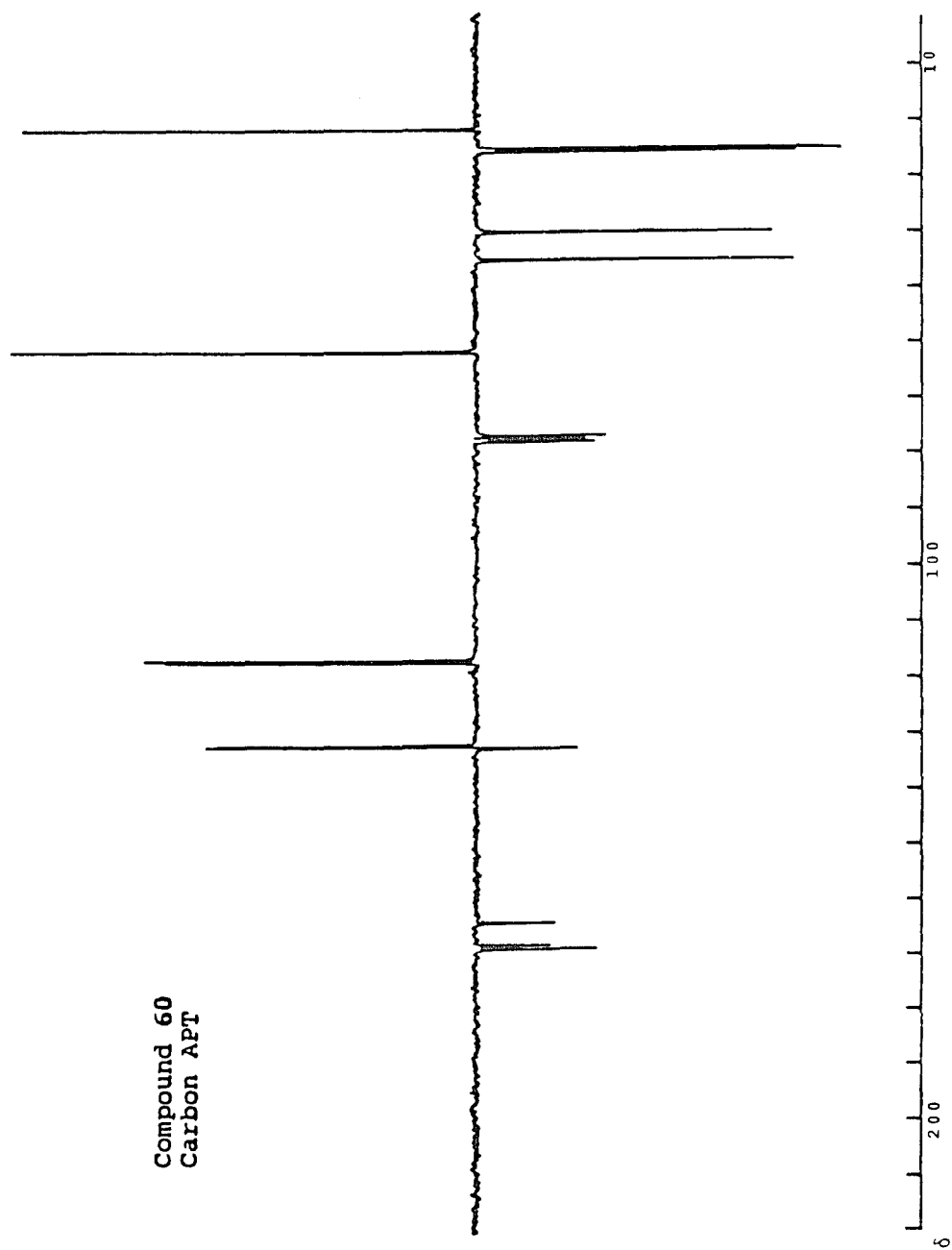
Compound 59
Proton

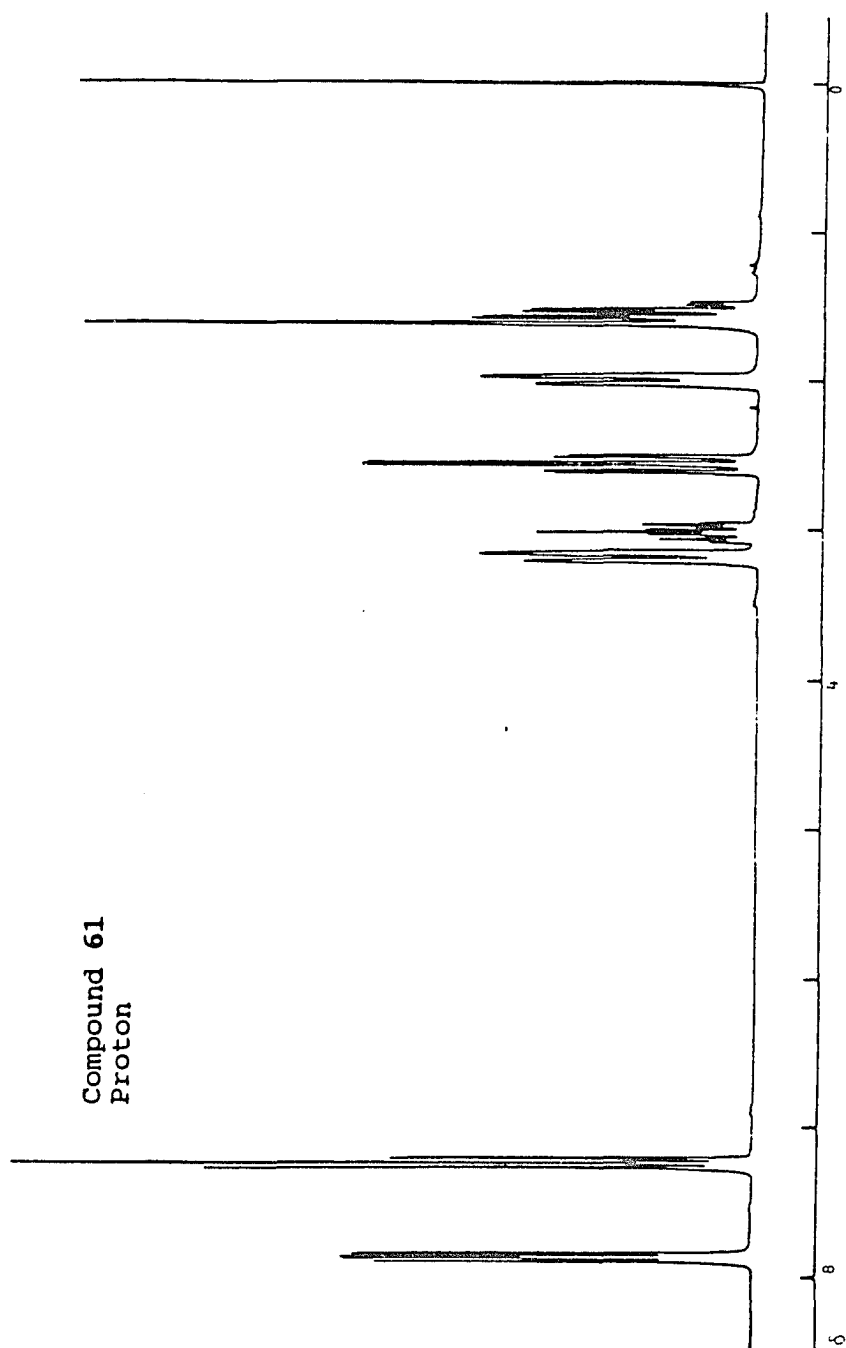


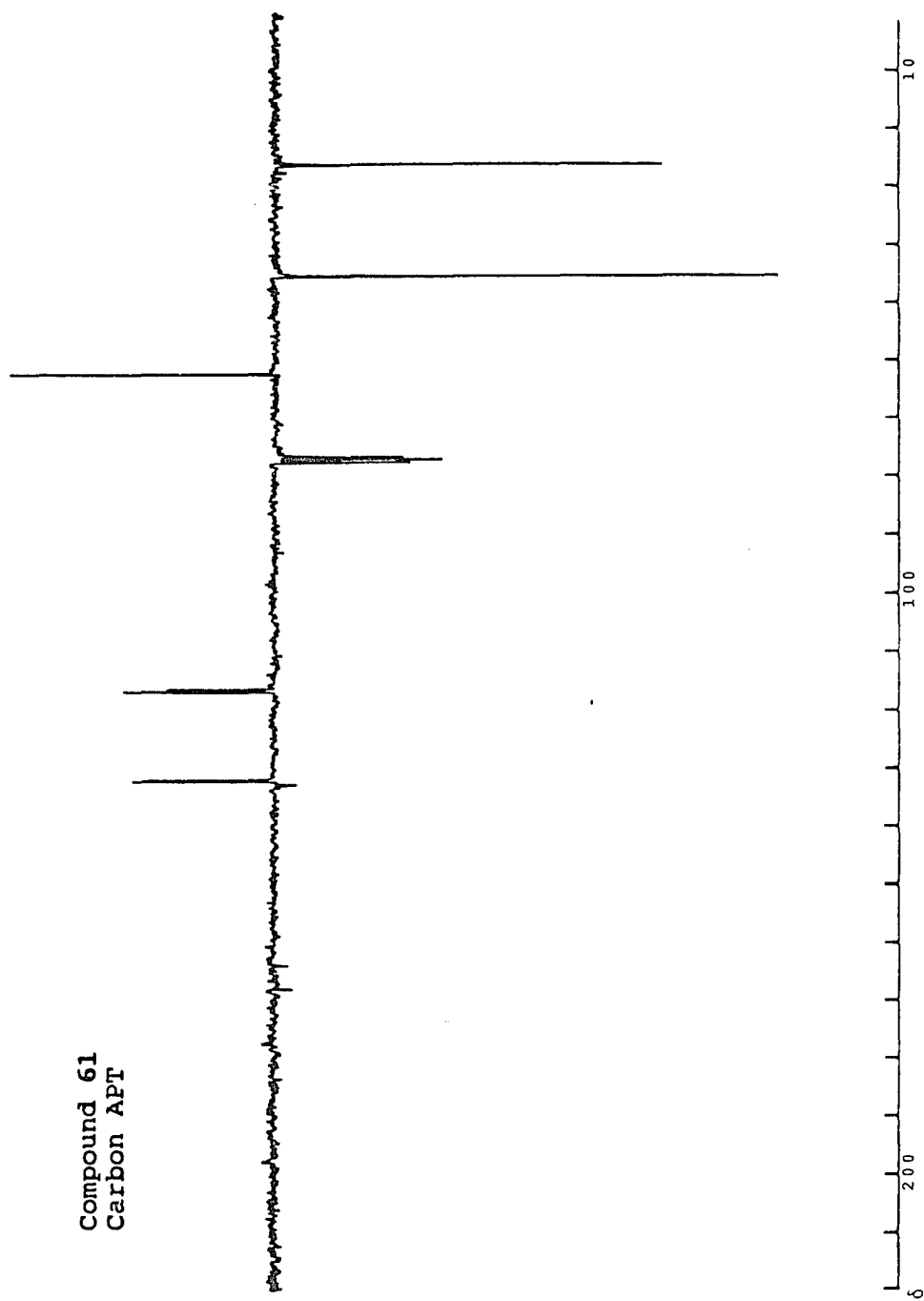


Compound 60
Proton

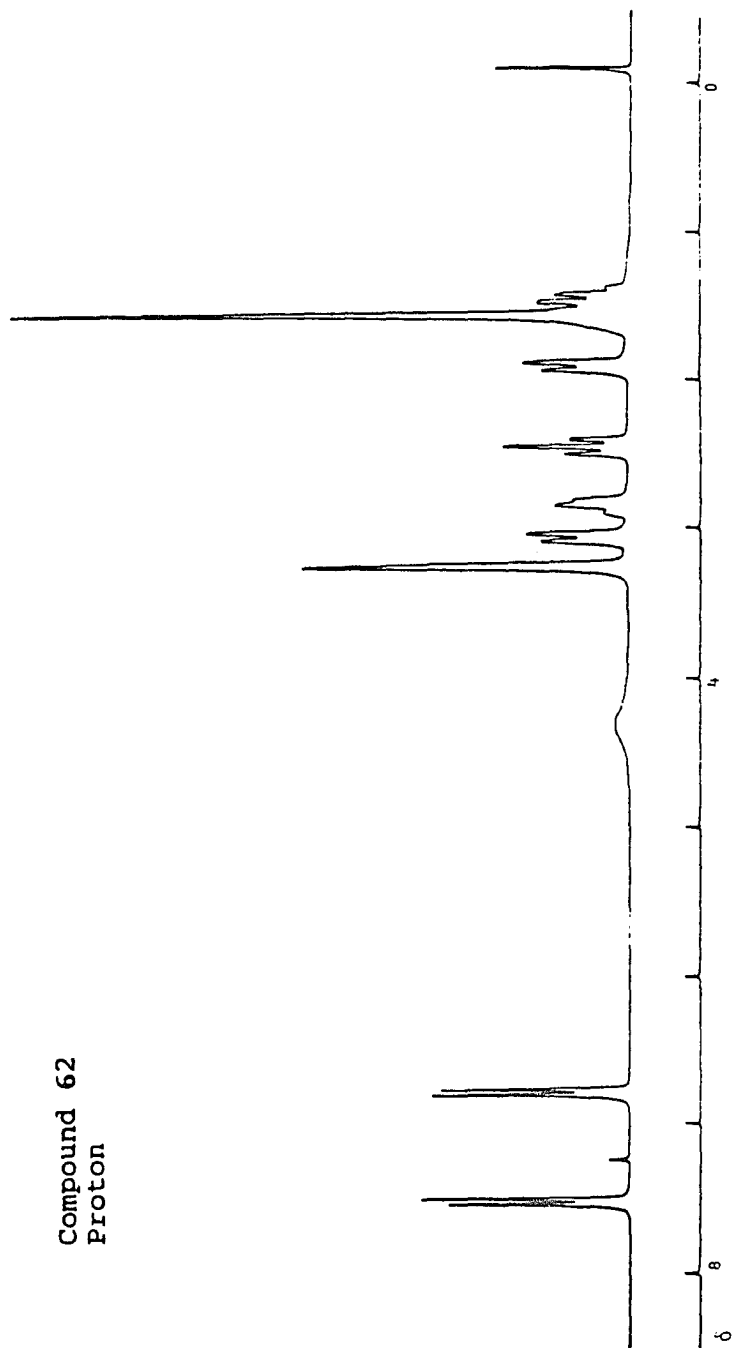


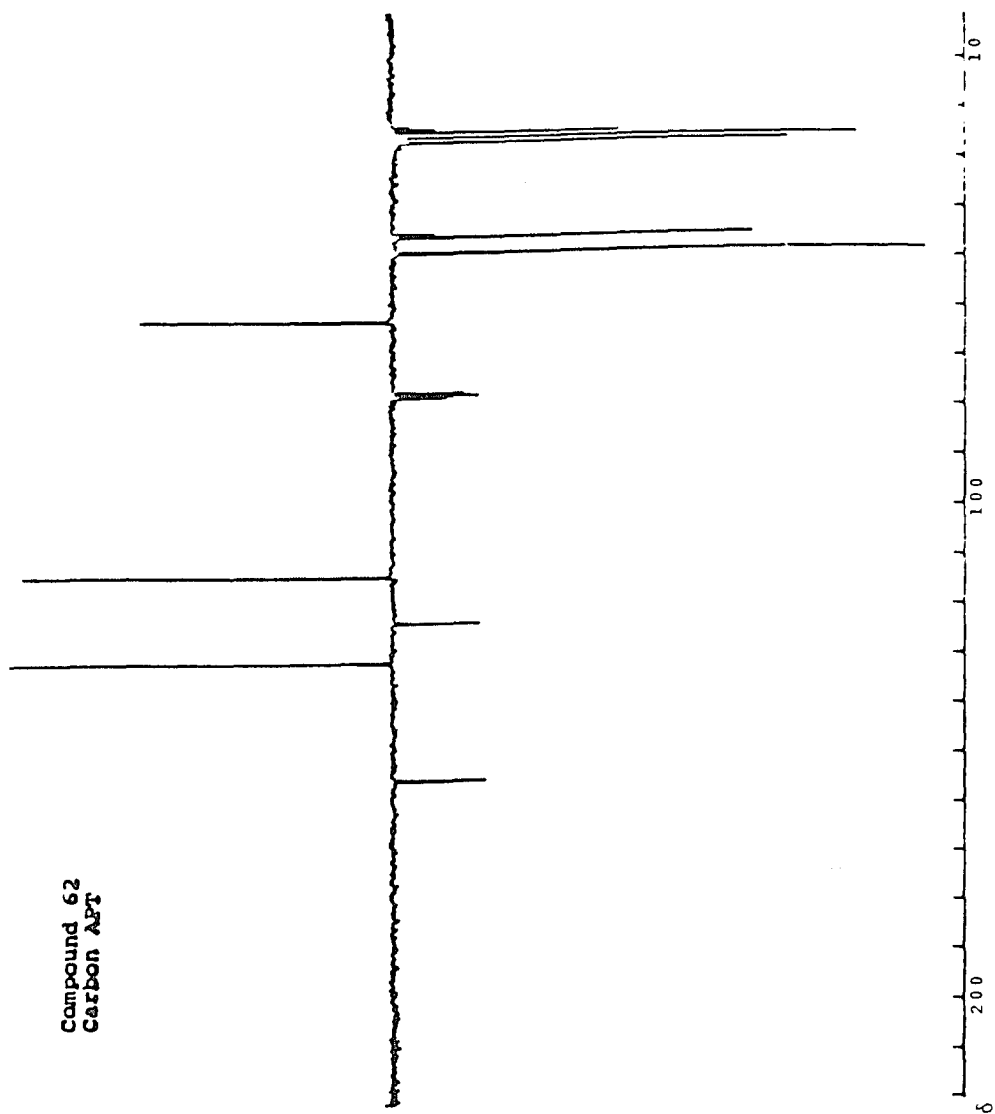


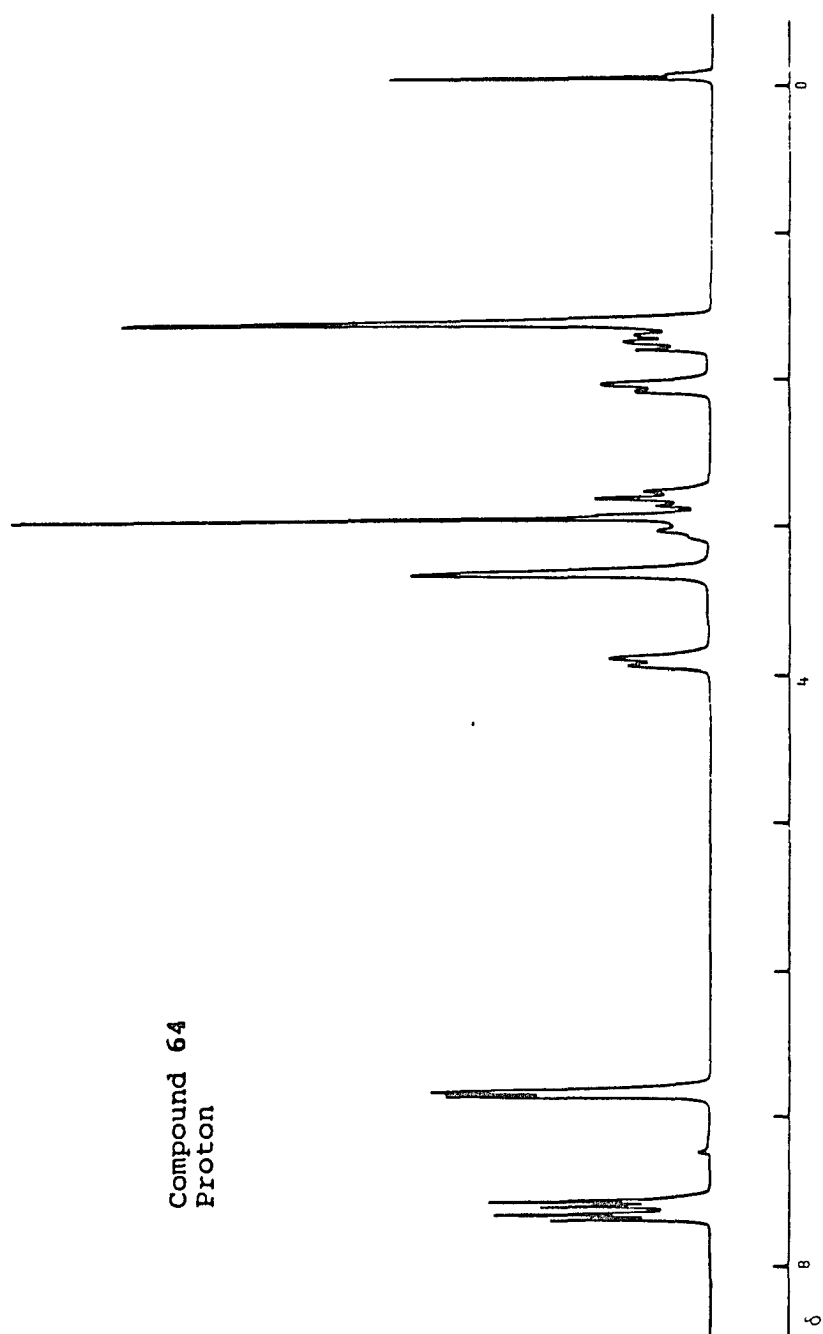




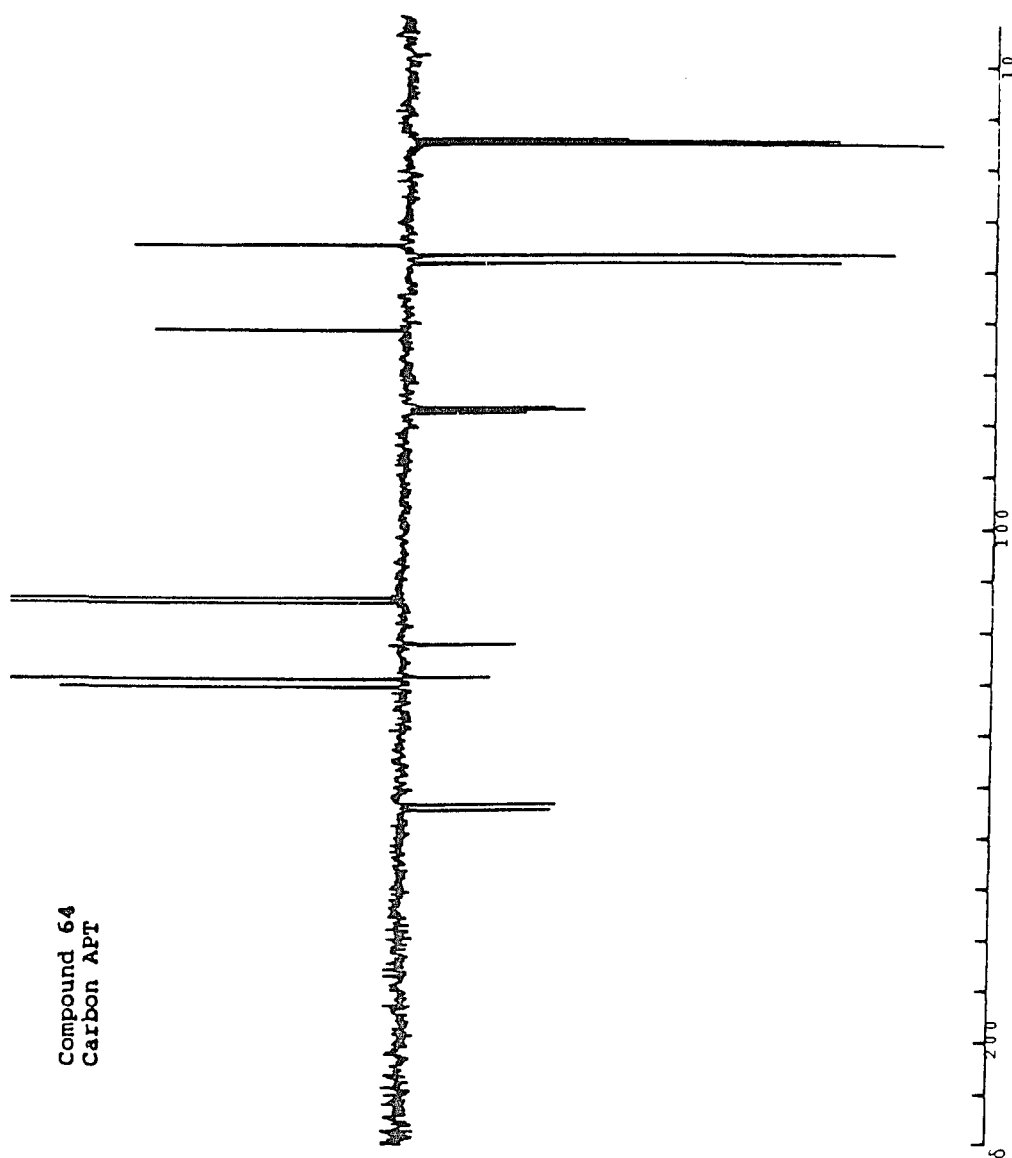
Compound 62
Proton

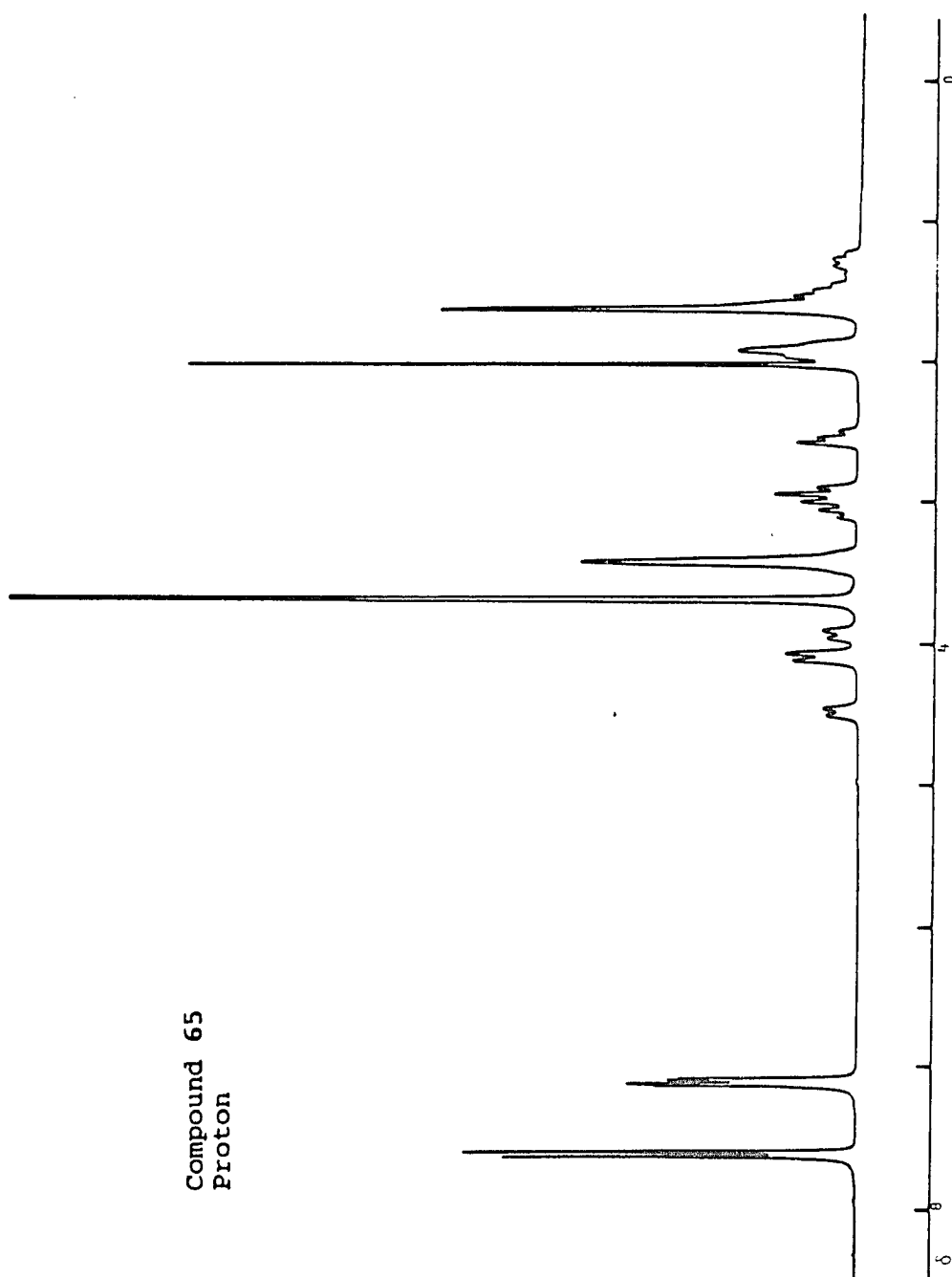


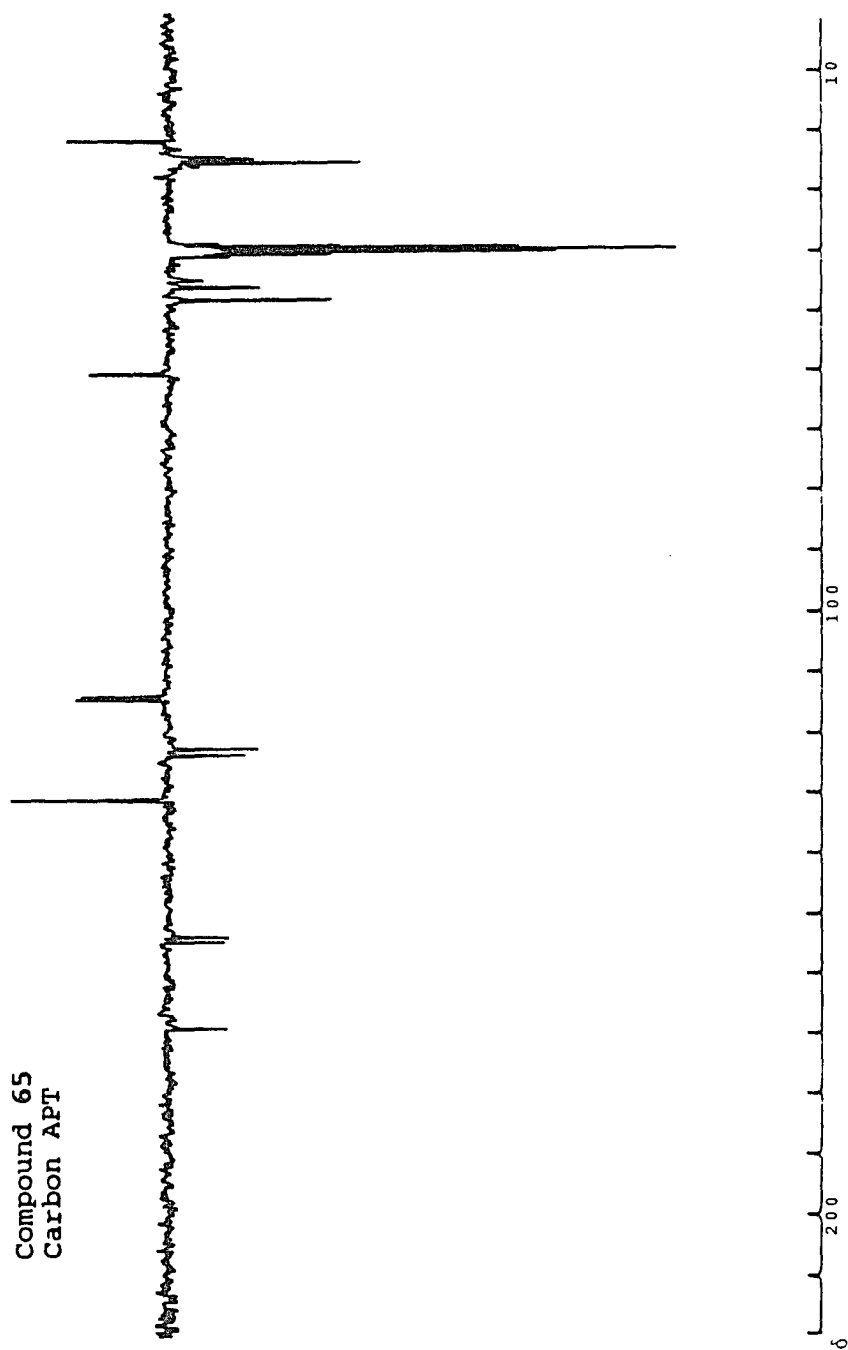


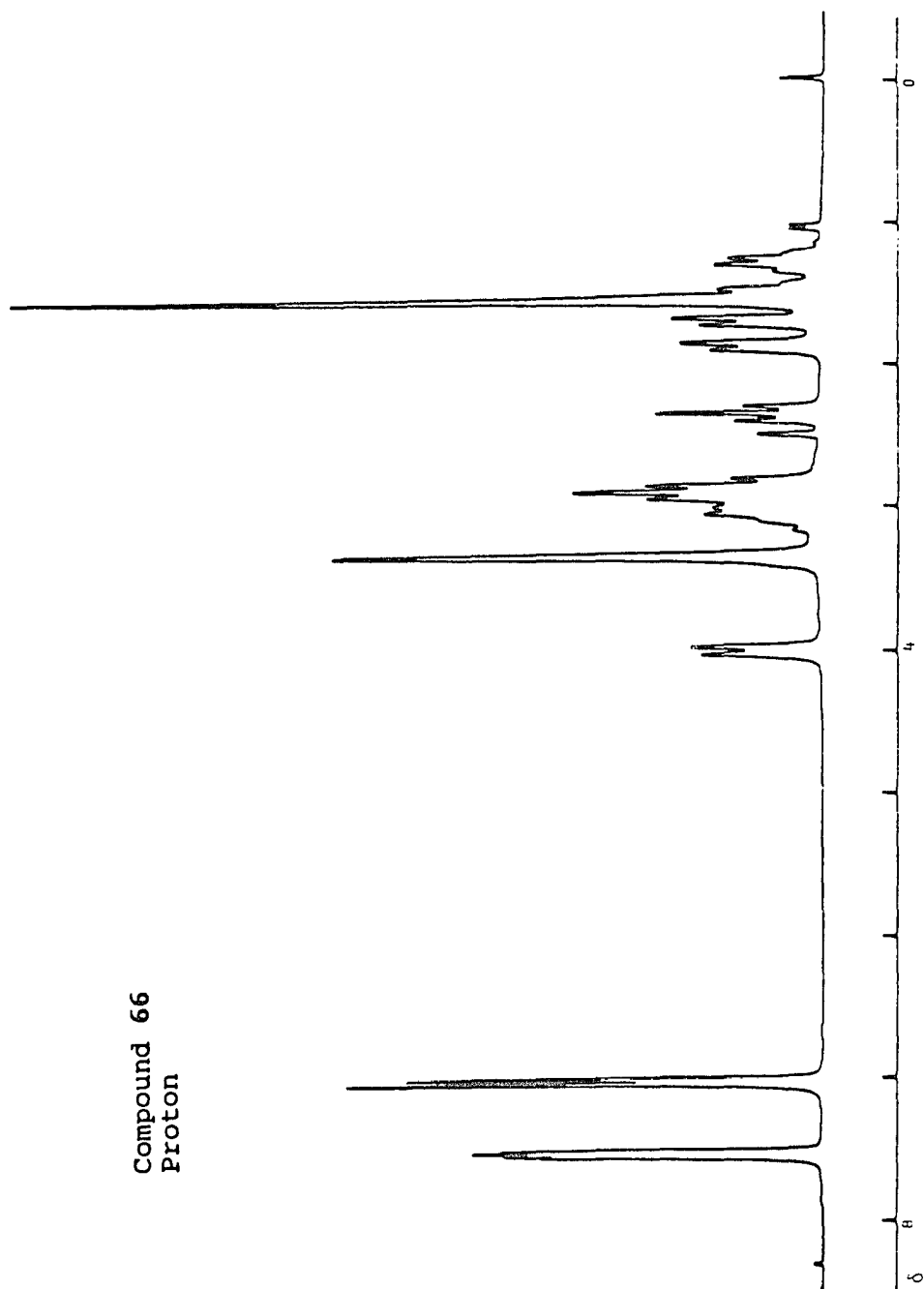


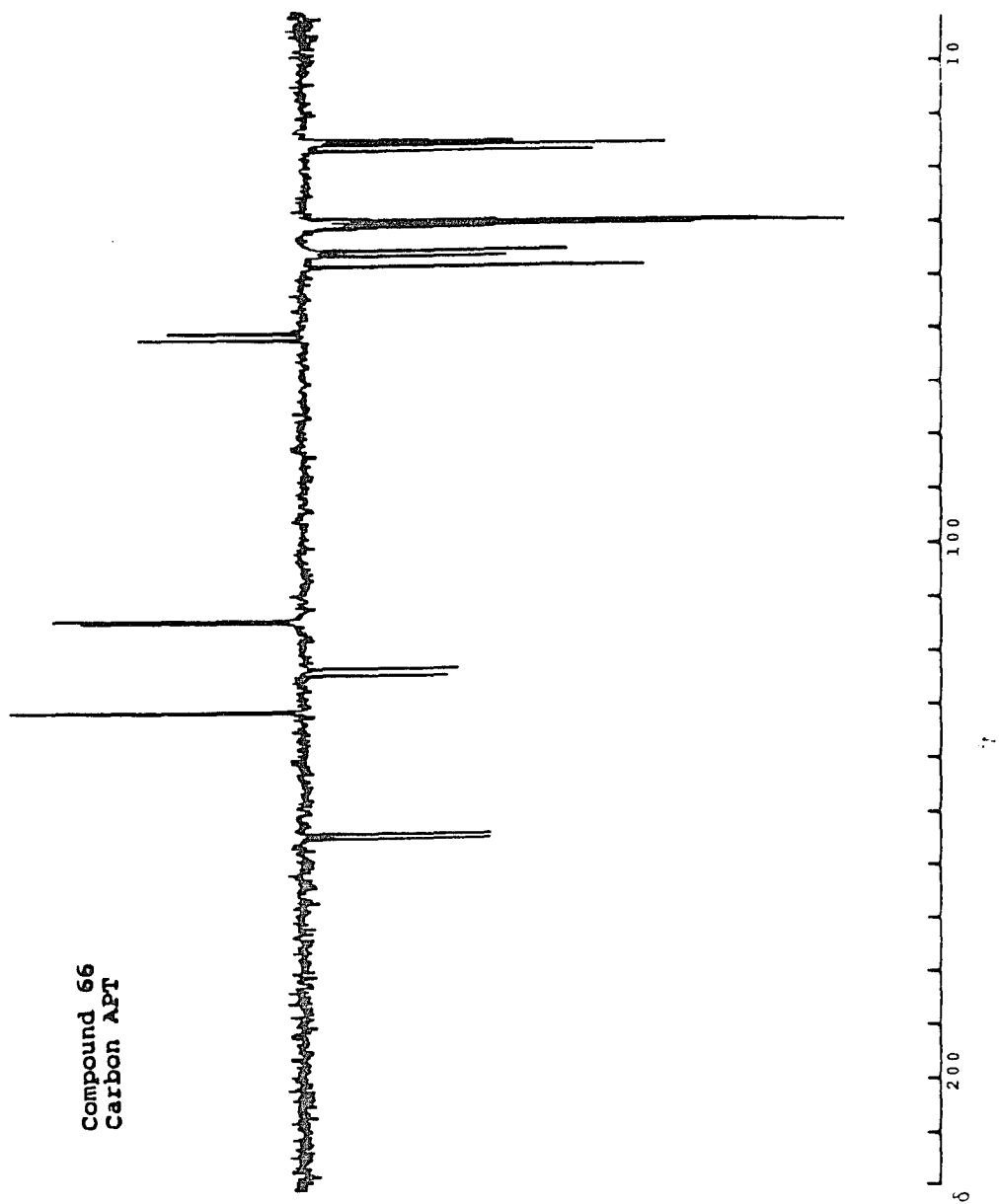
Compound 64
Proton

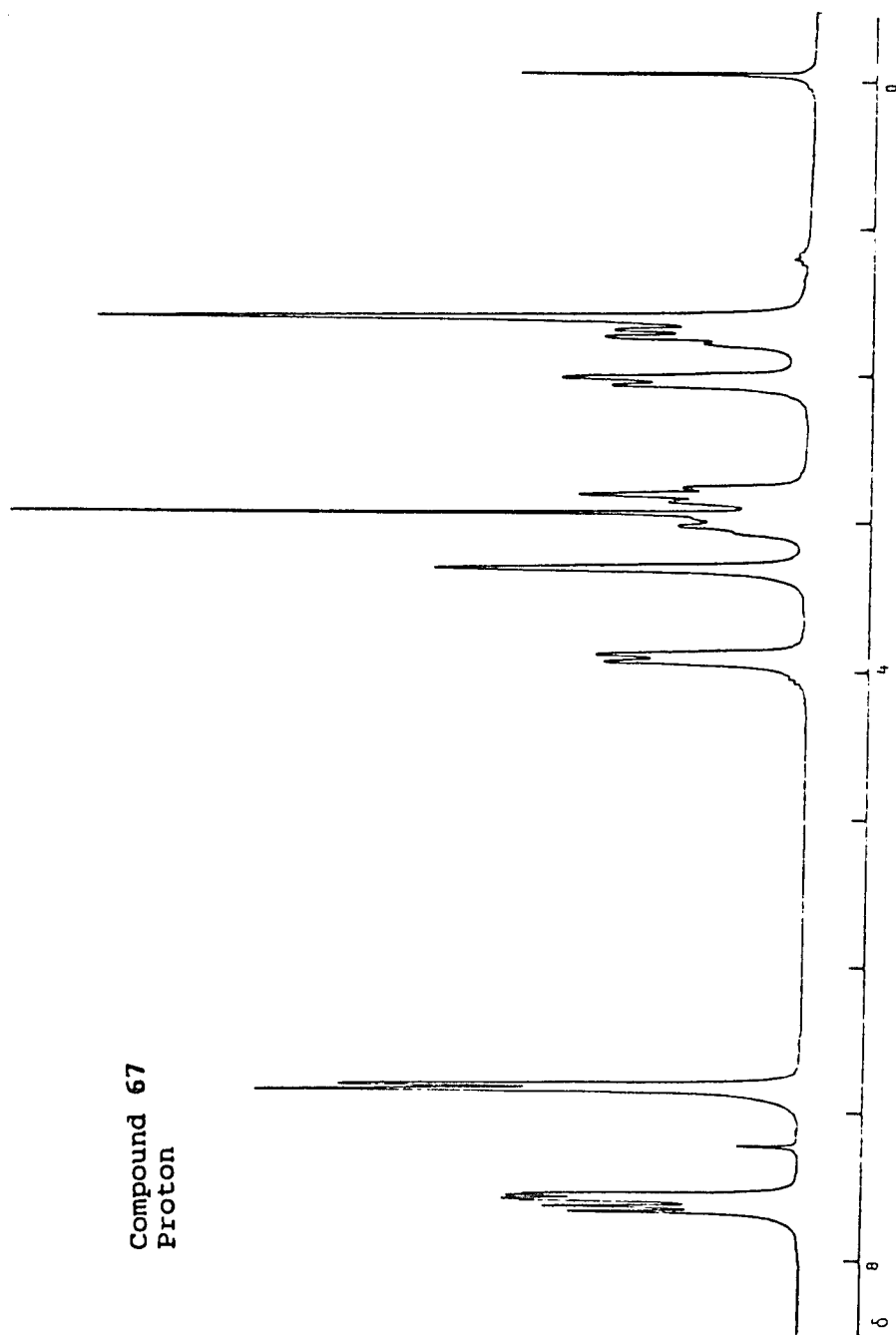


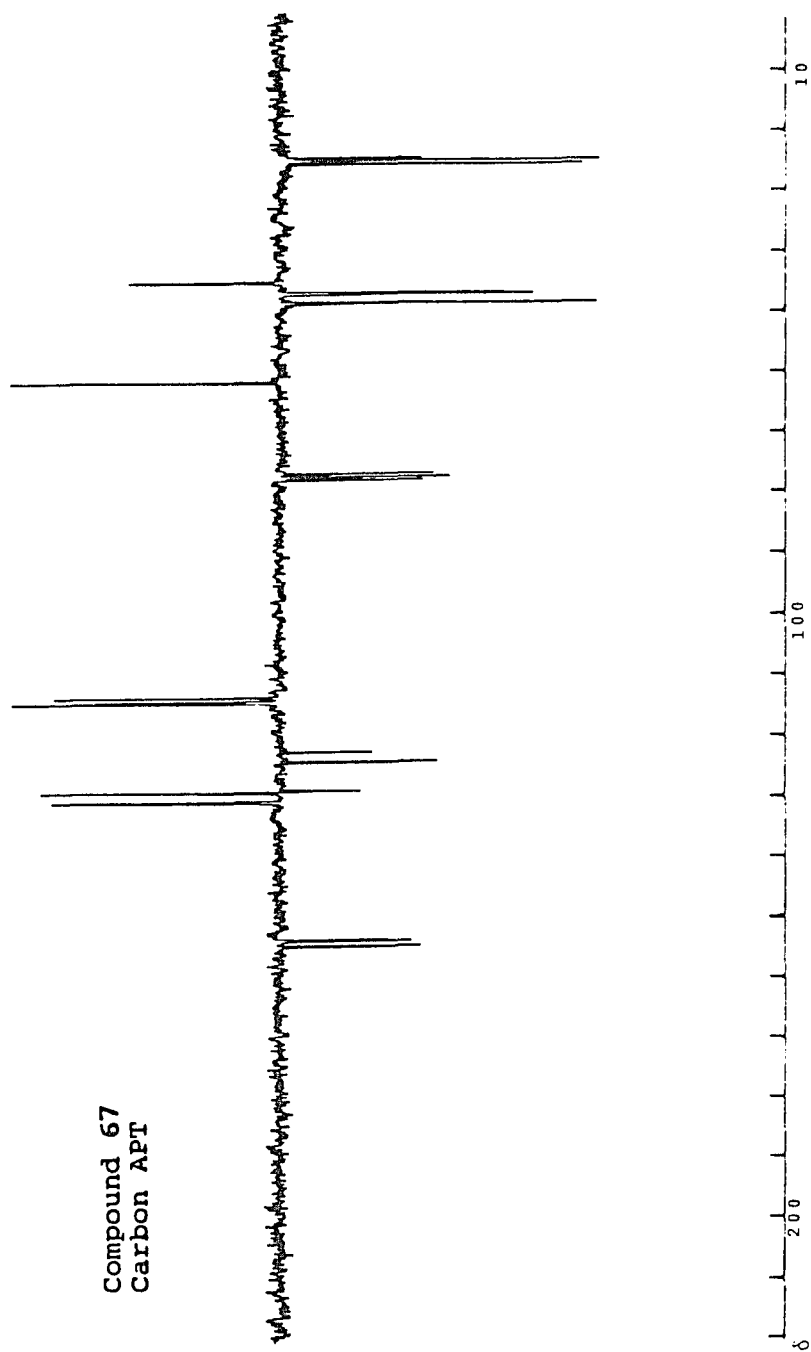




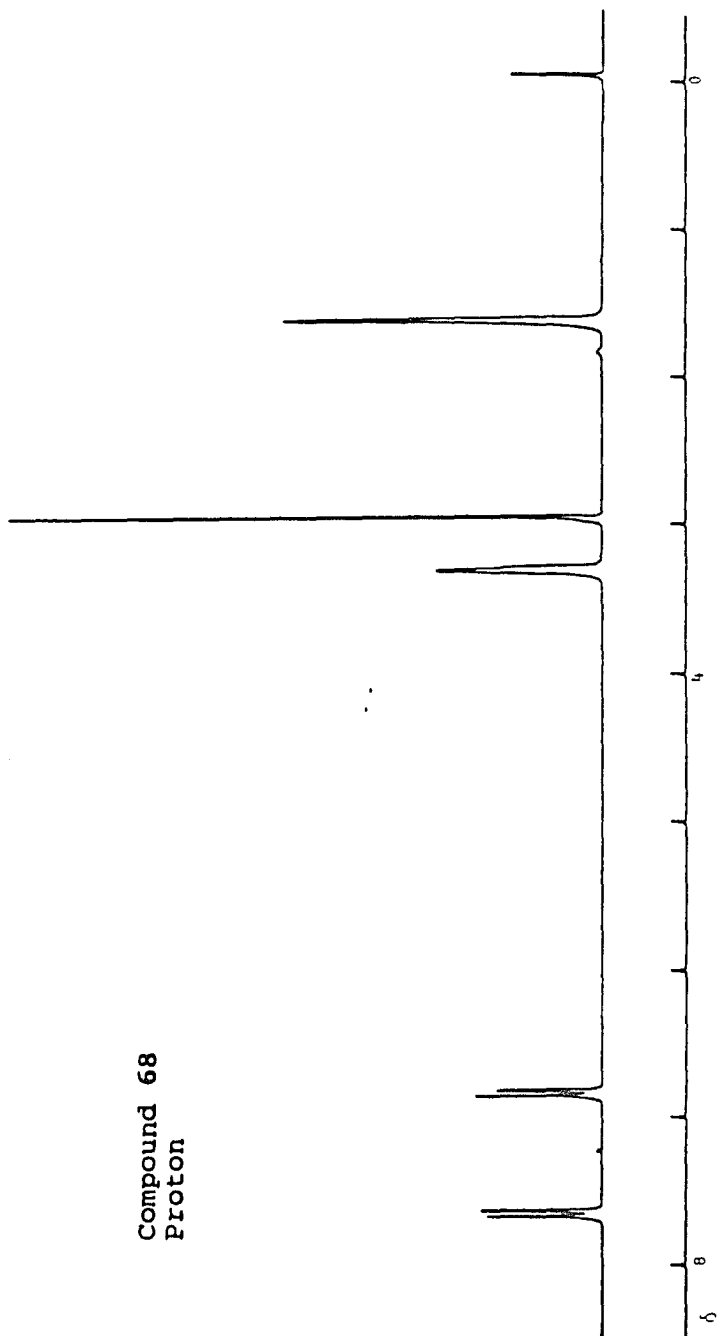


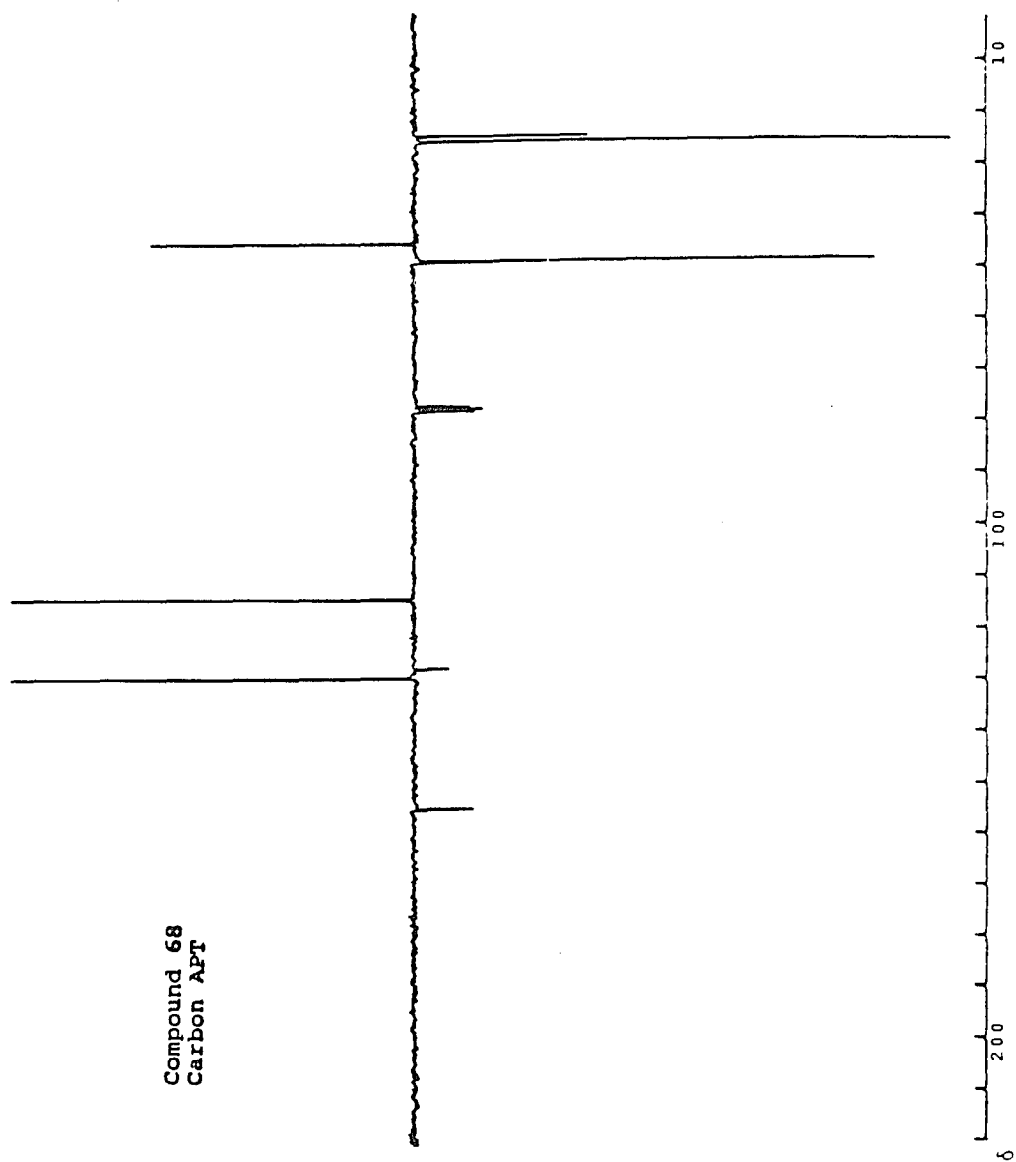




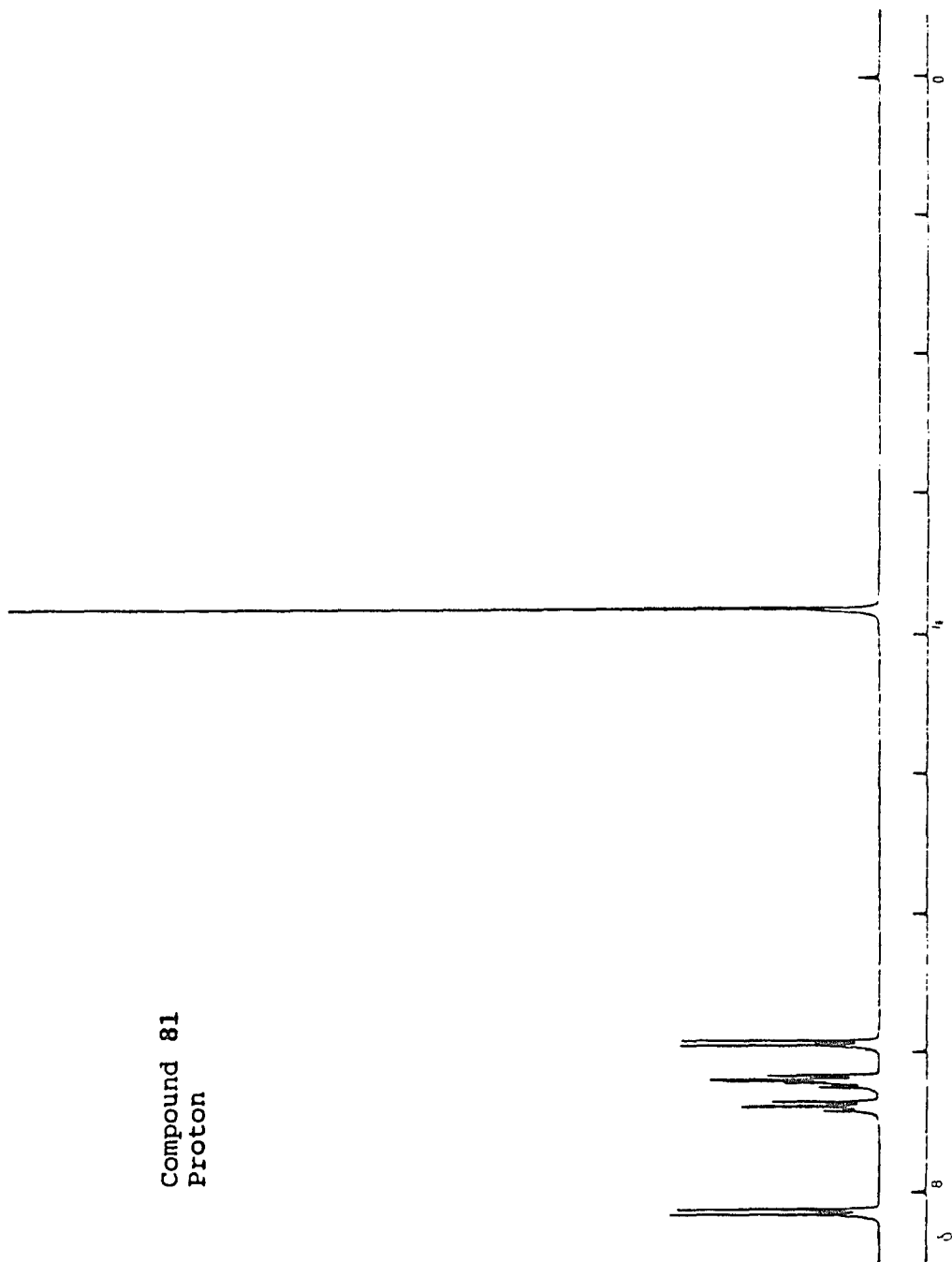


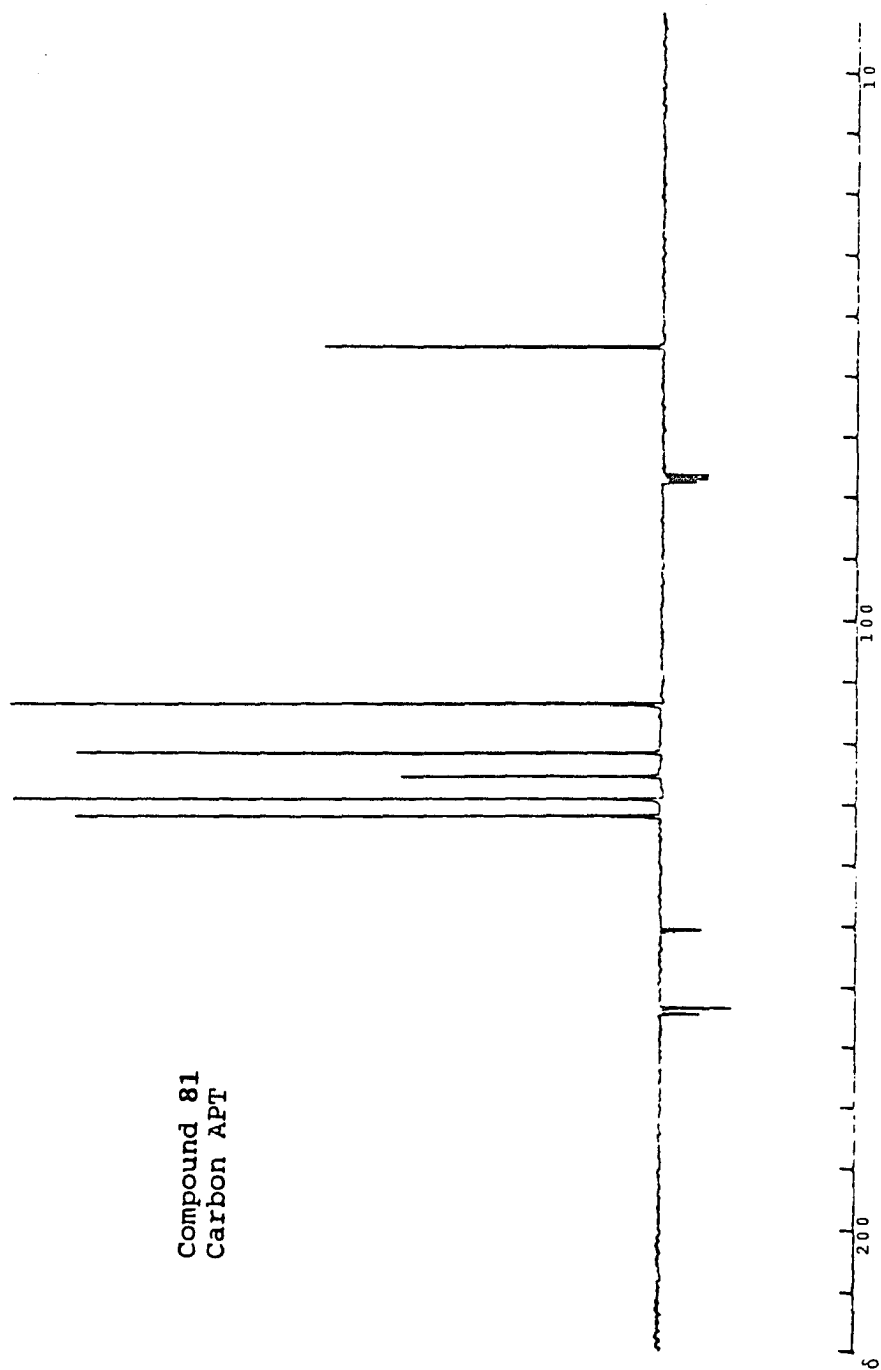
Compound 68
Proton



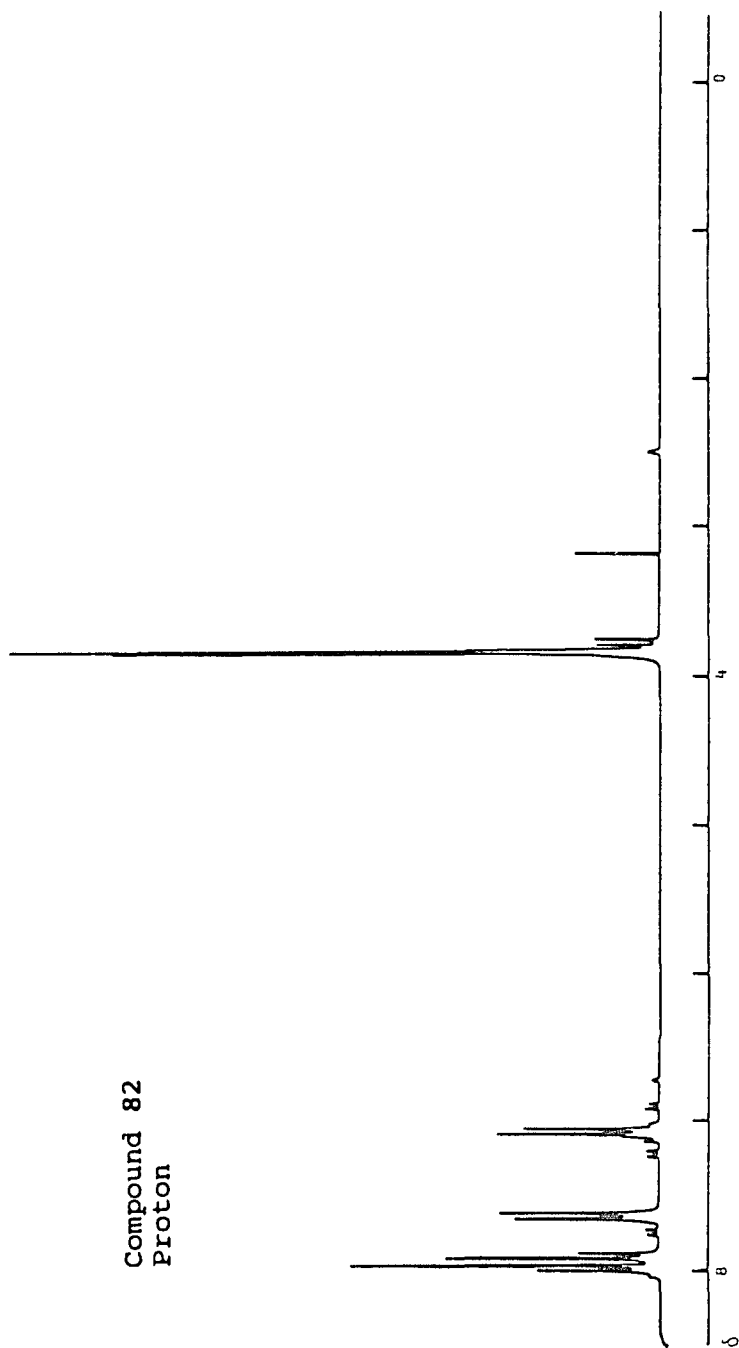


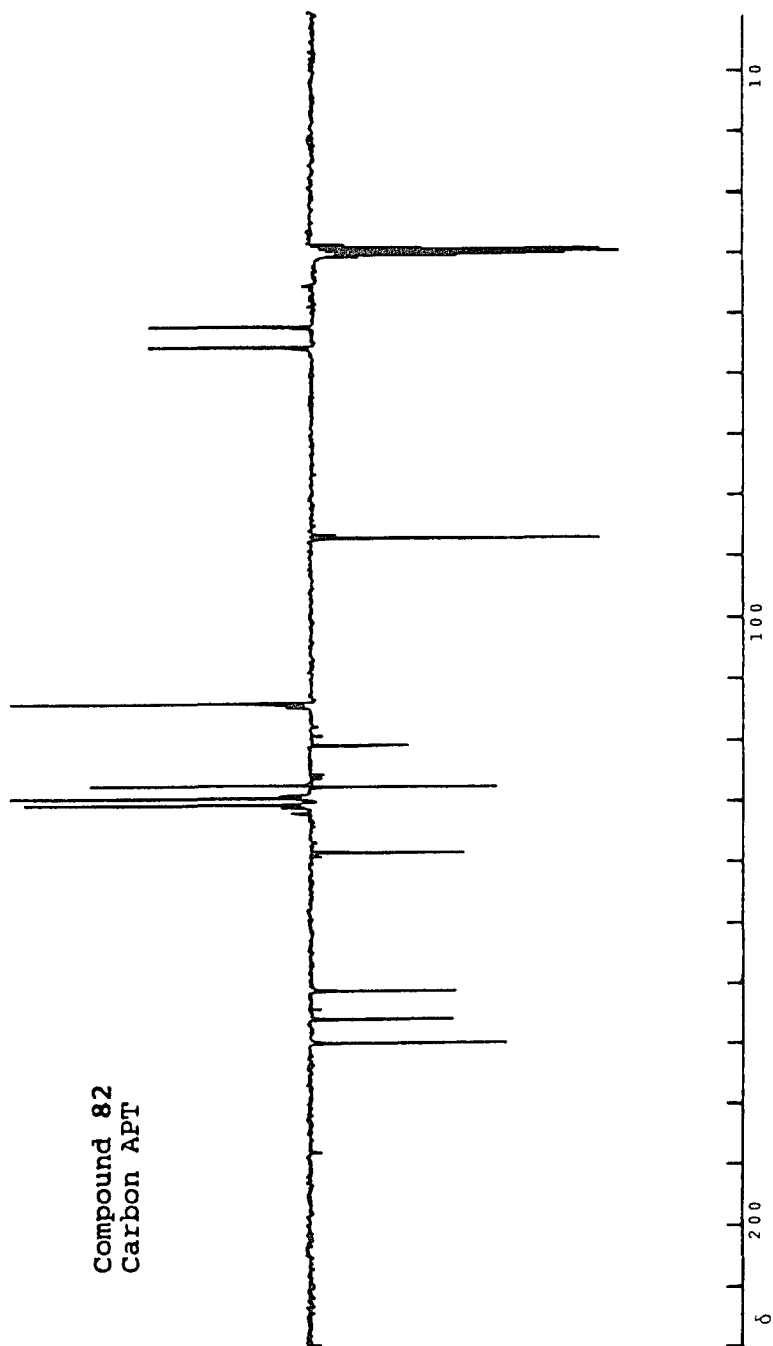
Compound 81
Proton



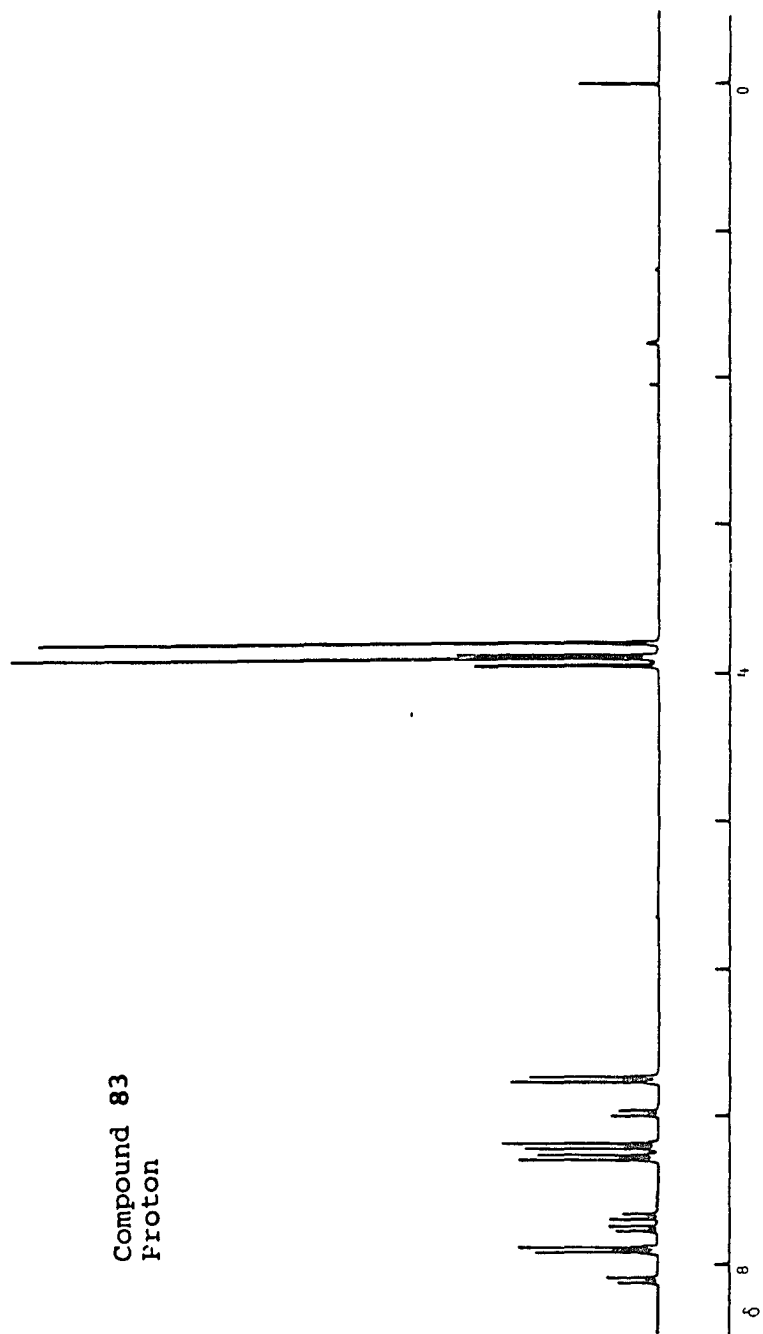


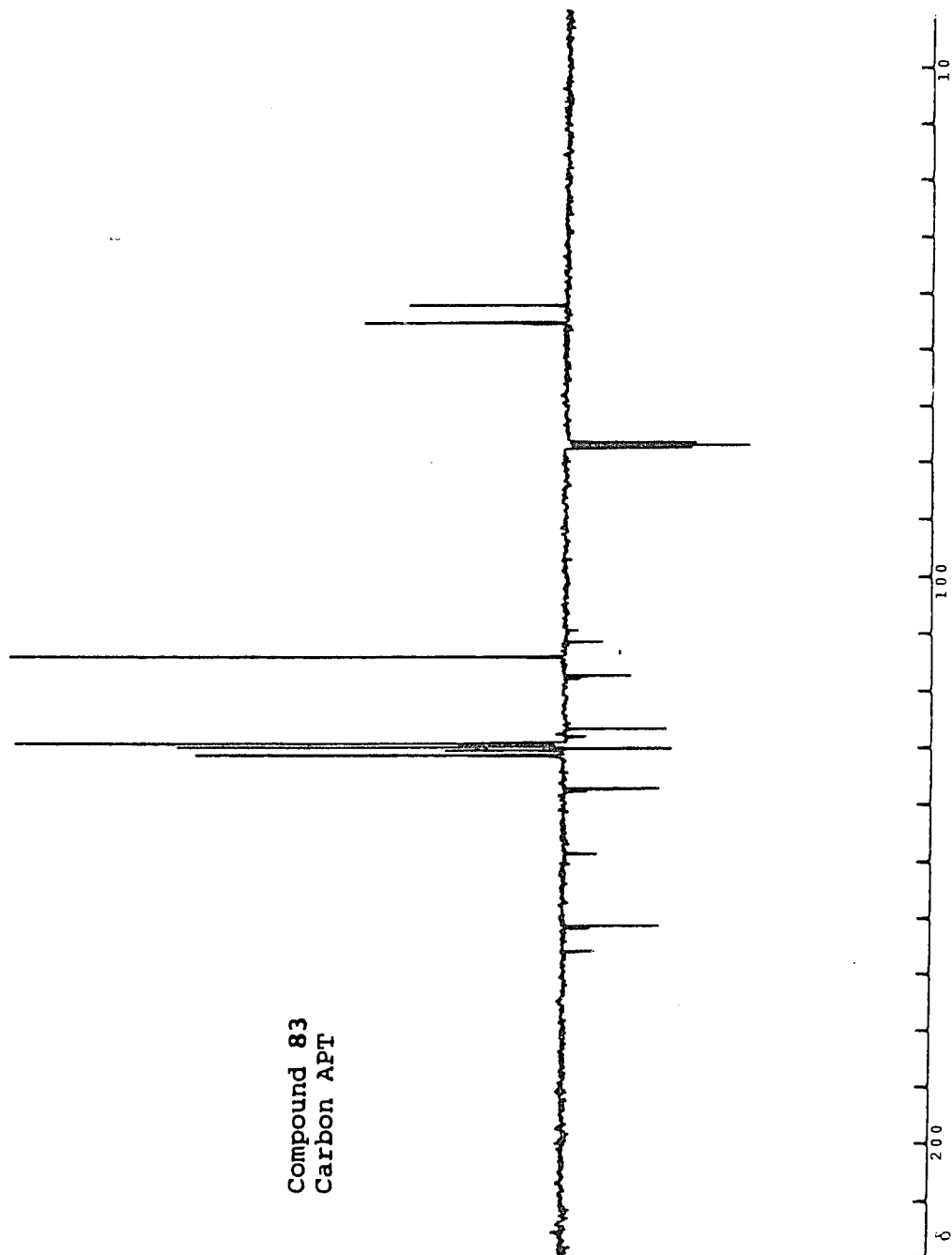
Compound 82
Proton

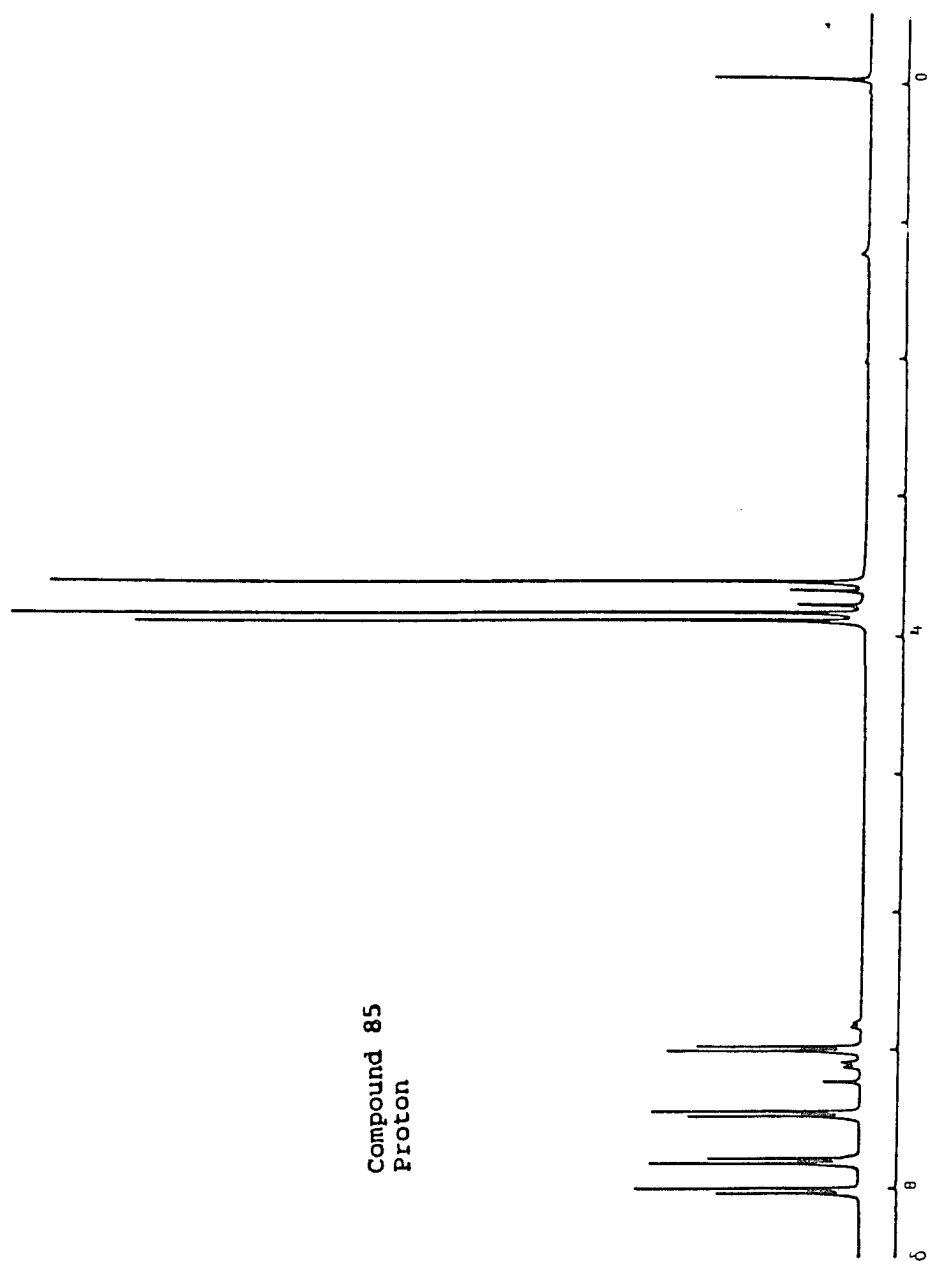


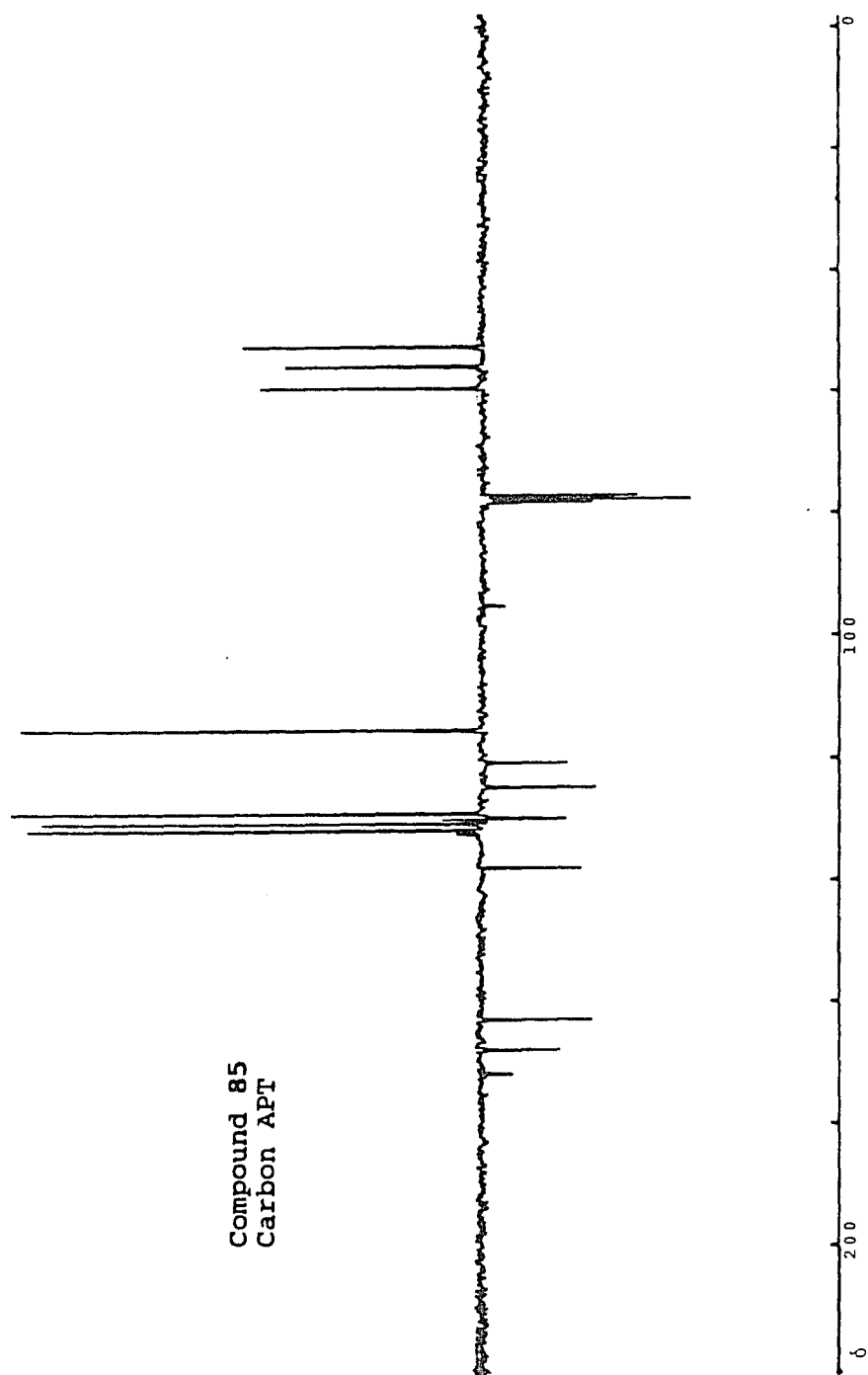


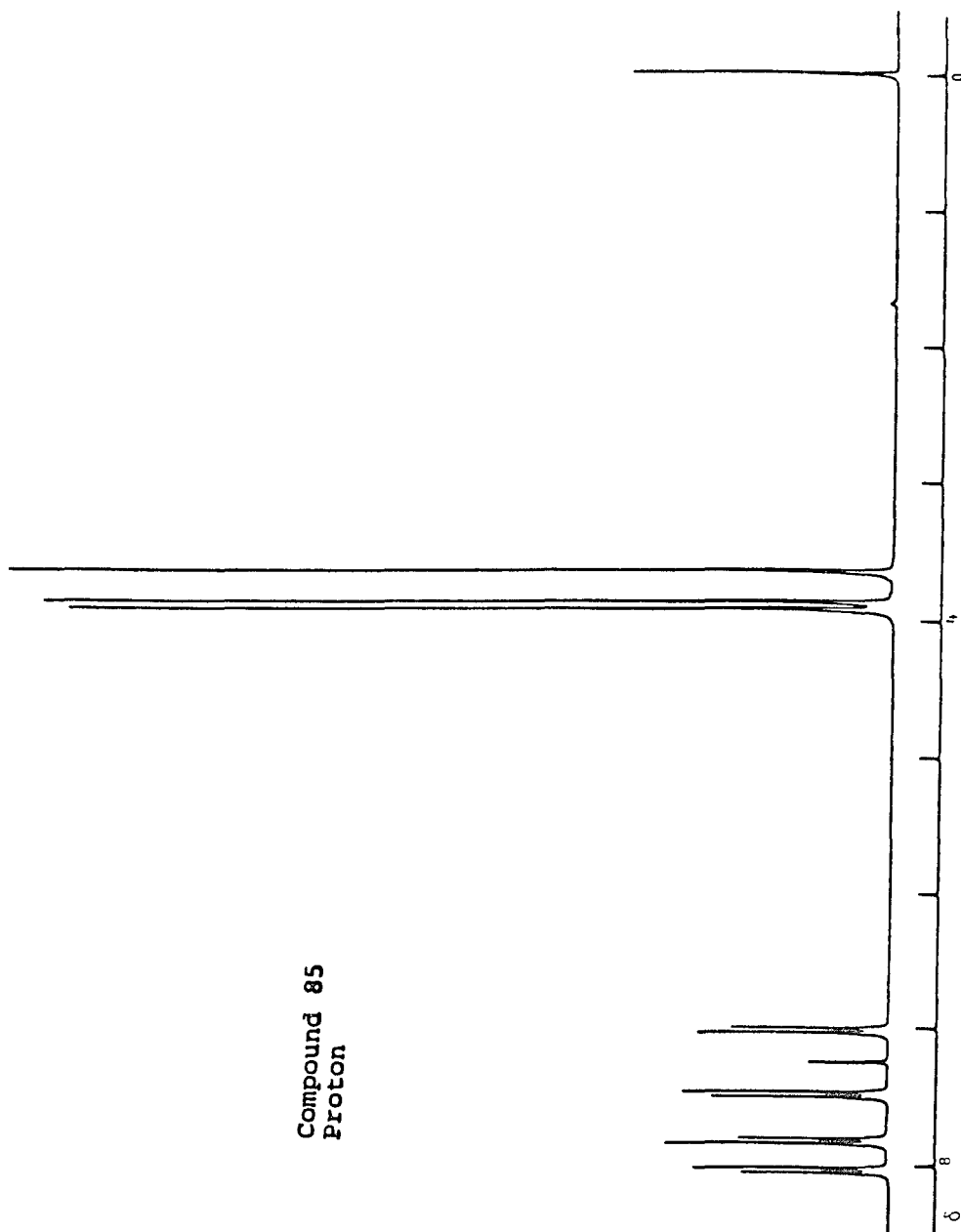
Compound 83
Proton



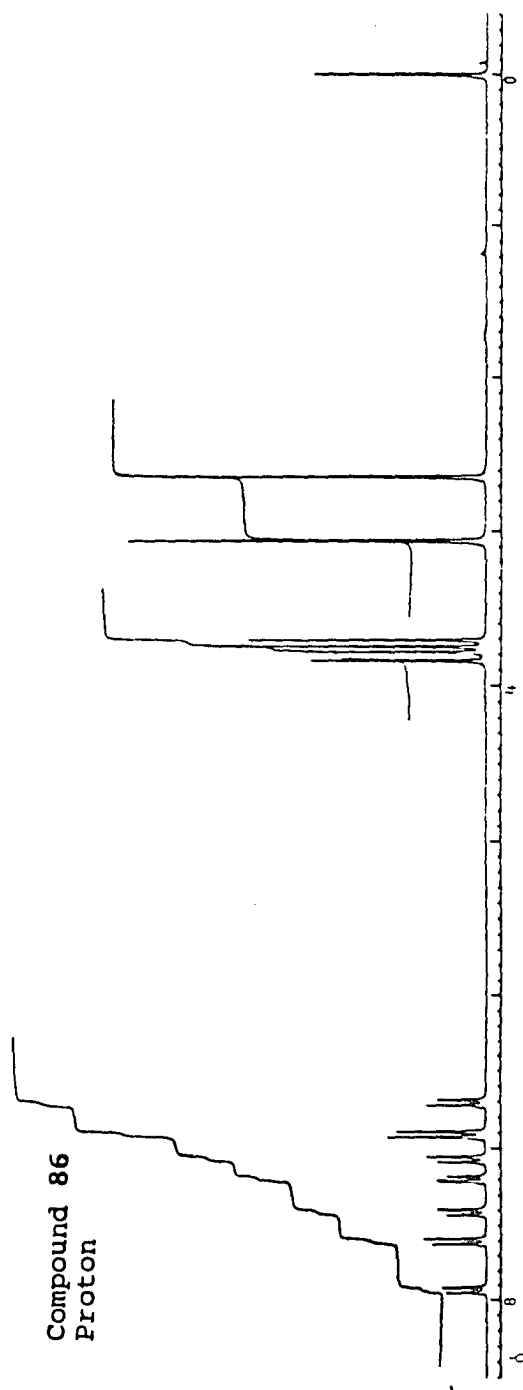




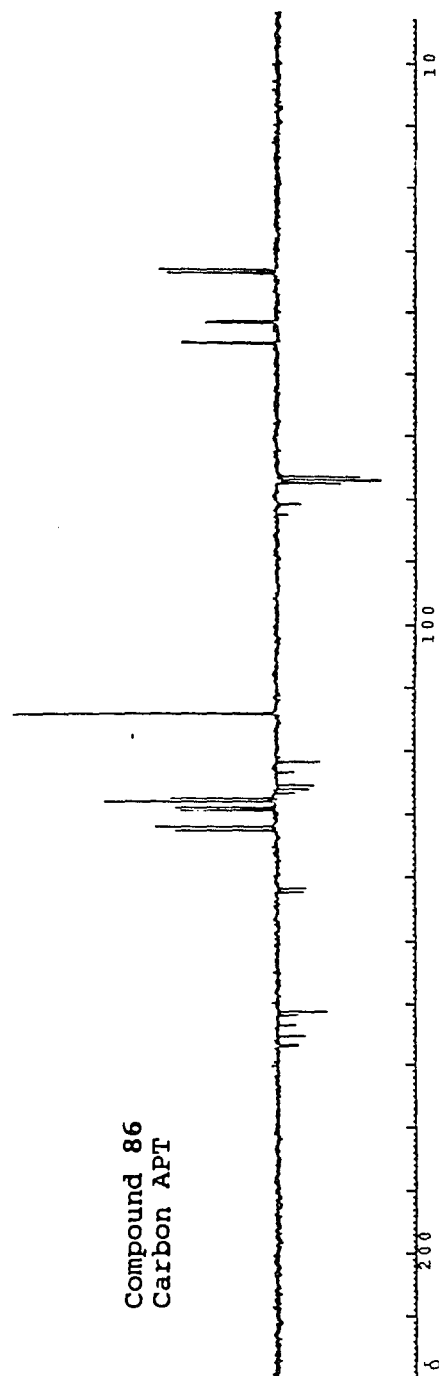




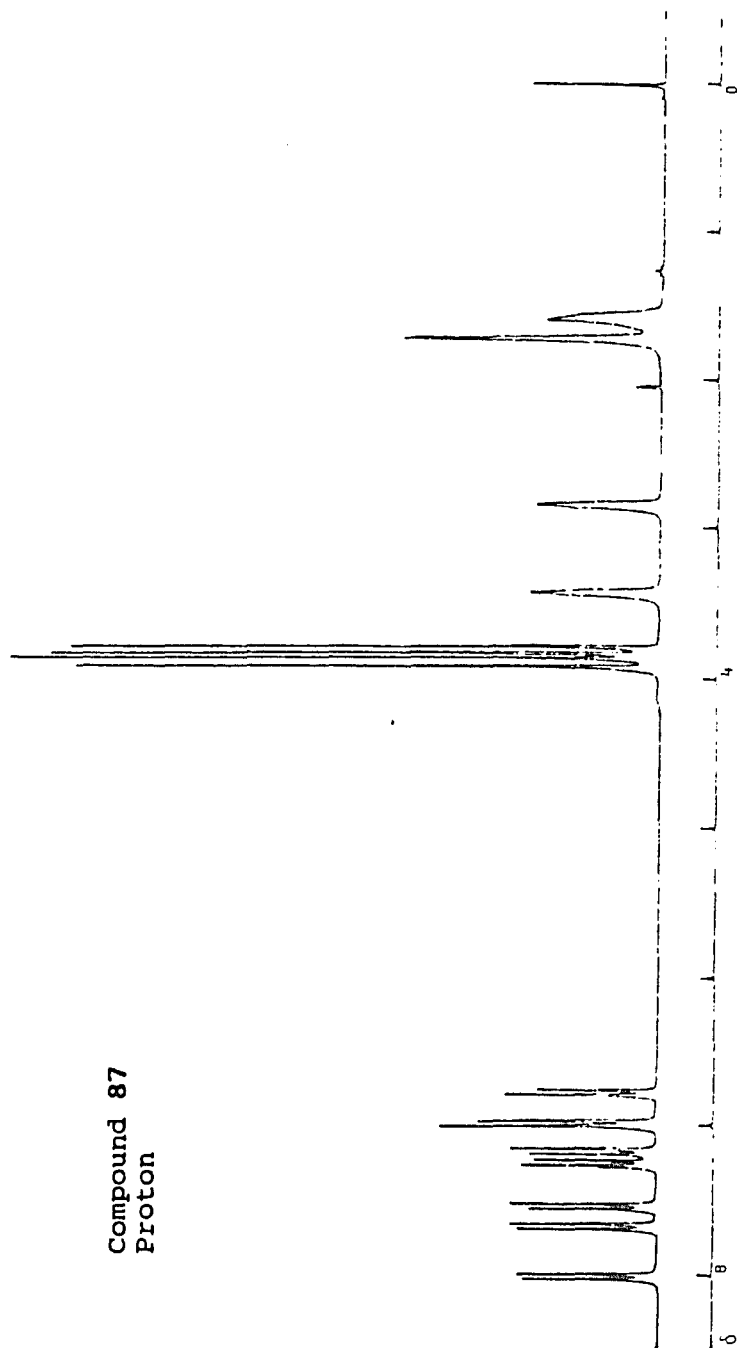
Compound 86
Proton

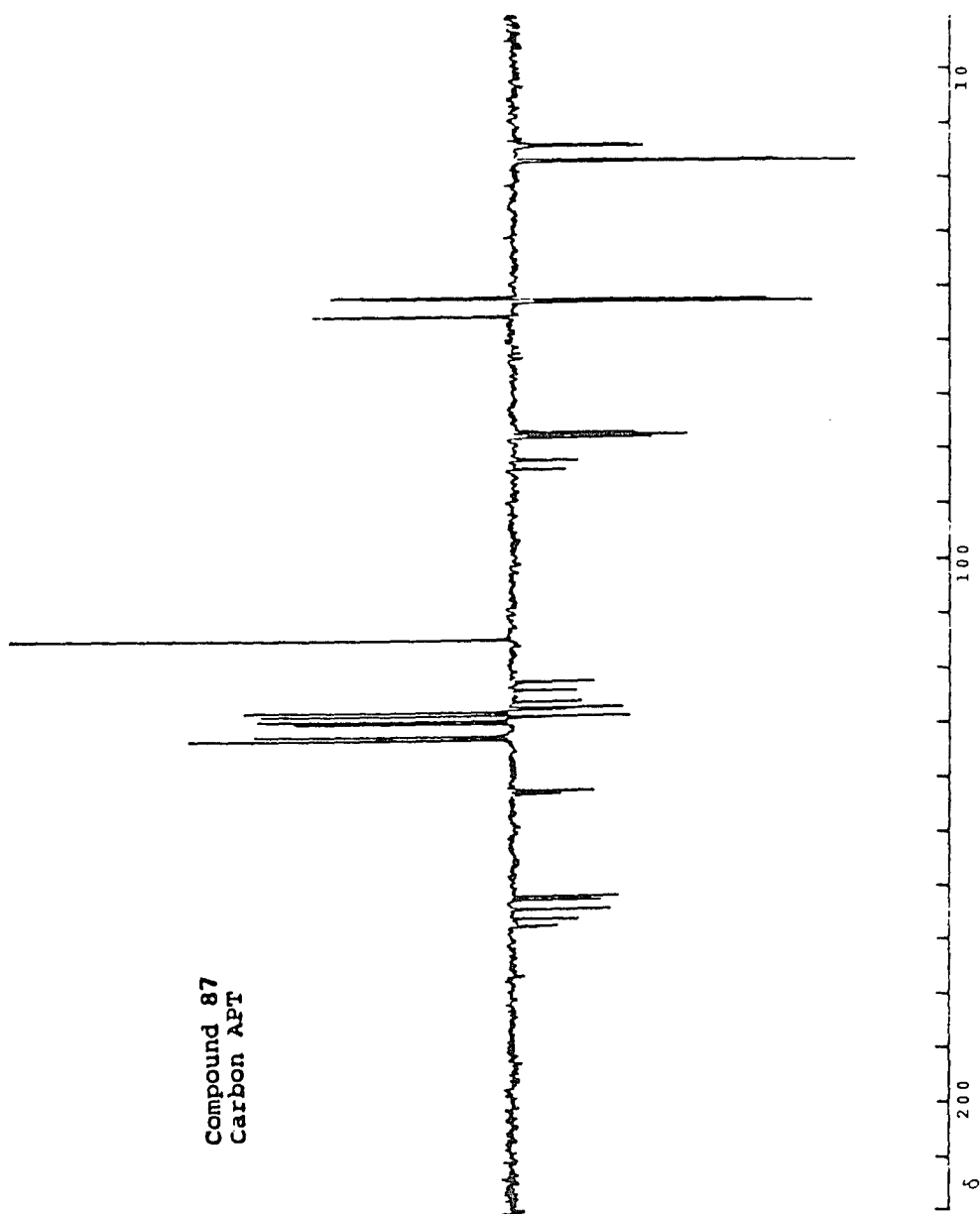


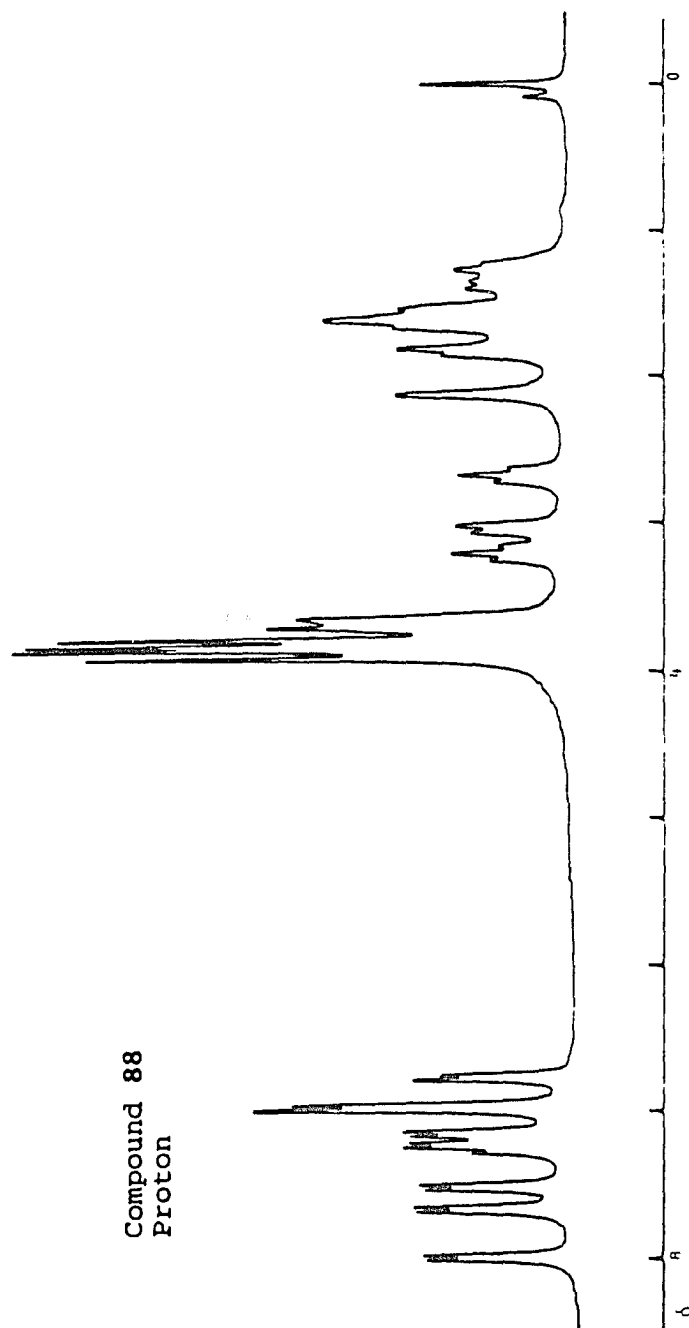
Compound 86
Carbon APT

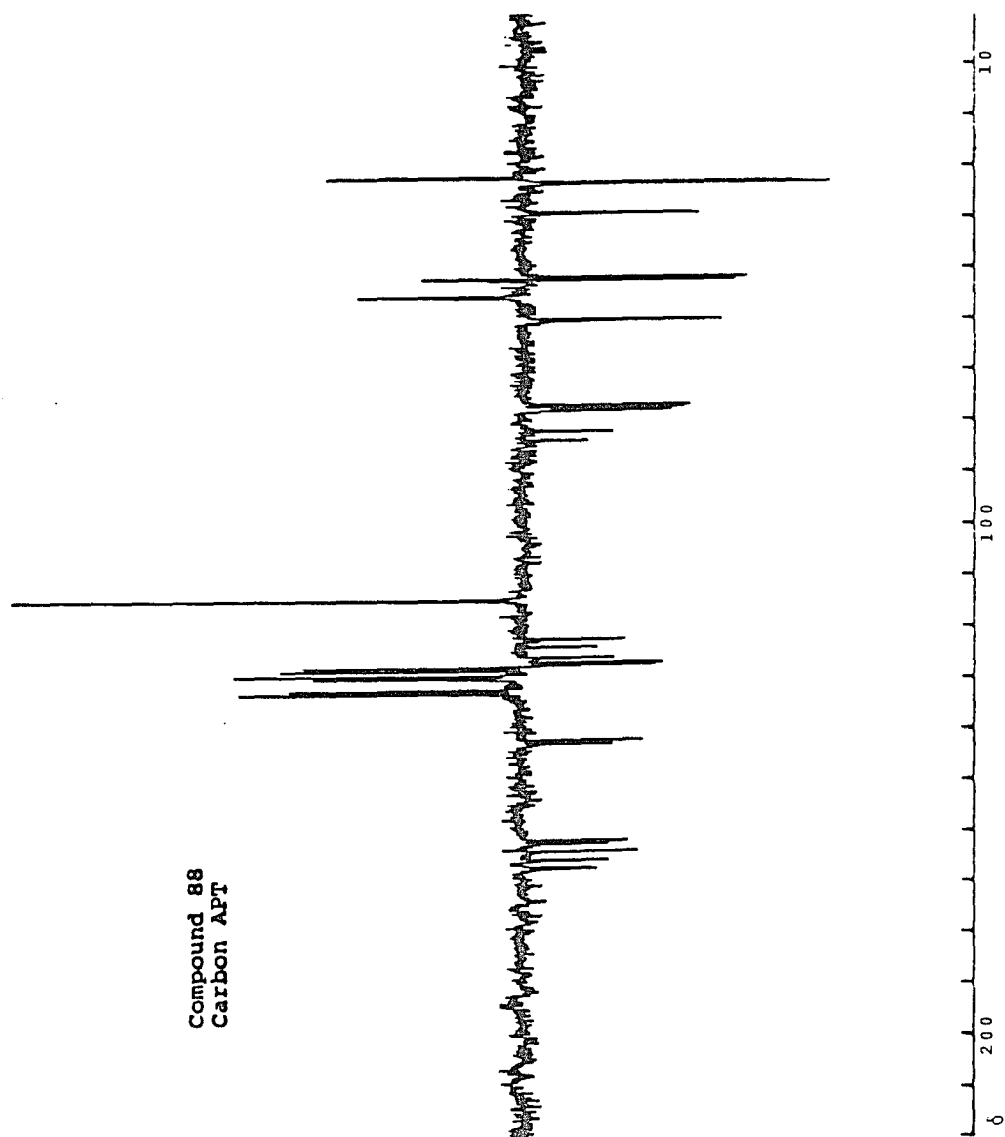


Compound 87
Proton

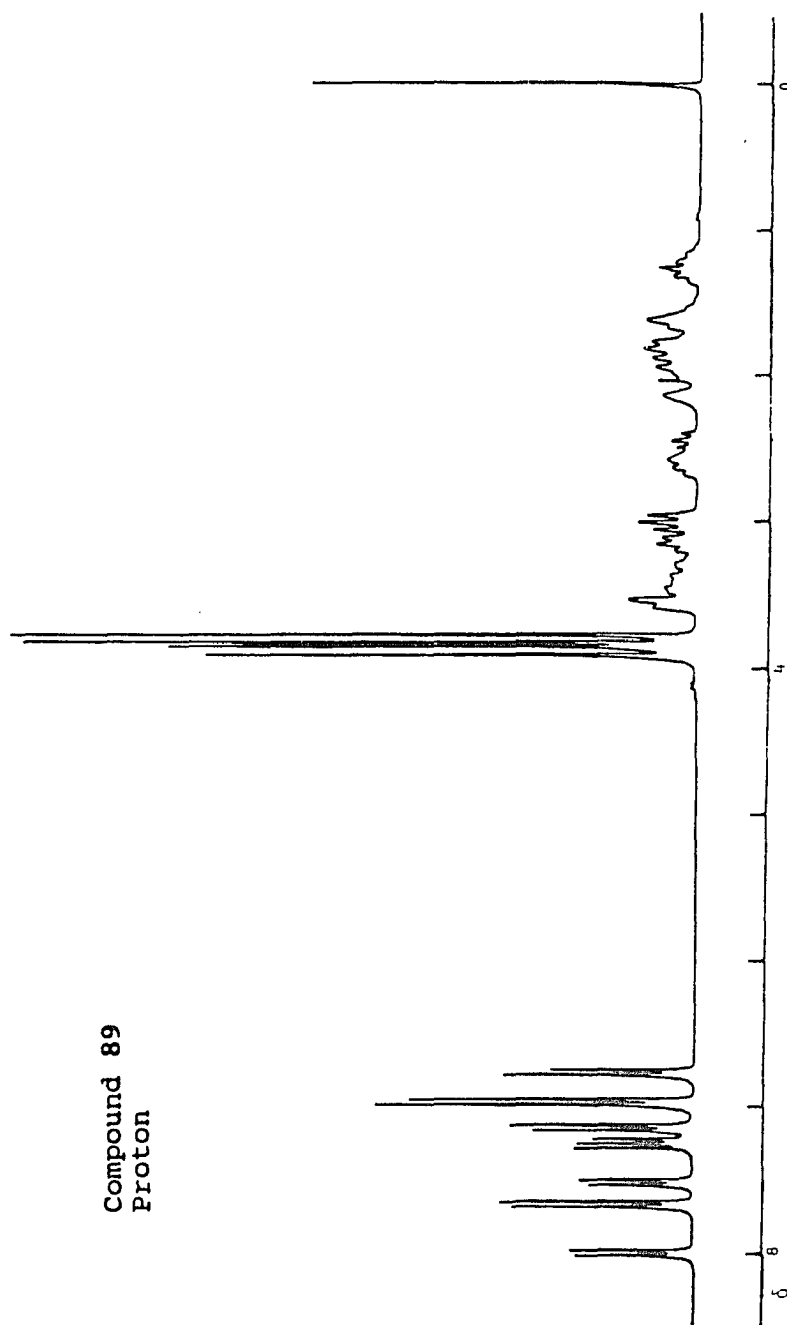


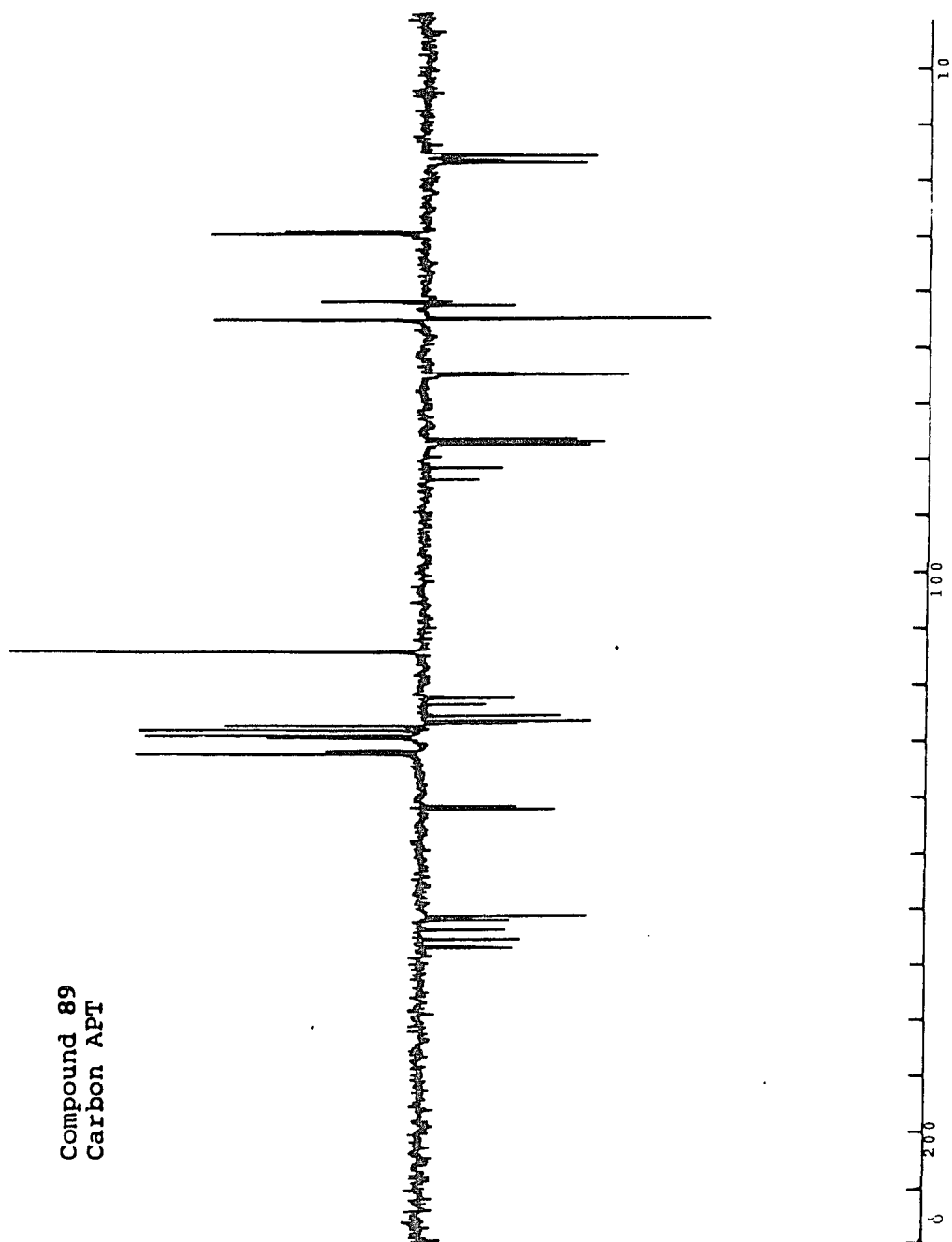


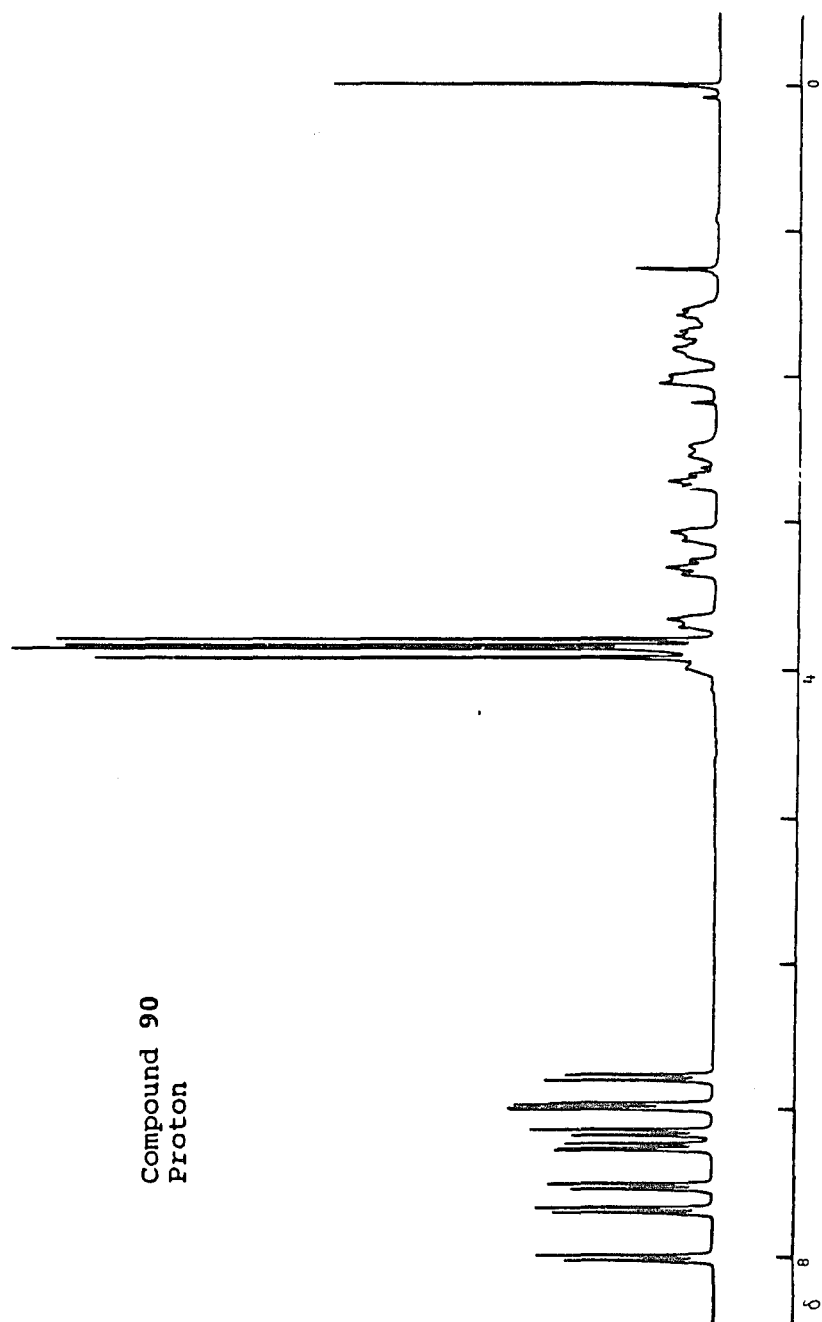


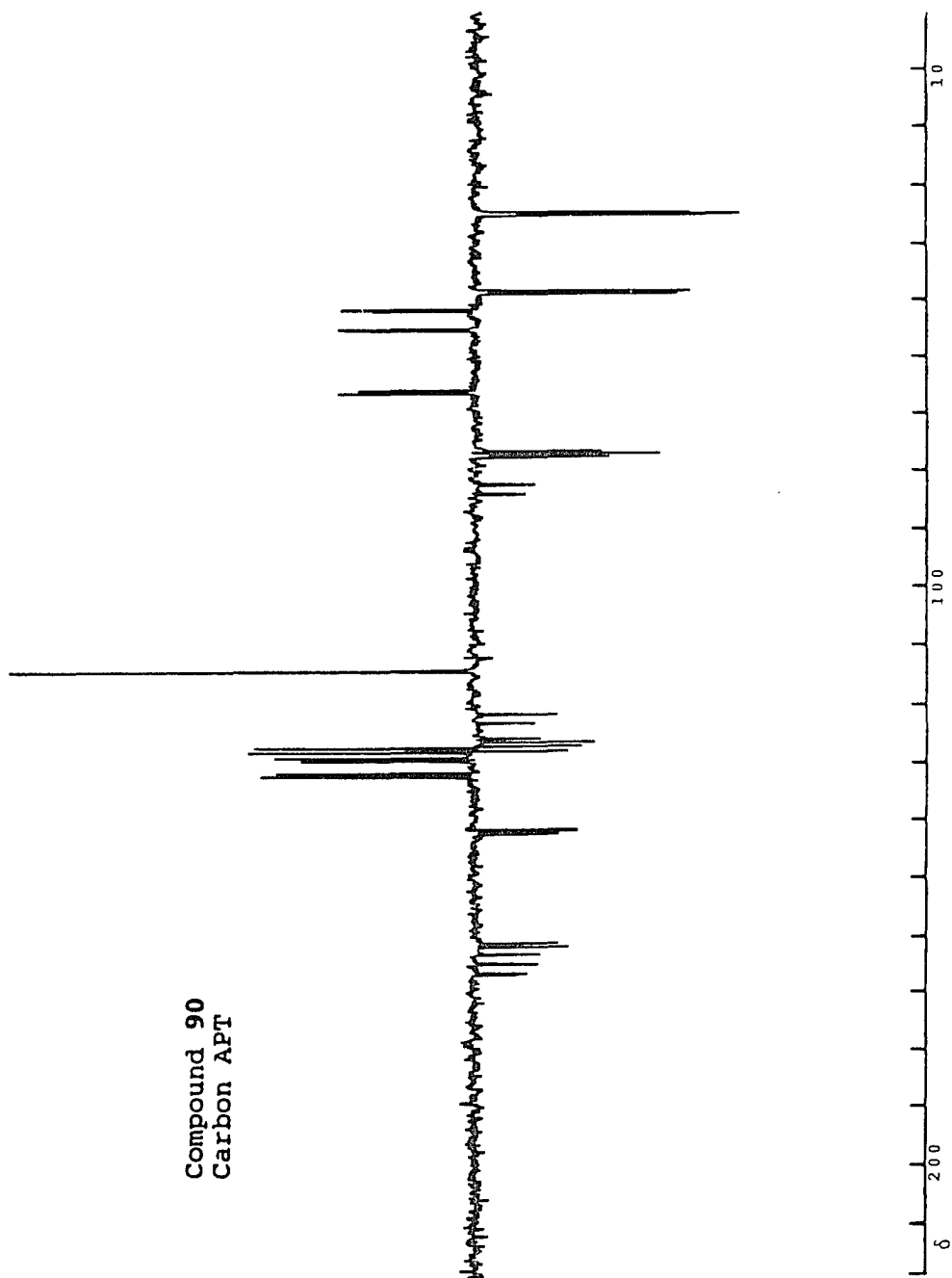


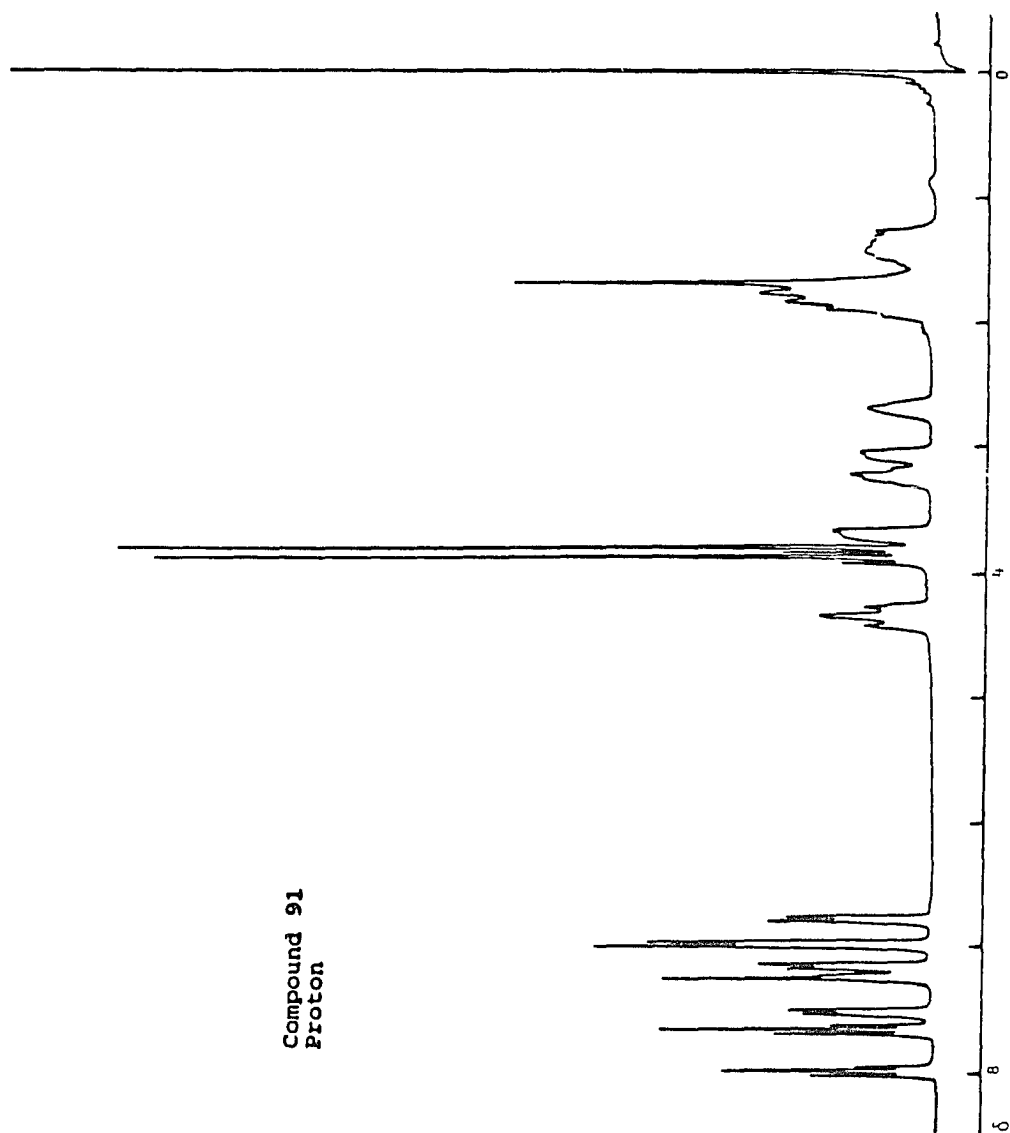
Compound 89
Proton

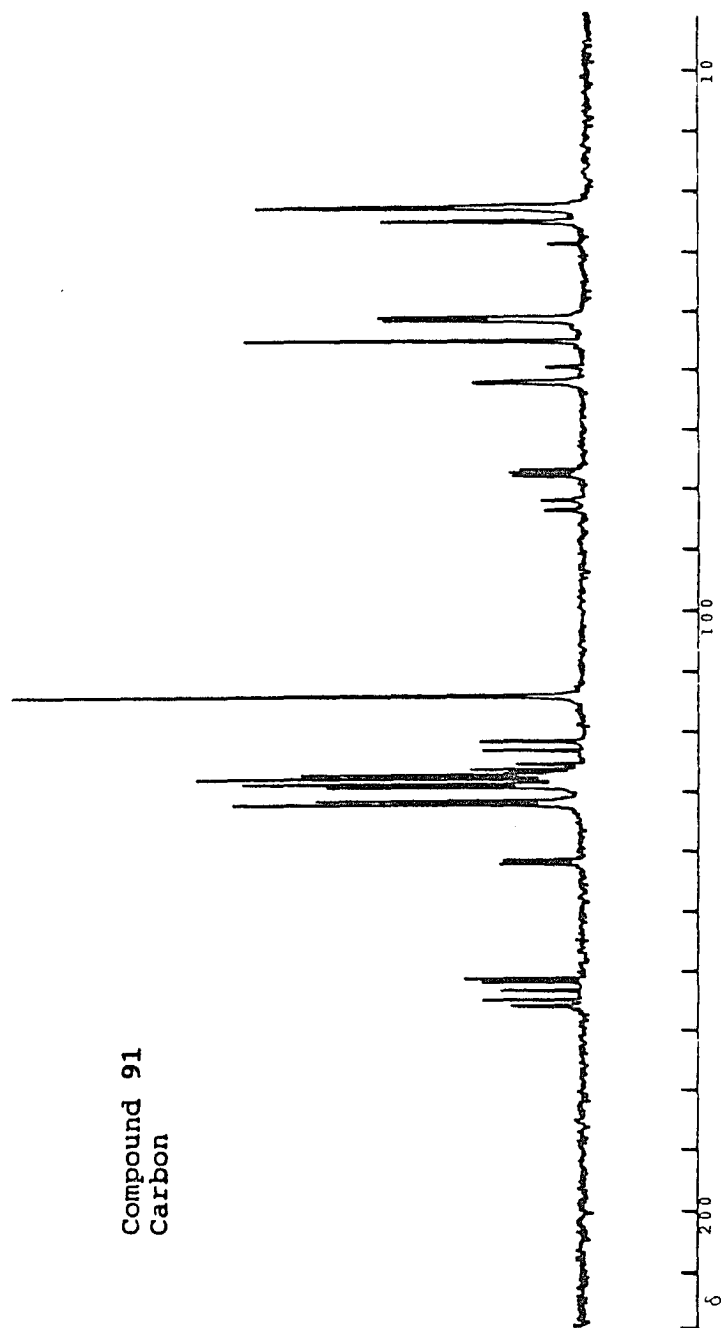




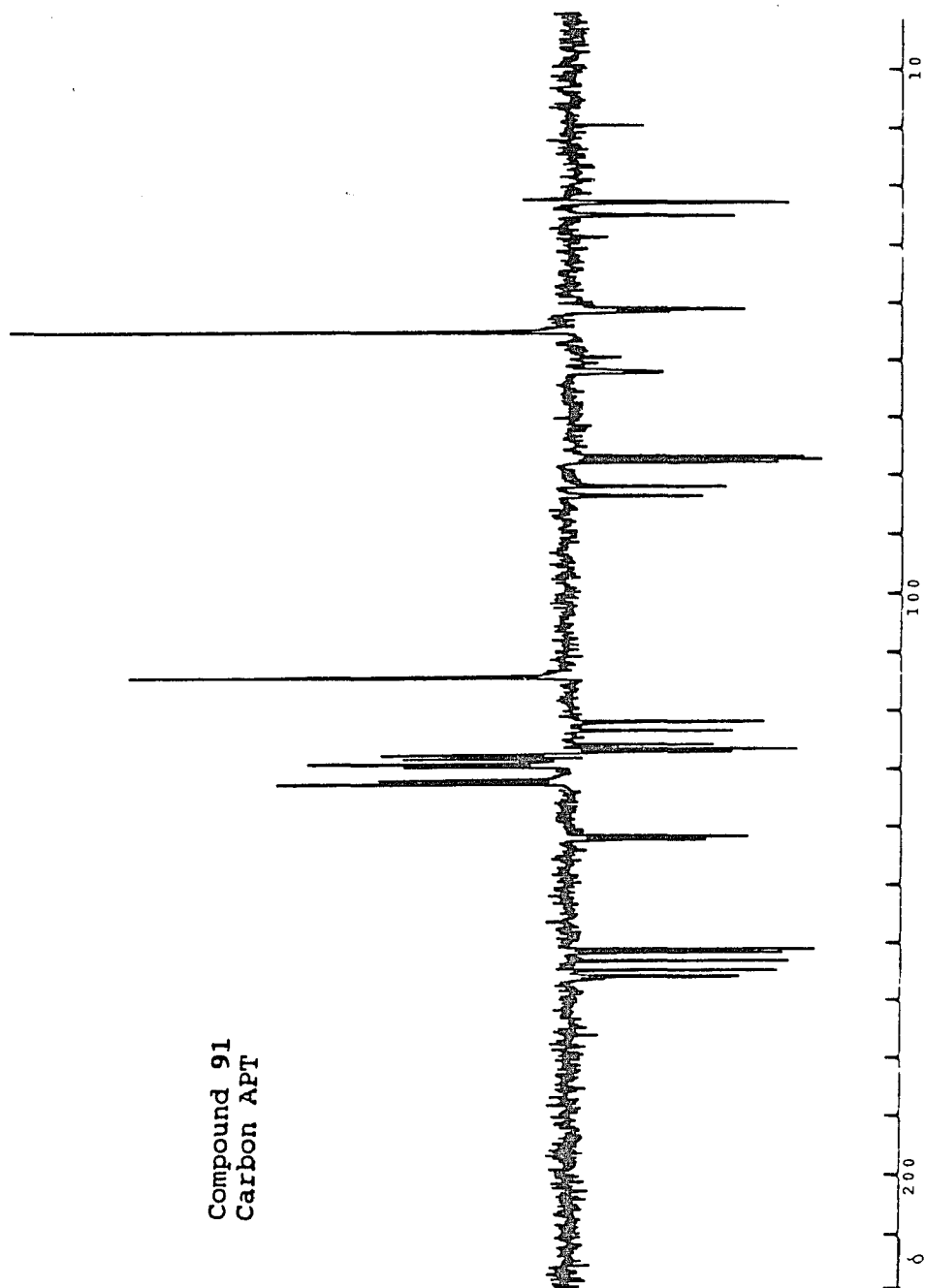


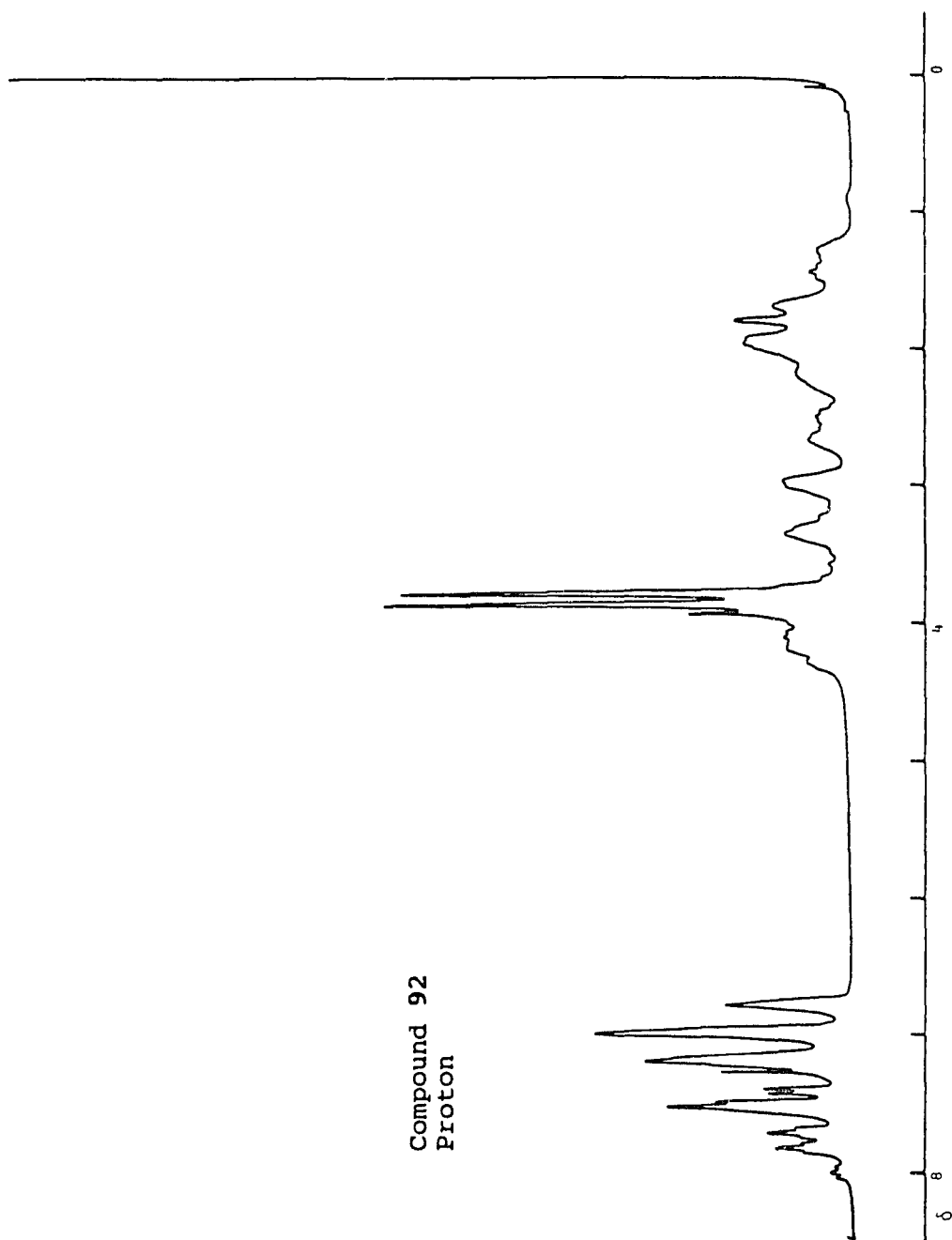


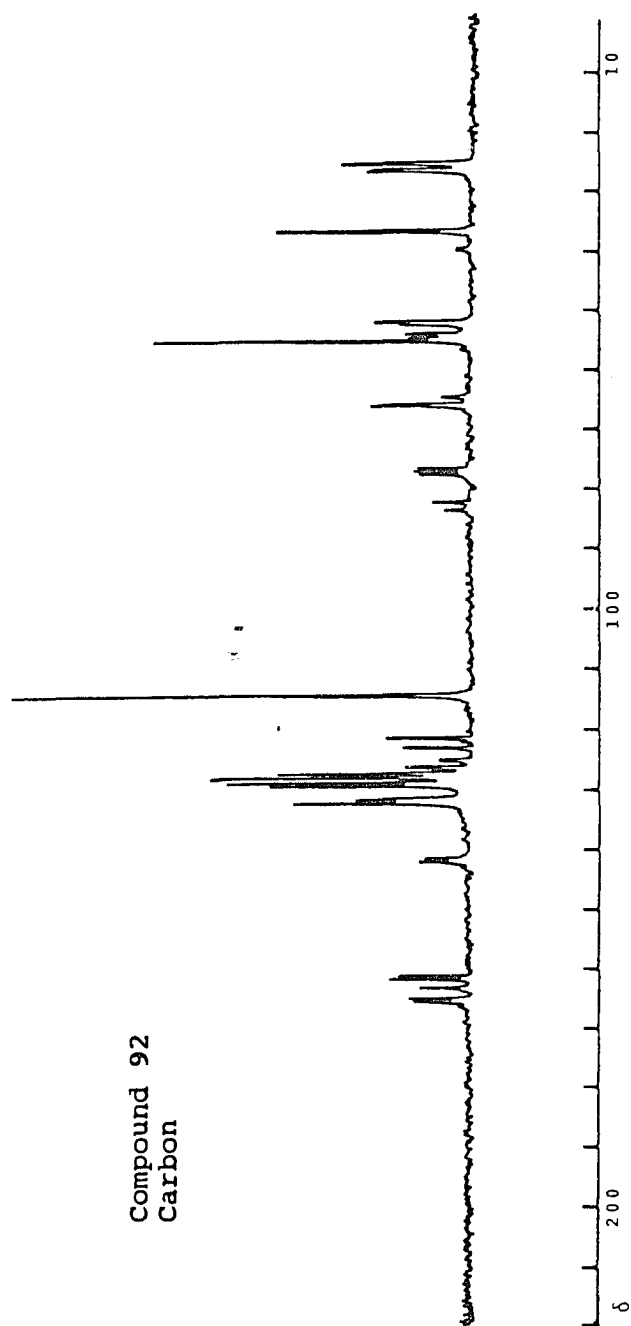




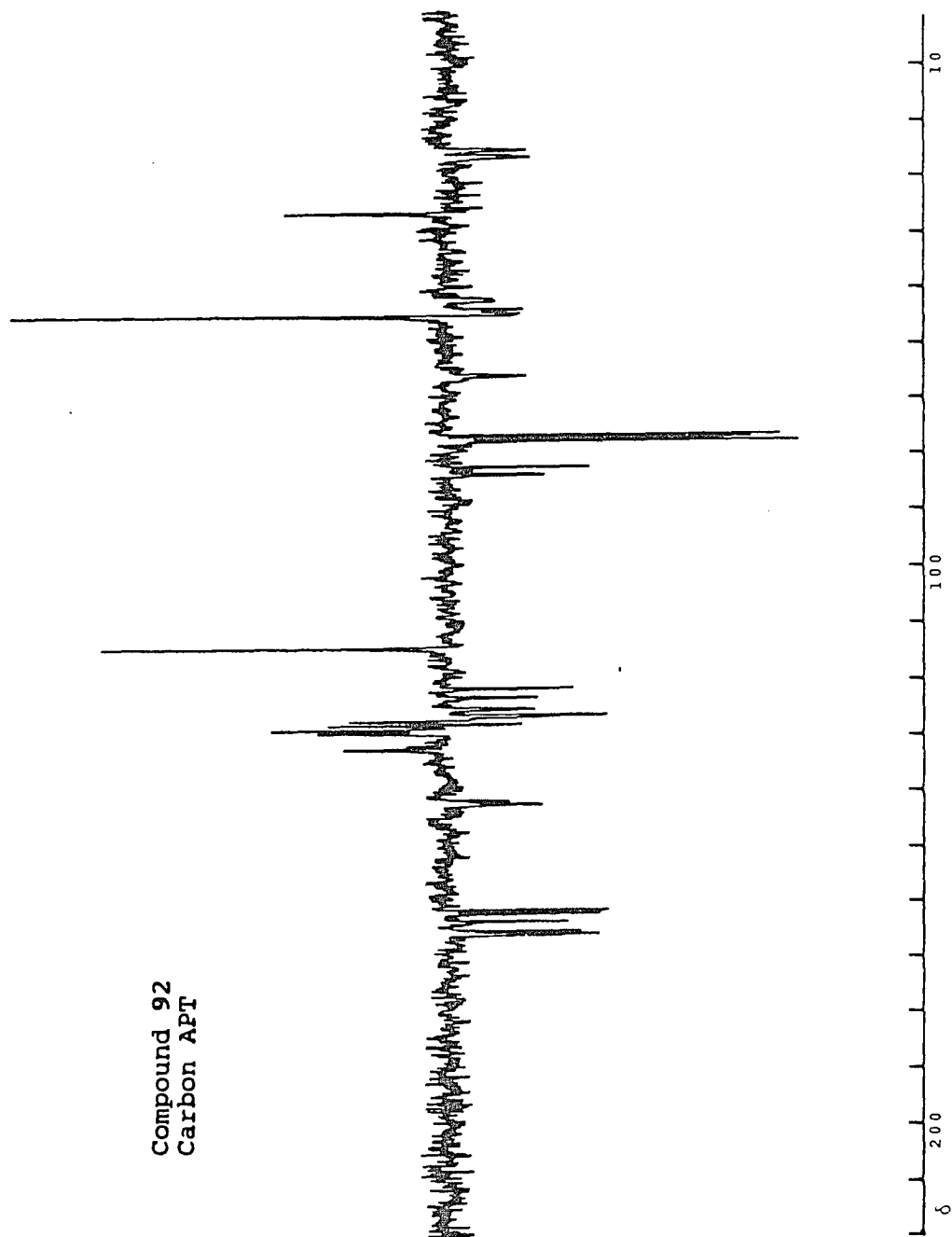
Compound 91
Carbon APT

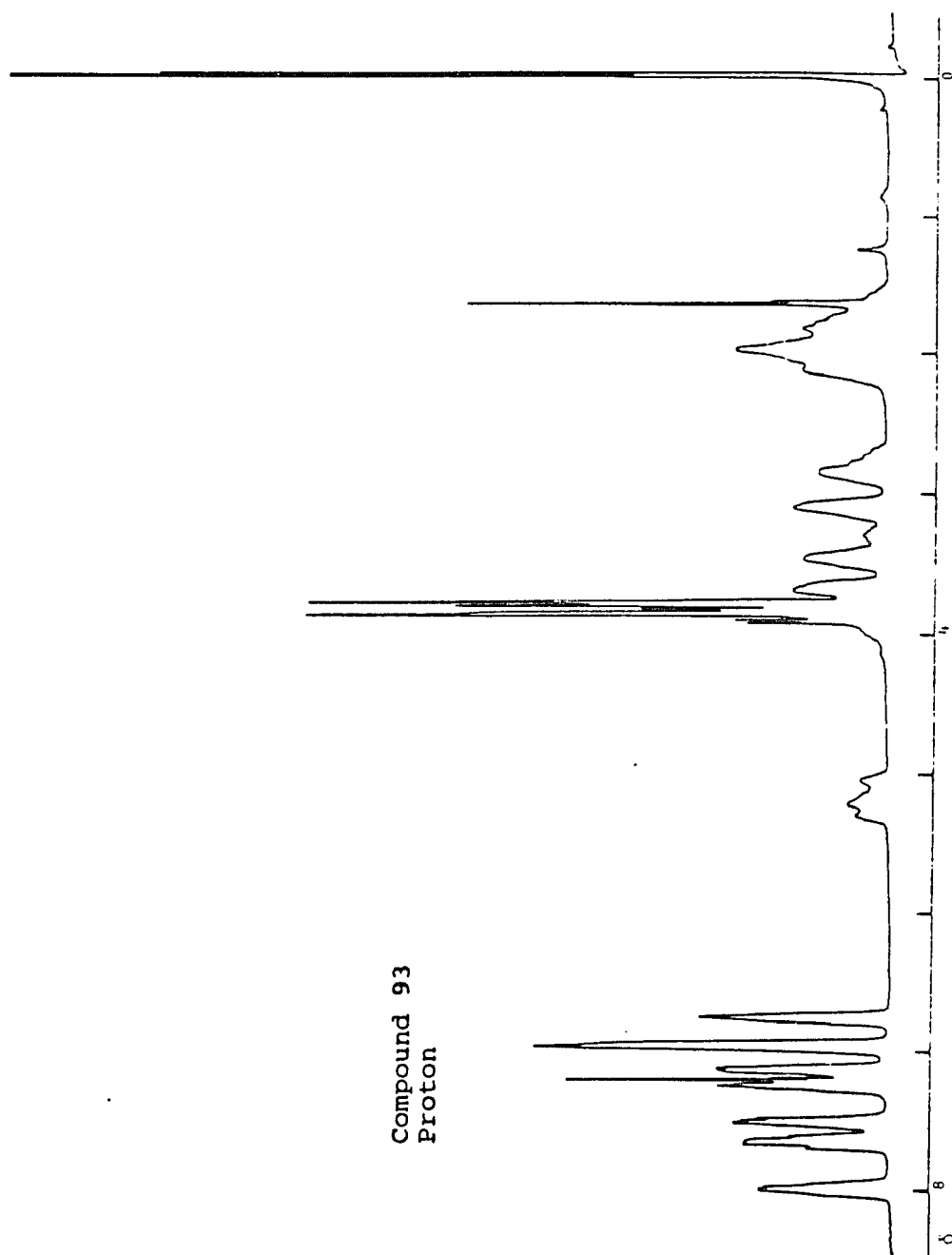




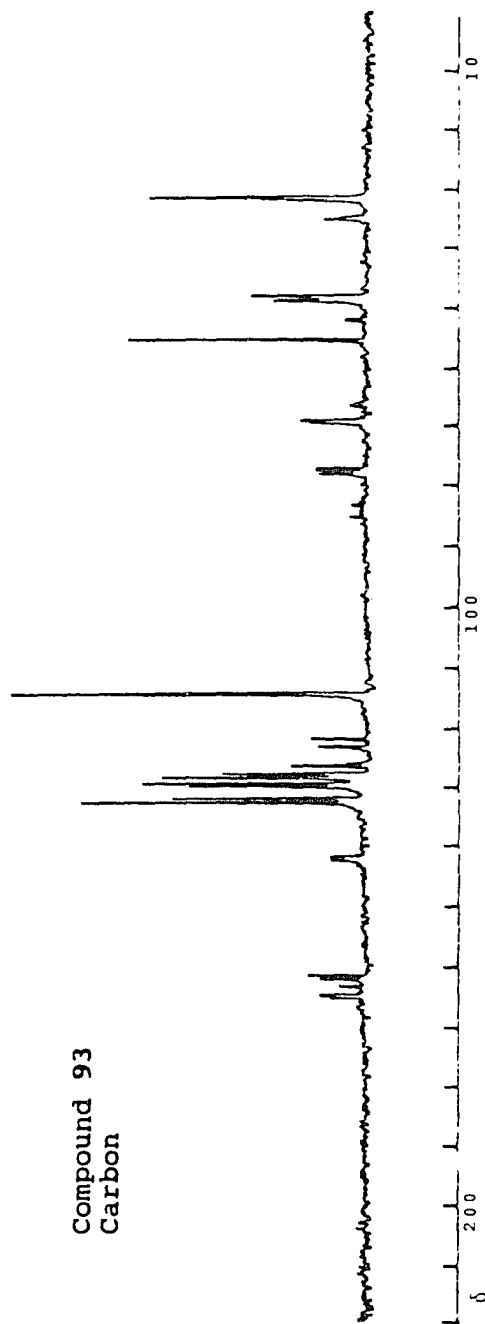


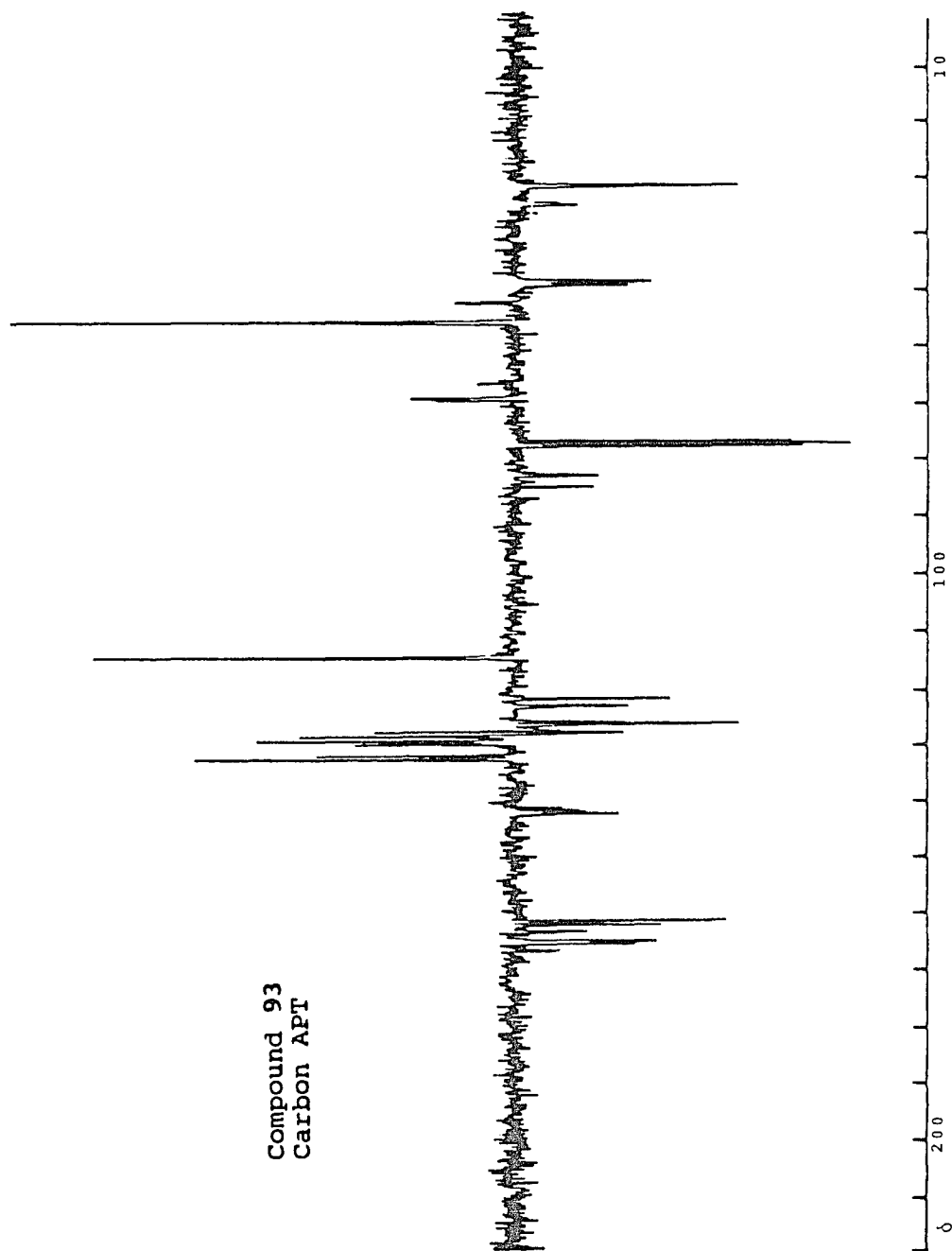
Compound 92
Carbon APT



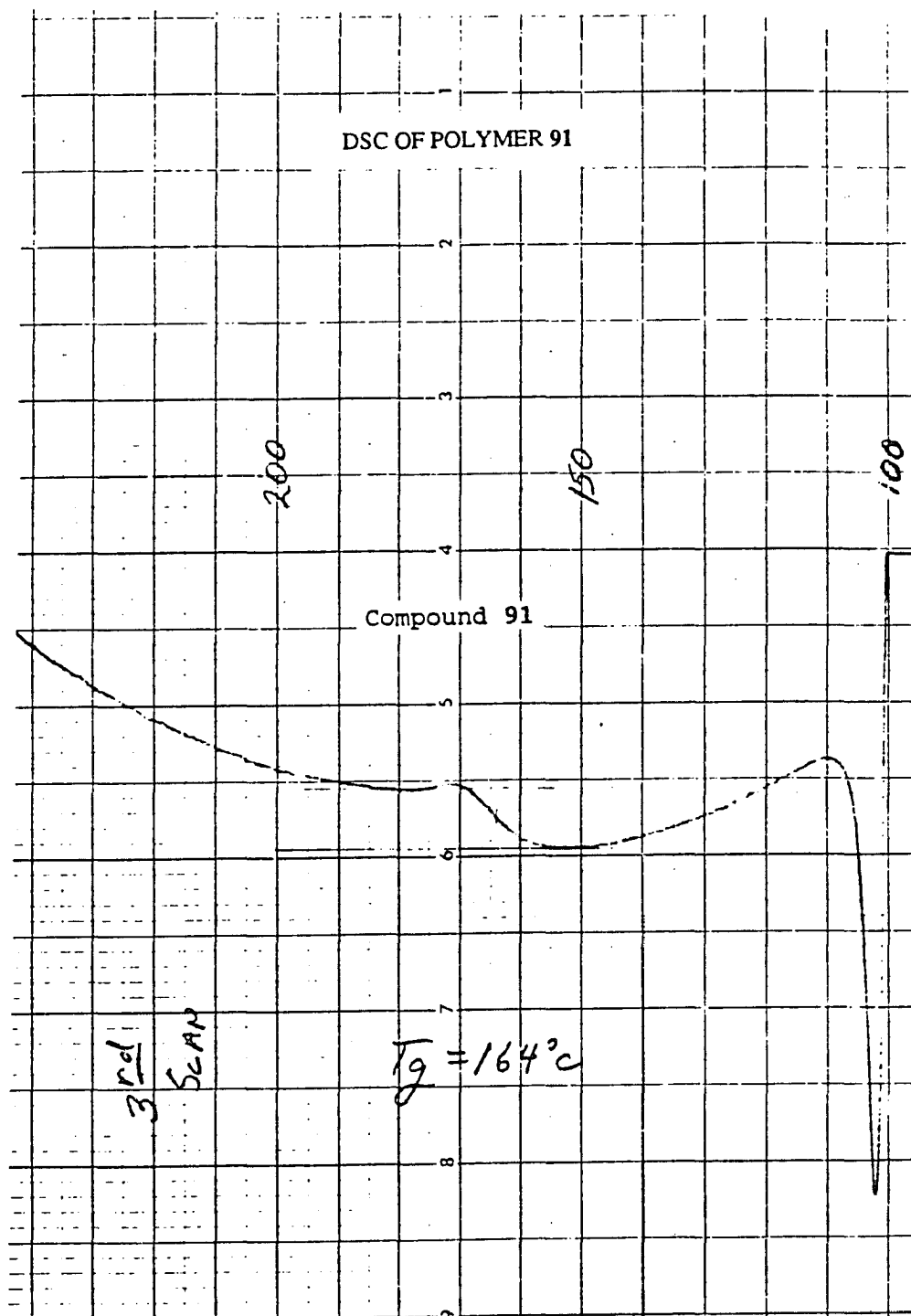


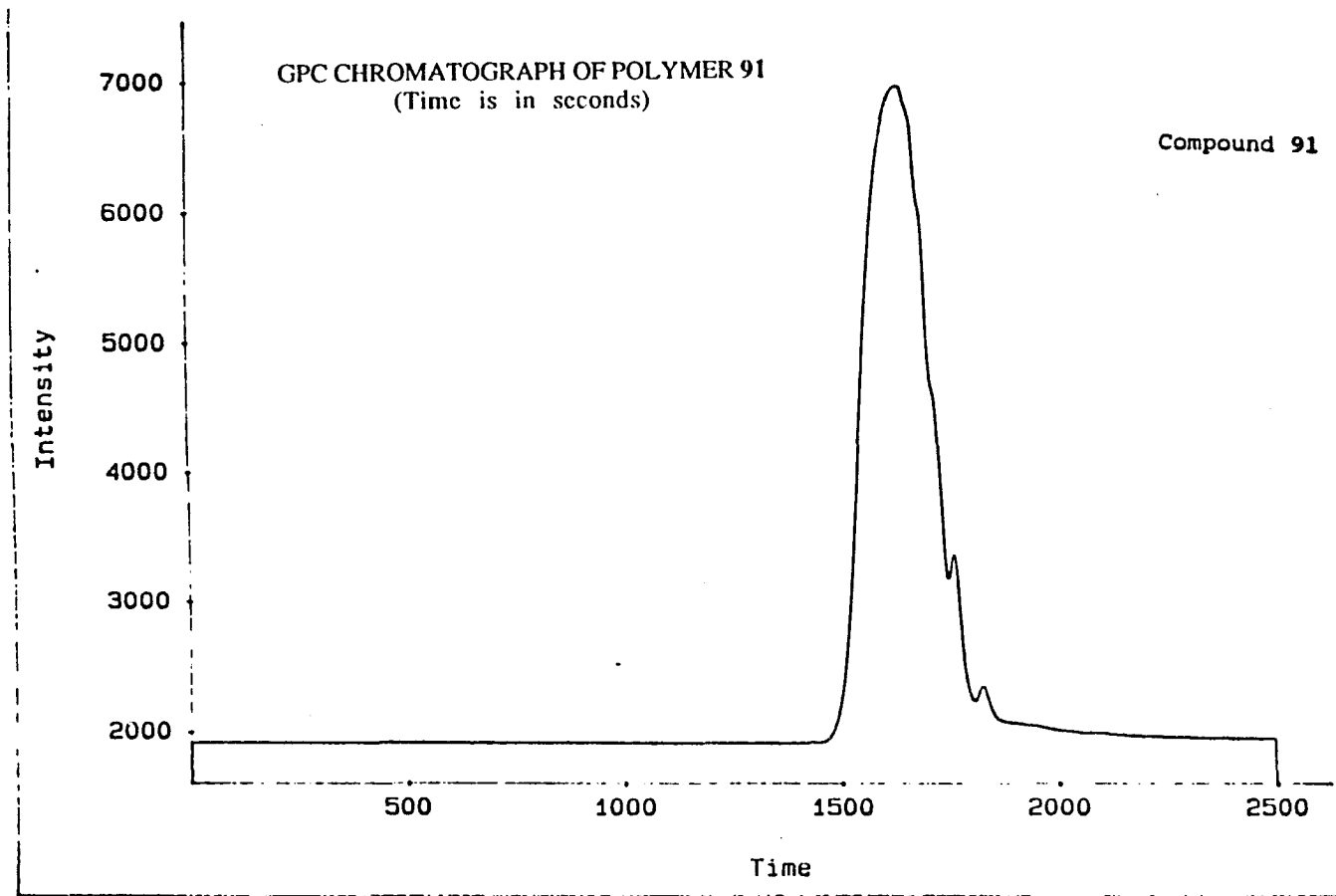
Compound 93
Carbon

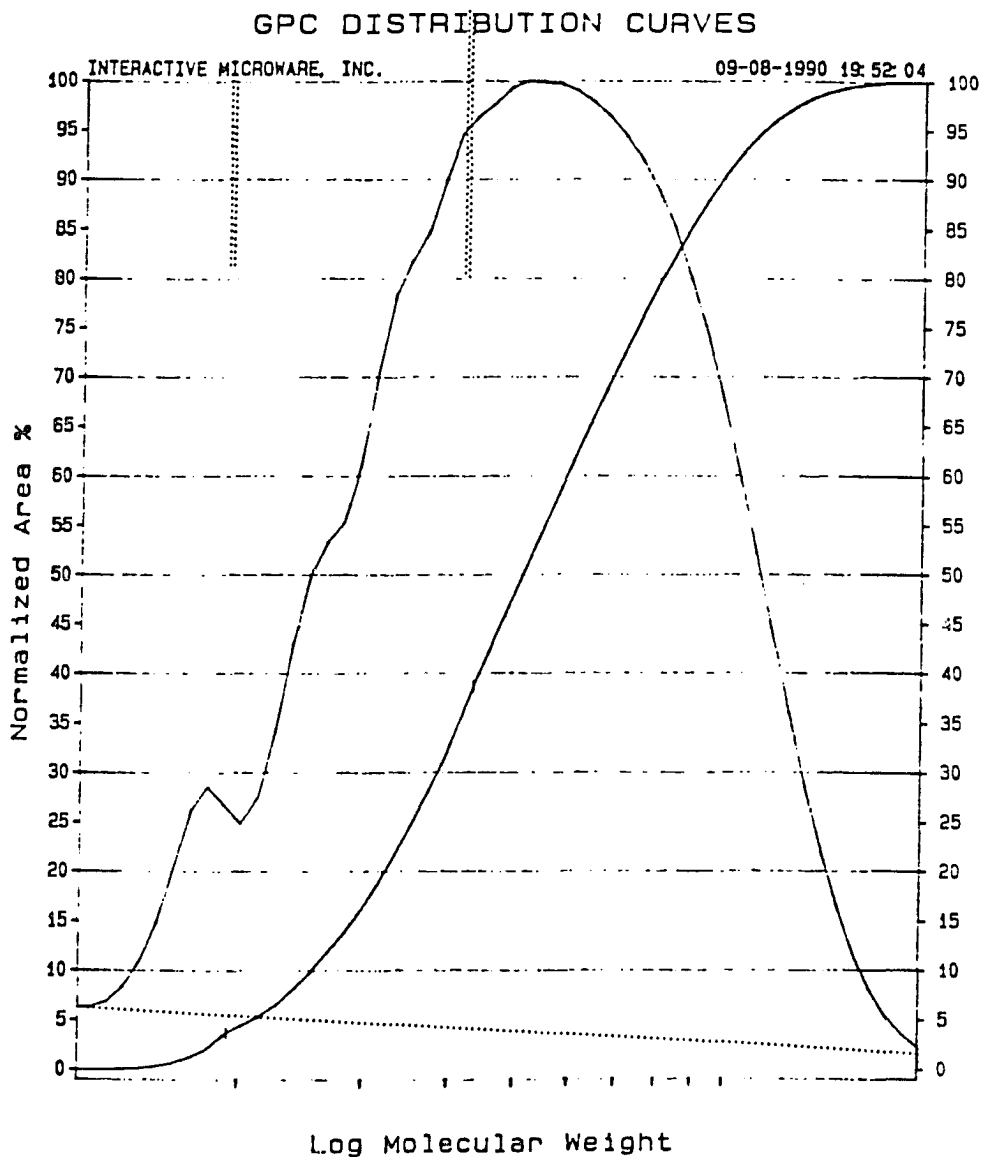




APPENDIX B
DSC AND SEC DATA







Compound 91

Integration Range : 1479 to 1804 seconds; 1198 to 19123 amu.

Maximum Intensity : 6991 Minimum Intensity : 2003

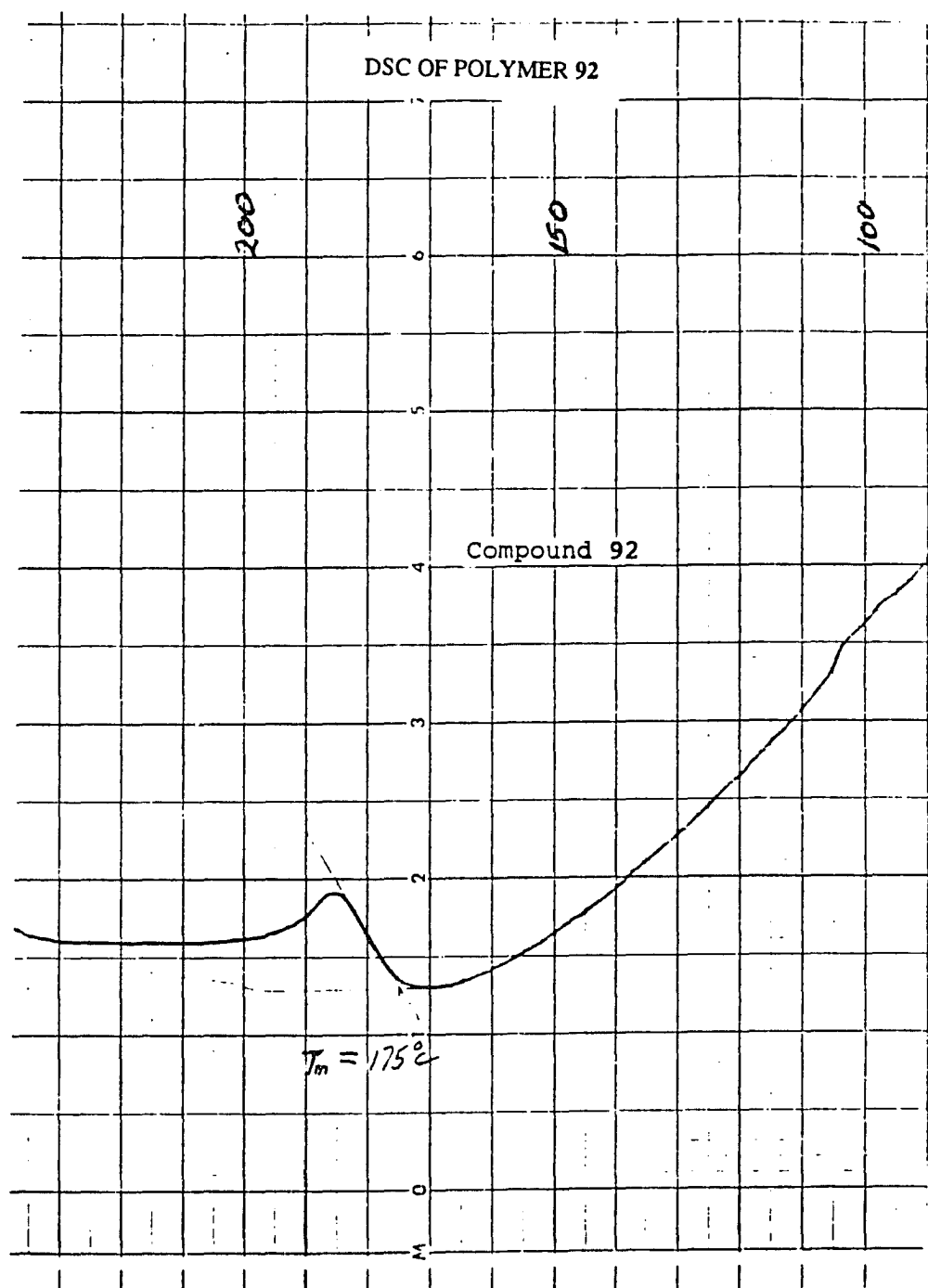
Mn = 4856

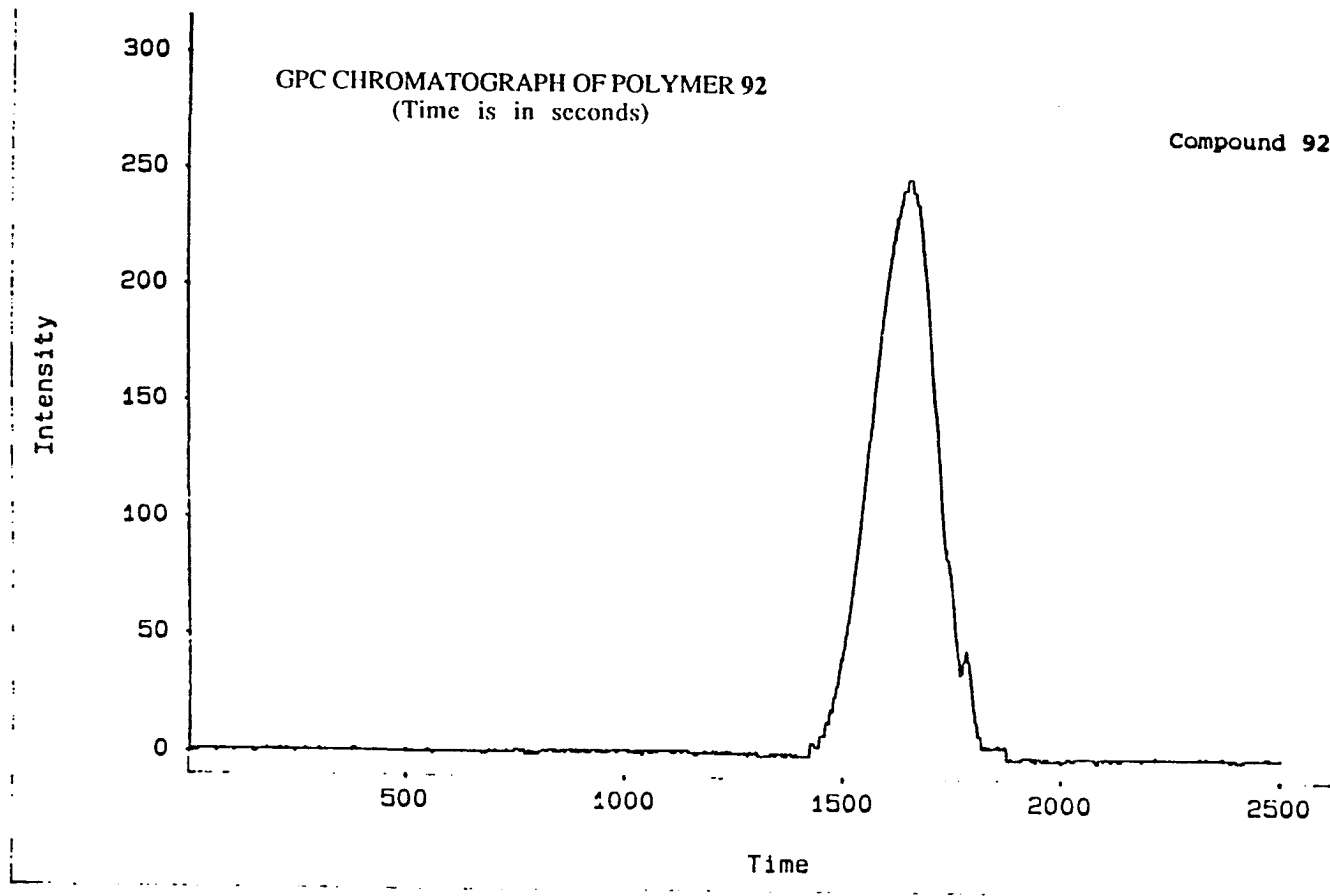
Mw = 6270

Mz = 7726

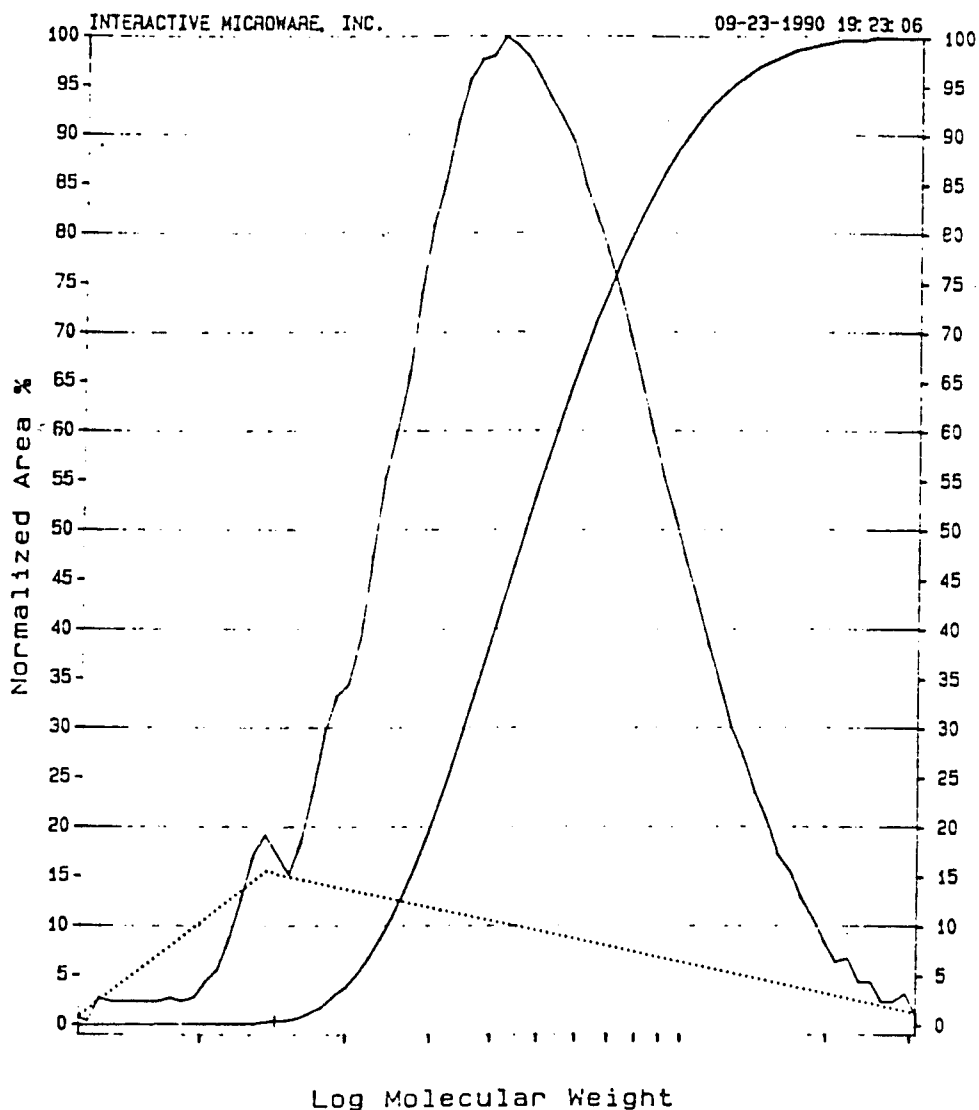
Mz+1 = 9056

PDI = 1





GPC DISTRIBUTION CURVES

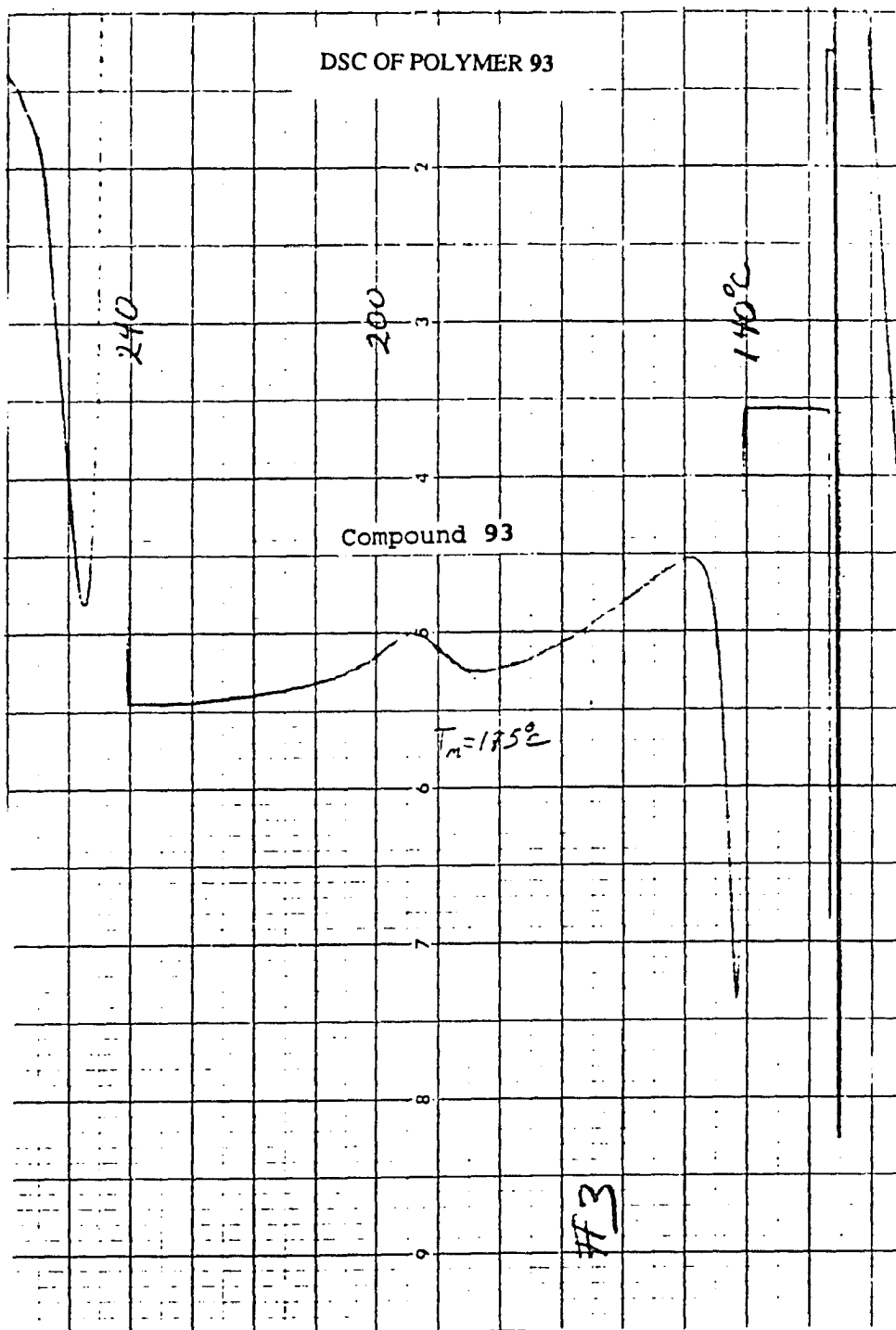


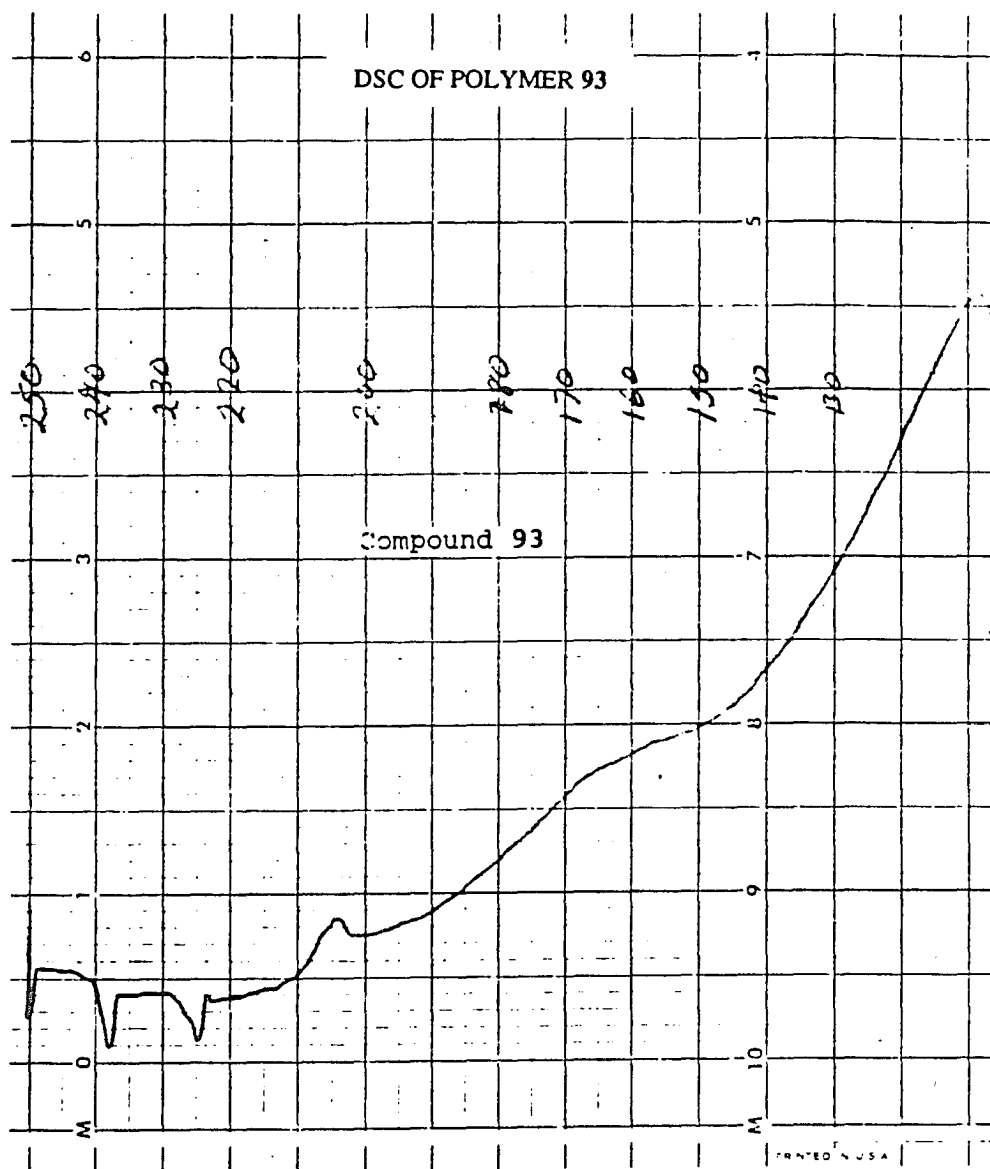
Compound 92

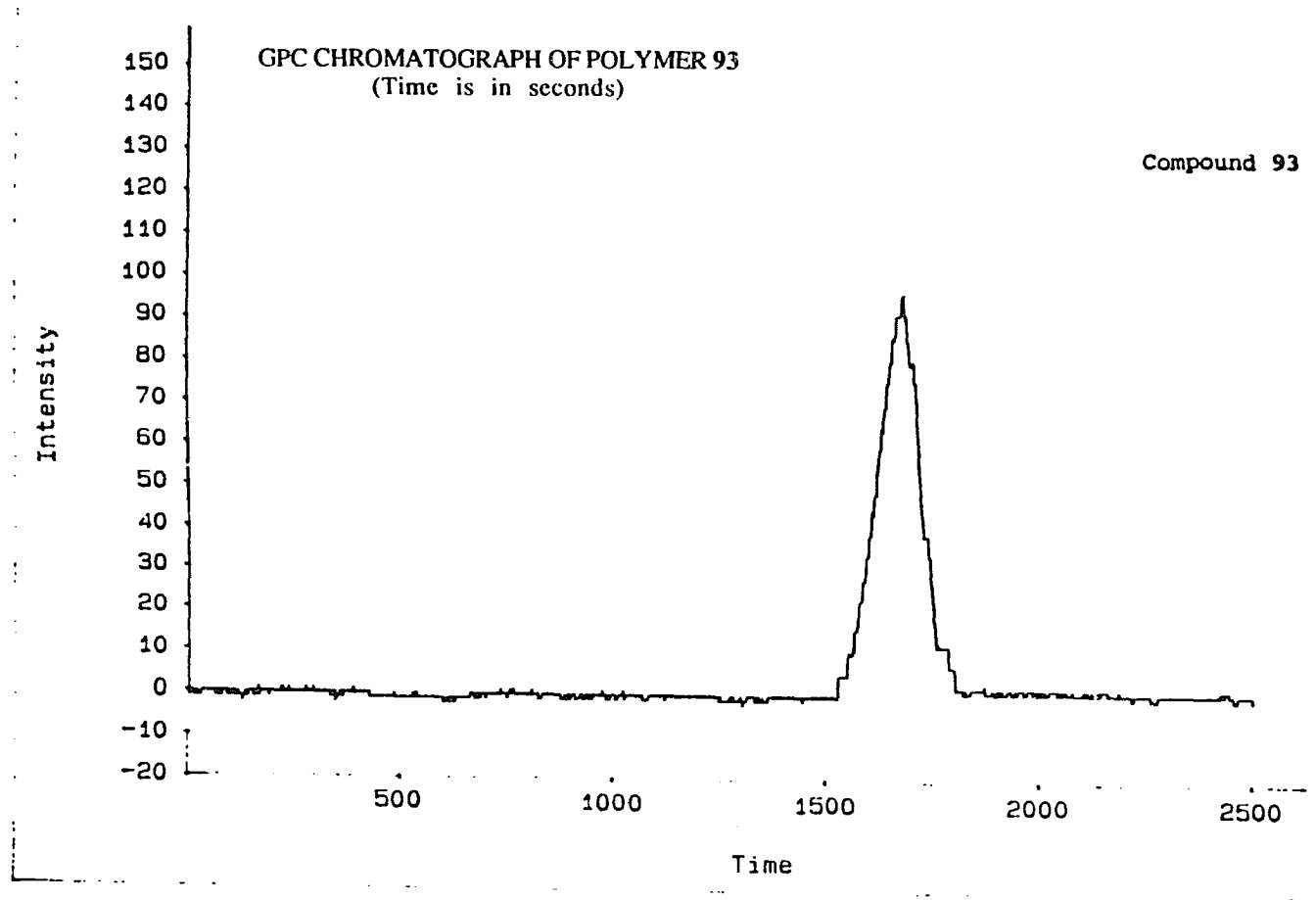
Integration Range : 1415 to 1874 seconds; 567 to 31095 amu.

Maximum Intensity : 248 Minimum Intensity : -1

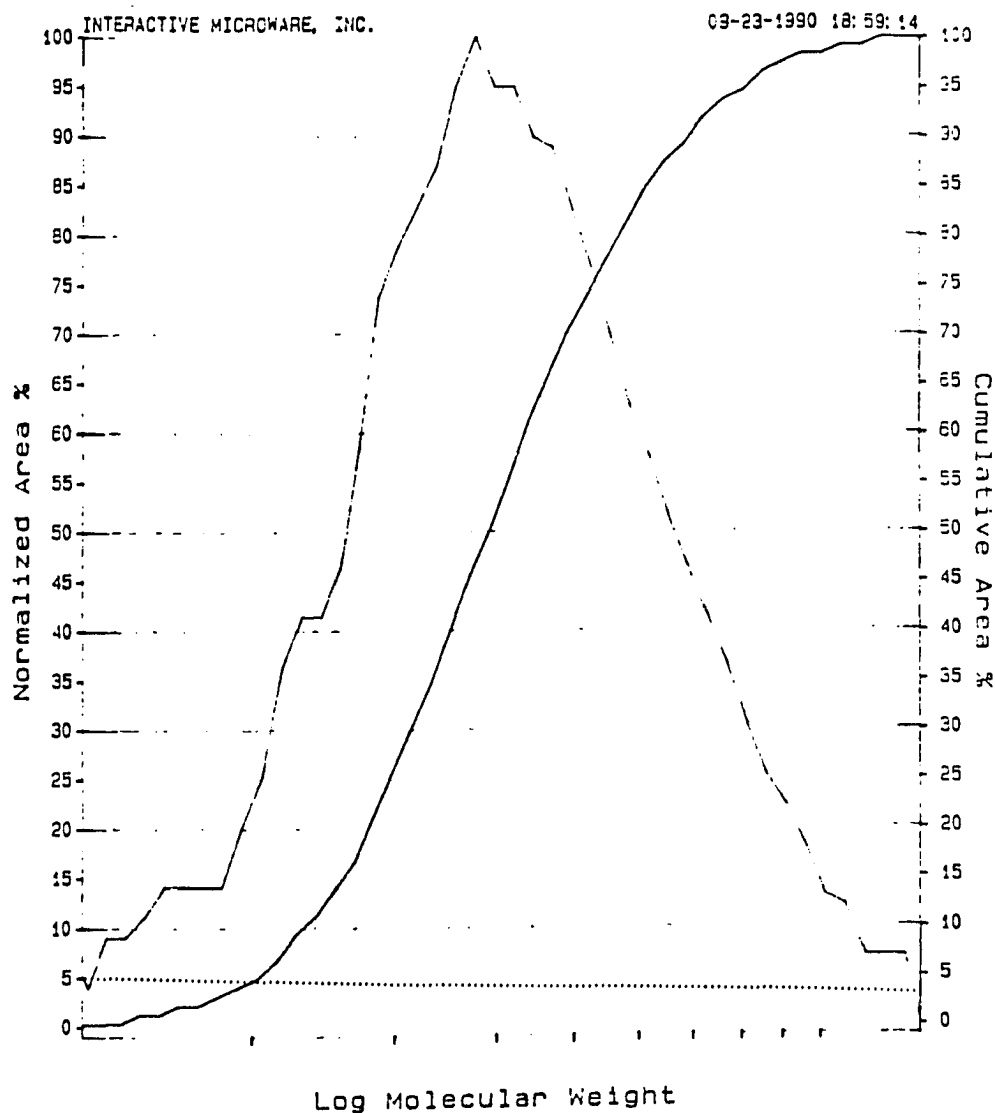
Mn = 5185
Mw = 6747
Mz = 8817
Mz+1 = 11270
PDI = 1







GPC DISTRIBUTION CURVES



Compound 93

Integration Range : 1525 to 1801 seconds; 1235 to 13449 amu.

Maximum Intensity : 97 Minimum Intensity : 2

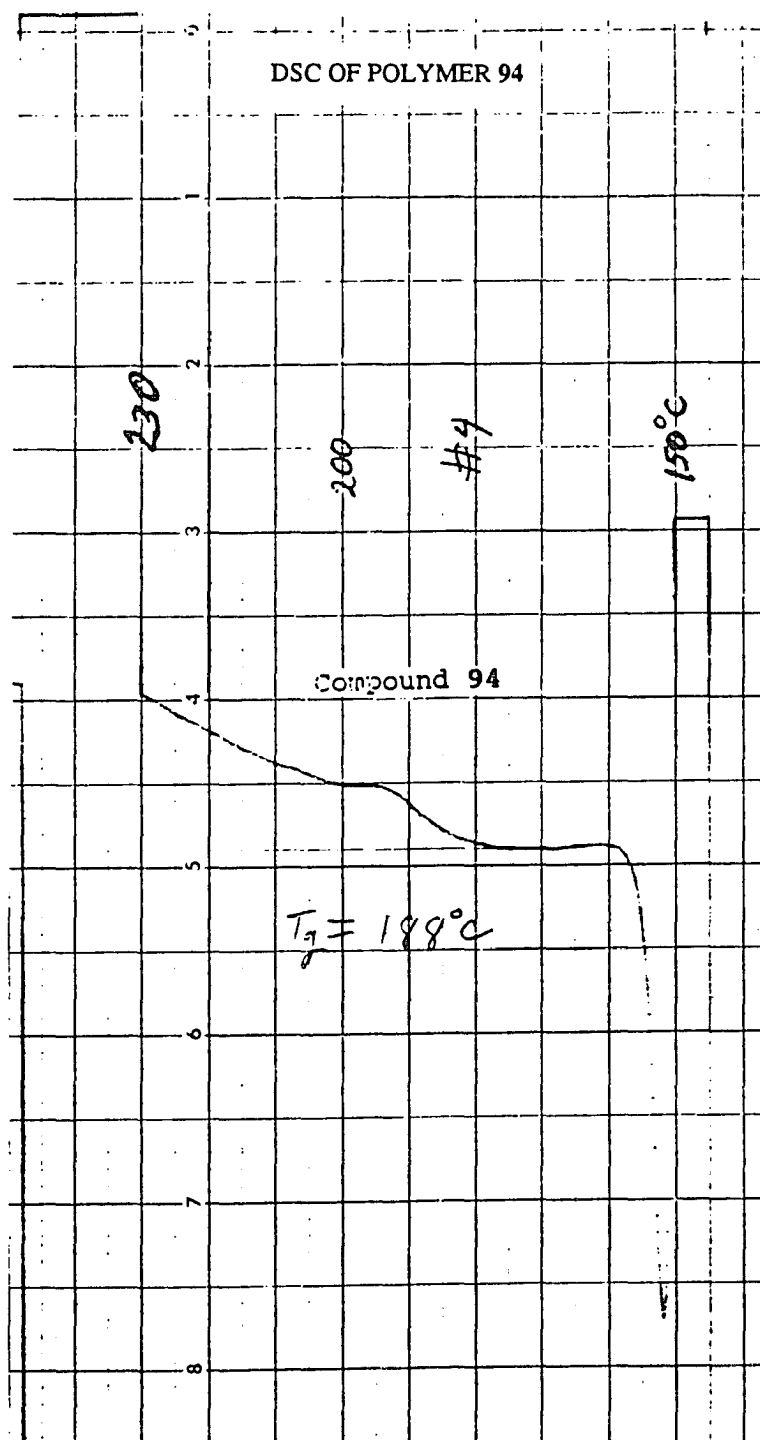
Mn = 3959

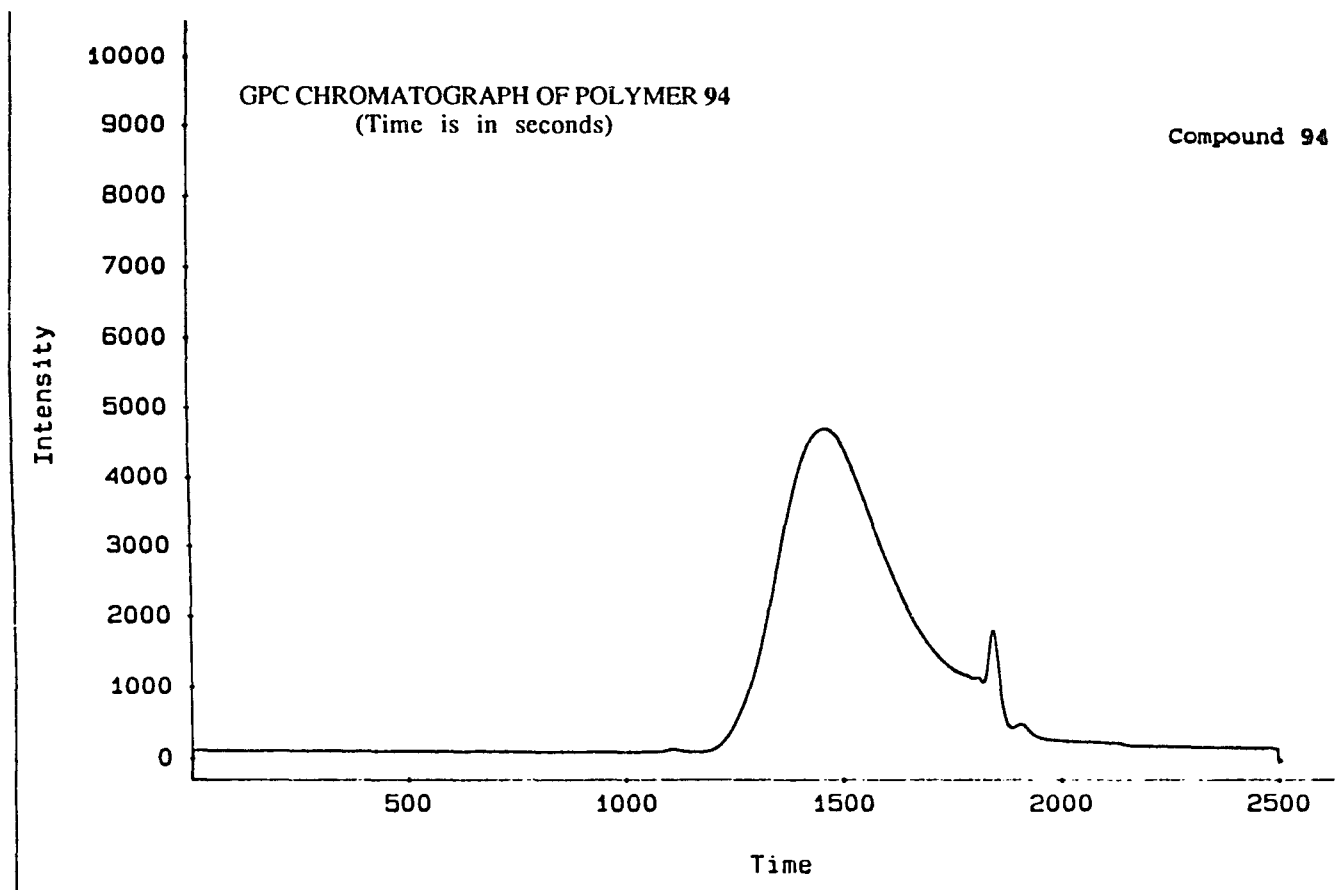
Mw = 4715

Mz = 5570

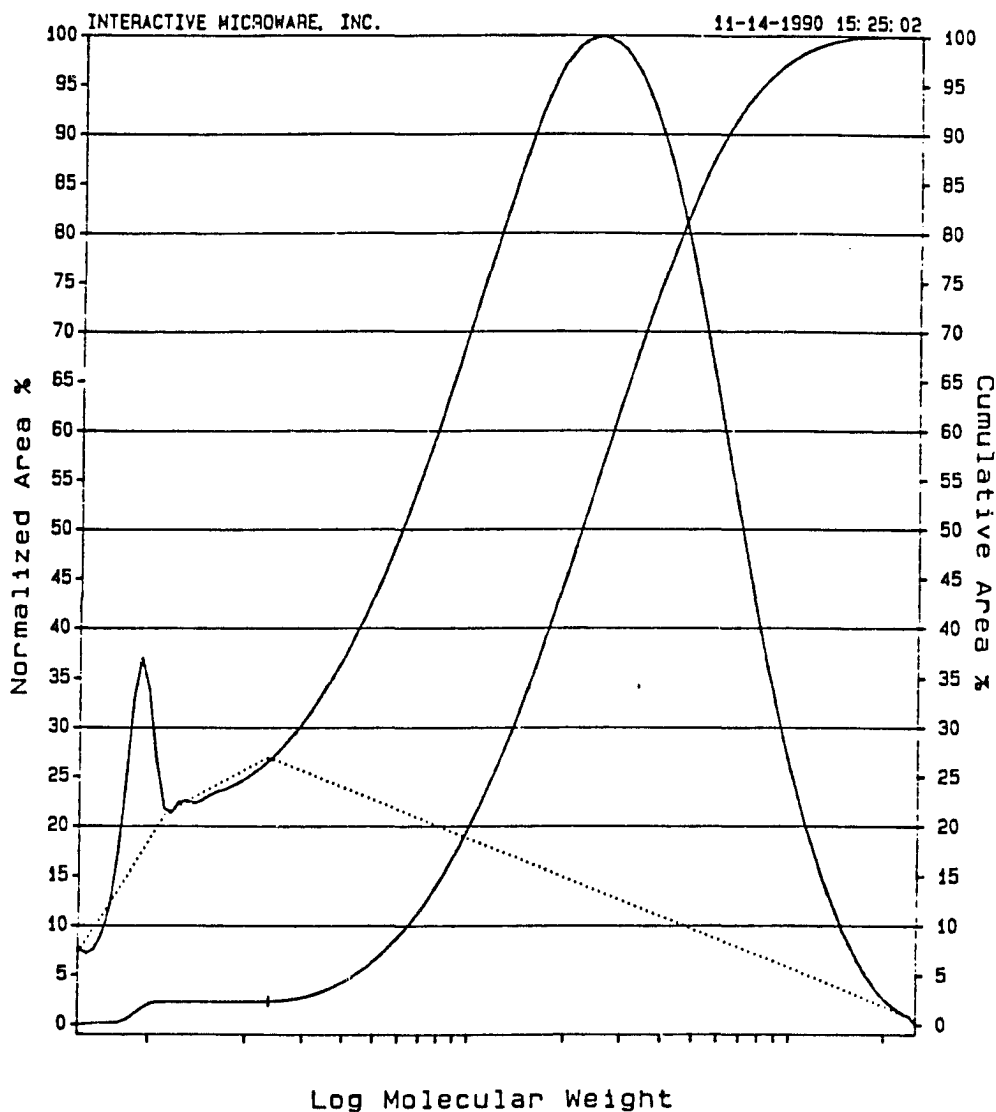
Mz+1 = 6489

PDI = 1





GPC DISTRIBUTION CURVES



Compound 94

Integration Range : 1186 to 1889 seconds; 613 to 255710 amu.

Maximum Intensity : 4705 Minimum Intensity : 120

Mn = 12822

Mw = 30254

Mz = 49179

Mz+1 = 70083

PDI = 2

REFERENCES

1. Kerr, J. Philos. Mag. **1875**, 50, 337.
2. Kerr, J. *ibid*, 446.
3. Tripathy, S.; Cavicchi, E.; Kumar, J.; Kumar, R.S. Chemtech, **1989**, Oct., 620.
4. Franken, P.A.; Hill, A.E.; Peters, C.W.; Weinreich, G. Phys. Rev. Lett. **1961**, 7(4), 118.
5. Laud, B.B. "Lasers and Nonlinear Optics", Wiley Eastern Limited, New Delhi, 1985.
6. Zernike, F.; Midwinter, J.E. "Applied Nonlinear Optics", John Wiley & Sons, Inc., New York, 1973.
7. Bailey, R.T.; Cruickshank, F.R.; Guthrie, S.M.G.; McArdle, B.J.; McGillivray, G.W.; Morrison, H.; Pugh, D.; Shepherd, E.A.; Sherwood, J.N.; Yoon, C.S. "Nonlinear Optical Materials"; Roosen, G.: SPIE - The International Society for Optical Engineering, Bellingham, 1989, 114.
8. Bloembergen, N.; Armstrong, J.A.; Ducuing, J.; Pershan, P.S. Phys. Rev. **1962**, 127(6), 1918.
9. Tanguay, A.R., Jr. Optical Engineering **1985**, 24(1), 2.
10. Markoff, J. New York Times **1990**, Jan. 31, A1.
11. Lee, S.H.; Athale, R.A. Optical Engineering **1989**, 28(4), 297.
12. Carpenter, G.A.; Grossberg, S. Applied Optics **1987**, 26(23), 4909.
13. Hecht-Nielsen, R. Spectrum **1988**, 25(3), 36.
14. Grossberg, S. Optics News **1988**, 14(8), 5.
15. Southgate, P.D.; Hall, D.S. J. Appl. Phys. **1972**, 43(6), 2765.
16. Derkacheva, L.D.; Krymova, A.I.; Sopina, N.P. JETP Lett. **1970**, 11(10), 319.
17. Southgate, P.D.; Hall, D.S. J. Appl. Phys. **1971**, 42(11), 4480.

18. Davydov, B.L.; Derkacheva, L.D.; Dunina, V.V.; Zhabotinskii, M.E.; Zolin, V.F.; Koreneva, L.G.; Samokhina, M.A. JETP Lett. 1970, 12(1), 16.
19. Cheng, L.T.; Tam, W.; Meredith, G.R.; Rikken, G.L.J.A.; Meijer, E.W. Proc. SPIE- Int. Soc. Opt. Eng. 1989, 1147, 61.
20. Williams, D.J. Angew. Chem. Int. Ed. Engl. 1984, 23, 690.
21. Dulcic, A.; Sauteret, C. J. Chem. Phys. 1918, 69, 3453.
22. Dulcic, A.; Flytzanis, C.; Tang, C.L.; Pepin, D.; Fitizon, M.; Hoppilliard, Y. *ibid* 1981, 74, 1559.
23. Itoh, Y.; Oono, K.; Isogai, M.; Kakuta, A. "Nonlinear Optical Materials", G. Roosen: SPIE - The International Society for Optical Engineering, Bellingham, 1989, 127.
24. Twieg, R.W.; Jain, K. "Nonlinear Optical Properties of Organic and Polymeric Materials"; D.J. Williams: ACS Symposium Series 233, American Chemical Society, Washington, 1983, 57.
25. Zyss, J.S.; Nicoud, J.F.; Koquillay, M. J. Chem. Phys. 1984, 81, 4160.
26. Zyss, J.S., *et. al.* *ibid* 1981, 74, 4800.
27. Marder, S.R.; Perry, J.W.; Schaefer, W.P. Science 1989, 245, 626.
28. Stucky, G.D.; Cox, S.D.; Gier, T.E.; Bierlein, J. J. Am. Chem. Soc. 1988, 110, 2986.
29. Finkelman, H.; Ringsdorf, H.; Wendorf, J. Makromol. Chem. 1978, 179, 273.
30. Stegman, G.S.; Normandin, R.; So, V.C.Y. J. Opt. Soc. Am. 1979, 69, 1166.
31. Williams, D.J.; Meredith, G.R.; Van Dusen, J.G. "Nonlinear Optical Properties of Organic and Polymeric Materials"; D.J. Williams: ACS Symposium Series 233, American Chemical Society, Washington, 1983, 109.
32. Kohler, W.; Robello, D.R.; Dao, P.T.; Willand, C.S.; Williams, D.J. J. Chem. Phys. 1990, In Press.
33. Lindsay, G.A., Naval Weapons Center, China Lake, CA; Personal Communication.

34. Leslie, T.M., Hoechst Celanese Research Center, Summit, NJ; Personal Communication.
35. Robello, D.R.; Ulman W.A.; Willand C.S. U.S. Patent 4,796,971; Jan. 10, 1989.
36. Reck, B.; Eich, M.; Tungbauer, D.; Twieg, R.J.; Willson, C.G.; Yoon, D.Y.; Bjorklund, G.C. Proc. SPIE - Int. Soc. Opt. Eng. **1989**, 1147, 74.
37. Green, G.D.; Hall, H.K., Jr.; Mulvaney, J.E.; Noonan, J.; Williams, D.J. Macromolecules **1987**, 20, 716.
38. Green, G.D.; Weinschenk, J.I.; Mulvaney, J.E.; Hall, H.K., Jr. *ibid*, 722.
39. Willand, C.S.; Feth, S.E.; Scozzafava, M.; Williams, D.J.; Green, G.D.; Weinschenk, J.I.; Hall, H.K., Jr.; Mulvaney, J.E. "Nonlinear Optical and Electroactive Polymers"; P.N. Prasad and D.R. Ulrich: Plenum Press, New York, 1988, 107.
40. Hall, H.K., Jr. J. Macromol. Sci. - Chem. **1988**, A25(5-7), 729.
41. Halbout, J.M.; Tang, C.L. "Nonlinear Optical Properties of Organic Molecules and Crystals", Volume 1; D.S. Chemla, J. Zyss: Academic Press, Inc., Orlando, 1987, 385.
42. Zyss, J.; Berthier, G. J. Chem. Phys. **1982**, 77, 3635.
43. Katz, H.E.; Schilling, M.L. J. Am. Chem. Soc. **1989**, 111, 7554.
44. Imai, Y.; Ueda, M.; Ii, M. Macromol. Chem. **1978**, 179, 2989.
45. Johnson, R.N.; Farnham, A.G.; Clendinning, R.A.; Hale, W.F.; Merriam, C.N. J. Polymer Sci. - Part A1 **1967**, 5, 2375.
46. Hale, W.F.; Farnham, A.G.; Johnson, R.N.; Clendinning, R.A. *ibid*, 2399.
47. Rose, J.B. Polymer **1974**, 15, 456.
48. Zahn, H.; Zuber, H. Chem. Ber. **1953**, 86, 172.
49. Yamawaki, J.; Ando, T. Chem. Lett. **1979**, 755.
50. Yamawaki, J.; Ando, T.; Hanafusa, T. *ibid* **1981**, 1143.
51. Brown, H.C.; Narasimhan, S.; Choi, Y.M. Synthesis Comm. **1981**, 996.

52. Paradisi, C.; Galvagni, M.; Kelleher, F.; Scorrano, G. J. Org. Chem. **1990**, 55, 4454.
53. Kennedy, R.J.; Stock, A.M. J. Org. Chem. **1960**, 25, 1901.
54. Trost, B.M.; Curran, D.P. Tet. Lett. **1981**, 22(14), 1287.
55. Smith, E.D.; Sheppard, H. Nature **1965**, 208, 878.
56. Rogozhin, S.V.; Davidovich, Y.A.; Yurtanov, A.I. Synthesis **1975**, 113.
57. Ohtsuka, Y.; Oishi, T. Chem. Pharm. Bull. **1983**, 31, 454.
58. DeMartino, R.N.; Khanarian, G.; Leslie, T.M.; Sansone, M.J.; Stamatoff, J.B.; Yoon, H.N. SPIE - Materials for Optical Switches, Isolators, and Limiters **1989**, 1105, 2.
59. Fouguey, C.; Lehn, J.-M.; Levelut, A.-M. Adv. Materials **1990**, 2(5), 254.
60. Hunter, C.A.; Sanders, J.K.M. J. Am. Chem. Soc. **1990**, 112, 5525.
61. Hallas, G.; Marsden, R.; Hepworth, J.D.; Mason, D. J. Chem. Soc., Perkin Trans. **1984**, 2, 149.
62. Hepworth, J.D.; Mason, D.; Hallas, G.; Marsden, R. Dyes and Pigments **1985**, 6, 389.
63. Hallas, G.; Marsden, R. *ibid*, 463.
64. Stenger-Smith, J.D.; Fischer, J.W.; Henry, R.A.; Hoover, J.M.; Lindsay, G.A.; Hayden, L.M. Makromol. Chem., Rapid Comm. **1990**, 11, 141.
65. Moore, J.A.; Robello, D.R. Macromolecules **1989**, 22, 1084.
66. Rappoport, Z.; Avramovitch, B. J. Org. Chem. **1982**, 47, 1397.
67. Lodder, G.; van Dorp, J.W.J.; Avramovitch, B.; Rappoport, Z. *ibid* **1989**, 54, 2574.
68. Moore, J.A.; Robello, D.R. Polymer Preprints **1986**, 27(1), 127.
69. Shi, S.; Wudl, F. J. Org. Chem. **1988**, 53, 5379.
70. Codington, J.F.; Mosettig, E. J. Org. Chem. **1952**, 17, 1035.

71. Weisskopf, K; Meyerhoff, G. Makromol. Chem. 1986, 187, 401.
72. Hayashi, T. J. Org. Chem. 1966, 31, 3253.
73. Iwatsuki, S.; Itoh, T.; Iwai, T.; Sawada, H. Macromolecules 1985, 18(12), 2726.
74. Kurtz, S.K.; Perry, T.T. J. Appl. Phys. 1968, 39, 3798.
75. Kurtz, S.K. IEEE J. Quant. Electr. 1968, QE-4, 578.
76. Kajzar, F.; Messier, J. "Nonlinear Optical Properties of Organic Molecules and Crystals", Volume 2; D.S. Chemla and J. Zyss: Academic Press, Inc. Orlando, 1987, 51.
77. Robello, D.R., Eastman Kodak Company, Rochester, NY; Personal Communication.
78. Levine, B.F.; Bethea, C.G. J. Chem. Phys. 1975, 63(6), 2666.
79. Oudar, J.L. J. Chem. Phys. 1977, 67, 446.
80. Paley, M.S.; Harris, J.M.; Looser, H.; Baumert, J.C.; Bjorklund, G.C.; Jundt, D.; Twieg, R.J. J. Org. Chem. 1989, 54, 3774.
81. Teng, C.C.; Garito, A.F. Phys. Rev. Lett. 1983, 50, 350.
82. Levine, B.F.; Bethea, C.G. J. Chem. Phys. 1976, 65, 2429.
83. Oudar, J.L.; Chemla, D.S. J. Chem. Phys. 1977, 66, 2664.
84. Oudar, J.L. *ibid* 1977, 67, 446.
85. Buckley, A.; Choe, E.; DeMartino, R.; Leslie, T.; Nelson, G.; Stamatoff, J.; Stuetz, D.; Yoon, H. Polymeric Materials: Sci. and Eng., Proc. of the ACS Division of Polymeric Materials, Sci. and Eng. 1986, 54, 502.
86. Oudar, J.L.; Zyss, J. Phys. Rev. A 1982, 26(4), 2016.
87. Shoemaker, D.P.; Garland, C.W.; Steinfeld, J.I.; Nibler, J.W. "Experiments in Physical Chemistry", Fourth Ed.; McGraw-Hill, Inc., New York, 1981.
88. Bonilla, A.; Vassos, B. J. Chem. Education 1977, 54(2), 130.
89. Liptay, W. Angew. Chem., Int. Ed. Engl. 1969, 8, 177.
90. Buncel, E; Rajagopal, S. J. Org. Chem. 1989, 54, 798.

91. Hermant, R.M.; Bakker, N.A.C.; Scherer, T.; Krijnen, B.; Verhoeven, J.W. J. Am. Chem. Soc. **1990**, 112, 1214.
92. McRea, E.G. J. Phys. Chem. **1957**, 61, 562.
93. Liptay, W. Z. Naturforschg. **1965**, 20a, 1441.
94. Bakhshiev, N.G.; Knyazhanskii, M.I.; Minkin, V.I.; Osipov, O.A.; Saidov, G.V. Russ. Chem. Rev. **1969**, 38(9), 740.
95. Bilot, L.; Kawski, A. Z. Naturforschung. **1962**, 17a, 621.
96. Mataga, N.; Kaifu, Y.; Koizumi, M. Bull. Chem. Soc. Jap. **1956**, 29(4), 465.
97. Block, H.; Walker, S.M. Chem. Phys. Lett. **1973**, 19(3), 363.
98. Lippert, V.E. Z. Naturforschung. **1955**, 10a, 541.
99. Koutek, B. Coll. Czech. Chem. Comm. **1984**, 49, 1680.
100. Koutek, B. *ibid* **1978**, 43, 2368.
101. Bakhshiev, N.G. Opt. Spektrosk. **1965**, 19, 345.
102. Minkin, Vladimir Isaakovich "Dipole Moments in Organic Chemistry"; translated by B.J. Hazzard, translation edited by Worth E. Vaughan, Plenum Press, New York, 1970.
103. Ulman, A.; Willand, C.S.; Kohler, W.; Robello, D.R.; Williams, D.J.; Handley, L. J. Am. Chem. Soc. **1990**, 112(20), 7083.
104. Li, D.; Ratner, M.A.; Marks, T.J. J. Am. Chem. Soc. **1988**, 110(6), 1707.